

Wilfrid Laurier University

Scholars Commons @ Laurier

---

Theses and Dissertations (Comprehensive)

---

2004

## Temporal variability in nutrient transport in a first-order agricultural basin in southern Ontario

Merrin L. Macrae  
*Wilfrid Laurier University*

Follow this and additional works at: <https://scholars.wlu.ca/etd>



Part of the [Agriculture Commons](#), and the [Hydrology Commons](#)

---

### Recommended Citation

Macrae, Merrin L., "Temporal variability in nutrient transport in a first-order agricultural basin in southern Ontario" (2004). *Theses and Dissertations (Comprehensive)*. 492.  
<https://scholars.wlu.ca/etd/492>

This Dissertation is brought to you for free and open access by Scholars Commons @ Laurier. It has been accepted for inclusion in Theses and Dissertations (Comprehensive) by an authorized administrator of Scholars Commons @ Laurier. For more information, please contact [scholarscommons@wlu.ca](mailto:scholarscommons@wlu.ca).



National Library  
of Canada

Bibliothèque nationale  
du Canada

Acquisitions and  
Bibliographic Services

Acquisitons et  
services bibliographiques

395 Wellington Street  
Ottawa ON K1A 0N4  
Canada

395, rue Wellington  
Ottawa ON K1A 0N4  
Canada

*Your file* *Votre référence*

*ISBN: 0-612-86627-0*

*Our file* *Notre référence*

*ISBN: 0-612-86627-0*

The author has granted a non-exclusive licence allowing the National Library of Canada to reproduce, loan, distribute or sell copies of this thesis in microform, paper or electronic formats.

L'auteur a accordé une licence non exclusive permettant à la Bibliothèque nationale du Canada de reproduire, prêter, distribuer ou vendre des copies de cette thèse sous la forme de microfiche/film, de reproduction sur papier ou sur format électronique.

The author retains ownership of the copyright in this thesis. Neither the thesis nor substantial extracts from it may be printed or otherwise reproduced without the author's permission.

L'auteur conserve la propriété du droit d'auteur qui protège cette thèse. Ni la thèse ni des extraits substantiels de celle-ci ne doivent être imprimés ou autrement reproduits sans son autorisation.

---

In compliance with the Canadian Privacy Act some supporting forms may have been removed from this dissertation.

Conformément à la loi canadienne sur la protection de la vie privée, quelques formulaires secondaires ont été enlevés de ce manuscrit.

While these forms may be included in the document page count, their removal does not represent any loss of content from the dissertation.

Bien que ces formulaires aient inclus dans la pagination, il n'y aura aucun contenu manquant.

**Canada**

**TEMPORAL VARIABILITY IN NUTRIENT TRANSPORT IN A FIRST-ORDER  
AGRICULTURAL BASIN IN SOUTHERN ONTARIO**

BY

Merrin L. Macrae  
B.E.S., York University, 1992  
M.Sc., York University, 1996

THESIS

Submitted to the Department of Geography and Environmental Studies  
in partial fulfillment of the requirements  
for the Doctor of Philosophy degree

Wilfrid Laurier University  
2003

© Merrin Macrae, 2003

## **ABSTRACT**

This thesis examines phosphorus and nitrate transport in a first-order agricultural catchment in Southern Ontario. Specific areas of concern relate to (1) long- and short-term temporal variability in nutrient export patterns, (2) the role of drainage tiles in annual nutrient export, (3) the effects of antecedent hydrologic conditions (AHC) on nutrient export patterns and (4) temporal variability in the nutrient retention in riparian buffer strips and streams.

Temporal variability in hydrochemical export from the study basin over a two-year period is described and quantified and the importance of high magnitude events is highlighted. This is the first comprehensive study to examine the role of such events in annual nutrient export from agricultural catchments (17-58% of annual nutrient export). The significance of winter thaws and in particular major snowmelt events in annual nutrient export from agricultural catchments in Southern Ontario is shown and the need to include the winter period in sampling regimes is demonstrated. The importance of sampling frequency is examined and an improved sampling strategy is suggested for the study basin.

The role of drainage tiles in annual hydrochemical export from the basin is quantified and the dominance of drainage tiles as a nutrient source is shown. Tiles account for approximately 42% of annual discharge, but account for the majority of SRP, TP and  $\text{NO}_3^-$  export. Tiles within the study basin exhibit spatial and temporal variability in hydrochemical export patterns but the discharge from all tiles within the basin can be predicted from one continuously monitored tile.

The effect of antecedent hydrologic conditions in hydrochemical export and the complex effects of successive events on hydrochemical export patterns are also demonstrated. In general, hydrochemical export increases as conditions become successively wetter, although empirical relationships between hydrological variables in the catchment and hydrochemical export are weak. Hydrologic connectivity between surface horizons and drainage tiles by macropores and preferential flowpaths appears to be critical in exporting nutrients from the catchment, and the role of these flowpaths increases as conditions become wetter.

The in-stream retention of phosphate during low flows is examined. Stream sediments are unable to retain large pulses of phosphate during very low flow periods due to poor mixing in the water column. The stream is therefore unable to retain pulses of phosphate that may occur following the irrigation of fields receiving liquid manure applications or when fertilizers are directly applied into ditches.

These individual studies improve our general understanding of nutrient dynamics and export from agricultural watersheds. This thesis increases our ability to predict nutrient export by (a) suggesting a new sampling strategy to improve the precision of nutrient export estimates in basins; and (b) identifying critical periods of nutrient export and linking these to antecedent hydrologic conditions in the basin.

## **CONTRIBUTION TO KNOWLEDGE**

This thesis has increased knowledge regarding the physical and chemical processes affecting spatial and temporal variability in hydrochemical export from first-order agricultural basins in several ways. These are noted below.

(1) High magnitude events account for 17-58% of the annual hydrochemical export from the study basin.

(2) This thesis has improved our understanding of dominant processes within the basin by linking hydrochemical export patterns to antecedent hydrologic conditions (AHC). Successive events play a critical role in hydrochemical export patterns and complicate empirical relationships between basin export and indications of AHC such as water table position and pre-event flow conditions.

(3) This thesis quantifies the significance of the major snowmelt event in annual hydrochemical export and suggests that in any given year this event is critical to sample as it may be a high magnitude event.

(4) A new sampling strategy has been proposed to improve the precision of nutrient export estimates in small basins such as the study basin and has identified critical periods of nutrient export and linked these to AHC in the basin. Sampling frequencies must increase in intensity around storm and thaw events. These findings have improved our ability to predict nutrient export from small agricultural basins.

(5) An extensive data set based on intensive sampling through all seasons of the year has been generated. Such data sets are rare. This data set will allow modeling exercises to be conducted in this basin in future research.

(6) This thesis has examined the importance of drainage tiles in basin hydrochemical export and has identified them as a dominant nutrient source compared to other sources in the study basin. The role of drainage tiles is examined in all seasons of the year and studies such as this have not been previously conducted .

(7) This thesis has shown that all tiles within the study basin behave in a similar manner hydrologically under some conditions and the hydrologic behaviour of all tiles within the basin may be predicted from one continuously monitored tile. Tile hydrology has been examined elsewhere, but this is the first study to look at discharge patterns from all tiles within a small basin over a one year period. The development of these relationships improves our understanding of the hydrology of the study basin and such relationships may be useful in models.

(8) This thesis has shown that Strawberry Creek, a representative first-order agricultural stream is not effective at retaining pulses of phosphate during low flow periods due to poor mixing in the water column. The ineffectiveness of stream sediments to retain phosphate is in contrast to other studies that have identified in-stream sediments as an important mechanism by which phosphate is removed from streamwater.

## **ACKNOWLEDGEMENTS**

This thesis could not have been produced without the help of many people. First I would like to thank my husband Richard and my family for their love, support and encouragement.

I would also like to thank my supervisor, Mike English and committee members Sherry Schiff and Mike Stone for their valuable suggestions throughout the production of this thesis.

For laboratory and field assistance I would like to thank Terry Amadio, Shauna Flanagan, Toby Gardner, Aaron Holmes, Steve Jackson, Kevin Maurice, Stephanie Monteith, Eric Michel, Jessica Mueller and Dave Woods, and the numerous undergraduate students who also spent time collecting samples at Strawberry Creek. I would especially like to thank Richard Elgood and Alex MacLean for laboratory and technical support.

Thanks are given to the Natural Sciences and Engineering Research Council of Canada (NSERC), the Ontario Graduate Scholarship program (OGS), and the Canadian Water Resources Association (CWRA) for their generous financial support throughout my graduate training. NOVARTIS is also thanked for financial assistance.

Finally, I would like to thank all those who provided encouragement and support along the way.



## **TABLE OF CONTENTS**

<u>Section</u>		<u>Page</u>
<b>1.0</b>	<b>Introduction and Literature Review</b>	<b>... 1</b>
1.1	Introduction	... 1
1.2	The current state of our understanding of patterns of nutrient export from agricultural systems	... 2
1.2.1	Long- and Short-term Temporal Variability in Nutrient Export Patterns	... 3
1.2.2	The Role of Drainage Tiles Within Various Watersheds	... 3
1.2.3	The Effects of Antecedent Hydrologic Conditions on Nutrient Export Patterns	... 4
1.2.4	Temporal Variability in the Effectiveness of Riparian Wetlands and/or Instream Processes	... 5
1.3	Specific Objectives of Thesis	... 6
1.4	Literature Review	... 8
1.4.1	Eutrophication and Human Health Risks: An Effect of Anthropogenic Additions of Nutrients to Agricultural Systems	... 8
1.4.2	Nutrient Cycling	... 9
1.4.2.1	The Phosphorus Cycle	... 9
1.4.2.2	The Nitrogen Cycle	... 12
1.4.3	Major Sources and Nutrient Pools in Agricultural Areas and Factors Influencing Availability	... 15
1.4.3.1	Phosphorus	... 16
1.4.3.2	Nitrate	... 17
1.4.4	Major Pathways of Nutrient Export in Agricultural Areas	... 18
1.4.4.1	Hydrological Pathways	... 18
1.4.4.2	Dominant Nutrient Pathways	... 22
1.4.5	Linkages Among Sources and Pathways: The Importance of Hydrology	... 25
1.4.6	Linking Nutrient Losses and Antecedent Hydrologic Conditions	... 26
1.4.7	Temporal Patterns in Hydrochemical Export	... 29
1.4.8	Nutrient Retention in Riparian Buffer Zones and Stream Sediments	... 30
1.4.9	Summary	... 34
<b>2.0</b>	<b>Site Description &amp; Methods</b>	<b>... 35</b>
2.1	Study Site	... 35
2.1.1	Land Use and Vegetation Cover	... 35
2.1.2	Surficial Geology and Topography	... 36
2.1.3	Climate	... 41
2.1.4	Drainage Characteristics/ General Hydrology	... 45
2.2	Methods	... 46
2.2.1	Hydrometric Variables	... 46
2.2.1.1	Intensively Monitored Tile	... 51
2.2.2	Water Chemistry	... 52
2.2.3	Data Analysis	... 56

<u>Section</u>	<u>Page</u>
2.2.3.1 Interpolation of Nutrient Concentrations in Stream Flow	... 56
2.2.3.2 Classification of Individual Events	... 57
<b>3.0 Temporal Patterns of Nutrient Export from a First-order Agricultural Basin in Southern Ontario</b>	<b>... 58</b>
3.1 Introduction	... 58
3.2 Site Description and Methods	
3.3 Results and Discussion	... 59
3.3.1 Inter-annual Comparison of Discharge and Nutrient Export Patterns	... 59
3.3.2 Seasonal Nutrient Export Patterns	... 64
3.3.3 Differences in Hydrochemical Export Between Events	... 65
3.3.4 Importance of Flowpaths to Nutrient Export	... 70
3.3.5 Importance of High-Magnitude Events in Annual Estimates	... 72
3.3.6 Importance of Sampling Frequency in Estimates of Nutrient Export	... 72
3.4 Conclusions	... 77
<b>4.0 Role of Drainage Tiles in Hydrochemical Export from a 1<sup>st</sup> Order Agricultural Catchment in Southern Ontario</b>	<b>... 79</b>
4.1 Introduction	... 79
4.2 Site Description and Methods	... 80
4.2.1 Diffuse Groundwater Flow	... 80
4.3 Results and Discussion	... 82
4.3.1 Hydrology: The Role of Drainage Tiles in Basin Discharge	... 82
4.3.1.1 Discharge from Tiles	... 82
4.3.1.2 Discharge from Diffuse Groundwater Sources	... 87
4.3.1.3 Empirical Relationships in Tile Discharge: Predicting the Annual Role of Tiles in Basin Discharge	... 94
4.3.2 The Role of Drainage Tiles in Basin Phosphate Export	... 96
4.3.2.1 Spatiotemporal Variability in Phosphate Concentrations in Tile Effluent	... 96
4.3.2.2 The Role of Tiles and Diffuse Groundwater Flow in Basin Phosphate Export	... 106
4.3.3 The Role of Drainage Tiles in Basin Nitrate Export	... 112
4.3.3.1 Spatiotemporal Variability in Nitrate Concentrations in Tile Effluent	... 112
4.3.3.2 The Role of Tiles and Diffuse Groundwater Flow in Basin Nitrate Export	... 115
4.4 The Contribution of Overland Flow to Basin Hydrochemical Export	... 119
4.5 Summary & Conclusions	... 120
<b>5.0 Influence of Antecedent Hydrologic Conditions on Patterns of Hydrochemical Export from a First-Order Agricultural Basin in Southern Ontario</b>	<b>... 122</b>
5.1 Introduction	... 122
5.2 Site Description and Methods	... 126

<u>Section</u>	<u>Page</u>
5.3	Results and Discussion ... 127
5.3.1	Hydrology ... 127
5.3.2	Nutrient Export ... 134
5.3.2.1	Individual Events ... 137
5.3.2.2	Summary of Individual Successive Events ... 159
5.3.2.3	Hysteresis Patterns ... 161
5.4	Summary & Conclusions ... 165
<b>6.0</b>	<b>Phosphate Retention in an Agricultural Stream Using Experimental Additions of Phosphate ... 166</b>
6.1	Introduction ... 166
6.2	Study Site and Methods ... 168
6.2.1	Characterization of Study Reaches ... 168
6.2.2	Experimental Approach ... 173
6.3	Results and Discussion ... 177
6.3.1	Environmental Conditions Prior to the SRP Addition Experiment Occasions ... 177
6.3.2	SRP Retention ... 178
6.3.3	Mechanisms of SRP Retention ... 184
6.4	Conclusions ... 187
<b>7.0</b>	<b>Summary and Major Conclusions of Thesis ... 189</b>
7.1	Long- and Short-term Temporal Variability in Nutrient Export Patterns ... 189
7.2	The Role of Drainage Tiles Within Various Watersheds ... 191
7.3	The Effects of Antecedent Hydrologic Conditions on Nutrient Export Patterns ... 193
7.4	Temporal Variability in the Effectiveness of Riparian Buffer Strips and/or Instream Processes ... 195
7.5	Summary of Major Processes Controlling Nutrient Export in the Strawberry Creek Watershed and Major Conclusions of Thesis ... 197
<b>8.0</b>	<b>References ... 202</b>

## LIST OF FIGURES

<u>Figure</u>		<u>Page</u>
	<b>Chapter Two</b>	
2.1	Map showing the Grand River Basin in Southern Ontario	... 37
2.2	Map of the Strawberry Creek Watershed. Catchment boundary, stream, residential buildings, woodlots, cultivated lands, and drainage tiles are shown in the figure.	... 38
2.3	Air Photo of Strawberry Creek. Type of fertilizer and crop grown for each field in the catchment are shown in the figure.	... 39
2.4	Total monthly precipitation (left y-axis) and air temperatures (right y-axis) in Southern Ontario. 1971-2000 30-year means for Waterloo-Wellington area are shown in (a). The error bars show one standard deviation for air temperature based on 30-year means. Precipitation and air temperature for 2000 and 2001 are shown in (b) and (c). The error bars in (b) and (c) show the maximum and minimum measured hourly air temperatures for each month during the study period.	... 43
2.5	Location of instruments in the Strawberry Creek Watershed.	... 48
2.6	Cross-section of the riparian zone at the continuously monitored (FR) site, facing the upstream direction. Locations of piezometers (black dots) and soil horizons are shown in the figure.	... 50
2.7	Diagram of V-notch weir box on continuously monitored drainage tile (FR tile).	... 53
2.8	Drainage tile network in the FR field. The header and feeder tiles in the FR field are shown in the inset.	... 54
	<b>Chapter Three</b>	
3.1	(a) Total daily precipitation and (b) daily mean hydrologic export for the 25-month study period.	... 60
3.2	(a) Hourly hydrologic export (left axis, grey line), and SRP (●) and TP (○) concentrations in stream water at the basin outflow. (b) Hourly hydrologic export and NO <sub>3</sub> <sup>-</sup> concentrations in stream water at the basin outflow.	... 62
3.3	Daily total mass export (kg ha <sup>-1</sup> d <sup>-1</sup> ) of (a) SRP, (b) TP and (c) NO <sub>3</sub> <sup>-</sup> for the study period	... 63

<u>Figure</u>		<u>Page</u>
3.4	Total export of (a) TP and (b) SRP and (c) $\text{NO}_3^-$ (the sum of kg $\text{ha}^{-1}$ over each entire event) are plotted against total hydrologic discharge (mm) throughout the duration of the storm (x axis). Winter storms are shown with dark circles and spring, summer, and fall storms are shown with white triangles. Storms that are of high magnitude in nutrient and hydrologic export are separated from all other storms with a line.	... 66
3.5	(a) Frequency histogram of daily basin discharge from the Strawberry Creek Watershed between 1996 and 2003, and (b) Basin discharge between 1996 and 2003. The three high magnitude events that occurred in 2000 and 2001 are marked with arrows in both graphs.	... 69
3.6	The effect of sampling frequency on the range of possible estimates of SRP export in December 2001, February 2001 and April 2001 are shown in (a), (b) and (c). The observed SRP export (based on 2-3 hour sampling intervals and a total of 20, 17 and 12 samples in a-c, respectively) are shown with a solid line. The ranges in possible estimates of SRP export based on fewer samples are shown by error bars. The right y-axis expresses the SRP export as a percentage of the observed SRP export during each event.	... 73
3.7	The effect of sampling frequency on the range of possible estimates of TP export in December 2001 and April 2001 are shown in (a) and (b). The observed TP export (based on 2-3 hour sampling intervals and a total of 20 and 12 collected samples in a and b, respectively) are shown with a solid line. The ranges in possible estimates of TP export based on fewer samples are shown by error bars. The right y-axis expresses the TP export as a percentage of the observed TP export during each event.	... 74
3.8	The effect of sampling frequency on the range of possible estimates of $\text{NO}_3^-$ export in December 2001, February 2001 and April 2001 are shown in (a), (b) and (c). The observed $\text{NO}_3^-$ export (based on 2-3 hour sampling intervals and a total of 20, 17 and 12 samples in a-c, respectively) are shown with a solid line. The ranges in possible estimates of $\text{NO}_3^-$ export based on fewer samples are shown by error bars. The right y-axis expresses the $\text{NO}_3^-$ export as a percentage of the observed $\text{NO}_3^-$ export during each event	... 75
 <b>Chapter Four</b>		
4.1	(a) Schematic Diagram of Calculations of Diffuse Groundwater Flow and Chemistry Along the FR Field. (b) A cross-section of the locations of piezometers in the riparian zone in the FR fields is shown.	... 83

<u>Figure</u>		<u>Page</u>
4.2	Precipitation (mm) and discharge at the basin outflow ( $L d^{-1}$ ) for the study period are shown in (a) and (b). Discharge from a continuously monitored drainage tile is shown in (c) and water table position beneath the ground surface near the basin outflow is shown in (d).	... 84
4.3	Contribution of Tiles to Basin Discharge Under Variable Flow Conditions. Dark circles indicate wet periods (regression equation corresponds to this data only). White squares and circles indicate transitional and dry periods, respectively.	... 86
4.4	The relative contribution of drainage tiles to streamflow throughout 3 selected events. The data in each of the three plots span a period of approximately one week.	... 88
4.5	The relationship between hourly water table position at the basin outflow and hourly discharge from the continuously monitored FR tile is shown in (a). The relationship between water table position at the basin outflow and cumulative discharge from all tiles in the basin is shown in (b).	... 89
4.6	Contribution of tiles and diffuse groundwater sources to basin discharge over a one year period. The stream hydrograph (line) and sampling periods (red dots) are shown in (a). The contribution of tiles (stacked bars) and streamflow at the outflow (black dots) are shown in (b). If black dots are above the bars, the difference between the dots and bars is water coming from diffuse sources.	... 92
4.7	Correlations (95% Confidence Interval) between the continuously monitored FR tile and instantaneous measurements of hydrologic discharge from 6 other tiles in the basin. Measured contribution of tiles is shown by black circles.	... 93
4.8	Contribution of Point sources to annual streamflow, predicted from the continuously monitored FR tile data. Total streamflow is shown by the solid line. The modelled contribution of all tiles in the basin is shown by the dashed line. The observed contribution of tiles to discharge is shown with black dots.	... 95
4.9	Tile Concentrations of SRP are shown against the basin hydrograph (solid line) illustrating seasonal and storm-related patterns in concentrations in tile effluent. The geometric mean concentration in seven tiles (solid circles) is shown in (a), and the observed range in concentrations (max and min) is shown by the error bars in (b).	... 97

<u>Figure</u>		<u>Page</u>
4.10	Tile Concentrations of TP are shown against the basin hydrograph (solid line) illustrating seasonal and storm-related patterns in concentrations in tile effluent. The geometric mean concentration in seven tiles (solid circles) is shown in (a), and the observed range in concentrations (max and min) is shown by the error bars in (b).	... 98
4.11	SRP export from FR tile during five successive rainstorms in April 2001. Precipitation is shown in (a), the FR tile hydrograph (solid line) and SRP concentrations (black dots) are shown in (b), and mass SRP export from the FR tile is shown in (c).	... 101
4.12	TP export from FR tile during five successive rainstorms in April 2001. Precipitation is shown in (a), the FR tile hydrograph (solid line) and TP concentrations (black dots) are shown in (b), and mass TP export from the FR tile is shown in (c).	... 102
4.13	Q-C relationship for SRP concentrations in effluent of 7 tiles in the basin are shown in (a) through (g).	... 107
4.14	Q-C relationship for TP concentrations in effluent of 7 tiles in the basin are shown in (a) through (g).	... 108
4.15	Contribution of tiles and diffuse groundwater sources to basin SRP export over a one year period. The stream hydrograph (line) and sampling periods (red dots) are shown in (a). SRP export from tiles (stacked bars) and in streamflow at the basin outflow (black dots) are shown in (b). If black dots are above the bars, the difference between the dots and bars is water coming from diffuse sources. If the dots are below the bars some retention is occurring in the stream.	... 109
4.16	Contribution of tiles and diffuse groundwater sources to basin TP export over a one year period. The stream hydrograph (line) and sampling periods (red dots) are shown in (a). TP export from tiles (stacked bars) and in streamflow at the basin outflow (black dots) are shown in (b). If black dots are above the bars, the difference between the dots and bars is water coming from diffuse sources. If the dots are below the bars some retention is occurring in the stream.	... 110
4.17	Tile Concentrations of NO <sub>3</sub> <sup>-</sup> shown against the basin hydrograph (solid line) illustrating seasonal and storm-related patterns in concentrations in tile effluent. The geometric mean concentration in 7 tiles (black dots) is shown in (a), and the observed range in concentrations (max and min) is shown by the error bars in (b).	... 113

<u>Figure</u>		<u>Page</u>
4.18	NO <sub>3</sub> <sup>-</sup> export from FR tile during three successive thunderstorms in April 2001. Precipitation is shown in (a), the FR tile hydrograph (solid line) and NO <sub>3</sub> <sup>-</sup> concentrations (black dots) are shown in (b), and mass NO <sub>3</sub> <sup>-</sup> export from the FR tile is shown in (c).	... 114
4.19	Q-C relationship for NO <sub>3</sub> <sup>-</sup> concentrations in effluent of 7 tiles in the basin are shown in (a) through (g).	... 116
4.20	Contribution of tiles and diffuse groundwater sources to basin NO <sub>3</sub> <sup>-</sup> export over a one year period. The stream hydrograph (line) and sampling periods (red dots) are shown in (a). NO <sub>3</sub> <sup>-</sup> export from tiles (stacked bars) and in streamflow at the basin outflow (black dots) are shown in (b). If black dots are above the bars, the difference between the dots and bars is water coming from diffuse sources. If the dots are below the bars some retention is occurring in the stream.	... 117
 <b>Chapter Five</b>		
5.1	Total nutrient losses (kg ha <sup>-1</sup> ) for each event for SRP (a), TP (b) and NO <sub>3</sub> <sup>-</sup> (c) are plotted against the total hydrologic inputs (precipitation = rainfall + snowmelt) to the basin for a given event	... 128
5.2	The total discharge for a given event is plotted against the total hydrologic inputs to the basin (precipitation, = rainfall + snowmelt) for that event.	... 129
5.3	Indicators of antecedent hydrologic conditions (AHC) in the basin are plotted against the ratio of total hydrologic outputs to total hydrologic inputs (Q/PPT) for 64 events. The various indicators of AHC are (a) pre-event streamflow (Q <sub>o</sub> ), Discharge lost over 2 weeks prior to the event onset (Q <sub>2wks</sub> ), and pre-event water table position (WT <sub>o</sub> ). The control of event 'magnitude' (total hydrologic inputs) on Q/PPT is shown in (d).	... 131
5.4	Influence of pre-event water table position at various locations in the basin on the ratio of total hydrologic outputs to total hydrologic inputs (Q/PPT) for 64 events. Pre-event water table position in the riparian zone at the basin outflow, in the riparian zone upstream from the basin outflow, and in a field upland from the stream are shown in (a), (b) and (c), respectively.	... 132



<u>Figure</u>		<u>Page</u>
5.5	Stepwise linear regressions showing the combined influences of the various indicators of AHC on the ratio of total hydrologic outputs to total hydrologic inputs (Q/PPT) for 64 events. $Q_o$ ( $L s^{-1}$ ), $WT_o$ in riparian zone upstream from basin outflow (m beneath soil surface), soil moisture at 25 cm (% saturation), and $Q_{2ks}$ (mm) are shown in the various plots.	... 135
5.6	Total hydrologic losses (discharge) from the basin for a given event are plotted against the total nutrient losses ( $kg ha^{-1}$ ) for each event for SRP (a), TP (b) and $NO_3^-$ (c).	... 136
5.7	Hydrologic and SRP export for a sequence of radiation melt days in March, 2001. Precipitation is shown in (a), stream discharge (solid line), discharge from one continuously monitored drainage tile (dashed line), and water table position (dotted line) are shown in (b), stream SRP concentration (dots) and mass output (bars) are shown in (c) and Q-SRP relationships are shown in (d). Melt 'days' are labelled (1-5) in (b) and (d).	... 139
5.8	Hydrologic and TP export for a sequence of radiation melt days in March, 2001. Precipitation is shown in (a), stream discharge (solid line), discharge from one continuously monitored drainage tile (dashed line), and water table position (dotted line) are shown in (b), stream TP concentration (dots) and mass output (bars) are shown in (c) and Q-TP relationships are shown in (d). Melt 'days' are labelled (1-5) in (b) and (d).	... 140
5.9	Hydrologic and $NO_3^-$ export for a sequence of radiation melt days in March, 2001. Precipitation is shown in (a), stream discharge (solid line), discharge from one continuously monitored drainage tile (dashed line), and water table position (dotted line) are shown in (b), stream $NO_3^-$ -N concentration (dots) and mass output (bars) are shown in (c) and Q- $NO_3^-$ -N relationships are shown in (d). Melt 'days' are labelled (1-5) in (b) and (d).	... 141
5.10	Hydrologic and SRP export for a sequence of rainstorms in April, 2001, following a prolonged wet period. Precipitation is shown in (a), stream discharge (solid line), discharge from one continuously monitored drainage tile (dashed line), and water table position (dotted line) are shown in (b), stream SRP concentration (dots) and mass output (bars) are shown in (c) and Q-SRP relationships are shown in (d). Individual storms are labelled (1-3) in (b) and (d).	... 142

<u>Figure</u>		<u>Page</u>
5.11	Hydrologic and TP export for a sequence of rainstorms in April, 2001, following a prolonged wet period. Precipitation is shown in (a), stream discharge (solid line), discharge from one continuously monitored drainage tile (dashed line), and water table position (dotted line) are shown in (b), stream TP concentration (dots) and mass output (bars) are shown in (c) and Q-TP relationships are shown in (d). Individual storms are labelled (1-3) in (b) and (d).	... 143
5.12	Hydrologic and NO <sub>3</sub> <sup>-</sup> export for a sequence of rainstorms in April, 2001, following a prolonged wet period. Precipitation is shown in (a), stream discharge (solid line), discharge from one continuously monitored drainage tile (dashed line), and water table position (dotted line) are shown in (b), stream NO <sub>3</sub> -N concentration (dots) and mass output (bars) are shown in (c) and Q- NO <sub>3</sub> -N relationships are shown in (d). Individual storms are labelled (1-3) in (b) and (d).	... 144
5.13	Hydrologic and SRP export for a sequence of rainstorms in October, 2001, following a prolonged dry period. Precipitation is shown in (a), stream discharge (solid line), discharge from one continuously monitored drainage tile (dashed line), and water table position (dotted line) are shown in (b), stream SRP concentration (dots) and mass output (bars) are shown in (c) and Q-SRP relationships are shown in (d). Individual storms are labelled (1-3) in (b) and (d).	... 145
5.14	5.14 Hydrologic and TP export for a sequence of rainstorms in October, 2001, following a prolonged dry period. Precipitation is shown in (a), stream discharge (solid line), discharge from one continuously monitored drainage tile (dashed line), and water table position (dotted line) are shown in (b), stream TP concentration (dots) and mass output (bars) are shown in (c) and Q-TP relationships are shown in (d). Individual storms are labelled (1-3) in (b) and (d).	... 146
5.15	Hydrologic and NO <sub>3</sub> <sup>-</sup> export for a sequence of rainstorms in October, 2001, following a prolonged dry period. Precipitation is shown in (a), stream discharge (solid line), discharge from one continuously monitored drainage tile (dashed line), and water table position (dotted line) are shown in (b), stream NO <sub>3</sub> -N concentration (dots) and mass output (bars) are shown in (c) and Q- NO <sub>3</sub> -N relationships are shown in (d). Individual storms are labelled (1-3) in (b) and (d).	... 147

<u>Figure</u>		<u>Page</u>
5.16	Hydrologic and SRP export for a rain-on-snow winter thaw event in December, 2001. Precipitation is shown in (a), stream discharge (solid line), discharge from one continuously monitored drainage tile (dashed line), and water table position (dotted line) are shown in (b), stream SRP concentration (dots) and mass output (bars) are shown in (c) and Q-SRP relationships are shown in (d).	... 148
5.17	Hydrologic and TP export for a rain-on-snow winter thaw event in December, 2001. Precipitation is shown in (a), stream discharge (solid line), discharge from one continuously monitored drainage tile (dashed line), and water table position (dotted line) are shown in (b), stream TP concentration (dots) and mass output (bars) are shown in (c) and Q-TP relationships are shown in (d).	... 149
5.18	Hydrologic and NO <sub>3</sub> <sup>-</sup> export for a rain-on-snow winter thaw event in December, 2001. Precipitation is shown in (a), stream discharge (solid line), discharge from one continuously monitored drainage tile (dashed line), and water table position (dotted line) are shown in (b), stream NO <sub>3</sub> -N concentration (dots) and mass output (bars) are shown in (c) and Q- NO <sub>3</sub> -N relationships are shown in (d).	... 150
5.19	Summary of 30 selected events. Sequences of successive events are divided by the solid vertical lines. Total precipitation (hydrologic inputs, sum of rainfall and snowmelt) for each event is shown in (a). Q/PPT is shown in (b). Nutrient export 'efficiency' (N <sub>EFF</sub> ) for SRP, TP and NO <sub>3</sub> -N are shown in (c-e). N <sub>EFF</sub> is the mass of nutrients exported per mm of discharge. Initial water table position (W <sub>o</sub> ) (black dots) and peak water table position (W <sub>peak</sub> ) (white dots) are shown in (f). Arrows indicate a rising or declining trend in the various variables.	... 160
5.20	Summary of prevalent forms of hysteresis loops observed in Q-C plots for various events throughout the study period	... 163
<b>Chapter Six</b>		
6.1	Morphological characteristics of experimental Site 1. Water and streambed surfaces (m.a.s.l.) are shown in (a), and streambed coverage is shown in (b). Locations of the point source addition of SRP, and sampling points <i>a</i> through <i>e</i> are shown in (a).	... 171
6.2	Morphological characteristics of experimental Site 2. Water and streambed surfaces (m.a.s.l.) are shown in (a), and streambed coverage is shown in (b). Locations of the point source addition of SRP, and sampling points <i>a</i> through <i>e</i> are shown in (a).	... 172

<u>Figure</u>		<u>Page</u>
6.3	Morphological characteristics of experimental Site 3. Water and streambed surfaces (m.a.s.l.) for June and October are shown in (a) and (b), and streambed coverage for June and October are shown in (c) and (d). Locations of the point source addition of SRP, and sampling points <i>a</i> through <i>e</i> are shown in (a).	... 173
6.4	Difference between expected SRP concentration and observed SRP concentrations downstream from point source addition of $K_2HPO_4$ in June. Observations 35 minutes (circles), 45 minutes (squares), and 55 minutes (triangles) after the beginning of the additions are shown. Data for 35 minutes is missing from Site 1 as the SRP plume had not passed the lower sections of the reach by 35 minutes into the experiment. SRP concentrations at Sites 1, 2 and 3 were elevated to 697, 2121, and $1134 \mu g L^{-1}$ , respectively (shown in brackets in each graph). Analytical error calculated from replicate analysis of samples is shown by error bars.	... 180
6.5	Difference between expected SRP concentration and observed SRP concentrations downstream from point source addition of $K_2HPO_4$ in October. Observations 35 minutes (dark circles), 45 minutes (dark squares), and 55 minutes (dark triangles) after the beginning of the additions are shown. Data is missing from Site 1 as the SRP plume did not pass into the lower sections of Site 1 at all during the 55-minute experiment in October. However, the plume was caught at the outflow (30 m downstream of Site 1) by the automated sampler 30 minutes later. SRP concentrations observed at the catchment outflow are shown for Site 1 (white symbols). SRP concentrations at Sites 1, 2 and 3 were elevated to 2897, 4225, and $3308 \mu g L^{-1}$ , respectively. Analytical error calculated from replicate analysis of samples is shown by error bars.	... 181
6.6	TSS (squares) (left y-axis) and PP (right y-axis) at sampling points along the three stream reaches during the June experiment. [PP] prior to and during the $K_2HPO_4$ additions are shown with diamonds and triangles, respectively. Error bars on the elevated PP symbols (triangles) show one standard deviation of the range of PP values observed at 35, 45 and 55 minutes at each location throughout the experiments.	... 185

<u>Figure</u>		<u>Page</u>
6.7	TSS (squares) (left y-axis) and PP (right y-axis) at sampling points along the three stream reaches during the October experiment. [PP] prior to and during the $K_2HPO_4$ additions are shown with diamonds and triangles, respectively. Error bars on the elevated PP symbols (triangles) show one standard deviation of the range of PP values observed at 35, 45 and 55 minutes at each location throughout the experiments.	... 186
6.8	TP (white circles) and SRP (black circles) observed at the catchment outflow prior to, during and following the October additions of $K_2HPO_4$ .	... 188
 <b>Chapter Seven</b>		
7.1	Conceptual Diagram of Major Sources, Pathways and Fate of Phosphate in the Study Basin	... 198
7.2	Conceptual Diagram of Major Sources, Pathways and Fate of Nitrate in the Study Basin	... 199

## LIST OF TABLES

<u>Table</u>	<u>Page</u>
<b>Chapter Three</b>	
3.1	Annual Nutrient Export from Strawberry Creek. Total nutrient export for each study year and the 25-month study period are presented. This number is expressed as the percentage (%) contribution of these events to total annual export in brackets. The number of events contributing to this value is shown in italics on the right hand side outside of the brackets. Nutrient contributions during baseflow periods and events are shown, and events are also sub-divided into ‘extreme’ and ‘normal’ events. ... 64
<b>Chapter Four</b>	
4.1	Estimates of groundwater discharge to the stream based on Darcy’s Law and the measured range of hydraulic gradients ( $dh/dx$ ) and measured hydraulic conductivities ( $K_{HS}$ ). Groundwater gained per metre of stream length (GW/m) and total groundwater gained along the entire stream reach ( $\Sigma GW_{Reach}$ ) are also shown. ... 91
4.2	Pearson Correlation ( $r$ ) of various tiles in the study basin. The FR tile was continuously monitored, whereas other tiles were monitored with spot samplings during all seasons, and during wet, dry, storm and snowmelt periods. ... 94
4.3	Average, standard deviation and range in nutrient concentrations for tiles in the study basin over the study period. Land use and fertilizer type are also shown in the table. ... 100
4.4	Changes in Hydrologic Storage in the FR Field During Successive Rainstorms. Available storage ( $S_A$ ) is calculated from Measured soil moisture ( $\theta_v$ ) and a measured porosity of 0.5. Rainfall prior to the tile response ( $PPT_{resp}$ ), the total rainfall throughout the event ( $\Sigma PPT$ ), the total tile discharge throughout the event ( $\Sigma Q_{tile}$ ), and storage in the fields throughout the event ( $S_F$ ) are also shown. ... 104
4.5	Comparison of P Mass Export from Diffuse Groundwater Sources and Drainage Tiles in the FR Cultivated Fields. Discharge, ( $Q$ ) ( $L s^{-1}$ ), P concentrations, [ $P$ ] ( $\mu g L^{-1}$ ), and the calculated mass of P, $\Sigma P$ ( $\mu g s^{-1}$ ) are shown at upstream (1) and downstream (2) locations along the reach and in the FR tile to calculate the observed change in P mass along the reach, $Obs\Delta P$ ( $\mu g s^{-1}$ ). This is compared to the estimated flux of groundwater, $Pred\Delta P$ ( $\mu g s^{-1}$ ) to calculate P retention, $R$ . ... 111

<u>Table</u>		<u>Page</u>
4.6	Comparison of $\text{NO}_3^-$ Mass Export from Diffuse Groundwater Sources and Drainage Tiles in the FR Cultivated Fields. Discharge ( $Q$ ), ( $\text{L s}^{-1}$ ), $\text{NO}_3^-$ concentrations, $[N]$ ( $\text{mg N L}^{-1}$ ), and the calculated mass of N, $\Sigma N$ ( $\text{mg N s}^{-1}$ ) are shown at upstream (1) and downstream (2) locations along the reach and in the FR tile to calculate the observed change in $\text{NO}_3^-$ mass along the reach, $\text{Obs}\Delta N$ ( $\text{mg N s}^{-1}$ ). This is compared to the estimated flux of groundwater, $\text{Pred}\Delta N$ ( $\text{mg N s}^{-1}$ ) to calculate $\text{NO}_3^-$ attenuation, $R$ .	... 118
 <b>Chapter Five</b>		
5.1	Proportion of Precipitation Discharged from Basin During Successive Storms	... 137
5.2	Comparison of Variability in the Magnitude of Nutrient Export During Events with Similar Discharge	... 138
 <b>Chapter Six</b>		
6.1	SRP Retention Rates Along Three Experimental Reaches for Two Experiments. All units are in $\mu\text{g m}^{-2} \text{s}^{-1}$ . Retention rates between each of the sampling points ( $a$ through $e$ ) were calculated from the mean retention for the 35, 45 and 55 minutes sampling intervals.	... 182

## **1.0 Introduction & Literature Review**

### **1.1 Introduction**

The transfer of nutrients from terrestrial to aquatic systems is of global concern due to its impact on human health risks (nitrate) and the eutrophication of water bodies (phosphate, nitrate). The scientific community and International governing bodies (*e.g.* UN, UNESCO) have identified the need to better understand nutrient dynamics in natural and disturbed systems. From a management perspective, it is important to quantify present day nutrient export patterns from agricultural systems in order to make predictions regarding the effect of land use change and best management practices on future export patterns (PLUARG, 1978; IJC, 2000). The goal of reduced nutrient loading has been attempted using management practices such as conservation tillage in agricultural regions, and the use of riparian or buffer zones in both agricultural and urban areas. Although such measures have been shown to reduce nutrient export in some agricultural catchments, runoff from agricultural areas still contributes large quantities of nutrients to surface waters (Carpenter *et al.*, 1998).

The goal of this thesis is to improve our understanding of nutrient transport in agricultural systems. Several gaps exist within our current understanding of nutrient export patterns from agricultural systems. These gaps form the basis of this thesis. Specific areas where the current scientific understanding of nutrient dynamics is lacking are identified and summarized below. Research questions pertaining to these areas are posed and the specific objectives of the thesis are stated. This is followed by a general review of the current understanding of nutrient dynamics in agricultural systems and where gaps exist within this understanding. A more specific review of the literature as it



pertains to each chapter is given at the beginning of each of the four major chapters in this thesis.

## **1.2 The current state of our understanding of patterns of nutrient export from agricultural systems**

Substantial progress has been made over the past several decades in advancing the understanding of the major processes controlling nutrient export from agricultural catchments but significant gaps are still present in our understanding. There is still an inability to adequately quantify and predict patterns of nutrient cycling and nutrient export from agricultural watersheds and explain their spatial and temporal variability.

Soil characteristics, nutrient availability and hydrologic flowpaths are important factors controlling nutrient export from agricultural systems but a complete understanding of how these variables interact is lacking. The current state of research in this area is focused on the characterization of *when* and *how* hydrologic flowpaths, nutrient pools and soil characteristics interact.

Some specific gaps in the current scientific understanding of nutrient export from agricultural systems include (1) long- and short-term temporal variability in nutrient export patterns; (2) the role of drainage tiles within various watersheds; (3) the effects of antecedent hydrologic conditions (AHC) on nutrient export patterns and (4) temporal variability in the effectiveness of riparian wetlands and/or instream processes. These gaps are summarized below and discussed in more detail in the literature review that follows.

### ***1.2.1 Long- and Short-term Temporal Variability in Nutrient Export Patterns***

Temporal variability in nutrient export patterns is poorly understood because of data limitations related to the frequency with which storm events are often sampled. Annual estimates of nutrient export are often extrapolated from small data sets that may exclude sampling during certain times of the year (B. Metcalfe, Pers. Comm., 2003). Moreover, estimates may be generated from inadequate sampling frequencies during individual events. Few studies have employed an extensive monitoring programme that includes intensive high resolution sampling during storms and melt periods. Furthermore, a substantial portion of the scientific understanding of nutrient cycling and export patterns has been developed in different geographic locations (e.g. southern U.S.A. and Europe) where climate and soils differ substantially from Southern Ontario.

Specific research questions on this topic addressed in this thesis examine the distribution and range in magnitude of storms throughout all seasons in a first order agricultural catchment in Southern Ontario and the importance of individual events to annual export. It is hypothesized that the bulk of nutrients are lost during storms and thaw events and that specific high magnitude events account for a substantial proportion of annual nutrient export.

### ***1.2.2 The Role of Drainage Tiles Within Various Watersheds***

The contribution of drainage tiles to hydrochemical export within and among various watersheds differs and there is still controversy over the relative importance of drainage tiles in nutrient export (Dils and Heathwaite, 1999). It has been suggested by some researchers that tiles reduce nutrient export by lowering the water table and

preventing overland flow (Sims *et al.*, 1998), whereas others suggest that tiles are ‘conduits’ for nutrients (e.g. Stamm *et al.*, 1998; Dils and Heathwaite, 1999) and allow them to bypass soils and hinder natural soil processes.

Specific research questions on this topic addressed in this thesis revolve around temporal variability in nutrient export in tile effluent and the overall role of tiles in annual basin export. It is hypothesized that a substantial portion of nutrients is delivered to the stream by drainage tiles rather than diffuse groundwater sources. It is also hypothesized that tiles will exhibit variability throughout events as a result of changing flowpaths.

### ***1.2.3 The Effects of Antecedent Hydrologic Conditions on Nutrient Export Patterns***

The effects of antecedent hydrologic conditions (AHC) on nutrient export patterns are also poorly understood by the scientific community. AHC affect the storage capacity within a basin (e.g. Dingman, 2002) as well as how easily water can pass through soils, which affects hydrochemical flowpaths. Although AHC are referred to extensively in the literature, scientists have yet to be able to adequately quantify their effects on nutrient export patterns.

Specific research questions investigated within this thesis concern linkages between temporal variability in discharge and nutrient export and AHC. It is hypothesized that a greater portion of precipitation will pass through the basin and be discharged as AHC become wetter in the basin. It is also hypothesized that both P and  $\text{NO}_3^-$  are affected by AHC, but they respond in different manners. For example, high quantities of P may be exported through macropores following dry periods, or, high quantities of P may be exported along with overland flow during very wet periods.  $\text{NO}_3^-$

export is expected to increase under wetter conditions due to the interaction of runoff with  $\text{NO}_3^-$  pools in higher soil horizons.

#### ***1.2.4 Temporal Variability in the Effectiveness of Riparian Wetlands and/or Instream Processes***

Temporal variability in nutrient dynamics related to stream riparian buffers and/or instream processes is an area that has been examined by few researchers. Studies are typically conducted during low flow conditions in summer and do not account for high flow periods or the winter months. Although stream riparian buffers and in-stream sediments play a role in the reduction of nutrients in runoff during low summer flows, they are less effective during periods of high runoff (Karr and Schlosser, 1978).

Although temporal variability in nutrient retention in riparian areas is poorly understood and represents a gap in our understanding of nutrient dynamics, it is not considered in this thesis. This is an area where future research is necessary. In-stream processes of nutrient retention represent another gap in our understanding, and are considered in this thesis. Sediments are thought to be an important mechanism by which phosphate is retained in streams (e.g. McCallister and Logan, 1978) but how this changes under different flow conditions is poorly understood. A few studies have observed rare occasions where pulses of soluble reactive phosphorus (SRP) may occur following irrigation or the application of manure (e.g. Stone and Krishnappan, 2003; Dean and Foran, 1992; Cook and Baker, 1998; Geohring *et al.*, 1998; Sims *et al.*, 1998). Stamm *et al.* (1998) suggested that such pulses were a result of SRP transport through macropores into tile drains. Specific research questions addressed in this thesis involve the ability of in-stream sediments to retain pulses of SRP under low flow conditions. It is hypothesized

that in-stream sediments will effectively attenuate large pulses of SRP at low flows through sorption processes.

### **1.3 Specific Objectives of Thesis**

The goal of this thesis is to improve our understanding of patterns of hydrochemical export from a first-order agricultural basin in Southern Ontario. The study approach is to examine temporal patterns of nutrient export and use these patterns to understand the physical processes governing temporal variability in nutrient export. This is accomplished by intensively monitoring hydrochemical export and nutrient dynamics within the study basin. Few studies have undertaken such an intensive monitoring programme.

Several gaps have been identified and specific research questions and hypotheses regarding these questions have been stated (Section 1.2). The approach of this thesis is to address some aspect of each of the four gaps that have been identified to obtain a more complete understanding of nutrient dynamics in agricultural systems. These are examined in the following four chapters:

Chapter Three: “Temporal Patterns of Nutrient Export from a First-order Agricultural Basin in Southern Ontario”

This chapter intensively examines temporal variability in discharge and nutrient export patterns from the study basin. The specific objectives of this chapter are (1) to quantify annual SRP, total phosphorus (TP) and nitrate ( $\text{NO}_3^-$ ) export (2 years) from a first order agricultural basin in Southern Ontario; (2) to examine temporal variability in nutrient export, especially the significance of the snowmelt period and high magnitude

events in annual nutrient export; (3) to quantify the potential error associated with missing one or more high magnitude events; and (4) to examine the importance of sampling frequency in generating estimates of export rates during storm events.

#### Chapter Four: “Role of Drainage Tiles in Hydrochemical Export from a 1<sup>st</sup> Order Agricultural Catchment in Southern Ontario”

This chapter illustrates the importance of drainage tiles in annual hydrochemical export from a first order agricultural basin in Southern Ontario. The specific objectives of the chapter are (1) To quantify the proportion of basin discharge that comes from point (tiles) and non-point (primarily diffuse groundwater) sources and demonstrate temporal variability in these sources over a one year period; and (2) To demonstrate the importance of drainage tiles in SRP, TP, NO<sub>3</sub><sup>-</sup> export from the basin.

#### Chapter Five, “Influence of Antecedent Hydrologic Conditions on Patterns of Hydrochemical Export from a First-Order Agricultural Basin in Southern Ontario”

The goal of this chapter is to relate hydrochemical export patterns and AHC in a first-order agricultural basin in Southern Ontario. The specific objectives of this chapter are (1) to show linkages between AHC in the basin and the proportion of hydrologic inputs (rainfall, snowmelt) that are lost via discharge; (2) to show linkages between AHC in the basin and the export of SRP, TP and NO<sub>3</sub><sup>-</sup> in streamflow; and (3) to describe prevalent types of hysteresis loops that are found in storms in the study basin and link these to AHC.

## Chapter Six, “Phosphate Retention in an Agricultural Stream Using Experimental Additions of Phosphate

This chapter examines the SRP retention potential of an agricultural stream under highly elevated SRP concentrations at low flows. Various concentrations of SRP were added to the stream to simulate elevated SRP concentrations found in streams receiving effluent from upland areas. The specific objectives of the study are: (1) to determine SRP retention rates when SRP concentrations in the stream are highly elevated during low flow periods; (2) to examine whether retention rates vary spatially among areas having different physical characteristics such as horizontal gradient, groundwater flux direction, bathymetry, and vegetative cover; and (3) to examine the effects of dredging the stream bottom on the ability of the stream to retain SRP.

### 1.4 Literature Review

#### *1.4.1 Eutrophication and Human Health Risks: An Effect of Anthropogenic Additions of Nutrients to Agricultural Systems*

The application of fertilizers to agroecosystems has led to the eutrophication of surface waters in many areas of the world (Carpenter *et al.*, 1998). High levels of nitrate ( $\text{NO}_3^-$ ) in drinking water have been associated with human health risks (Goss *et al.*, 1998). Eutrophication involves accelerated biological productivity in aquatic systems. In particular, massive algal blooms in surface waters result from high levels of nitrogen (N) and phosphorus (P) loading from atmospheric and terrestrial sources. Eutrophication reduces oxygen levels, and causes fish kills, unpalatability of drinking water, odour and aesthetic problems (Daniel *et al.*, 1998).

$\text{NO}_3^-$  is a potential human health threat especially to infants, causing the condition known as methemoglobinemia, also called "blue baby syndrome". Unlike  $\text{NO}_3^-$ , P is not directly toxic to humans (Daniel *et al.*, 1998). However, the reduction of P loading has been focused on for several reasons. First, P cycling does not involve a gaseous flux between water and the atmosphere like N and C, and may therefore be easier to control. Secondly, P is considered to be the limiting nutrient in freshwater bodies (Schindler, 1977).

## ***1.4.2 Nutrient Cycling***

### **1.4.2.1 The Phosphorus Cycle**

P cycling in nature is unique from the cycles of other major nutrients because it is not found in a gaseous form and is almost always present in the +5 (oxidized) valence state as orthophosphate ( $\text{PO}_4^{3-}$ ) (Jahnke, 1992). P is found in both organic and inorganic forms, and may be present as particulate or dissolved material (Jahnke, 1992). The forms of P in aquatic systems are generally classified as either dissolved (soluble) or particulate P (PP). The soluble fraction can be subdivided into soluble reactive P (SRP) (which is considered to be biologically available) and soluble unreactive P (SUP) (Henderson-Sellers & Markland, 1987). The forms of P in soils and/or aquatic sediments are often classified based on a series of sequential chemical extractions, and are therefore operationally defined. Stone (1993) provides a review of the approaches used to characterize the forms of P in sediments.

The primary natural source of P is apatite, a calcareous mineral. P is liberated from apatite via physical and chemical weathering processes in terrestrial landscapes (Jahnke,



1992). Secondary sources of P external to a watershed include deposition from the atmosphere and the addition of P from anthropogenic sources such as the addition of fertilizer to agricultural fields. Internal sources of P include desorption from soils, the erosion of PP, the dissolution of minerals or leaching from plants. P sinks in terrestrial and/or aquatic environments include uptake by plants and other biota, the deposition of particulate P onto soils or sediments, adsorption by soils or sediments and precipitation as phosphate minerals. Soils and plants are both capable of acting as P sources and sinks. In terrestrial and aquatic systems, P may participate in two general types of biogeochemical processes: physico-chemical reactions with soils, and biological cycles.

#### Physico-chemical Reactions

Inorganic exchanges of P with soil / sediment particles have been widely described (e.g. Barrow, 1978; Parfitt, 1978; Syers *et al.*, 1973). Two reactions are described in the literature: adsorption-desorption reactions and precipitation-dissolution reactions.

##### (a) Adsorption – Desorption Reactions

Adsorption involves P being held by the surfaces of particles, and therefore its removal from solution. Adsorption is higher with metal oxygen hydroxides and affected by grain size, pH, redox conditions and organic matter (Syers *et al.*, 1973; Patrick and Khalid, 1974; Meyer, 1979; Hill, 1982; Klotz, 1985; Stone and Mudroch, 1989; Stone and English, 1993). Desorption involves the release of P from particles into solution. The rates of adsorption-desorption of P between particles and solution are quantified using sorption isotherms (e.g. Langmuir, Freundlich). These equations predict sorption reasonably well within limited ranges.

### (b) Precipitation – Dissolution Reactions

When ions in solution such as  $\text{Al}^{3+}$ ,  $\text{Fe}^{3+}$  and  $\text{Ca}^{2+}$  combine with phosphate ions, sparingly soluble minerals form and precipitate out of solution (Holtan *et al.*, 1988; Miller & Donahue, 1990). In calcareous soils, the formation of calcium phosphates occurs, whereas in acidic or non-calcareous soils, aluminum and ferric phosphates tend to form (Foth and Ellis, 1997).

### Biological Cycles

P is an essential nutrient required by all living organisms, and therefore plays an integral role in biogeochemical cycles. P is found in DNA, RNA and ATP (Jahnke, 1992) and is important in cell genetics as well as the storage, transfer and release of energy in living organisms (Troeh & Thompson, 1993). Terrestrial plants obtain dissolved inorganic P from solution (Troeh, & Thompson, 1993), and subsequently convert it to organic compounds in their bodies as phosphate ester bonds (Jahnke, 1992; Smeck, 1985). Heterotrophic organisms consume P in organic and inorganic forms from the bodies of primary producers (Villem *et al.*, 1989). When the plants or organisms die, organic P is released in both particulate and dissolved forms. The organic compounds are decomposed by microbial and bacterial organisms (heterotrophs) and inorganic phosphates are subsequently released (Kucey, 1983; Smeck, 1985) or retained as refractory compounds in the soils or sediments (Gachter and Meyer, 1993; Smeck, 1985). It is thought that much of the organic P in soil originates from microbial synthesis rather than the accumulation of plant or animal residues (Smeck, 1985). The microbial solubilization of “unavailable” forms of P in soil is important in biological cycles, as

more phosphate is taken up by plants than is supplied by simple desorption or dissolution of phosphate minerals alone (Kucey, 1983).

While plants and other biota are considered as potential sources and sinks, they are transient in their ability to retain or release P (e.g. Reddy *et al.*, 1999). Organisms are subject to life cycles that involve the uptake of P for growth and its subsequent release upon death, which can be seasonally dependant.

#### 1.4.2.2 The Nitrogen Cycle

The biological N cycle begins with N gas ( $N_2$ ) in the atmosphere. This gas, though it occupies 78% of the atmosphere by volume (Henderson-Sellers & Markland, 1987), cannot be utilized by most organisms and is therefore not biologically available. Some organisms, however, are capable of utilizing  $N_2$  gas. These organisms, termed the *nitrogen fixers*, take in the  $N_2$  gas and convert it into biologically available forms. Other organisms then obtain N by either consuming the nitrogen fixers, or by ingesting the various forms of N they produce. If conditions are anaerobic, *fixed* N can be converted back to  $N_2$  gas (denitrification) and subsequently returned to the atmosphere, thereby completing the N cycle. These processes are described in more detail below.

#### Nitrogen Fixation

N fixation is a process where  $N_2$  in the atmosphere reacts to form any N compound (Jaffe, 1992). Biological N fixation is a process whereby organisms convert  $N_2$  gas into biologically available forms by combining the  $N_2$  gas with hydrogen, carbon (C) and oxygen, creating proteins and other essential organic compounds (Berner &

Berner, 1996; Jaffe, 1992). In biological fixation, ammonia ( $\text{NH}_3$ ), a substance that is available for use in amino acid structures, is generated (Henderson-Sellers & Markland, 1987). Two forms of ammonia may occur:  $\text{NH}_3$  and  $\text{NH}_4^+$  (ammonium), with the latter simply being the ionic form of the former, resulting from ammonia hydrolysis.



Once created, this ammonia or ammonium is either *assimilated* by organisms, or is oxidized into other available forms by the *nitrification* process (Henderson-Sellers & Markland, 1987).

In terrestrial systems, the major N fixers are legumes and lichens (Berner & Berner, 1996). Examples of legumes include clover, soybeans and chickpeas (Jaffe, 1992). These plants are often used in agriculture to replenish soil N (Jaffe, 1992). The N fixers in surface water bodies are microorganisms such as bacteria and blue-green algae, who possess the enzyme nitrogenase (Vymazal, 1995).

#### Ammonification/Mineralization

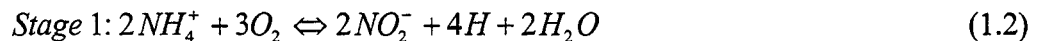
During the process of N mineralization, organic N from decaying plant and animal residues (proteins, nucleic acids, amino sugars, urea) is converted to ammonia ( $\text{NH}_3$ ) and ammonium ( $\text{NH}_4^+$ ). The resultant ammonia can be converted back to organic N (immobilization) where it can be taken up by microbes and plants (assimilated) or nitrified to  $\text{NO}_3^-$ . Once N has been fixed in soils as either  $\text{NH}_3$  or  $\text{NH}_4^+$ , it is subject to either ammonia assimilation or nitrification.

### Ammonia Assimilation

Ammonia assimilation is the process by which ammonia is taken up by organisms and incorporated into their biomass as organic N compounds (Jaffe, 1992).

### Nitrification

Nitrification, which results from bacterial metabolism, is a two-stage process. In the first stage of nitrification, fixed ammonia is oxidized by the bacteria *Nitrosomonas*, generating nitrite ( $\text{NO}_2^-$ ). This  $\text{NO}_2^-$  is subsequently oxidized by the bacteria *Nitrobacter*, creating  $\text{NO}_3^-$ .  $\text{NO}_3^-$ , the most highly reactive form of N, is easily dissolved, and is therefore biologically available (Henderson-Sellers & Markland, 1987). The two reactions are summarized by the following equations.



The two stages can be combined into the following equation.



$\text{NO}_3^-$  in soils has two major fates: (1) it may act as an electron acceptor under anaerobic conditions (denitrification); or (2) it may be assimilated and reduced into an organism's biomass (assimilatory  $\text{NO}_3^-$  reduction) (Jaffe, 1992). Alternatively,  $\text{NO}_3^-$  may be removed by leaching and erosional losses.

### Denitrification

When conditions are anaerobic, bacteria reduce  $\text{NO}_2^-$  and  $\text{NO}_3^-$  to form  $\text{N}_2$  gas or nitrous oxide ( $\text{N}_2\text{O}$ ), thereby returning them to the atmosphere (Jaffe, 1992).



In agricultural systems, denitrification typically occurs in riparian wetlands and in the hyporeic zone of streams as these conditions are anaerobic. This is the only process in the biological N cycle where the major end-product is removed from the internal biological N cycle (Jaffe, 1992). As such, denitrification is the principal means of balancing inputs from biological N fixation (Jaffe, 1992). However, the increased use of N fertilizers has increased levels of denitrification in agricultural systems, and is thought to be responsible for contributing large quantities of N<sub>2</sub>O to the atmosphere (Jaffe, 1992).

#### ***1.4.3 Major Sources and Nutrient Pools in Agricultural Areas and Factors Influencing Availability***

The major sources of nutrients in agricultural areas are fertilizers and manure. Phosphoric acid, anhydrous ammonia, urea and ammonium NO<sub>3</sub><sup>-</sup> are important compounds used in fertilizers (McDowell *et al.*, 2001; Steinheimer *et al.*, 1998) and some fertilizers are composed of a mixture of N, P and potassium (K). NO<sub>3</sub><sup>-</sup> is more of a limiting nutrient to terrestrial plant growth than P and manure applications have historically been based on crop N requirements (McDowell *et al.*, 2001).

In the case of both P and N, fertilizers and manure are applied at far greater rates than is needed for optimum crop growth. As a result, there has been a build up of these nutrients in soils over time, which is susceptible to removal in runoff. Agricultural areas often receive between 10 and 100 kg ha<sup>-1</sup> yr<sup>-1</sup> of P in the form of fertilizers (e.g. Sharpley, 1985b; Sharpley *et al.*, 1981). N is often applied in the form of fertilizers at a rate of 30 - 60 kg ha<sup>-1</sup> yr<sup>-1</sup> (Haag and Kaupenjohann, 2001; Sharpley *et al.*, 1983).

In watersheds that are not impacted by agriculture, nutrient deposition from the atmosphere has been identified as a major source of nutrients (e.g. Stoddard, 1994). However, these inputs are smaller than fertilizer inputs. For example, gains of N through atmospheric deposition average approximately  $1 \text{ kg N ha}^{-1} \text{ yr}^{-1}$  over the United States, but are  $10 \text{ kg N ha}^{-1} \text{ yr}^{-1}$  in the Great Lakes region (Wetzel, 1983). P concentrations in rainfall and particulate material fallout vary but tend to be less than concentrations of N (Wetzel, 1983).

#### 1.4.3.1 Phosphorus

The availability of PP for transport in runoff is primarily a function of soil properties, slope characteristics and rainfall intensity and duration. The ability of soils to release SRP into solution is largely affected by the type of inputs (i.e. fertilizers or manure), soil type (i.e. clay vs sand vs organic soils), soil management practices (i.e. till or no-till) (McDowell *et al.*, 2001) and soil moisture characteristics. As soil P concentrations increase, the potential for the transfer of SRP from soil to solution also increases (McDowell *et al.*, 2001). Larger losses of SRP have been observed in areas where manure is applied, particularly when rainstorms follow manure or fertilizer application (Burwell *et al.*, 1975; Haygarth, 1997), although these losses decrease as the interval between application and storms increases because SRP is bound to surface soils through sorption.

Fine grained particles have the highest capacity to sorb SRP (Stone and Mudroch, 1989), while organic soils tend to release SRP because organic colloids block P sorption sites (Dils and Heathwaite, 1999). Soil characteristics that influence SRP solubility

include pH, concentrations of aluminum, iron, calcium and magnesium, surface area and soil moisture content (McDowell *et al.*, 2001). Once SRP in the soil solution is lost via plant uptake or runoff, it is replenished by the solid soil phase (McDowell *et al.*, 2001). This is controlled by equilibria exchange between the soil adsorption system, soil solution and precipitated P compounds (McDowell *et al.*, 2001; Sample *et al.*, 1980). The 'availability' of easily desorbable P can also change temporally due to the seasonal drying of soils (Pote *et al.*, 1998).

#### 1.4.3.2 Nitrate

$\text{NO}_3^-$ , the predominant form of inorganic N in aerobic agricultural soils, is soluble in water and highly mobile in runoff. In terrestrial systems, N is often translocated as  $\text{NO}_3^-$ , which is subject to mass flow and leaching. The available  $\text{NO}_3^-$  pool in soils is a result of the balance between the various parts of the  $\text{NO}_3^-$  cycle that produce or consume  $\text{NO}_3^-$ . The critical factors that have been shown to control N in agricultural systems include (1) the state of ecosystem maturation (age); (2) the in situ decomposition rate (microbial status, soil fertility, moisture regime; (3) C- and N- limitation status; (4) the physical and chemical soil characteristics; and (5) the availability of moisture (Cirimo & McDonnell, 1997).

The rate of N mineralization is affected by soil depth, the quality of the substrate (i.e. N and C) (Updegraff *et al.*, 1995), temperature and redox conditions. Denitrification can only occur in saturated anoxic conditions but may also be limited by acidity, C and phosphate availability, soil morphology, and temperature (Cirimo & McDonnell, 1997; Haag and Kaupenjohann, 2001). Denitrification is minor in upland areas, except under



saturated conditions (*i.e.* following snowmelt), but can be very important in riparian wetlands in the near-stream zone (Cirimo & McDonnell, 1997; Hill, 1996). The size of the potential mineralizable pool of N in saturated near stream zones can be very large in humid temperate environments (Cirimo & McDonnell, 1997). Whether these saturated zones are a source or sink of N will depend on biological N requirements and the availability of C (Cirimo & McDonnell, 1997; Haag and Kaupenjohann, 2001).

Compared to natural systems, agroecosystems are “leaky” systems and greater transfers of nutrients occur (Haag and Kaupenjohann, 2001). Just how ‘leaky’ a system will be is a function of the ‘availability’ or ‘mobility’ of a particular nutrient and the pathways through which the nutrients are transported. The previous section has shown that the available pools of nutrients vary in time and space. However, the pathways for nutrient export can also vary and will be discussed below.

#### ***1.4.4 Major Pathways of Nutrient Export in Agricultural Areas***

##### **1.4.4.1 Hydrologic Pathways**

Nutrients are largely exported in hydrologic runoff during irrigation, rain or snow melt events. These inputs may pass over the soil surface as overland flow, or may infiltrate soils and move through soil horizons as subsurface flow. Water from soils may be subsequently returned to the atmosphere through evapotranspiration.

##### **Runoff Via Overland Flow**

Overland flow may occur due to two reasons: (1) Hortonian Overland Flow (HOF) or (2) Saturation Overland Flow (SOF) (Dingman, 2002). HOF occurs when the

atmospheric input rate of water exceeds the infiltration capacity of basin soils. This seldom occurs during summer months in Southern Ontario but may readily occur in winter months when basin surficial soils are frozen. SOF occurs when basin soils are saturated and the storage capacity of the soils is exceeded. Hewlitt and Hibbert (1967) postulated that such flow originated from specific areas in a drainage basin and termed this the Variable Source Area concept.

### Runoff Via Subsurface Flow and Groundwater

Water that infiltrates into terrestrial soils may take several pathways that may include interflow, soil moisture storage, percolation, groundwater storage and groundwater flow (Khaleel, 1980). Interflow consists of infiltrated water that moves laterally through upper soil layers to aquatic systems. Water that does not move overland or as interflow percolates through soils and contributes to soil moisture storage within a landscape or recharges groundwater.

The bulk of water movement in a saturated porous media is governed by Darcy's Law,

$$q = \frac{Q}{A} = -k_{HS} \frac{dh}{dx} \quad (1.6)$$

where  $q$  ( $\text{m s}^{-1}$ ) is the specific discharge,  $Q$  is the volume rate of flow ( $\text{m}^3 \text{s}^{-1}$ ), and  $A$  is the area of porous medium at right angles to the  $x$  direction ( $\text{m}^2$ );  $k_{HS}$  is the saturated hydraulic conductivity of the medium ( $\text{m s}^{-1}$ ) in the  $x$  direction, and  $h$  is the total hydraulic head of the fluid (Dingman, 2002). Saturated hydraulic conductivities in porous media are low, owing to the compact nature of soils and the tortuosity of pathways within

the soil matrix. Consequently, groundwater movement is very slow, and moves at a pace on the order of  $10^{-6}$  to  $10^{-8}$  m s<sup>-1</sup> in many glacial tills (Dingman, 2002).

### Runoff Via Preferential Flow Pathways

Water movement through subsoils does not always follow Darcy's Law and may instead pass rapidly through soils through preferential pathways. Darcy's Law is based on the assumption that flow occurs as *distributed flow*, where water permeates the entire porous network of the soil and passes through the entire soil volume (Hillel, 1998). However, water may instead move as preferential flow which occurs through distinct pathways that constitute a small fraction of the total soil volume (Hillel, 1998). Preferential pathways follow preexisting features in the soil profile such as clay or sand lenses, cavities or fissures. Flow in macropores can approach 1 m s<sup>-1</sup> (Dingman, 2002).

Preferential flow often occurs in clay and peat soils due to the presence of shrinkage cracks and/or biopores such as worm burrows (Bevan & Germann, 1982; Hillel, 1998). Water may move along vertical fingers via preferential flow paths toward the water table due to unstable wetting fronts (Ritsema *et al.*, 1998). Unstable wetting fronts occur if (a) soil hydraulic conductivity increases with depth (Hillel and Baker, 1988; Baker and Hillel, 1990; Ritsema and Dekker, 1994); (b) soils are water repellent (Ritsema *et al.*, 1993) and (c) if air entrapment occurs (Glass *et al.*, 1990).

The use of tracers has allowed scientists to see how quickly water may be moved from the surface through soils. For example, Kung *et al.* (2000a) applied tracers to a surface and observed these tracers in drainage tile effluent within 13 minutes. If water

was moving as matrix flow, given the measured  $K_{HS}$  values for the soils in their study (e.g. following Darcy's Law), runoff should not have reached the tile outlet for two days.

It is still very difficult to quantify the importance of preferential flowpaths in hydrologic and contaminant transport. Conventional sampling protocols such as coring and soil lysimeters are not suitable for monitoring field scale leaching of contaminants through preferential flow paths (Ghodrati and Jury, 1990; Ju *et al.*, 1997; Kung *et al.*, 2000b). However, tile drainage networks can be useful in quantifying solute transport dynamics (Richards and Steenhuis, 1988). Jury and Roth (1990) describe the concept of *transfer function*, where the breakthrough curve of a conservative tracer can be used to determine solute transport under field conditions. However, this breakthrough curve would only be directly applicable to the field in which the experiment was conducted.

#### Runoff Via Assisted Drainage / Weeping Tiles

A steady flow of groundwater discharge through drainage tiles is given by

$$q = Kh_m F(L, r, D) \quad (1.7)$$

where  $q$  ( $m\ d^{-1}$ ) is the specific drainage runoff,  $K$  ( $m\ d^{-1}$ ) is the hydraulic conductivity of the soil,  $h_m$  (m) is the groundwater table elevation above the level of drains taken in the mid distance between the drains and  $F$  ( $m^{-1}$ ) is a geometrical factor which depends on the drain spacing (m), the effective drain radius  $r$  (m) and the effective depth  $D$  (m) of an impermeable bedrock beneath the drains (Dolezal *et al.*, 2001; van Schilfgaarde, 1974). Thus, drainage runoff depends linearly on water table position (Dolezal *et al.*, 2001).

However, flow through drainage tiles is not always a steady flow of groundwater and may vary both spatially and temporally (Dolezal *et al.*, 2001). For example, at low or

zero discharge, the hydrogeology of the drained land is important in determining discharge patterns, as tiles may either be ephemeral or may drain an aquifer (Dolezal *et al.*, 2001). At moderate discharges, tile drainage patterns are linked to the removal of water from the soil profile itself (Dolezal *et al.*, 2001). At high discharges, tile drainage is influenced by the hydraulic capacity of the drainage system (Dolezal *et al.*, 2001). Stochastic aspects of tile drainage (in particular both flood and drought conditions) are difficult to quantify and consequently Dolezal *et al.* (2001) suggested the use of probability of exceedence curves (PoE) for modelling purposes.

#### 1.4.4.2 Dominant Nutrient Pathways

In agricultural landscapes, elevated nutrient losses have long been associated with surface runoff (Cirimo and McDonnell, 1997; Douglas *et al.*, 1998; Haag & Kaupenjohann, 2001) largely because of the abundance of nutrients in surface soil horizons and increased soil erodability. This is particularly in the case of P as most P in surface runoff from agricultural watersheds is adsorbed to sediment particles (Sommers *et al.*, 1975) and is lost via erosion during periods in which overland flow occurs. In particular, P tends to be associated with fine sediments (Cooper and Gilliam, 1987; Stone and Mudroch, 1989). Rainfall and/or snowmelt events also tend to result in large fluxes of  $\text{NO}_3^-$  with overland flow, in which near-stream anoxic environments are bypassed (Cirimo & McDonnell, 1997).

$\text{NO}_3^-$  losses in subsurface runoff can also be substantial. First,  $\text{NO}_3^-$  is mobile in soils and the process of denitrification requires anoxic conditions. Thus where oxic conditions predominate,  $\text{NO}_3^-$  will be actively transported with runoff and discharged into

surface waters. Interflow has been identified as an important mechanism for the rapid transport of  $\text{NO}_3^-$  towards streams, particularly under stormflow and snowmelt conditions (Haag & Kaupenjohann, 2001; Mosley, 1982).

Subsurface flow has less potential than overland flow for removing P from soils. This is largely a result of the P-deficiency of subsoils (Sharpley *et al.*, 1995b). Moreover, water percolating through soils has increased residence times and increased contact with soil particles due to the tortuosity of flow paths. Particulate P may become trapped in pore spaces, allowing only dissolved fractions to pass through soils. P is therefore filtered from water as it percolates vertically through soils. In many systems, P export via subsurface flow has been neglected (Sharpley, 1995b). There are some exceptions to this, however. For example, soils lacking in their ability to sorb or retain P (e.g. some organic soils and sands) have been found to release appreciable quantities of dissolved P through leaching (Sharpley, 1995b).

Macropores and preferential flowpaths have recently been identified as major pathways of both P and  $\text{NO}_3^-$  in agricultural systems. Ryden *et al.* (1973) showed that subsurface flow may constitute losses of P that are equal or greater to those in surface runoff. Cirimo and McDonnell (1997), Haag and Kaupenjohann (2001) and Stamm *et al.* (1998) also stressed the importance of macropores and preferential transport in transporting large quantities of  $\text{NO}_3^-$  and P into surface waters.

Often, macropores or preferential pathways work in conjunction with drainage tiles to export large quantities of nutrients. In the past, the role of drainage tiles in nutrient export has been unclear. Some researchers have suggested that drainage tiles lower the water table and reduce overland flow and tend to reduce nutrient losses. Haygarth *et al.*,

1998 found that tiles reduced TP export in runoff by reducing the amount of surface runoff. Lindsay (1979) suggested that tiles may reduce the spatial extent of waterlogging, which increases soil redox potential and encourages the adsorption of P. However, others have shown that tiles facilitate the export of nutrients by allowing drainage waters to bypass the soil matrix and hinder natural processes that remove nutrients from runoff (Dils and Heathwaite, 1999; Laubel *et al.*, 1999; Ulen and Persson, 1999; Haag and Kaupenjohann, 2001; Gentry *et al.*, 2000; Ryden *et al.*, 1973). Patterns of nutrient export in tile effluent have been linked to both spatial and temporal factors. Researchers have related tile export of nutrients to fertilizer type and application (Haygarth, 1997; Gentry *et al.*, 2000), and soil type (Beauchemin *et al.*, 1998). Others have related tile export to soil moisture properties and the degree of connectivity between tiles and surface layers through preferential flowpaths (e.g. Beauchemin *et al.*, 1998; Stamm *et al.*, 1998; Welsch *et al.*, 2001). Often, tiles exhibit strong temporal variability in nutrient concentrations in effluent (e.g. Ulen, 1995). For example, Dils and Heathwaite (1999) observed that TP losses in tile effluent were low during stable baseflow periods ( $< 100 \mu\text{g L}^{-1}$ ), but could be quite high during high discharge events ( $> 1000 \mu\text{g L}^{-1}$ ).  $\text{NO}_3^-$ -N concentrations in tile effluent have been shown to range from 2 to 20  $\text{mg L}^{-1}$  in mineral soils in Europe (Haag & Kaupenjohann, 2001). But the transport of nitrate through macropores into drainage tiles resulted in concentrations averaging 70  $\text{mg L}^{-1}$  and as high as 136  $\text{mg L}^{-1}$  in tile effluent in one study (Bronswijk *et al.*, 1995).

Tile effluent can account for a substantial portion of nutrient losses from agricultural catchments. Moreover, nutrient export through tiles may occur over a short period of time in response to storms (David *et al.*, 1997; Johnson *et al.*, 1976). In a study

in Illinois, tiles accounted for 60% of annual  $\text{NO}_3^-$  losses (Kohl *et al.*, 1971). In a large watershed in New York, Johnson *et al.* (1976) demonstrated that tiles accounted for only 35% of annual basin export. Ulen (1995) observed that both  $\text{NO}_3^-$  and P export through drainage tiles in an agricultural basin in Sweden were episodic and occurred over a small portion of the year, although this was more prevalent for P than  $\text{NO}_3^-$ . Overall, the role of drainage tiles in the export of nutrients in agricultural runoff is still poorly understood. Temporal variability in hydrochemical export is difficult to quantify and predict, and the role of drainage tiles during winter months has not been adequately characterized.

#### ***1.4.5 Linkages Among Sources and Pathways: The Importance of Hydrology***

Landscapes are heterogeneous ‘patchworks’ where varying biological and geological patterns and processes interact to produce domains in which either the retention or transport of matter dominates (Haag and Kaupenjohann, 2001). In other words, the mass of nutrients exported from a system is simply a function of the available pool of nutrients in the soil, and the hydrologic conditions that transport the nutrients to surface waters (Cirimo & McDonnell, 1997; McDowell *et al.*, 2000). The highest losses, therefore, will occur when nutrient availability is very high and hydrologic flowpaths such as overland flow and preferential flowpaths are ‘activated’. To adequately characterize nutrient losses to surface waters, it is necessary to understand how nutrient dynamics in soils and hydrology interact. Cirimo and McDonnell (1997) suggest that future research on N-fluxes should focus on the critical juncture between temporal, spatial and biogeochemical conditions in the near-stream environment. Future research



on P-fluxes should focus on the interaction of particular hydrologic flowpaths and 'vulnerable' areas of catchments where P pools are high (Gburek and Sharpley, 1998).

#### ***1.4.6 Linking Nutrient Losses and Antecedent Hydrologic Conditions***

The role of AHC in hydrochemical export in agricultural landscapes is poorly understood. While it is widely acknowledged that AHC should influence hydrologic discharge and nutrient export, it is difficult to demonstrate this quantitatively and to develop predictive models.

#### Hydrology

Antecedent moisture in basin upland areas can have a dramatic effect on the ability of a basin to store or discharge water but also on the flowpaths through which runoff drains into adjacent waterways. Under very dry conditions, the storage capacity of the basin is very high, whereas under very wet conditions, the storage capacity is low (Dingman, 2002).

Hydrologic flow paths vary spatially and temporally. Whether or not a system will experience overland flow or subsurface flow is determined by a variety of factors, such as the topography of the landscape, its underlying geology, vegetative cover and root systems, climate and AHC. Flow pathways and discharge from a basin change in response to precipitation events (e.g. storms) and by season. For example, in northern ecosystems, soils freeze for a portion of the year, which reduces their infiltration capacity. Consequently, overland flow prevails in these systems in winter and spring during hydrologic events. Also, under saturated conditions, flowpaths are largely

governed by the limited storage capacity of the drainage basin, and precipitation is forced to travel over the ground surface to adjacent waterways.

Under very dry conditions, runoff is forced to move via preferential ‘finger like’ flow (e.g. Ritsema *et al.*, 1998). This runoff may be retained within the soil matrix, or may pass through the soil matrix and be exported to drainage systems (tiles) or surface waters. Kung *et al.* (2000b) demonstrated that the movement of both conservative and reactive tracers through a soil profile became faster as soils became wetter during a precipitation event. This pattern indicates that water movement through preferential flowpaths changes throughout a precipitation event and some flow paths are ‘activated’ once soil conditions become wetter. As this occurs, the role of macropores and preferential flow pathways appears to increase and water movement shifts toward increasingly larger pores of preferential flow pathways (Kung *et al.*, 2000b).

### Nutrient Export

AHC can also affect patterns of nutrient export but the effects of AHC on chemical export patterns are unclear (Muscutt *et al.*, 1993; Biron *et al.*, 1999; Welsch *et al.*, 2001). The chemical constituents in runoff have been found to vary depending on whether a given event is preceded by drought or wet conditions. Some authors report a pulse of nutrients following periods of drought, while others report an increase in nutrient export as moisture levels rise. Biron *et al.* (1999) and Walling and Foster (1975) showed that initial chemical concentrations were higher following a period of drought rather than following a period of wet antecedent conditions. Pote *et al.* (1998) showed in laboratory tests that SRP was more easily desorbed in water following the drying of soil samples

and implied that this may lead to variable losses in runoff in different seasons and/or under variable AHC. Welsch et al (2001) linked  $\text{NO}_3^-$  export to topographic indices and found that such relationships were strengthened as moisture levels increased due to increased hydrologic connectivity in the basin. The rates and magnitudes of nutrient export vary by season. Dils and Heathwaite (1999) observed that TP losses in drainage tile effluent were highest in autumn as conditions became wetter following summer drought. N may accumulate in subsoils during seasonal water table drawdown, and the subsequent mobilization of this accumulation of N by wetting up later in the season can lead to a large flushing of N (Cirimo & McDonnell, 1997).

Hydrologic connectivity with upper soil horizons appears to be critical in flushing chemicals into streams (Creed and Band, 1998; Biron *et al.*, 1999; Welsch *et al.*, 2001) and, this connectivity has been linked to AHC (Biron *et al.*, 1999; Welsch *et al.*, 2001). It is hypothesized that macropores and preferential flowpaths are critical features controlling nutrient loss. Finger-like flow through macropores allows surface waters to bypass natural soil processes and be exported to drainage tiles and/or surface waters (Beauchemin *et al.*, 1998; Gachter *et al.*, 1998; Ritsema *et al.*, 1998; Stamm *et al.*, 1998). Nutrient loss from soils may occur under dry, moist or wet conditions due to drainage through macropores and preferential flow pathways. 'Pulses' of nutrient losses are often observed under such dry conditions following rainfall (e.g. Beauchemin *et al.*, 1998; Stamm *et al.*, 1998) or irrigation (Stone & Krishnappan, 2003). However, under wetter antecedent conditions, preferential flow paths may increase in importance. Kung *et al.* (2000a) demonstrated that the size distribution of preferential pathways increased as soils became wetter (i.e. larger pores are activated as soils become wetter and that

contaminants at the surface were transported more rapidly through these larger pores. This implies that surface contaminants are routed more rapidly through the soil column with increasing soil moisture content. Therefore, it is hypothesized that AHC control the degree of 'connectivity' or 'activeness' of preferential flowpaths and govern rates of nutrient export in discharge.

#### ***1.4.7 Temporal Patterns in Hydrochemical Export***

Estimates of nutrient export from agricultural systems range considerably (0.02 – 48 kg TP ha<sup>-1</sup> yr<sup>-1</sup>, 0.01 – 2.2 kg SRP ha<sup>-1</sup> yr<sup>-1</sup>, 0.04 – 44.8 kg NO<sub>3</sub><sup>-</sup>-N ha<sup>-1</sup> yr<sup>-1</sup>) (Vanni *et al.*, 2001; Correll *et al.*, 1999; Cooke & Prepas, 1998; Douglas *et al.*, 1998; Jordan *et al.*, 1997; Mueller *et al.*, 1995; Puckett, 1995; Baker, 1993; Cleresci *et al.*, 1986; Beaulac & Reckhow, 1982; Hill, 1981; Sharpley and Syers, 1981; Miller, 1979; Dillon & Kirchner, 1975; Schuman *et al.* 1973). The literature shows that the majority of annual nutrient export occurs during a few events during the year. For example, McDowell *et al.* (2001) noted that a few short and intense storms can account for as much as 90% of annual exports delivered from less than 5% of the basin area. In Australia, Cosser (1989) observed that mid summer storms accounted for 3% of runoff time but accounted for 75-80% of annual TP export. Edwards and Owens (1991) reported that 66% of erosional losses over a period of 28 years were lost in five storms. The dominance of a few major events in annual estimates of nutrient mass exports has also been reported by Ulen & Persson, (1999), Brunet & Astin, (1998), Douglas *et al.*, (1998) Pionke *et al.*, (1996), Zuzel *et al.*, (1993), Douglas *et al.*, (1988) McCool *et al.*, (1982), Hill, (1981), and Schuman *et al.*, (1973).

During snowmelt, a significant proportion of nutrient export can be lost from agricultural basins (Zuzel *et al.*, 1993; McCool *et al.* 1982; Cooke and Prepas 1998). In areas where seasonal periods of frost occur, agricultural fields are vulnerable to nutrient export during winter melt events because ground frost enhances the possibility of overland flow by reducing soil permeability. Mid-winter or spring runoff events coupled with the application of organic fertilizers can result in excessive export of SRP (Cooke & Prepas, 1998; Schuman *et al.*, 1973). The flushing of N due to episodic periods of snowmelt is a large annual source of N from forested environments in eastern USA (Cirimo & McDonnell, 1997).

Although the dominance of a few major storms in annual nutrient export estimates has been reported by several authors, such studies have been in geographic regions outside of Southern Ontario and have been undertaken at different spatial and temporal scales. Temporal variability in hydrochemical export patterns and in particular the influence of high magnitude events on such estimates is still widely unknown. Few studies have examined nutrient export patterns during winter periods. Moreover, few studies undertake intensive monitoring programmes, and at present, annual estimates are often generated from inadequate sampling regimes. The importance of sampling interval on estimates of nutrient export must be explored in more detail.

#### ***1.4.8 Nutrient Retention in Riparian Buffer Zones and Stream Sediments***

Riparian buffer zones are critical interfaces between uplands and receiving water bodies due to their ability to retain nutrients (Meyer, 1979; Klotz, 1985; Richardson,

1985; Reddy *et al.*, 1999). The retention of nutrients may occur in both riparian areas and within streams.

Riparian buffer zones are vegetated strips of land that reduce the transfer of nutrients to surface waters in overland flow (Norris, 1993). These areas effectively remove nutrients in surface and subsurface runoff (Norris, 1993; Daniels & Gilliam, 1996). Norris (1993) has noted, however, that though riparian zones are effective filters under small scale experimental conditions, they are less successful on a broad catchment basis. Norris (1993) explains that the purpose of a riparian zone is to divide or spread incoming overland flow, thereby reducing its velocity. This process acts to increase infiltration and reduce surface runoff, which in turn allows the deposition of coarse particulate and the filtration of suspended particles through leaf litter and soil. The retention of these materials in the soils promotes their decay, uptake by plants or adsorption to plants and soil surfaces. It should be noted that P may be subsequently removed from riparian areas by (1) erosion of the enriched sediment; or (2) desorption to the overlying water (Cooper & Gilliam, 1987).

It appears that P retention in riparian areas is mainly controlled by physical or chemical factors rather than biological (Cooper and Gilliam, 1987, Lee *et al.*, 1989). Cooper and Gilliam (1987) report that riparian zones can serve as sinks for P in runoff in two ways: (1) through the sorption of P from overlying water by soil and sediments (precipitation and adsorption reactions) and (2) they act as a site of deposition for enriched sediment.

There is a general agreement that the land-water interface regulates water quality in agricultural basins (Haag and Kaupenjohann, 2001; Dillaha *et al.*, 1989). In the case of

$\text{NO}_3^-$  export, the predominant role of riparian zones is through the process of denitrification (Haag and Kaupenjohann, 2001). In a large number of studies, riparian  $\text{NO}_3^-$  removal has been shown to exceed 90% (Hill, 1996). However, in other studies, little to no  $\text{NO}_3^-$  is retained (Devito *et al.*, 1990). Cirimo and McDonnell (1997) state that because riparian zones may be the last biogeochemical environment encountered by converging hydrologic pathways, their importance in regulating stream N concentrations cannot be overemphasized. However, they also suggest that during large hydrologic events or snowmelt, the riparian environment may be bypassed by the N fluxes.

The effectiveness of a riparian zone as a nutrient filter is affected by physical features such as (1) the length, gradient and shape of the riparian area and upland areas; (2) the hydrologic source to the riparian zone and the proximity of the riparian area to the nutrient source; (3) the structure and species of riparian vegetation; (4) soil composition in the riparian zone and/or the availability of C; (5) the type of pollutant encountered and the size distribution of incoming sediments; (6) the age of the riparian area; and (7) the season and temporal distribution of the hydrologic or pollutant inflows (Cooper & Gilliam, 1987; Daniels & Gilliam, 1996; Haag & Kaupenjohann, 2001; Karr & Schlosser, 1978; Lee *et al.* 1989; Norris, 1993; Osborne & Kovacic, 1993; Richardson, 1985; Schlosser & Karr, 1981).

During baseflow, in-stream processes can regulate nutrient export from agricultural catchments (Burns, 1998; Svendsen *et al.*, 1995). The retention of SRP is a function of a number of biotic and abiotic processes (Reddy *et al.*, 1999). Biotic mechanisms of P retention include assimilation by vegetation, plankton, periphyton and

microorganisms, whereas abiotic mechanisms include sedimentation, adsorption by sediments and precipitation (Reddy *et al.*, 1999). While biotic mechanisms play an important role (Meyer, 1979; Hill, 1982; Mulholland *et al.*, 1985), the abiotic exchange of P between the water column and suspended and/or bottom sediments is a major component of the P cycle in many fluvial systems (McCallister and Logan, 1978; Meyer, 1979; Hill, 1982; Klotz, 1985). Exchange processes are governed by factors such as pH, redox potential and organic matter content but appear to be most affected by sediment composition (mineralogy, texture) (Syers *et al.*, 1973; Patrick and Khalid, 1974; Meyer, 1979; Hill, 1982; Klotz, 1985; Stone and Mudroch, 1989; Stone and English, 1993).

The hyporheic zone is an active ecotone between the surface stream and groundwater, where nitrification (Triska *et al.*, 1990) or denitrification (Burns, 1998; Christensen *et al.*, 1990; Hill, 1981) may dominate but the overall role of in-stream denitrification is much less than adjacent riparian buffer zones (Fennessy and Cronk, 1997; Haag & Kaupenjohann, 2001). N transformations in hyporheic zones have been examined by Triska *et al.* (1989; 1990; 1993) Duff and Triska (1990), Mulholland (1992), and Findlay (1995). Sediments have been shown to act as sinks for  $\text{NO}_3^-$  (Gilbert *et al.*, 1990; Hill, 1997). Denitrification in sediments is limited by the availability of organic C and temperature (Haag & Kaupenjohann, 2001). However, N transformations in hyporheic zones have also been linked to length and intensity of light, substrate grain size, hydraulic gradient, stream velocity, and the concentrations of N (Burns, 1998).

Although in-stream processes are generally effective at low flows, the majority of nutrient export from agricultural catchments typically occurs during storm periods (Svendsen *et al.*, 1995; Gburek and Sharpley, 1998) during which in-stream retention



processes may be rendered ineffective. For example, during storms associated with high rates of discharge, P originally retained in streams can be subsequently transported as PP due to the resuspension of streambed sediments (Hill, 1982; Svendsen *et al.*, 1995).

#### ***1.4.9 Summary***

The goal of this thesis is to improve our understanding of nutrient dynamics in agricultural systems. Several gaps in the current scientific understanding of nutrient export from agricultural systems have been identified. The study approach taken was to examine some aspect of all four gaps and examine nutrient cycling within the study basin at a range of spatial and temporal scales. An alternative approach would be to select one of these gaps and focus the thesis around it. However the approach taken was preferred as it provided a broader understanding of major processes occurring within the study basin, which is a typical first-order agricultural catchment in Southern Ontario.

Research questions addressed in this thesis involve (1) long- and short-term temporal variability in nutrient export patterns; (2) the role of drainage tiles within various watersheds; (3) the effects of antecedent hydrologic conditions (AHC) on nutrient export patterns; and (4) the SRP retention potential of an agricultural stream under highly elevated SRP concentrations at low flows.

## **2.0 Site Description & Methods**

### **2.1 Study Site**

The study was conducted in the Strawberry Creek Watershed, near Maryhill, Ontario (80°23'15"W, 43°33'10"N). Strawberry Creek is a small (2.7 km<sup>2</sup>), perennial first-order stream that drains into Hopewell Creek and subsequently into the Grand River (Figure 2.1).

#### ***2.1.1 Land Use & Vegetation Cover***

The catchment is typical of first-order agricultural catchments in the Grand River Watershed in terms of its land use. Specific land-use in the basin consists of woodlots and hedgerows (10%), cultivated (85%) and residential (5%) lands (Figure 2.2). Six residential properties are located within the watershed. The woodlots in the basin are poorly drained and dominated by Sugar Maple (*Acer saccharum*) and Red Maple (*Acer rubrum*) (Harris, 1999). Crops include corn, soybeans, winter wheat and strawberries (Figure 2.3).

Organic (cattle, poultry) fertilizers are applied periodically throughout the year, including the winter months. Organic fertilizers are applied to 40% of the basin (generally in the upper portion of the basin, Figure 2.3) at a rate of approximately 33 kg NO<sub>3</sub>-N ha<sup>-1</sup> yr<sup>-1</sup> and 9 kg P ha<sup>-1</sup> yr<sup>-1</sup> (calculated from the typical daily constituents in the waste per cattle provided by Fleming and Ford (2001) x 100 beef cattle in the basin). Inorganic fertilizers are applied to 35% of the middle and lower portions of the basin in the spring months (Figure 2.3). N is applied in the spring months at a rate of

approximately  $113 \text{ kg N ha}^{-1} \text{ yr}^{-1}$  (P. Renkema. Pers.Comm., 2003). The precise quantity of P applied in this basin is not known, but it is most likely on the order of  $25\text{-}30 \text{ kg P}_2\text{O}_5 \text{ ha}^{-1} \text{ yr}^{-1}$  (J.Lauzon. Pers. Comm. 2003). Two fields in the lower portion of the basin are in fallow and do not receive fertilizer (10% of the basin). Thus, the basin receives a total of approximately  $1.5 \times 10^5 \text{ kg NO}_3\text{-N ha}^{-1} \text{ yr}^{-1}$  and  $2 \times 10^3 \text{ kg P ha}^{-1} \text{ yr}^{-1}$  in the form of manure and fertilizers. It is often difficult to obtain an exact estimate of quantities of N and P applied via manure and fertilizers in agricultural catchments because this information is not always documented by landowners, and, there is some hesitation by landowners to provide this information to environmental managers.

A narrow riparian buffer strip (3-10 m wide) is present on either side of the stream along its length. Riparian areas are dominated by tall grasses (*Gramineae spp.*) but also contain native vegetation species such as Canada Goldenrod (*Solidago canadensis*), Yarrow (*Achillea millefolium*), Thistle (*Cirsium spp.*), Common Milkweed (*Asclepias syriaca*), Queen Anne's Lace (*Daucus carota*) and Common burdock (*Arctum minus*) (Harris, 1999). A few trees (*Salix spp.*) are also present in riparian areas at the lower end of the basin.

### ***2.1.2 Surficial Geology and Topography***

Much of Southern Ontario is underlain by stratified glacial tills (Presant and Wicklund, 1971) and bedrock of Silurian origin. The presence of compact basal tills in regions extending from London Ontario to regions east of Guelph have a dramatic effect on the hydrology of this region. The study site is located within this region and is therefore representative of much of southern Ontario.

**Figure 2.1 Map showing the Grand River Basin in Southern Ontario**

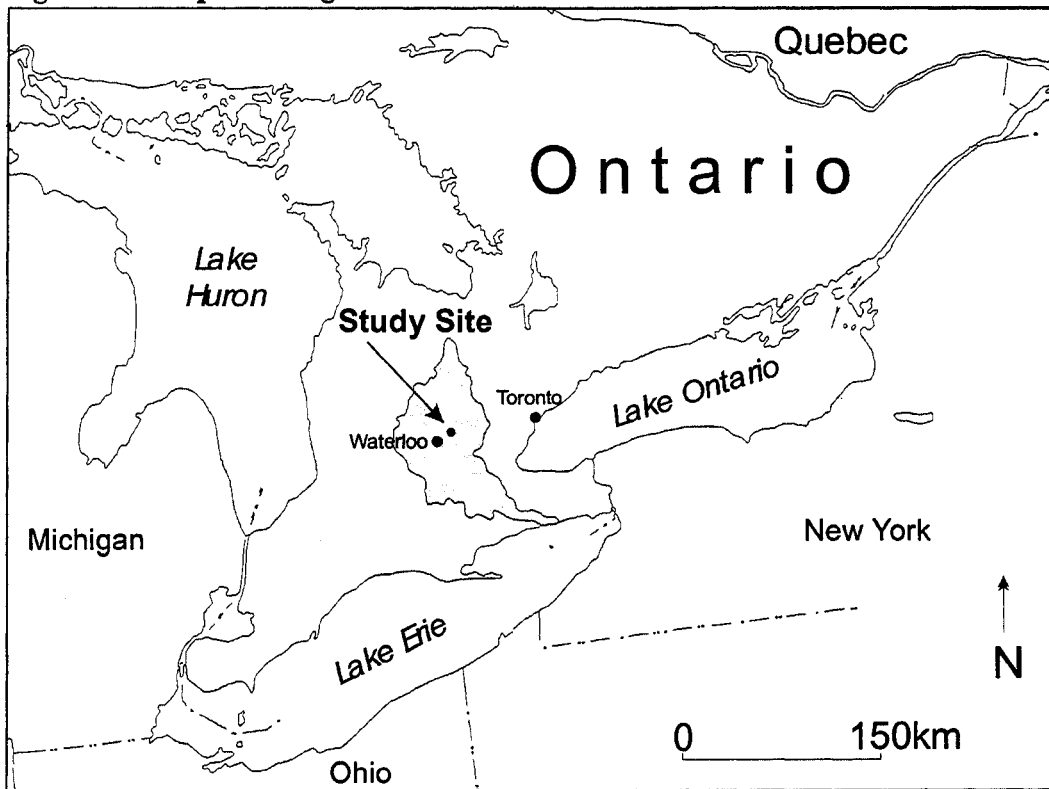


**Figure 2.2 Map of the Strawberry Creek Watershed. Catchment boundary, stream, residential buildings, woodlots, cultivated lands, and drainage tiles are shown in the figure.**

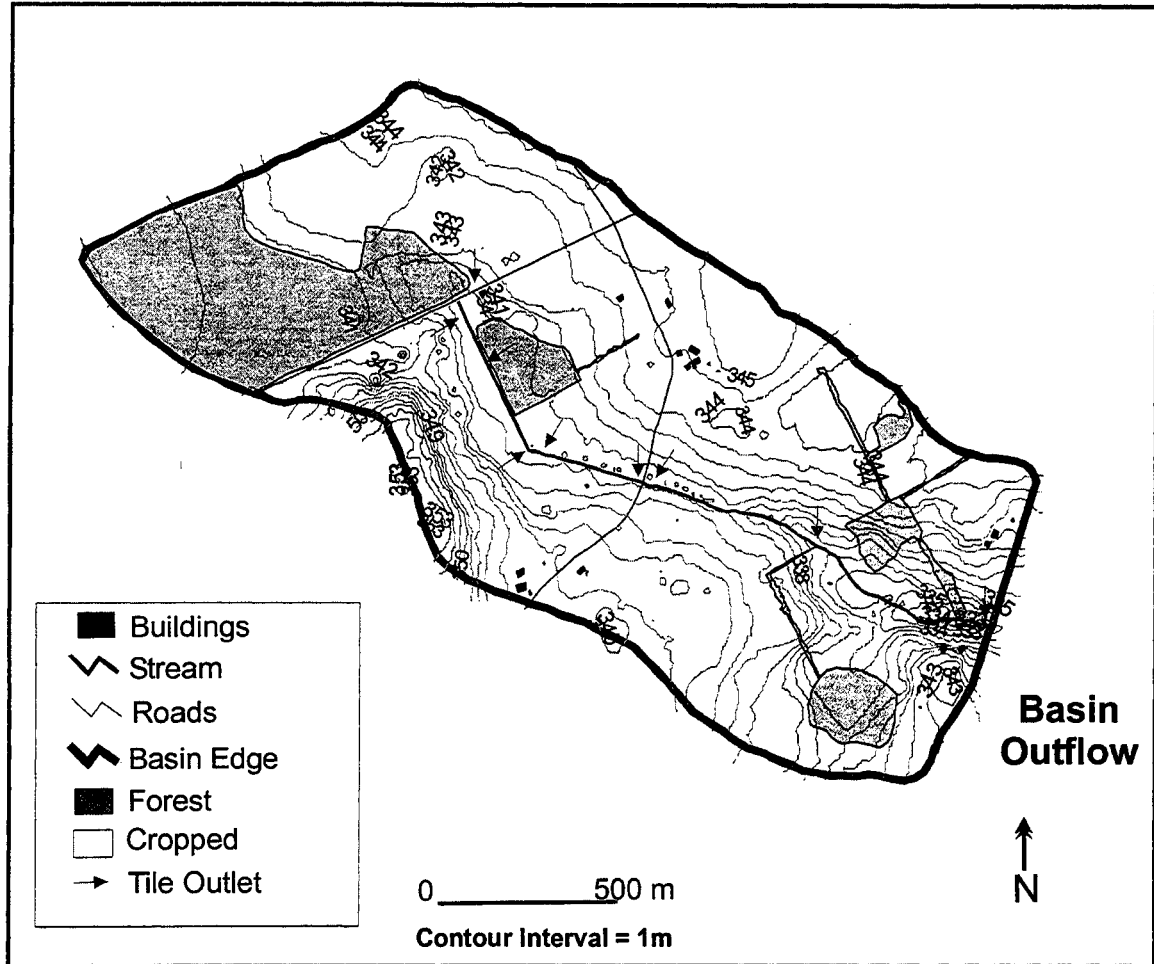
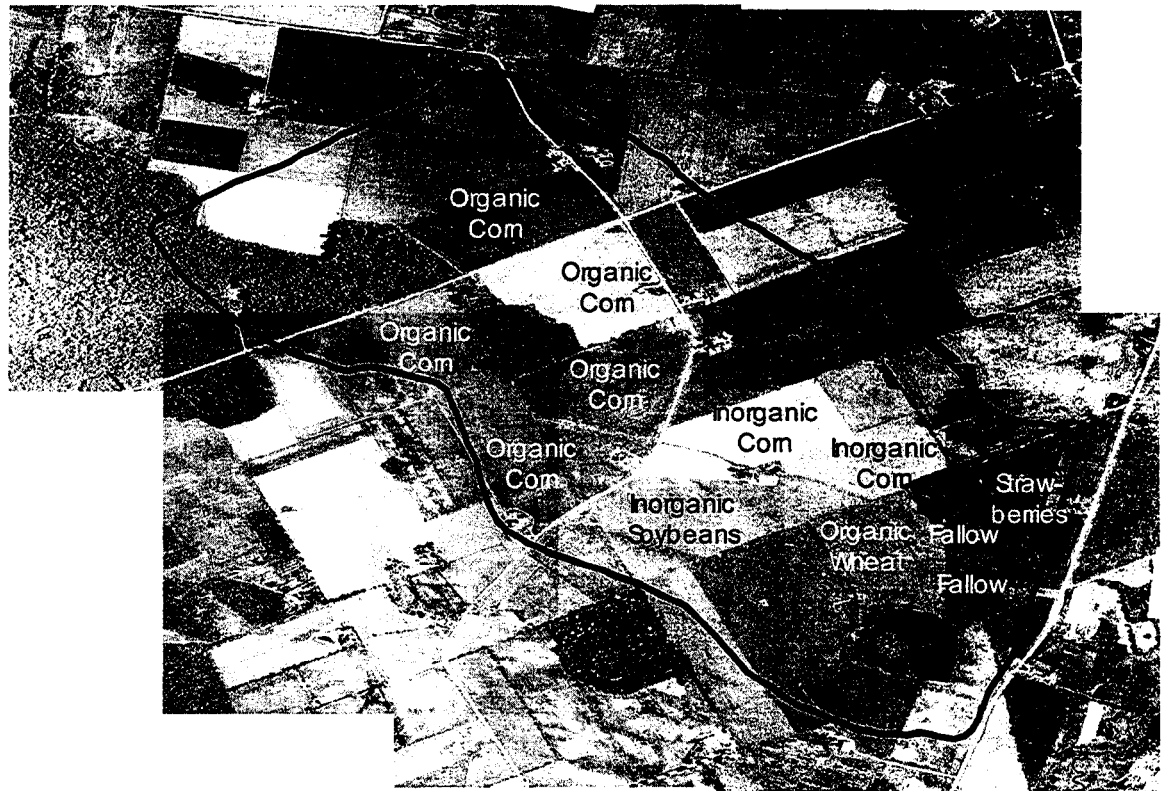


**Figure 2.3 Air Photo of Strawberry Creek. Type of fertilizer and crop grown for each field in the catchment are shown in the figure.**



This central portion of the Grand River basin is rugged and hilly compared to the upper and lower areas of the basin. More northern areas of the Grand River watershed are predominantly covered by till plains and are characterized by a gently rolling, marshy landscape. Soils in the upper portion of the Grand River watershed are generally poorly drained sandy silt clays. Lower areas of the Grand River watershed are flat and characterized by shallow soils composed of sand, clay, and till plains, which were once at the bottom of glacial lakes.

The Strawberry Creek Watershed is located within the Guelph Drumlin Field. The physiography of the region is shaped by glacial processes (Chapman & Putnam, 1984), where much of the central part of the Grand River watershed is characterized by moraines, drumlins and sandy hills (GRCA, 1998). Drumlins in the region have long axes trending in an east-west direction, and areas between the drumlins are of low relief (Karrow, 1974). More detailed information about the surficial geology of the region is provided by Karrow (1974) and Chapman and Putnam (1984).

In general, upland areas of the basin slope gently, and have a topographic gradient of 0.05 (Harris, 1999). One exception to this is a large hill at the western edge of the catchment, which rises 15 m above the surrounding terrain. This hill is part of the Breslau Moraine (Karrow, 1974). Riparian areas range in structure from wide and flat to steep and narrow. In the downstream, low-lying areas of the basin, riparian buffer strips are typically 8-10 m wide, with a slope that is similar to upland areas (0.05). In sections of the basin that are closer to the headwaters, riparian buffer strips are steeper and narrower (4-6 m wide, and with a slope of 0.10).

Soils in the basin are classified as a combination of Gray Brown luvisols, Melanic Brunisols and Humic gleysols (Presant & Wicklund, 1971). These soils are a combination of loam and silt loam (Guelph and London series) that developed on Port Stanley till, a heterogeneous mixture of sand and silt. Soils in riparian areas are similar to basin surficial soils although a thin organic layer of sediments is present around the stream perimeter. At approximately 2 m depth in the basin a layer of fine, clay-rich till is present (Karrow, 1974) which acts as an aquiclude between shallow and deep soils in the basin. Agricultural fields located on the eastern side of Waterloo Township and throughout much of Wellington Township have tile drains as a result of the presence of this clay-rich till layer at such a shallow depth beneath the loam (Presant and Wicklund, 1971). Catfish Creek till is found in the basin at a depth of approximately 5m, which is composed of large quantities of cobbles and boulders. The Guelph-Lockport formation of cream to brown dolomitic bedrock is located between 25 and 50 m below the surface (Karrow, 1974).

### ***2.1.3 Climate***

The study years were 2000 and 2001. Both of the study years were drier than long-term precipitation averages for Southern Ontario, although the distribution of rainfall resulted in a very wet summer in 2000 and a very dry summer in 2001. In 2000 and 2001, 743 (37 mm as snow) and 633 (52 mm as snow) mm of precipitation fell,, respectively. 30-year mean annual precipitation for the region is 909 mm (160 mm as snowfall) (Environment Canada, 2003). In the frost-free months, precipitation is generally evenly distributed throughout the year in Southern Ontario (Figure 2.4). Mean

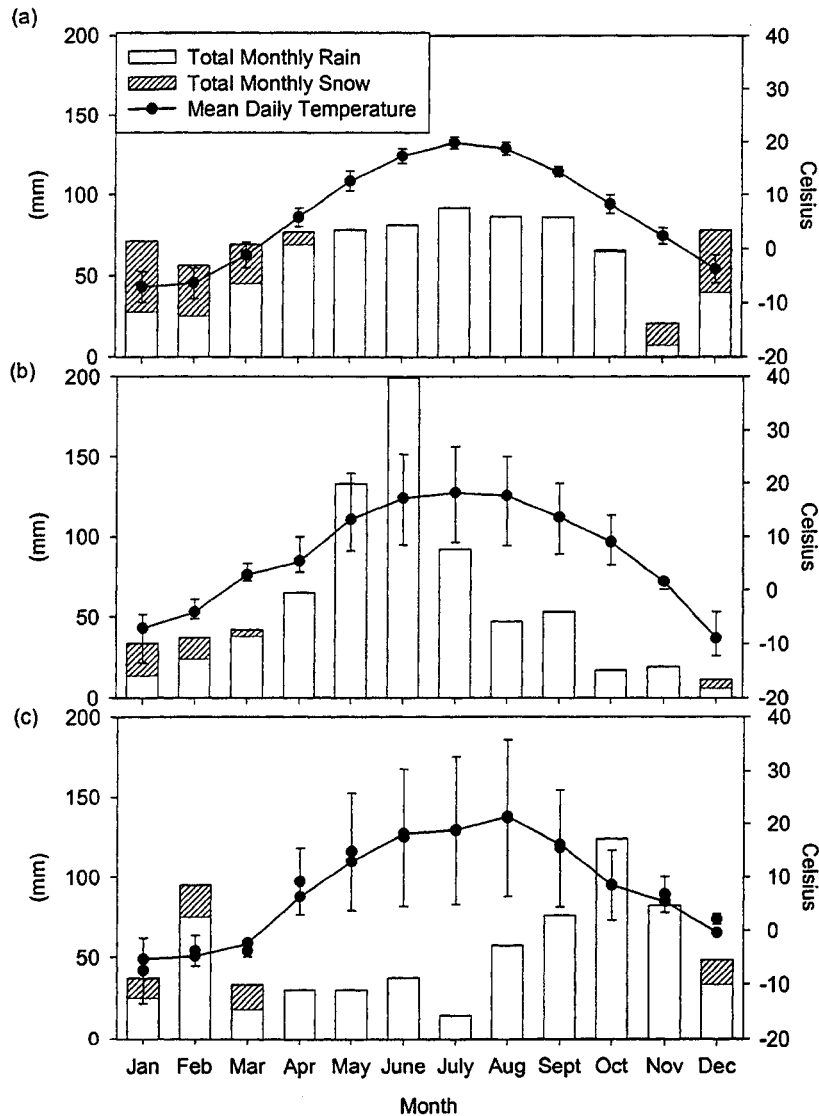


totally monthly precipitation ranges from 51.5 mm to 91 mm per month in this region (Environment Canada, 2003).

The winter of 2000 (37 mm snow (water equivalent) + 38 mm rainfall) was drier than the winter of 2001 (52 mm snow (water equivalent) + 100 mm rainfall). Snowfall typically falls in small quantities in this region, with most snowfall events falling at intensities of  $< 2 \text{ mm d}^{-1}$ . Events with snowfall intensities of  $5 \text{ mm d}^{-1}$  generally occur 2 days per month during the winter months, and snowfall intensities exceeding this are far less common (e.g. 0.4 – 0.7 days per month) (Environment Canada, 2003). Winter rainfall events most often occur in intensities  $< 1 \text{ mm d}^{-1}$ . Occurrences of  $10 \text{ mm d}^{-1}$  typically occur 0.9 days per month in January and February based on 30-year means; however, rainfall events  $> 25 \text{ mm d}^{-1}$  are uncommon in winter (0.1 days per month) (Environment Canada, 2003). The distribution of rainfall events over the study period resembled these long-term averages (i.e. generally events were less than  $1 \text{ mm d}^{-1}$ , but were occasionally higher than this). An unusually large precipitation event only occurred once over the study period (February 2001), when 50 mm of rainfall fell over a 24 hour period.

Rainfall events in summer are typically higher in magnitude than winter rainfall events, although events exceeding  $25 \text{ mm d}^{-1}$  are less common (0.37 to 0.87 days per month) (Environment Canada, 2003). The early summer of 2000 was wet (a total of 332 mm of rain fell in May and June, 2000), whereas the summer of 2001 was exceptionally dry (130 mm of rain fell between May 1 and August 31, 2001). 30-year means for rainfall in the summer months range from 64 to 92 mm per month (Environment Canada, 2003).

**Figure 2.4 Total monthly precipitation (left y-axis) and air temperatures (right y-axis) in Southern Ontario. 1971-2000 30-year means for Waterloo-Wellington area are shown in (a). The error bars show one standard deviation for air temperature based on 30-year means. Precipitation and air temperature for 2000 and 2001 are shown in (b) and (c). The error bars in (b) and (c) show the maximum and minimum measured hourly air temperatures for each month during the study period.**



The autumn of 2000 was dry (89 mm fell between September 1 and November 31) whereas the autumn of 2001 was wet (282 mm from September 1 to November 21).

Air temperatures in Southern Ontario show a seasonal trend with maxima in summer and minima in winter (Figure 2.4). Mean monthly air temperatures (recorded in Breslau, Ontario, 30-year mean, Environment Canada, 2003) are below the freezing mark in winter (December, January, February and March), but may range considerably. For example, maximum air temperatures have reached 13-18°C in December, January and February, and 24 °C in March, but minimum air temperatures have plummeted to as low as -25°C to -32 °C in the winter months. Mean daily air temperatures in summer (June-August) are typically 17-20 °C. Maximum daily air temperatures reached are 36 °C, and minimum daily temperatures are 1-5 °C (Environment Canada, 2003).

Air temperatures over the study period fell within the range of temperatures observed over 30 years (Fig. 2.4). The winter of 2000 was cold, whereas the winter of 2002 was very mild. The winter of 2001 routinely had strong fluctuations in air temperature ranging from warm (12 °C) to very cold (-15 °C) within a 24-48 hour period. The 30-year mean January and February air temperatures for the region are -7.1 °C and -6.4 °C, respectively. The winters of 2000, 2001 and 2002 had mean January and February temperatures of -7.1 °C and -4.1 °C, -5.4 °C and -4.9 °C, and -1.9 °C and -2.9 °C, respectively. Air temperatures during the months of April through September were typical of Southern Ontario, averaging 14.2 °C in 2000, and 15.6 °C in 2001. This compared to a 30-year normal of 14.7 °C (Environment Canada, 2003).

#### ***2.1.4 Drainage Characteristics/ General Hydrology***

The stream, (approximately 2 kilometres in length) is generally narrow (1 m wide), varying from 0.5 m at summer baseflow to 2.5 m at bankfull storage at the stream outlet. This translates to flow rates ranging from  $< 1 \text{ L s}^{-1}$  to  $> 400 \text{ L s}^{-1}$ . The change in streambed elevation is 8.3 m over the entire stream length. However, more than half of the change in elevation occurs over a 500 m reach located in the middle section of the stream. The upper portion (750 m) of the stream is deeply incised and has been periodically channelized and straightened to improve drainage. The lower end of the stream, conversely, is a gentle meander, and is likely natural in origin (Harris, 1999).

Surface inputs from two deciduous swamps, as well as perennial groundwater flow contribute to the flow of Strawberry Creek (Figure 2.2). Groundwater input is distributed along the reach and is spatially and temporally irregular (Cabrera, 1998). One of the deciduous swamps forms the headwaters of the stream and the other swamp feeds a very small ephemeral tributary at the lower end of the basin (Figure 2.2). Groundwater flow through the riparian zone is primarily lateral due to the compact layer of Maryhill till at 2m depth (Mengis, 1999). A dense network of macropores in the basin subsoils allows groundwater to pass rapidly through soils (Harris, 1999; House, 2000).

Approximately 60% of the drainage basin is underlain by drainage tiles (House, 2000), and a total of nine tile outlets drain into Strawberry Creek. Drainage tile networks within a given field are composed of 'feeder' tiles, which feed into 'header' tiles, which subsequently flow into a common outlet where they are exported to the stream (House, 2000). Tile networks in the basin are typically composed of either perforated clay or

polyethylene tubing (4" in diameter) installed approximately 1m below the soil surface and lie approximately 40 feet apart.

During the snowmelt period and exceptionally wet periods in the summer months, surface runoff enters the creek as overland flow. During dry periods, tiles do not flow and the surface flow from the swamps to the stream stops. During such periods, perennial groundwater inputs sustain stream baseflow. Under exceptionally dry periods such as the summer of 2001, the streamflow ceases altogether. However, farmers who have lived in the basin for longer than 30 years report that these dry periods are uncommon.

## **2.2 Methods**

Intensive field research for this study was conducted between January 2000 and February 2002. Data were collected in all months of the year, including winter. Although data collection was more intensive around storm and/or thaw events, it was also conducted between events.

### ***2.2.1 Hydrometric Variables***

Precipitation was measured continuously using a tipping-bucket rain gauge and recorded on a Campbell Scientific 21X data logger. The locations of the hydrometric instruments in the basin are shown in Figure 2.5.

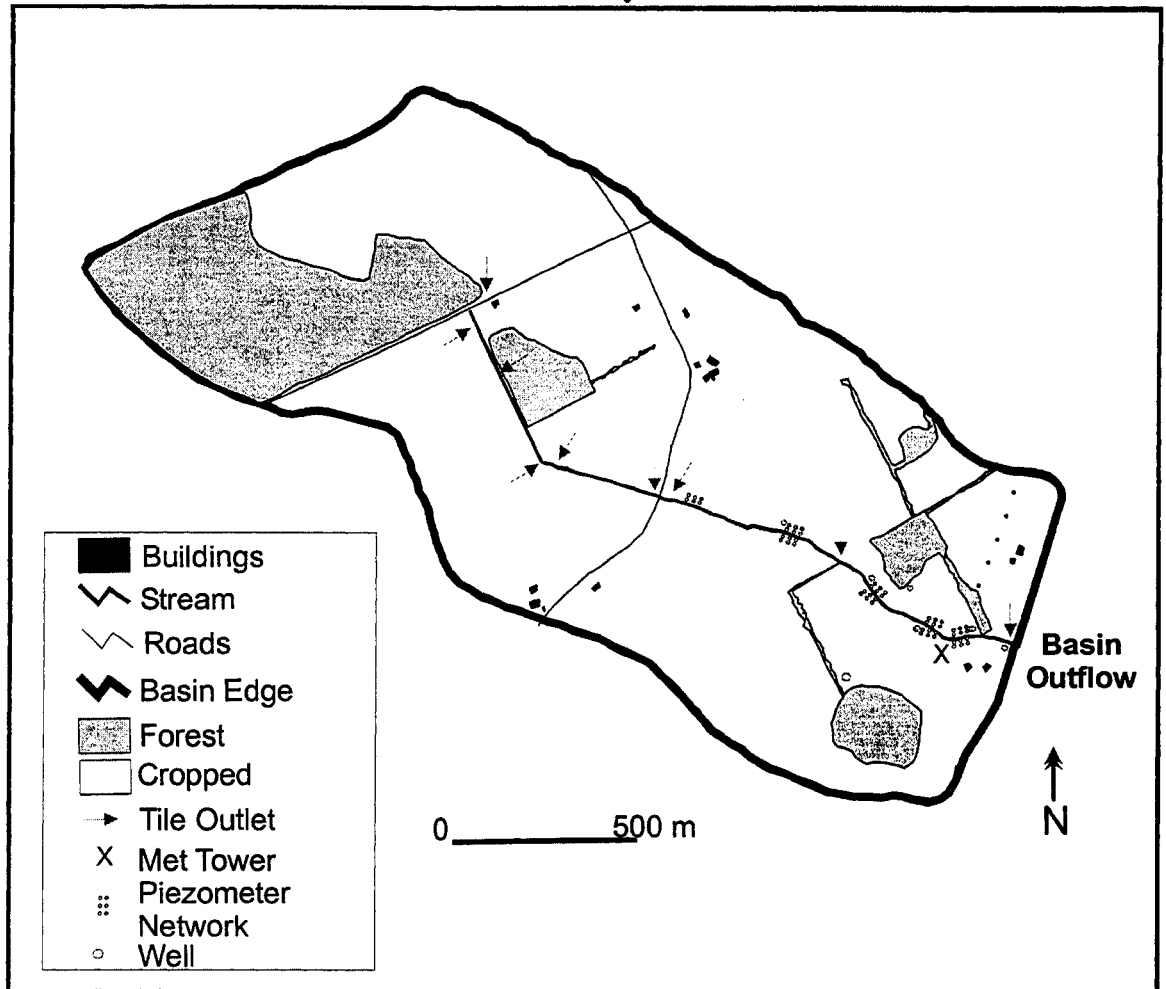
Stream discharge was recorded continuously at the basin outflow over the two-year period. Stream stage was measured by a potentiometer in an enclosed stilling well and recorded at 5-minute intervals by a Campbell Scientific CR10 data logger. Stream discharge was estimated from a stage-discharge relationship curve that was developed

from manual discharge measurements taken at the basin outflow over a five year period. Discharge values predicted by the stage-discharge relationship are within 13% of measured values.

The position of the water table was monitored at various locations in the study basin. Water table position in the near-stream zone at the basin outflow was recorded at 5-minute intervals by a Campbell CR10 data logger. The water table position was measured by a potentiometer and float in a PVC pipe (2-inch inner diameter) drilled into the riparian zone to a depth of 2 m. The water table position was also monitored manually at seven additional locations in the study basin (Figure 2.5) using a water level recorder. All wells were constructed of PVC pipe (2-inch inner diameter), and were screened along the entire length of the well. Most of the wells were inserted to 2.5 m depth, with the exception of one well in the riparian zone at the lower end of the basin, which was installed using an Envirocorer to a depth of 5 m.

Soil moisture in the unsaturated zone was measured manually using Time Domain Reflectometry (TDR), which uses the dielectric properties of water and soil to measure soil water content (Topp *et al.*, 1980). Four profiles of TDR probes were installed within the basin, three of which were in the near-stream zone (one fallow field and two cultivated fields) and the fourth set of probes was installed at the upland edge of a fallowing field) (Figure 2.5). At each site, four TDR probes were inserted horizontally into an 'undisturbed' wall of a 1.5 m soil pit and the soil pit was subsequently backfilled. In the soil pits, TDR probes were installed at 20, 40, 60 and 80 cm in the riparian zone of the fallow field and at 25, 50, 75 and 125 cm at the other two riparian zones. Probes were installed at 25, 75 and 125 cm in the upland fallow field.

**Figure 2.5 Location of instruments in the Strawberry Creek Watershed.**



Groundwater flow was monitored in the riparian zone at two locations along the stream reach but only intensively at one location (Figures 2.5, 2.6). Groundwater hydraulic gradients, a measure of the difference in hydraulic head over a given distance, were measured in piezometers. Piezometers were constructed of white PVC pipe (2" ID), screened over 25 cm. Piezometers were installed at depths ranging from 25 cm to 200 cm beneath the soil surface and were installed in transects across the riparian zone (Figures 2.6). Piezometer tips were covered with plastic caps to prevent rainwater from entering the pipes. Water levels inside of piezometers were measured with a water level recorder, and were monitored throughout all seasons of the year with sampling periods focused around hydrologic events.

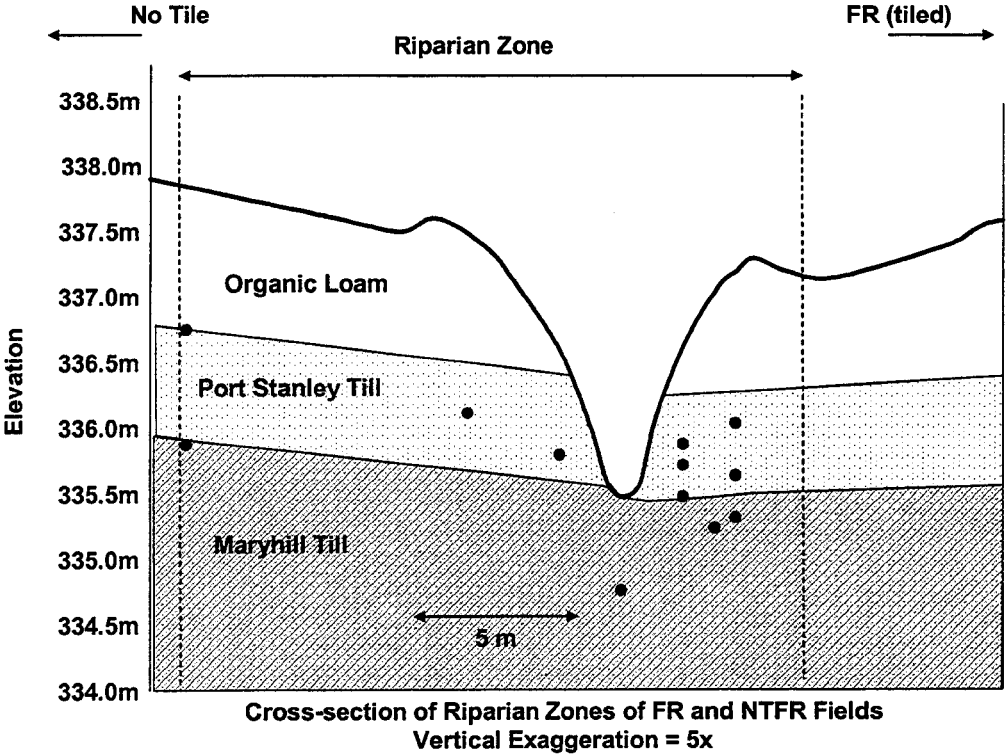
Hydraulic conductivities of riparian soils were determined using bail tests (Hvorslev, 1951). Piezometers were purged with a peristaltic pump and water levels inside of the piezometers were monitored until they had recovered to at least 63% of their initial levels. Hydraulic conductivity was then calculated by

$$K = \frac{r^2 \ln(L/R)}{2LT_o} \quad (2.1)$$

Where  $K$  is the hydraulic conductivity ( $\text{cm s}^{-1}$ ),  $r$  is the radius of the well casing (cm),  $R$  is the radius of the well screen (cm),  $L$  is the length of the well screen (cm),  $T_o$  is the time after the initiation of the test,  $H$  is the initial depth of water in the piezometer,  $H_o$  is the depth of water in the piezometer after bail extraction and  $H$  is the depth of water in the piezometer at time  $t$ .



**Figure 2.6 Cross-section of the riparian zone at the continuously monitored (FR) site, facing the upstream direction. Locations of piezometers (black dots) and soil horizons are shown in the figure.**



Diffuse groundwater (saturated) flow to the stream was predicted from Darcy's Law:

$$Q_D = kiA \quad (2.2)$$

where  $Q_D$  is the hydrologic export from diffuse (non-point) groundwater sources ( $\text{m}^{-3} \text{s}^{-1}$ ),  $k$  is the hydraulic conductivity ( $\text{m s}^{-1}$ ),  $i$  is the hydrologic gradient ( $\text{m/m}$ ) and  $A$  is the cross-sectional area of one metre of stream length ( $\text{m}^2$ ). Groundwater flow across the riparian zone was measured on both sides of the stream at two locations along the stream reach.

Discharge from seven of the nine tiles in the basin was monitored routinely over a 2.5 year period (January 2000 – February 2002). Two of the nine tiles in the basin are plugged and have not been flowing for several years (J. Renkema. Pers. Comm., 2002). Consequently, these tiles are not factored into calculations of tile discharge in the basin. Discharge was measured manually during low flow periods (bucket and stopwatch) or using a velocity metre (Marsh-McBirney) when the tile was partially or fully submerged beneath the stream water surface. During such periods, discharge was calculated as

$$Q_T = vA \quad (2.3)$$

where  $Q_T$  is hydrologic discharge from the tile ( $\text{m}^{-3} \text{s}^{-1}$ ),  $v$  is average flow velocity ( $\text{m s}^{-1}$ ) determined from velocity measured at increments across the tile outlet and  $A$  is the cross-sectional area of water flowing through the tile ( $\text{m}^2$ ) (Grant, 1981).

#### 2.2.1.1 Intensively Monitored Tile

Tile discharge was continuously recorded from one of the 9 tiles in the basin (FR tile) using a V-notch weir at the end of a tile (Figure 2.7). The tile drains 28 000  $\text{m}^2$  of the 84 500  $\text{m}^2$  field (33%) (Figure 2.8). The FR tile outlet is approximately 23 cm in

diameter. A 125 cm (h) x 50 cm (w) x 50 cm (l) stainless steel box was sealed to the end of the FR tile outlet pipe using a rubber connector, hose clamps and plumbing putty. A V-notch (15°) was cut into the front of the box (at the top). The base of the V was 50 cm above the base of the box (25 cm above the top of the tile), and extended to the top of the box. An enclosure welded into the inside of the box acted as a stilling well for a water level recorder. This enclosure was open at the bottom so that water levels would not be affected. Water levels in the enclosure were measured using a potentiometer and recorded at 5-minute intervals using a Campbell Scientific CR-10 data logger. Water level in the weir and the corresponding discharge through the V-notch were calibrated over a 1.5 year period. A propane heater was placed in the weir box in the winter months to prevent water in the weir box from freezing and sealing the base of the tile.

### ***2.2.2 Water Chemistry***

Stream water samples were collected both manually and using an automated ISCO sampler during “event” and “non-event” (baseflow) conditions between February 2000 and February 2002. All samples were collected in acid-washed (10% H<sub>2</sub>SO<sub>4</sub>) plastic nalgene bottles. Sample bottles were rinsed three times with stream water before the final sample was collected. Event samples were generally collected at 2 hour intervals throughout each event. Samples were collected less frequently between events, with the longest period between sampling periods being less than one month. A total of 553 samples were analyzed for SRP and NO<sub>3</sub><sup>-</sup> and a subset of 234 samples was analyzed for TP.

**Figure 2.7 Diagram of V-notch weir box on continuously monitored drainage tile (FR tile).**

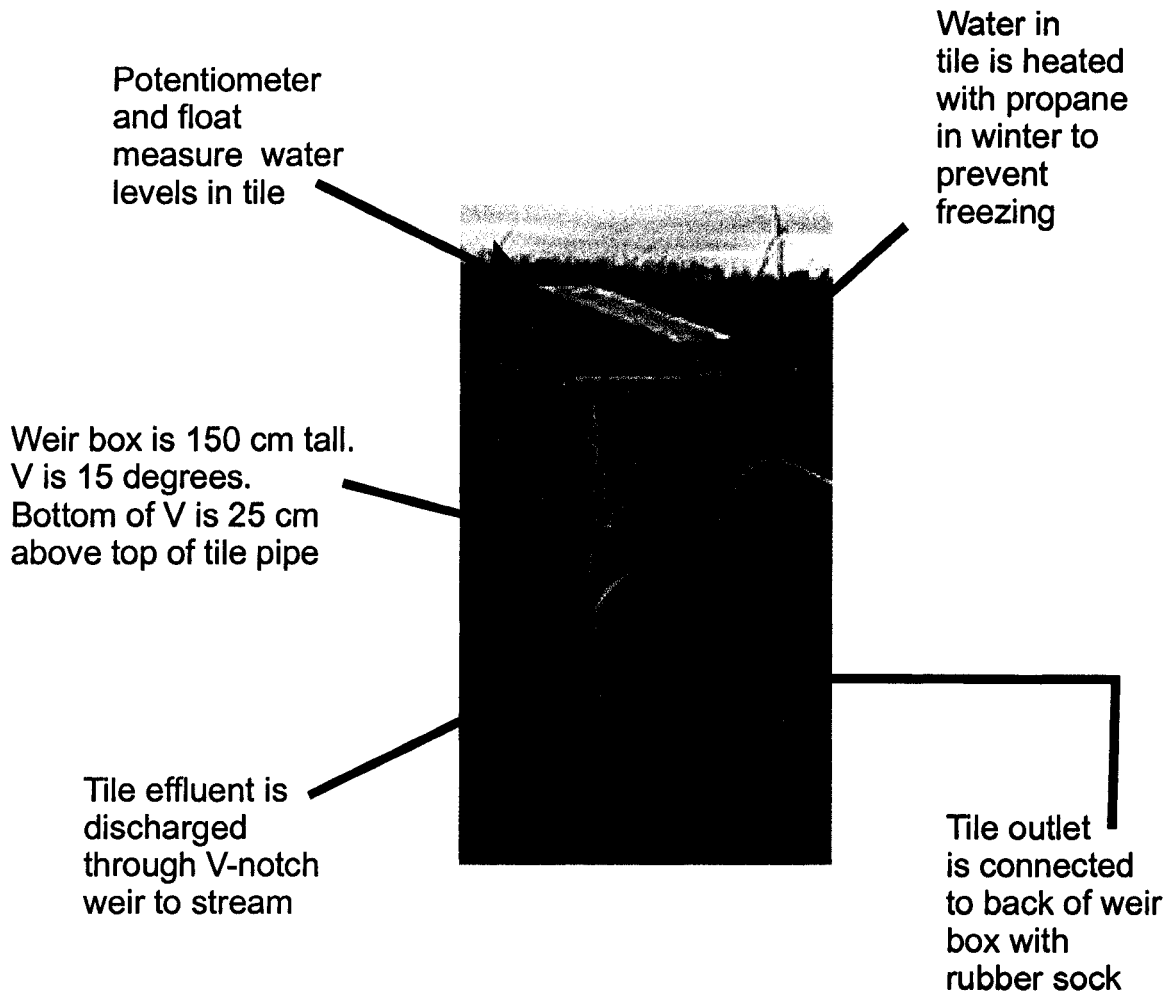
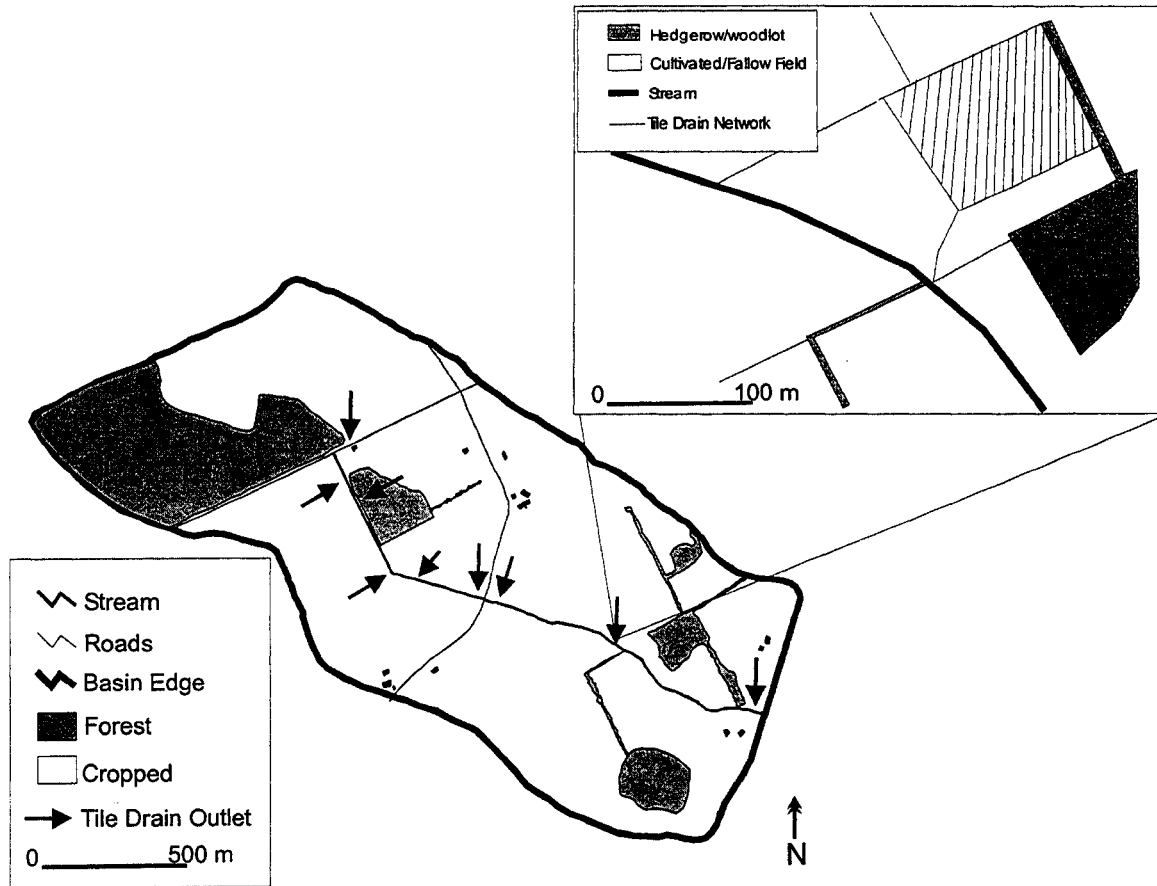


**Figure 2.8 Drainage tile network in the FR field. The header and feeder tiles in the FR field are shown in the inset.**



Tile effluent and groundwater samples were collected in acid-washed triple-rinsed 250 mL nalgene bottles. Groundwater samples were collected using a peristaltic pump. Pump tubing was rinsed with de-ionized water and flushed with a small amount of the groundwater sample before a sample was collected. Piezometers were purged and allowed to recharge prior to sampling to ensure that a good quality sample was obtained.

During low to moderate flow conditions, samples of tile effluent were collected at the tile outlet. However, during higher flows, tiles were frequently submerged, and samples of tile effluent were collected using a peristaltic pump with its tubing inserted 1 m into the tile.

During selected storm periods, effluent from one tile (FR tile) was collected using an automated ISCO sampler. Tubing from the ISCO was inserted approximately 1 m into the tile outlet. Samples were collected at 2-12 hour intervals throughout the various events.

Water samples were filtered (0.45  $\mu\text{m}$ ) immediately and stored in the dark at 2-4  $^{\circ}\text{C}$ . A 100 mL aliquot of the sample was acidified (0.2 %  $\text{H}_2\text{SO}_4$ ) and subsequently stored for TP processing. Prior to analysis for TP, samples were digested in 25 mL aliquots with 0.3 mL of saturated potassium persulphate and heated on hot plates until 2-5 mL of sample remained (Stone, 1993). Samples were then diluted to 25 mL with de-ionized water and filtered for TP analysis.

Samples were analysed on a Technicon Autoanalyser for  $\text{NO}_3^-$ -N, using Automated Cadmium Reduction and SRP and TP using Ammonium Molybdate-Stannous Chloride Reduction linked to NAP software (Environment Canada, 1979). The detection limits were 1  $\mu\text{g P L}^{-1}$  for SRP and TP and 0.1  $\text{mg N L}^{-1}$  for  $\text{NO}_3^-$ . The high range for

samples was 160  $\mu\text{g P L}^{-1}$  for SRP, 200  $\mu\text{g P L}^{-1}$  for TP, and 20  $\text{mg N L}^{-1}$  for  $\text{NO}_3^-$ . Samples exceeding these concentrations were diluted and re-analyzed. Analytical precision based on replicate analysis of 5% of all samples was generally  $\pm 5\%$  of reported values. Samples were generally analysed for SRP and  $\text{NO}_3^-$  within 1-2 weeks of collection. Samples were analysed for TP within 10 days of processing.

### 2.2.3 Data Analysis

#### 2.2.3.1 Interpolation of Nutrient Concentrations in Stream Flow

Nutrient concentrations for periods where samples were not collected were estimated using a method described by Scheider *et al.* (1979), Vanni *et al.* (2001) and Hill (1981). In this approach, concentrations are determined using one of two interpolation techniques (simple and discharge ( $Q$ ) proportionate). In the  $Q$ -proportionate method, nutrient concentrations are determined from the slope of a linear regression of  $Q$ - $C$  where  $Q$  is stream discharge ( $\text{L s}^{-1}$ ) and  $C$  is nutrient concentration ( $\mu\text{g L}^{-1}$ ). Where  $r^2 > 0.50$ , the slope of the relationship was used to estimate concentrations for periods when samples were not collected, but if  $r^2 < 0.50$  (after Hill, 1981), the simple interpolation method was employed. In the simple interpolation method, the concentration at any given hour ( $C_h$ ) is given by

$$C_h = C_{prev} + [(C_{next} - C_{prev}) \cdot ((h - h_{prev}) / (h_{next} - h_{prev}))], \quad (2.4)$$

where  $C_{prev}$ ,  $C_{next}$ ,  $h_{prev}$ , and  $h_{next}$  are the concentration and time of previous and next sample, respectively. Due to high variability in the data, it was necessary to explore the  $Q$ - $C$  relationship on an individual event basis, and occasionally at small time steps within a given event (e.g. 12-24 hours).

#### 2.2.3.2 Classification of Individual Events

Individual events were identified using hydrograph analysis (McCuen, 1998). In this paper, events are defined based on hydrograph response rather than precipitation events. An event was considered to have started once the hydrograph began to rise following precipitation or melt. An event was considered to be finished once conditions had returned to baseflow. Baseflow was determined using the constant slope method (McCuen, 1998) where individual events could be isolated and stable flow was apparent during both pre- and post-event flow. If two or more successive events occurred, the hydrologic contribution of individual events was determined using a synthetic recession curve.



### **3.0 Temporal Patterns of Nutrient Export from a First-order Agricultural Basin in Southern Ontario**

#### **3.1 Introduction**

Nutrient export from agricultural areas can lead to the eutrophication of surface waters (Carpenter *et al.*, 1998). Nutrient export rates from agricultural areas are difficult to predict because they often come from non-point sources which depend on flowpaths (Carlyle and Hill, 2001; Gburek and Sharpley, 1998; Stamm *et al.*, 1998; Cirimo and McDonnell, 1997; Hill, 1996; Sharpley, 1995; Hill, 1990), and may vary temporally and spatially among catchments. It is well known that elevated rates of nutrient loading occur during storm events (*e.g.* Douglas *et al.*, 1998; Gburek and Sharpley, 1998; Sims *et al.*, 1998; Hill, 1981; Schuman *et al.* 1973) but the reasons why similar storms produce entirely different nutrient export patterns are poorly understood. There is a need to better understand how hydrological processes are coupled with nutrient sources (McDowell *et al.*, 2001; Daniel *et al.*, 1998; Gburek and Sharpley, 1998; Hill, 1996; Cirimo and McDonnell, 1997) and how this leads to temporal variability in nutrient export.

Budget and logistical constraints often limit the frequency with which storm events can be sampled. Annual estimates of nutrient export are often extrapolated from a small number of events and may exclude certain times of the year. These sampling frequencies may not be sufficient to generate accurate estimates of annual nutrient export.

The objectives of this study are (1) to quantify annual SRP, TP and NO<sub>3</sub><sup>-</sup> export (2 years) from a first order agricultural basin in Southern Ontario; (2) to examine temporal variability in nutrient export, especially the significance of the snowmelt period and high magnitude events in annual nutrient export; (3) to quantify the potential error associated

with missing one or more high magnitude events; and (4) to examine the importance of sampling frequency in generating estimates of export rates during storm events.

### **3.2 Site Description and Methods**

The research site and methods are provided in detail in Chapter Two.

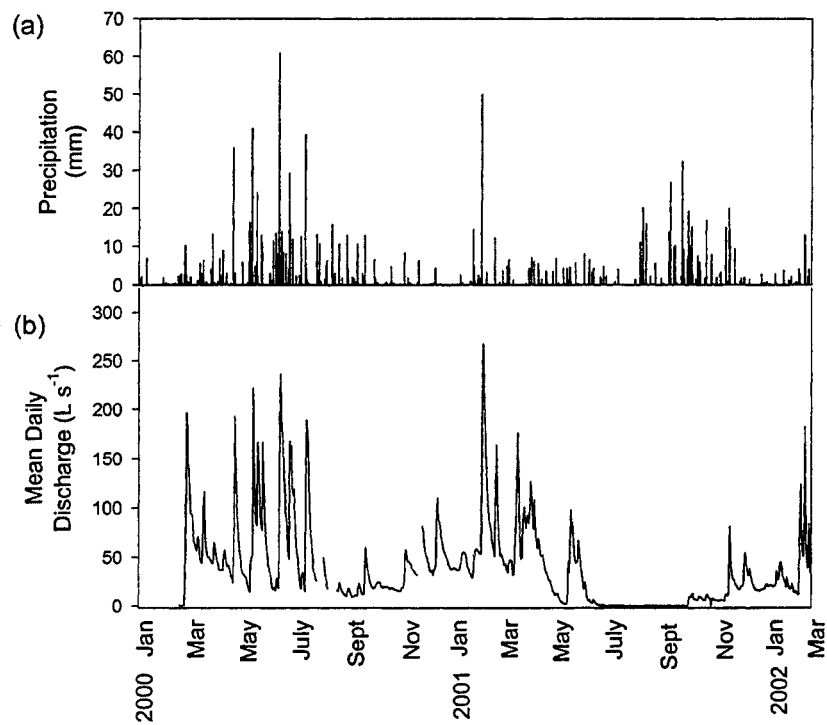
### **3.3 Results and Discussion**

#### ***3.3.1 Inter-annual Comparison of Discharge and Nutrient Export Patterns***

Hydroclimatic conditions differed between the two study years (Fig. 3.1). Total precipitation was similar in both study years (743 mm in 2000, 633 mm and 2001), but lower than the 30-year mean annual precipitation for the Waterloo region (908 mm; Environment Canada, 2003). However, the distribution of rainfall and runoff varied substantially between the study years (Fig. 3.1). The summer of 2000 (332 mm rainfall) was substantially wetter than the summer of 2001 (130 mm rainfall). The winter/early spring and autumn seasons of 2001 (52 mm snow + 100 mm rain in winter/early spring, 282 mm rain in autumn) were wetter than those in 2000 (37 mm snow + 38 mm rain in winter/early spring, 89 mm rain in autumn). Flow rates during low flow periods ranged from 0 (ephemeral) to 30 L s<sup>-1</sup> and event-related flow ranged from 30 to 450 L s<sup>-1</sup> (Fig.3.2).

Nutrient export was significantly higher in 2000 (0.40 kg TP ha<sup>-1</sup>, 0.12 kg SRP ha<sup>-1</sup> and 39.06 kg NO<sub>3</sub><sup>-</sup>-N ha<sup>-1</sup>) than in 2001 (0.27 kg TP ha<sup>-1</sup>, 0.06 kg SRP ha<sup>-1</sup> and 29.50 kg NO<sub>3</sub><sup>-</sup>-N ha<sup>-1</sup>; Table 3.1). These results are consistent with other studies of agricultural systems, where particulate P is the main form of P exported, and NO<sub>3</sub><sup>-</sup> is the predominant

**Figure 3.1: (a) Total daily precipitation and (b) daily mean hydrologic export for the 25-month study period.**



form of N exported (Vanni *et al.*, 2001; Baker, 1993; Logan, 1990). Annual estimates of nutrient export from Strawberry Creek are within the wide range of estimates of nutrient export that have been provided in the literature (0.02 – 48 kg TP ha<sup>-1</sup> yr<sup>-1</sup>, 0.01 – 2.2 kg SRP ha<sup>-1</sup> yr<sup>-1</sup>, 0.04 – 44.8 kg NO<sub>3</sub><sup>-</sup>-N ha<sup>-1</sup> yr<sup>-1</sup>) (Vanni *et al.*, 2001; Douglas *et al.*, 1998; Jordan *et al.*, 1997; Baker, 1993; Hill, 1981; Sharpley and Syers, 1981; Dillon and Kirchner, 1975; Schuman *et al.* 1973). The large range reported in the literature is attributed to factors including land use, soil type and basin geomorphology, fertilizer type and timing of application, tillage practice, and drainage characteristics.

Although these results are within the range of export coefficients reported in the literature, P export from the study basin is low, whereas NO<sub>3</sub><sup>-</sup> export is high. Higher levels of P export are often observed from fields with livestock and the application of organic fertilizers or in areas where erosion is prevalent. Organic fertilizers are applied to a small proportion of the Strawberry Creek Watershed (15%), and overland flow is uncommon in the basin. Consequently, soil losses due to erosion are small. NO<sub>3</sub><sup>-</sup> export from the study basin, however, is high. Although the stream is bounded by a grassed buffer strip, the riparian areas are narrow (<10m). Also, 60% of the drainage basin is tiled, causing a substantial portion of runoff to bypass soils.

Higher nutrient concentrations were not always observed during discharge peaks in both study years (Fig.3.2). However, most nutrient export occurred during winter thaw/snowmelt and storm events. Twenty-seven events occurred in 2000, accounting for 80%, 83%, and 73% of annual TP, SRP and NO<sub>3</sub><sup>-</sup> export, whereas 28 events occurred in 2001, accounting for 70%, 83%, and 67% of annual TP, SRP and NO<sub>3</sub><sup>-</sup> export (Table 3.1, Fig.3.3). Cumulatively, these events accounted for only 64% and 63% of annual

**Figure 3.2: (a) Hourly hydrologic export (left axis, grey line), and SRP (●) and TP (○) concentrations in stream water at the basin outflow. (b) Hourly hydrologic export and NO<sub>3</sub><sup>-</sup> concentrations in stream water at the basin outflow.**

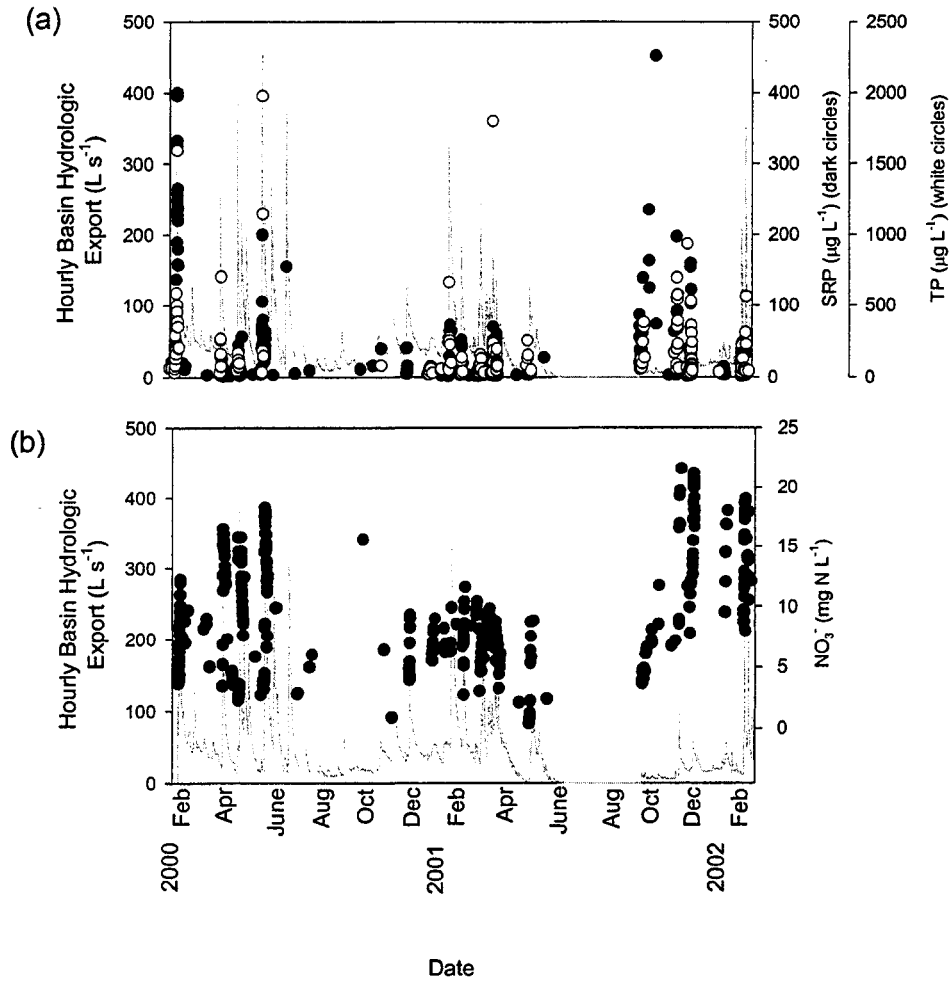
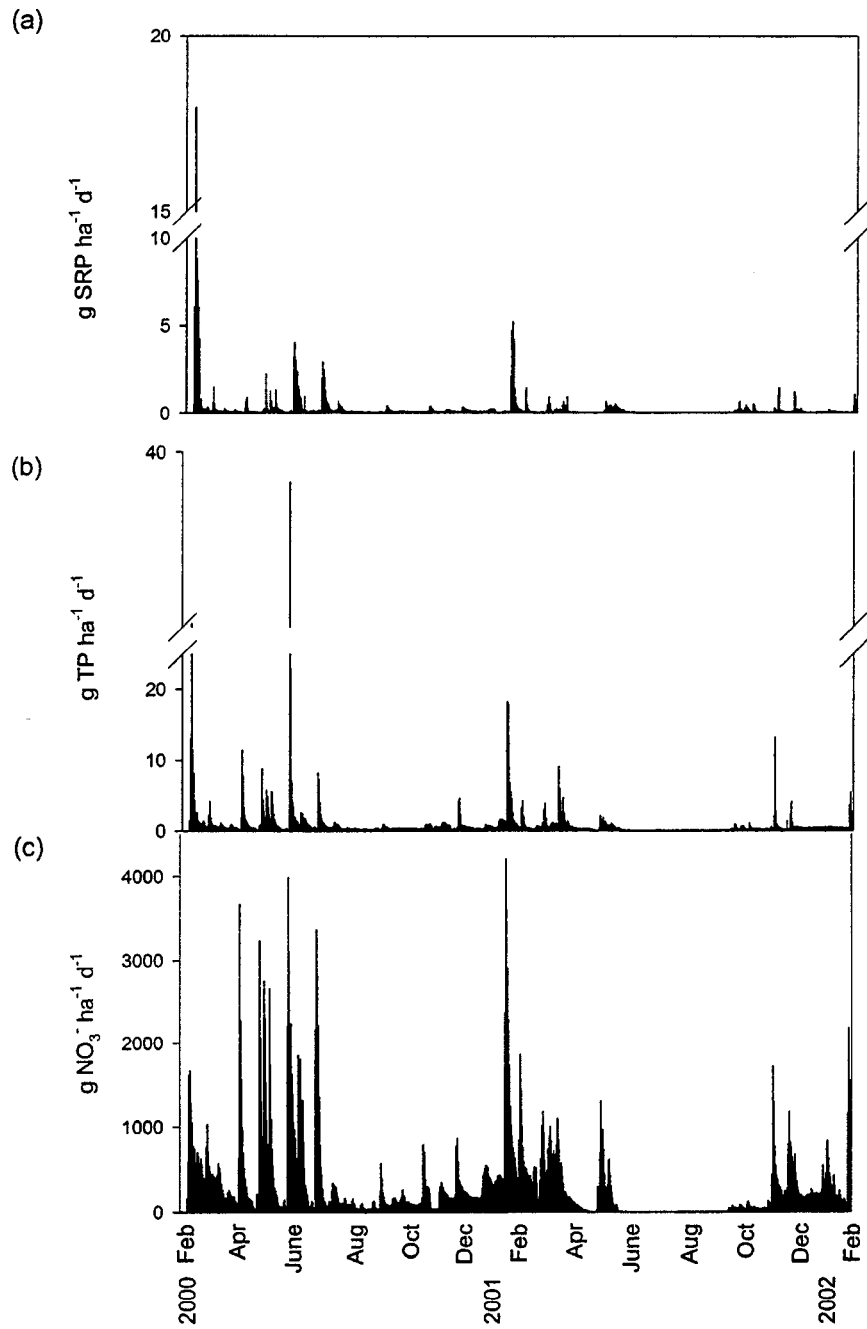


Figure 3.3: Daily total mass export ( $\text{kg ha}^{-1} \text{d}^{-1}$ ) of (a) SRP, (b) TP and (c)  $\text{NO}_3^-$  for the study period.



**Table 3.1: Annual Nutrient Export from Strawberry Creek. Total nutrient export for each study year and the 25-month study period are presented. This number is expressed as the percentage (%) contribution of these events to total annual export in brackets. The number of events contributing to this value is shown in italics on the right hand side outside of the brackets. Nutrient contributions during baseflow periods and events are shown, and events are also sub-divided into ‘high magnitude’ and ‘normal’ events.**

	kg TP ha <sup>-1</sup>	kg SRP ha <sup>-1</sup>	kg NO <sub>3</sub> <sup>-</sup> -N ha <sup>-1</sup>	Hydrologic Export (mm)
2000				
Σ all events	0.32 (80%) 27	0.10 (83%) 27	28.62 (73%) 27	320 (64 %) 27
Σ high mag. events	0.17 (43%) 2	0.07 (58%) 2	9.38 (24%) 2	97 (20 %) 2
Σ normal events	0.15 (37%) 25	0.03 (25%) 25	19.24 (49%) 24	223 (44 %) 25
Σ baseflow	0.08 (20%)	0.02 (17%)	10.44 (27%)	182 (36 %)
Σ annual export	0.40 (100%)	0.12 (100 %)	39.06 (100%)	502 (100 %)
2001				
Σ all events	0.19 (70%) 28	0.05 (83%) 28	19.75 (67%) 28	226 (63 %) 28
Σ high mag. events	0.05 (18%) 1	0.00 (0%) 0	3.87 (13%) 1	34 (9%) 1
Σ normal events	0.14 (52%) 27	0.05 (83%) 28	15.89 (54%) 27	193 (54%) 27
Σ baseflow	0.07 (30%)	0.01 (17%)	9.75 (33%)	135 (37%)
Σ annual export	0.27 (100%)	0.06 (100 %)	29.50 (100%)	361 (100 %)
Study Period (Feb/00- Feb/02)				
Σ all events	0.55 (75%) 64	0.15 (83%) 64	52.99 (69%) 64	580 (63%) 64
Σ high mag. events	0.22 (30%) 3	0.07 (39%) 2	13.25 (17%) 3	131 (15%) 3
Σ normal events	0.33 (45%) 61	0.08 (53%) 62	39.74 (52%) 61	449 (48%) 60
Σ baseflow	0.18 (25%)	0.03 (17%)	23.56 (31%)	347 (37%)
Σ export	0.73 (100%)	0.18 (100 %)	76.55 (100%)	927 (100 %)

hydrologic discharge in 2000 and 2001 suggesting that nutrients are exported more efficiently during thaw or storm events than during baseflow conditions.

### 3.3.2 Seasonal Nutrient Export Patterns

Twenty winter thaws occurred during the study period (Fig. 3.3). Winter thaw events (including the main snowmelt event) in 2000 and 2001 accounted for a substantial portion of annual TP (25% and 37%), SRP (48% and 42%), NO<sub>3</sub><sup>-</sup> (13% and 36%), and hydrologic export (13% and 32%).

In general, export during events did not differ in magnitude between summer and winter events. This was not expected, as biological nutrient uptake mechanisms differ

between seasons. Nutrient export during summer events was expected to be lower in magnitude due to the hydrologic flowpaths that dominate in summer, and, the activity of riparian vegetation and soil microorganisms. During the winter months in Southern Ontario, the presence of ground frost impedes drainage and overland flow may occur during thaw events. Also, riparian vegetation is dormant during this period, and biotic uptake is thought to be minimized. Consequently, winter storm export was expected to be higher than summer storm export.

The lack of seasonal variability may be partly explained by the presence of drainage tiles within the basin. Since 60% of the basin is tiled, nutrients may be bypassing natural soil processes, thereby reducing the biotic removal of nutrients. Furthermore, the tiles may rapidly route water out of the basin instead of allowing it to pass over soils as overland flow.

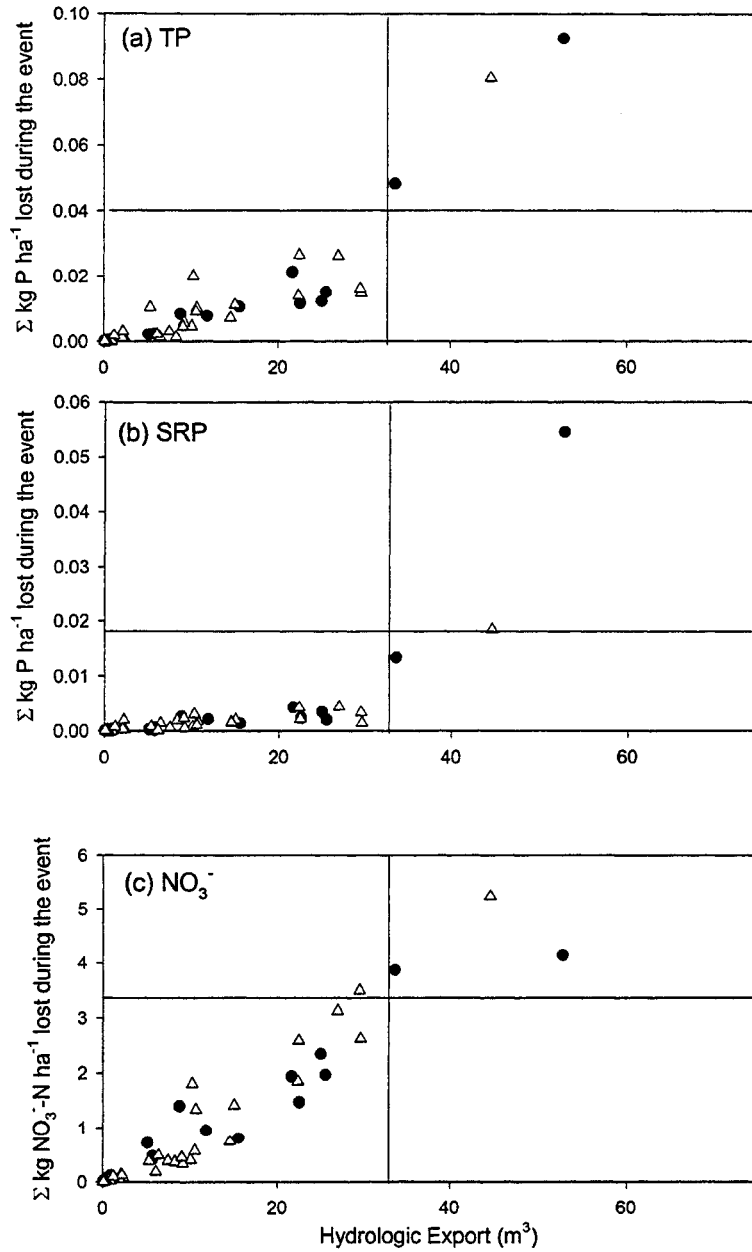
Although the magnitudes of events did not differ between winter and summer, the number of events and the proportion of annual export was higher in winter than in summer. Snowmelt often represents a significant proportion of nutrient export from agricultural basins (Zuzel *et al.*, 1993; McCool *et al.*, 1982). This illustrates the importance of including the winter period in sampling regimes.

### ***3.3.3 Differences in Hydrochemical Export Between Events***

Hydrologic discharge per event is compared to nutrient export in Figure 3.4. If nutrient export is simply a function of hydrologic export, there is expected to be a strong linear correlation in the figure.  $\text{NO}_3^-$  export is strongly related to discharge during events



**Figure 3.4: Total export of (a) TP and (b) SRP and (c)  $\text{NO}_3^-$  (the sum of  $\text{kg ha}^{-1}$  over each entire event) are plotted against total hydrologic discharge (mm) throughout the duration of the storm (x axis). Winter storms are shown with dark circles and spring, summer, and fall storms are shown with white triangles. Storms that are of high magnitude in nutrient and hydrologic export are separated from all other storms with a line.**



ranging from small to large in magnitude, suggesting that if discharge is recorded throughout a given event,  $\text{NO}_3^-$  export can be easily predicted. During events that are low in magnitude, the relationships between discharge and SRP and TP export are linear. These data suggest that for  $\text{NO}_3^-$  during all events, and, SRP and TP during events that are low in magnitude, the sampling of individual events is no longer necessary once the relationship between discharge and nutrient export is developed. However, for events that are high in magnitude, the relationships between discharge and SRP and TP change, hindering our ability to predict P export. This is likely due to changing flowpaths or delivery mechanisms. During events that are high in magnitude, overland flow typically occurs for a short period throughout the events, delivering a substantial quantity of P to the stream. TP concentrations measured in overland flow have exceeded  $10000 \mu\text{g L}^{-1}$ . The exceptionally high P export is a result of a large amount of runoff interacting with a large P source (surface soils). P export during these events is very unpredictable, demonstrating the importance of understanding how hydrology couples with P pools within a catchment.

A very limited number of events account for a large proportion of both discharge as well as nutrient export. These events are *high magnitude*, operationally defined as events exporting loads more than two standard deviations above the geometric mean (based on the range of events observed over the entire study period). Mean nutrient export coefficients of the 64 events over the study period were  $0.01 \pm 0.02 \text{ kg TP ha}^{-1}$ ,  $0.002 \pm 0.008 \text{ kg SRP ha}^{-1}$  and  $0.9 \pm 1.2 \text{ kg NO}_3^- \text{-N ha}^{-1}$ . Mean hydrologic discharge per event was  $10 \pm 12 \text{ mm}$  per event. Thus, export coefficients exceeding  $0.04 \text{ kg TP ha}^{-1}$ ,

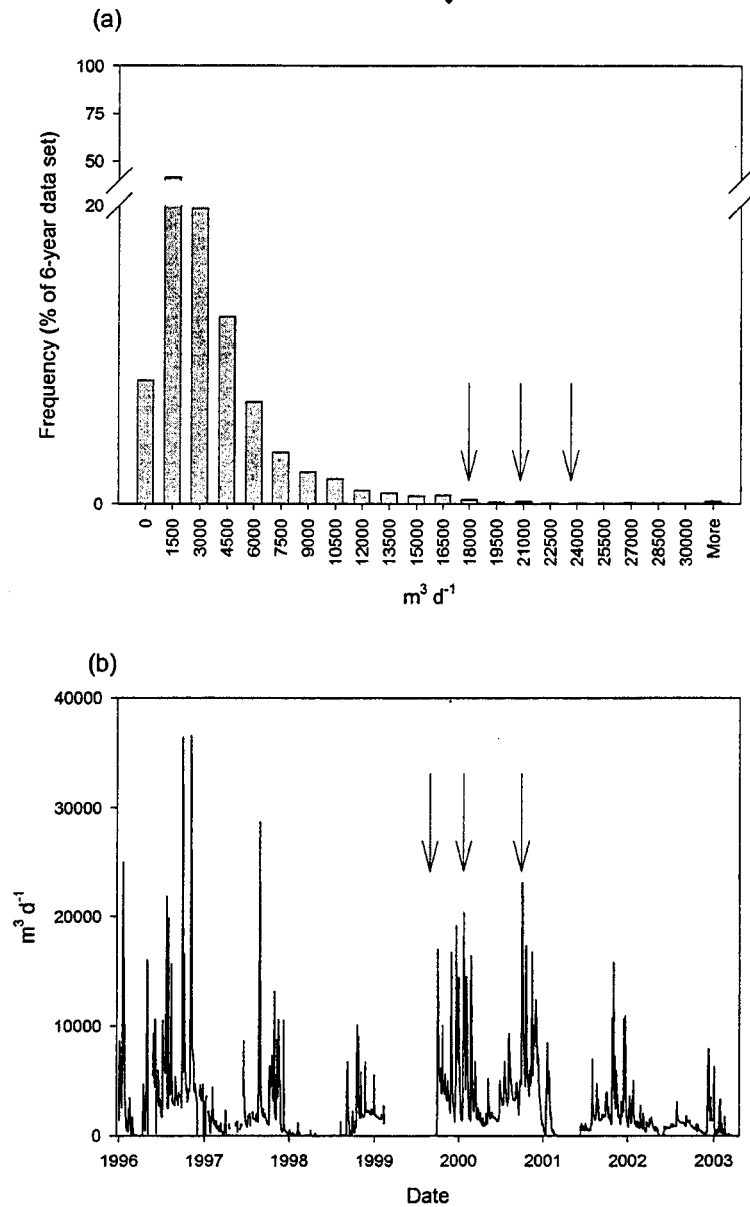
0.02 kg SRP ha<sup>-1</sup>, 3.35 kg NO<sub>3</sub><sup>-</sup>-N ha<sup>-1</sup> and 34 mm per event were classified as *high magnitude* based on the data collected in the current study.

Given these criteria, three of the 64 events over the study period can be classified as *high magnitude*. Two of the three high magnitude events were winter thaw events (February 2000 and February, 2001) and the third high magnitude event occurred in June, 2000 following more than 120 mm of rainfall (Table 3.1, Figures 3.3 and 3.4). Thus, high magnitude events are not limited to the winter period.

The dominance of a few major events in annual estimates of nutrient mass exports has been reported elsewhere (Ulen and Persson, 1999; Brunet and Astin, 1998; Douglas *et al.*, 1998; Pionke *et al.*, 1996; Zuzel *et al.*, 1993; Edwards and Owens, 1991; Douglas *et al.*, 1988; McCool *et al.*, 1982; Hill, 1981; Schuman *et al.*, 1973). However, these studies have been conducted on larger basins in different geographical regions and at larger scales. The study basin is a small first-order agricultural basin in Southern Ontario, and is likely representative of many headwater streams draining agricultural basins in this region.

A frequency histogram (Fig. 3.5a) shows that high magnitudes of discharge do not occur at high frequencies in the study basin. However, the hydrograph of basin discharge from 1996 to 2003 (Fig. 3.5b) shows the temporal distribution of the high magnitude events, and shows that such events occurred in each of the eight years of the data record. This suggests that the distribution of high magnitude events during 2000 and 2001 are representative of the distribution of high magnitude events in any given year (based on an eight year data record), and implies that an event of high magnitude can be expected in any given year.

**Figure 3.5: (a) Frequency histogram of daily basin discharge from the Strawberry Creek Watershed between 1996 and 2003, and (b) Basin discharge between 1996 and 2003. The three high magnitude events that occurred in 2000 and 2001 are marked with arrows in both graphs.**



### ***3.3.4 Importance of Flowpaths to Nutrient Export***

Changing hydrologic flowpaths can have a dramatic effect on nutrient export patterns and magnitudes. Also, individual events may export substantial quantities of one nutrient but not the other nutrient. Some events (e.g. February 2000 snowmelt) exported large quantities of SRP and TP, but not as much  $\text{NO}_3^-$ . Conversely, many events exported substantial quantities of  $\text{NO}_3^-$  but little SRP or TP. These observations are attributed to differences in the mechanisms and processes driving SRP, TP, and  $\text{NO}_3^-$  export. Elevated SRP and TP export have been linked to both overland flow, and the rapid routing of runoff from surface soils to aquatic systems via preferential flow into drainage tiles (Gburek and Sharpley, 1998; Stamm *et al.*, 1998). Elevated levels of  $\text{NO}_3^-$  export have been associated with a high water table, where  $\text{NO}_3^-$  that has accumulated in surface and shallow soils is rapidly routed through upper soil layers or through preferential flowpaths and drainage tiles toward aquatic systems. This further illustrates the importance of examining *processes* occurring within individual events to explain why a particular event may export large quantities of one nutrient, yet smaller quantities of another nutrient.

The three high magnitude events that occurred over the study period were driven by different processes. For example, during the high magnitude summer storm (June 2000), riparian areas were inundated and saturation overland flow occurred for several days. Substantial quantities of nutrients were exported during this time, due to the interaction of surface runoff with nutrient pools in higher soil horizons.  $\text{NO}_3^-$  export during this event was particularly high.

The February 2001 snowmelt event exported large quantities of discharge and TP and  $\text{NO}_3^-$ . This event followed 50 mm of rain and 25 mm (50%) of the snowpack was lost

during the event. During this period, standing water was observed in some of the fields, and runoff was observed entering the stream as overland flow from a few fields in the study basin.

The February 2000 event was of high magnitude in its discharge and export of SRP, TP and  $\text{NO}_3^-$ . For a period of six weeks prior to this event, temperatures were cold (mean air temperature was  $-8.9^\circ\text{C}$ ) and dry (streamflow  $< 1 \text{ L s}^{-1}$ ). At Strawberry Creek, manure was applied to 15% of the basin a few days prior to the February 2000 snowmelt event. The onset of this snowmelt event was prompted by a rain-on-snow event (12 mm) and high air temperatures (daily highs of  $+12^\circ\text{C}$ ). The entire snowpack (35 mm) was lost within three days. Standing water was observed on all of the fields during this period and riparian areas were inundated. Substantial quantities of SRP and PP were exported via overland flow as well as through drainage tiles. The substantial P export (80% of TP was as SRP) during this period was a result of the interaction of ponded water on the soil surface with the substantial P pool in the fields where manure had been applied. Mid-winter or spring runoff events coupled with the application of organic fertilizers has resulted in the excessive export of SRP in other studies (Cooke and Prepas, 1998; Schuman *et al.*, 1973).

The observed nutrient export during these high magnitude events results from a combination of the timing and type of fertilizer application, hydroclimatic conditions during and prior to the events themselves, and, the flowpaths through which the nutrients reached the stream channel. These factors have been shown to be important in other study basins (Gburek and Sharpley, 1998; Stamm *et al.*, 1998; Cirimo and McDonnell, 1997; Creed and Band, 1998; Sharpley *et al.*, 1983; Schuman *et al.*, 1973).

During all three high magnitude events, overland flow was observed for an extended period of time throughout the event. These prolonged periods of surface saturation resulted from the addition of large amounts of moisture to the basin (i.e. very large storms or thaws). Although overland flow occurred during other storms throughout the study period, such incidences were minimal and of very short duration. High magnitude events appear to be driven by the prolonged interaction of water at or near the soil surface with nutrient pools in upper soil horizons, and nutrients are exported from fields via both overland flow and drainage tiles during these events.

### ***3.3.5 Importance of High Magnitude Events in Annual Estimates***

*High magnitude* events accounted for substantial proportions of annual nutrient export in both study years (Table 3.1). Over the 25-month study period, three events accounted for 30% of total TP export and two events accounted for 39% of total SRP export. Three events accounted for 17% of total  $\text{NO}_3^-$  export. The same three events accounted for only 15% of the hydrologic discharge over the study period. If high magnitude events are missed, annual estimates of nutrient export would be significantly underestimated.

### ***3.3.6 Importance of Sampling Frequency in Estimates of Nutrient Export***

The sampling frequency of thaw or storm events can dramatically affect the estimated nutrient mass export. The ranges in possible estimates of SRP, TP and  $\text{NO}_3^-$  export under different sampling frequencies are shown in Figures 3.6, 3.7 and 3.8, respectively for portions of three selected events. The estimates presented are based on samples collected over 1.5 to 2 days (at 2-3 hour intervals) for each of the three events.

**Figure 3.6: The effect of sampling frequency on the range of possible estimates of SRP export in December 2001, February 2001 and April 2001 are shown in (a), (b) and (c). The observed SRP export (based on 2-3 hour sampling intervals and a total of 20, 17 and 12 samples in a-c, respectively) are shown with a solid line. The ranges in possible estimates of SRP export based on fewer samples are shown by error bars. The right y-axis expresses the SRP export as a percentage of the observed SRP export during each event.**

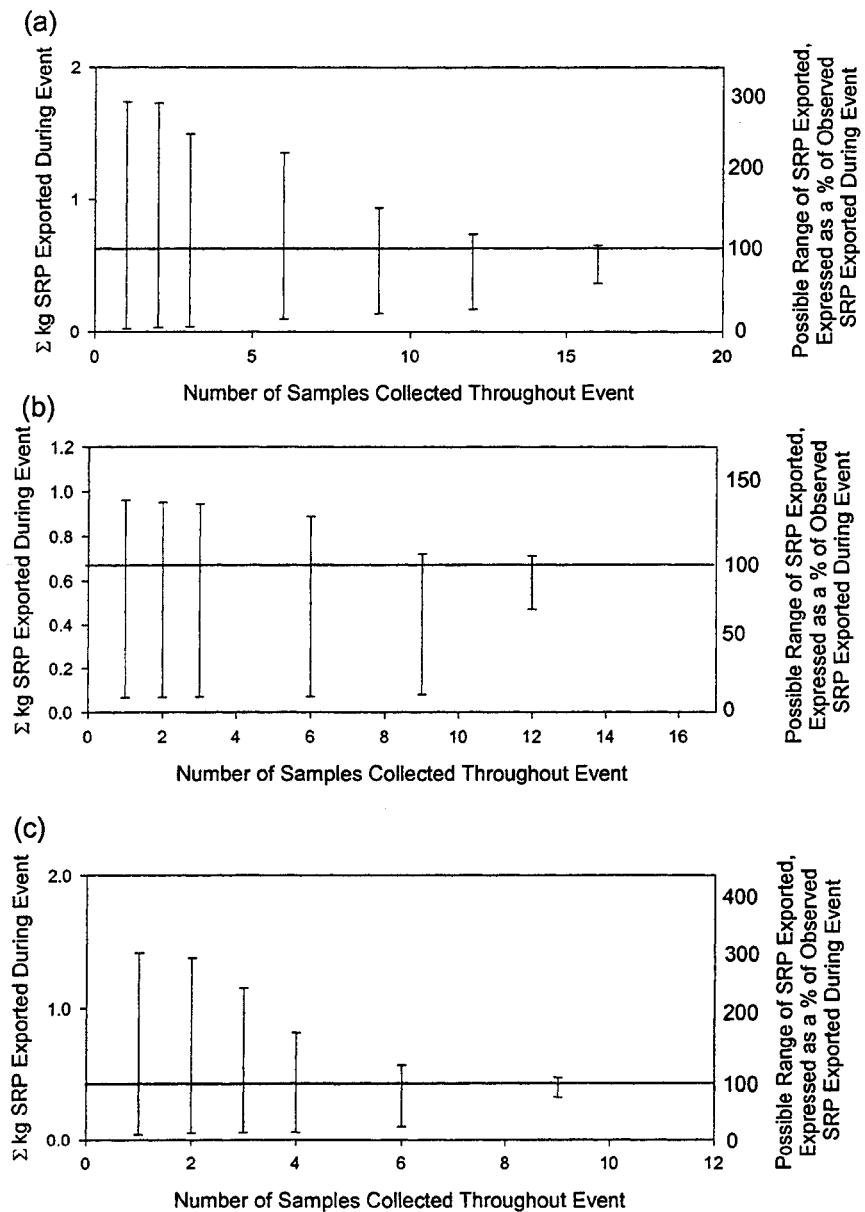




**Figure 3.7: The effect of sampling frequency on the range of possible estimates of TP export in December 2001 and April 2001 are shown in (a) and (b). The observed TP export (based on 2-3 hour sampling intervals, and a total of 20 and 12 collected samples in a and b, respectively) are shown with a solid line. The ranges in possible estimates of TP export based on fewer samples are shown by error bars. The right y-axis expresses the TP export as a percentage of the observed TP export during each event.**

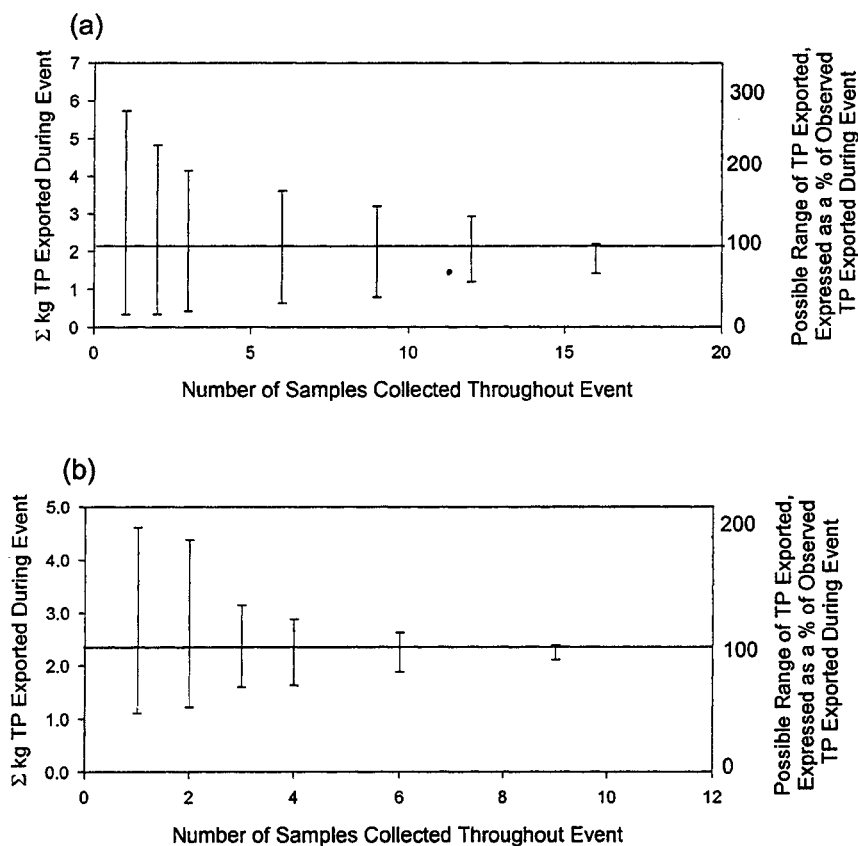
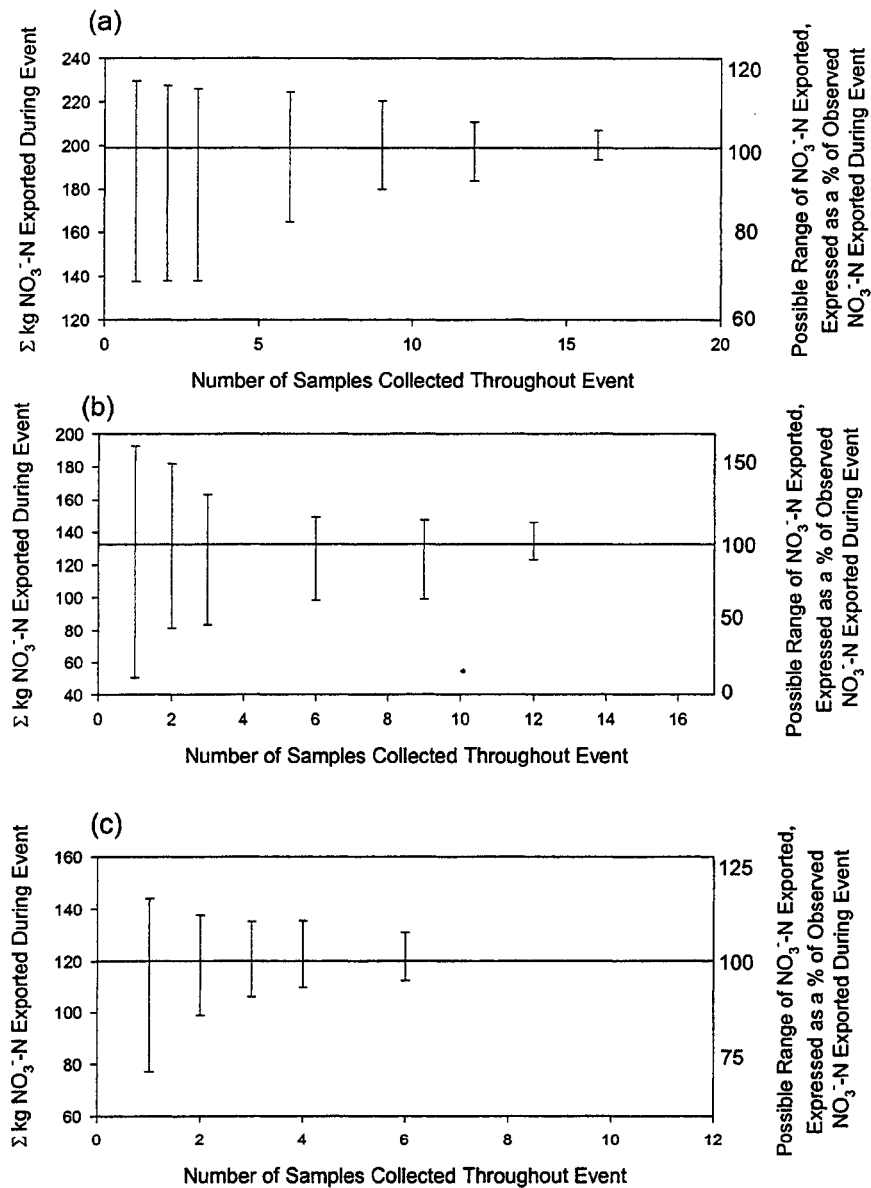


**Figure 3.8: The effect of sampling frequency on the range of possible estimates of  $\text{NO}_3^-$  export in December 2001, February 2001 and April 2001 are shown in (a), (b) and (c). The observed  $\text{NO}_3^-$  export (based on 2-3 hour sampling intervals and a total of 20, 17 and 12 samples in a-c, respectively) are shown with a solid line. The ranges in possible estimates of  $\text{NO}_3^-$  export based on fewer samples are shown by error bars. The right y-axis expresses the  $\text{NO}_3^-$  export as a percentage of the observed  $\text{NO}_3^-$  export during each event.**



Ranges in possible estimates were determined by selecting the maximum and minimum concentrations at each sampling frequency and interpolating between these values. Interpolated concentrations were subsequently multiplied by the observed discharge throughout the event to generate ranges in estimates of nutrient export. The range in estimates of nutrient export narrows as sampling frequency increases. This is because short pulses of high nutrient concentrations are less likely to be missed with a more frequent sampling regime. This is particularly important for P, which may be exported during very short time periods. Collecting 1-3 samples over a 2 day period is clearly inadequate as it may result in underestimations of nearly 100% and overestimations of several hundred percent for all three nutrients. However, an intensive sampling interval such as every two hours may not be essential to generate precise estimates of nutrient loading and a less frequent sampling interval may be sufficient. Phosphorus export occurs much more sporadically than  $\text{NO}_3^-$  and sampling interval can therefore be tailored to specific nutrients. For example, a 4-6 hour sampling interval would generate estimates of  $\text{NO}_3^-$  export within 10-20% of estimates obtained with a two-hour sampling interval. However, to remain within 20% of estimates obtained by a two-hour sampling interval, SRP and TP concentrations must be sampled at least every 3 hours. Sampling for SRP and TP less frequently than this (e.g. 4-6 hours) may result in estimates that are out by nearly 100%.

Given the importance of sampling frequency in attaining precise estimates of nutrient export rates, we need to rethink how we currently monitor nutrient export from small first-order drainage basins in Southern Ontario. This chapter has shown that the majority of nutrients are exported during storm and thaw events rather than baseflow

periods (Table 3.1). Figure 3.4 has shown that during low to moderate magnitude events, P export can be predicted from discharge, although these relationships break down for high magnitude events.  $\text{NO}_3^-$  export can be predicted from discharge during all events. Figures 3.6-3.8 have shown that an intensive sampling frequency (2-6 hours intervals throughout moderate to large events) is necessary to attain precise estimates of nutrient export.

Routine sampling frequencies (e.g. weekly) are inadequate to attain precise estimates of nutrient export given the episodic nature of nutrient export. A better monitoring strategy might be to sample intensively for an extended number of events to generate a discharge-mass relationship for a given basin (e.g. Fig. 3.4) and then apply this to subsequent events. High magnitude events, however, must be monitored intensively. Such events would include the snowmelt period in Southern Ontario, and major precipitation events year round.

### **3.4 Conclusions**

Intensive sampling over a 25-month period has demonstrated temporal variability in discharge and nutrient export patterns, and, has shown that the majority of nutrients are exported during storm and thaw events rather than baseflow conditions. A few high magnitude events exported substantially more discharge and nutrients than other events (17-58% of annual hydrochemical export), and occurred during both winter and summer months. Prolonged interaction of surface runoff with nutrient pools in upper soil horizons appears to be important in causing large quantities of nutrients to be exported.

Intensive sampling frequencies are critical in obtaining precise estimates of nutrient export rates, although threshold sampling frequencies differ for P and  $\text{NO}_3^-$  and may also vary for different events. Estimates of nutrient export generated from infrequent sampling frequencies can generate errors of more than 100% per event, and such errors can cumulatively result in major inaccuracies over time. An improved monitoring strategy may be to intensively sample a study basin during a range of hydrologic events to generate a discharge-mass relationship and predict nutrient export from subsequent events using this relationship. However, since discharge-mass relationships change for P during high magnitude events, and, substantial quantities of nutrients are exported during these periods, it is critical that such events are monitored intensively.

## **4.0 Role of Drainage Tiles in Hydrochemical Export from a 1<sup>st</sup> Order Agricultural Catchment in Southern Ontario**

### **4.1 Introduction**

Nutrient export from agricultural basins poses a serious problem to surface water quality through its contribution to eutrophication of aquatic ecosystem in downstream areas. Subsurface tile drainage is a commonly used agricultural management practice in areas with shallow groundwater or seasonally perched water tables. Tile drainage improves conditions for agriculture but alters hydrologic flow pathways. In addition, drainage tiles are point sources of nutrients that allow drainage waters to bypass natural filtration pathways, thus permitting the delivery of solids and nutrients to receiving streams (Dils and Heathwaite, 1999; Laubel *et al.*, 1999; Ulen and Persson, 1999; Haag and Kaupenjohann, 2001; Gentry *et al.*, 2000). Patterns of nutrient loading in tile effluent have been linked to both spatial and temporal factors. These factors include fertilizer type and application (Haygarth, 1997; Gentry *et al.*, 2000), soil type (Beauchemin *et al.*, 1998), antecedent hydrologic conditions and management practices. Temporal variability has also been observed where nutrient export during storms and snowmelt events is often characterized by a pulse of nutrients early in a storm due to preferential transport of surface water through macropores into tiles (Haygarth, 1997; Beauchemin *et al.*, 1998; Stamm *et al.*, 1998; Ulen and Persson, 1999). The role of tiles in agrochemical export has been the focus of several studies but factors governing temporal variability in nutrient export from tiles are still poorly understood. Much of the current understanding of hydrochemical export patterns from tiles has been developed in warmer geographic regions and little is known about nutrient export from tiles during winter months.

This chapter illustrates the dominance of drainage tiles in hydrochemical export from a first-order agricultural basin in Southern Ontario. In many regions, the majority of nutrients are lost during periods of elevated flow (Douglas *et al.*, 1998; Gburek and Sharpley, 1998; Sims *et al.*, 1998; Hill, 1981; Schuman *et al.* 1973), and much of this export occurs in winter months in Southern Ontario. In order to understand why these temporal patterns in hydrochemical export exist and to predict nutrient loading patterns it is first important to identify the dominant sources of these nutrients. The objectives of this chapter are:

- (1) To quantify the proportion of basin discharge that comes from point (tiles) and non-point (primarily diffuse groundwater) sources and demonstrate temporal variability in these sources over a one year period; and
- (2) To demonstrate the importance of drainage tiles in SRP, TP,  $\text{NO}_3^-$  export from the basin.

## **4.2 Site Description and Methods**

The research site and methods are provided in detail in Chapter Two. Methods specific to this chapter are outlined below.

### ***4.2.1 Diffuse Groundwater Flow***

Diffuse groundwater flow to the stream was predicted from Darcy's Law. The locations and depths of piezometers are described in Chapter Two. Hydraulic conductivities of riparian soils were determined using bail tests (Hvorslev, 1951).

Hydraulic gradients were monitored throughout each season of the year, with increased sampling intensity around rain and thaw events.

Groundwater flow to the stream was also estimated as a residual between measured flow volumes at selected points within the basin. Total basin groundwater flow to the stream ( $\Sigma GW_{\text{basin}}$ ) was estimated from

$$\Sigma GW_{\text{basin}} = \Sigma Q_{\text{basin}} - \Sigma Q_{\text{Tiles}} \quad (4.1)$$

where  $\Sigma Q_{\text{basin}}$  is discharge measured at the basin outflow and  $\Sigma Q_{\text{tiles}}$  is the sum of discharge from seven of the nine tiles in the basin. Two tiles are plugged and do not flow.

Groundwater flow ( $\Sigma GW_{\text{FR}}$ ) along a 500 m reach of the stream adjacent to the FR field was determined as a residual between stream discharge measured at upstream ( $Q_1$ ) and downstream ( $Q_2$ ) locations (Figure 4.1). Any discharge from tiles was also included in these calculations.

A quantity of P and  $\text{NO}_3^-$  gained through diffuse groundwater flow was predicted from the  $\Sigma GW_{\text{FR}}$  and observed concentrations of P (P) and  $\text{NO}_3^-$  (N) in piezometers in the riparian zone,  $[P_{\text{GW1}}, N_{\text{GW1}}]$

$$\text{Pred}\Delta_{(P,N)} = \Sigma GW_{\text{FR}} * [P_{\text{GW1}}, N_{\text{GW1}}] \quad (4.2)$$

This value was then compared to the observed change in nutrient mass along the stream reach ( $\text{Obs}\Delta_{(P,N)}$ )

$$\text{Obs}\Delta_{(P,N)} = \Sigma(P,N)_2 - \Sigma(P,N)_1 \quad (4.3)$$

where  $\Sigma(P,N)$  is the total mass of nutrients at the upstream (1) and downstream (2) locations, to generate an estimate of nutrient retention in the stream or hyporheic zone (R) (Figure 4.1).



This is also compared to nutrient retention in the riparian zone ( $R_{RZ}$ ), which was calculated using the predicted groundwater flow and concentrations in piezometers at the field-buffer edge (GW2) and at the buffer-stream edge (GW1).

Hydrologic storage in the FR field ( $S_A$ ) during successive rainstorms was calculated from measured soil moisture ( $\theta_V$ ) and a measured porosity of 0.5. Porosity was measured at 25, 50, 75 and 100 cm in three soil pits in the FR field using the traditional soil tin method (Hillel, 1998). Soil moisture was measured at the field edge of the riparian zone and is assumed to be representative of the entire field.

## **4.3 Results and Discussion**

### ***4.3.1 Hydrology: The Role of Drainage Tiles in Basin Discharge***

#### **4.3.1.1 Discharge From Tiles**

Discharge from tiles varies temporally. Discharge from the continuously monitored tile, basin discharge and water table position behaved in a similar manner over the one-year period (Figure 4.2). 2001 was a particularly dry year and no basin surface water export (streamflow) occurred during most of the summer. While the cessation of streamflow from the basin is not typical and resulted from an exceptionally dry summer, all of the tiles in the study basin are frequently dry during low-flow periods in both summer and winter months. The generally close correspondence between water table position and tile discharge is not surprising. Dolezal *et al.* (2001) showed that tile discharge is often a function of soil properties, drain spacing, the underlying bedrock and water table elevation above the drains. However, during some periods, water may enter tiles from the unsaturated zone via preferential flowpaths and macropores (Dolezal *et al.*, 2001; Stamm

**Figure 4.1 (a) Schematic Diagram of Calculations of Diffuse Groundwater Flow and Chemistry Along the FR Field. (b) A cross-section of the locations of piezometers in the riparian zone in the FR fields is shown.**

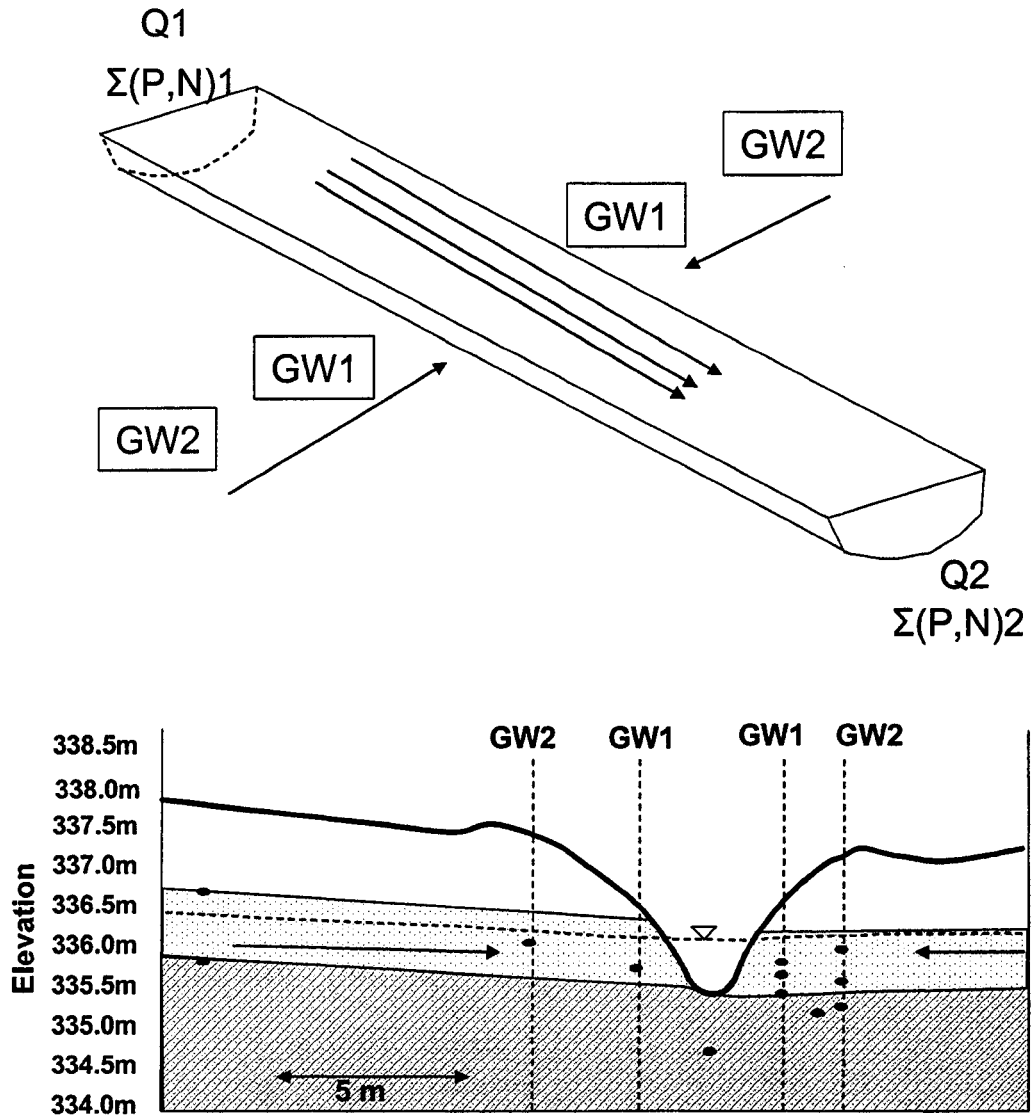
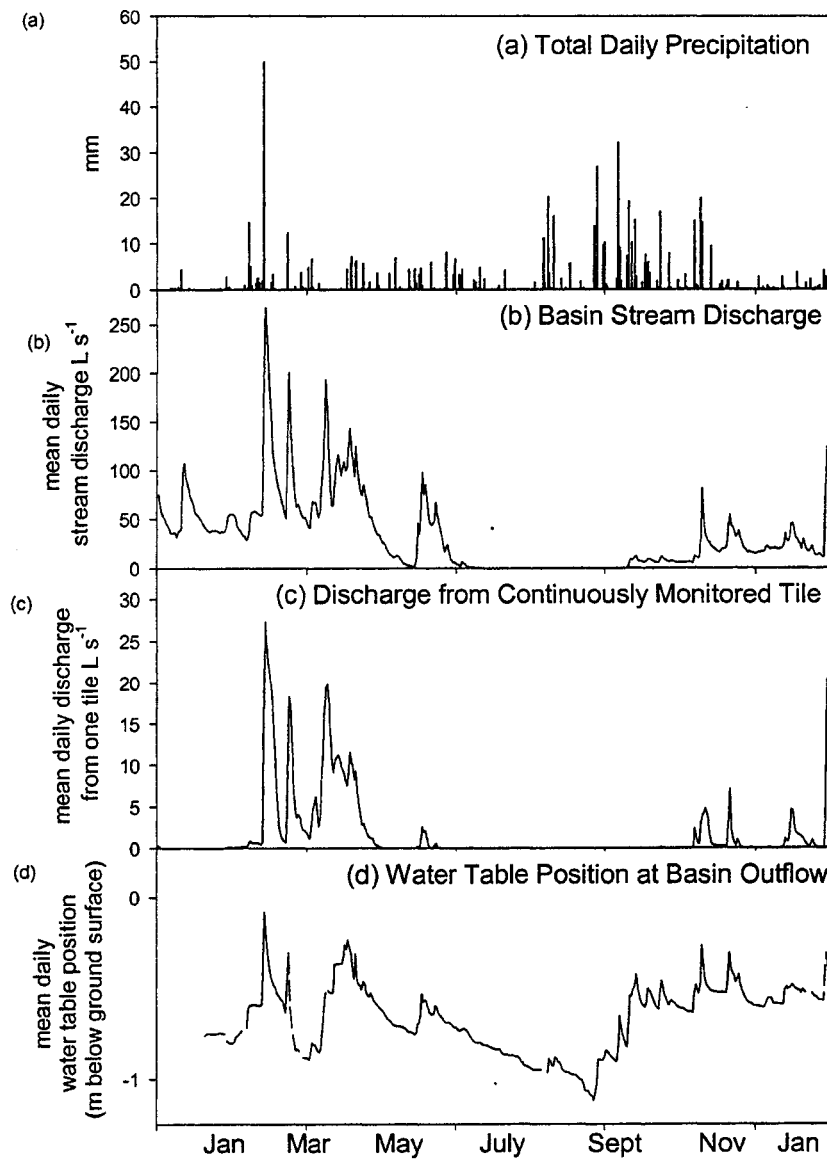


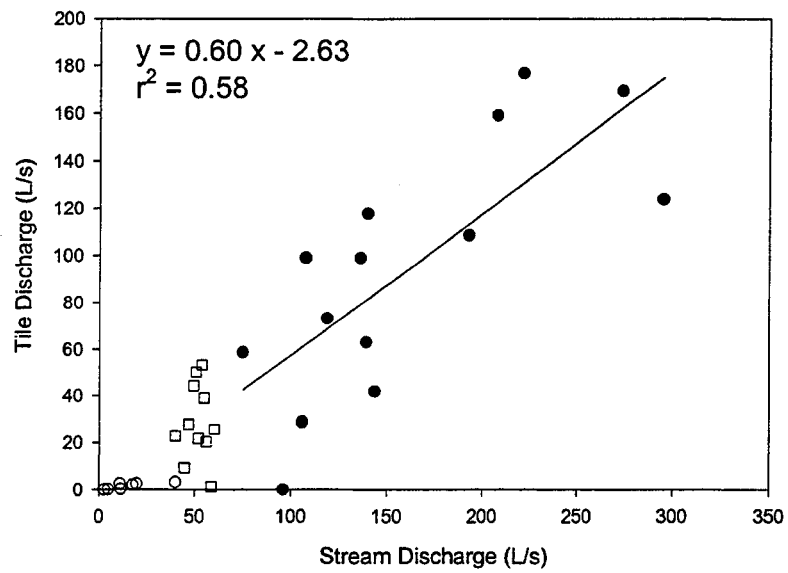
**Figure 4.2: Precipitation (mm) and discharge at the basin outflow ( $L d^{-1}$ ) for the study period are shown in (a) and (b). Discharge from a continuously monitored drainage tile is shown in (c) and water table position beneath the ground surface near the basin outflow is shown in (d).**



*et al.*, 1998). This weakens the relationship between water table position and tile discharge.

Tile and basin discharge are compared in Figure 4.3 to determine whether the contribution of tiles varies under different flow conditions. There is considerable spatial and temporal variability in tile discharge in the Strawberry Creek Watershed at both moderate (wet vs dry periods) and smaller (within-event) temporal scales, and the portion of streamflow contributed by drainage tiles is not constant. When stream discharge is less than  $40 \text{ L s}^{-1}$ , tiles generally do not flow or contribute very little to overall streamflow (open circles, Figure 4.3). When stream discharge is between 40 and  $60 \text{ L s}^{-1}$ , tiles show the largest range in their contribution to stream discharge, yielding between 0 and 90% of stream discharge (open squares, Fig. 4.3). When stream discharge is greater than  $60 \text{ L s}^{-1}$  (closed circles), there is a linear relationship between streamflow and tile discharge [tile discharge =  $(0.60 \times \text{stream discharge}) - 2.63$ ;  $r^2 = 0.58$ ]. During many storms and melt periods the contribution of drainage tiles varies, and may account for between 30% and 90% of overall basin discharge. The contribution of tiles to basin discharge can be easily predicted when streamflow is low ( $< 40 \text{ L s}^{-1}$ ) (i.e. tiles are not flowing) or high ( $> 60 \text{ L s}^{-1}$ ), but streamflow rates from  $40\text{-}60 \text{ L s}^{-1}$  are a critical period under which drainage tiles in the basin behave in a very unpredictable manner. Dolezal *et al.* (2001) suggested that at moderate discharge, tile drainage is simply the removal of water from the soil profile, whereas during high discharge periods, tile drainage is a function of the hydraulic capacity of the entire drainage system. The unpredictability of tile discharge at moderate flows in the Strawberry Creek Watershed is likely linked to soil heterogeneity within and among the various fields draining into the tiles. During higher discharge periods,

**Figure 4.3: Contribution of Tiles to Basin Discharge Under Variable Flow Conditions. Dark circles indicate wet periods (regression equation corresponds to this data only). White squares and circles indicate transitional and dry periods, respectively.**



differences among various fields in this basin become less apparent and tiles flow simultaneously as the entire catchment drains.

The contribution of tiles to streamflow varies throughout events (Fig. 4.4). During the February 2001 snowmelt event, tiles were more important in the early portion of the event. During the December 2001 winter thaw event (rain-on-snow), the contribution of tile flow in the early part of the event was low and became more important in the later stages of the event. This was also apparent in the early part of the February 2002 snowmelt event. This suggests that flowpaths vary both within and among various storms. This is likely due to antecedent hydrologic conditions in the basin (e.g. soil moisture, water table elevation and/or the presence of frost) as well as the rate of water input. Relationships between the water table position at the basin outflow and the contribution of tiles within the basin are weak (Fig. 4.5) suggesting that tile effluent is not fed by saturated groundwater flow alone.

#### 4.3.1.2 Discharge From Diffuse Groundwater Sources

In general, more than 50% of basin runoff is generated from diffuse groundwater sources at any given time. During dry periods when tiles are not flowing, groundwater flow accounts for 100% of streamflow. In 2001, this typically amounted to approximately 25-40 L s<sup>-1</sup> of stream discharge gained along the entire 2 km length of Strawberry Creek during January through mid-June 2001 and December 2001 through February 2002 (inclusive). Between mid-June and late November 2001, conditions in the basin were very dry and stream flow was low (0 - 10 L s<sup>-1</sup>).

**Figure 4.4: The relative contribution of drainage tiles to streamflow throughout 3 selected events. The data in each of the three plots span a period of approximately one week.**

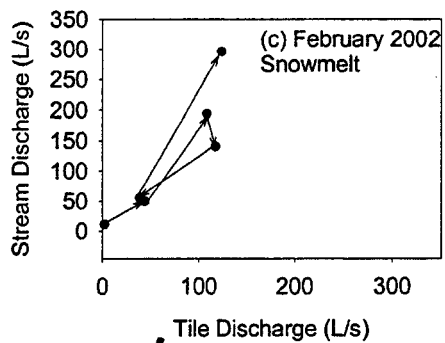
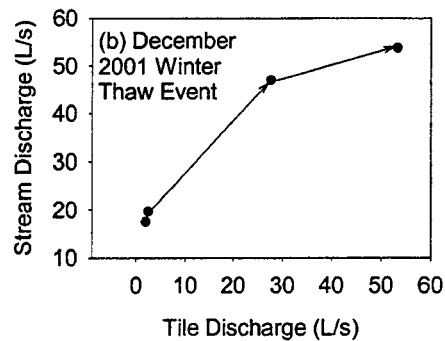
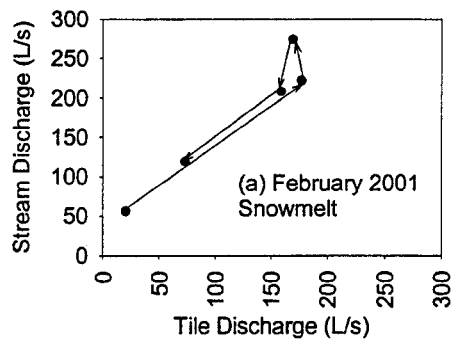
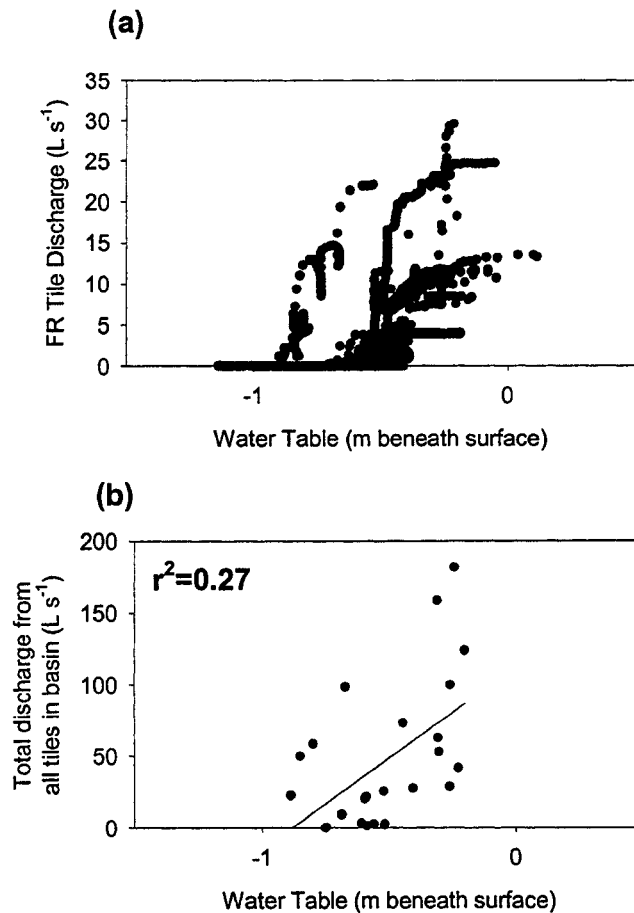


**Figure 4.5: The relationship between hourly water table position at the basin outflow and hourly discharge from the continuously monitored FR tile is shown in (a). The relationship between water table position at the basin outflow and cumulative discharge from all tiles in the basin is shown in (b).**





During wetter periods, the role of drainage tiles in basin drainage increases and a smaller proportion of streamflow originates from diffuse sources. However, the actual quantity of water entering the stream via diffuse groundwater flow increases under wet periods. During such periods (e.g. streamflow  $\sim 150 \text{ L s}^{-1}$ ) more than  $100 \text{ L s}^{-1}$  of stream discharge may originate from diffuse groundwater sources within the basin. These rates were determined as the residual between measured discharge at the basin outflow and from tiles within the basin. No overland flow was apparent during these periods. Although overland flow was observed on several occasions throughout the study period, occurrences were short in duration and difficult to quantify. This is discussed below (Section 4.4).

Predicted groundwater flow based on hydraulic head and hydraulic conductivity measurements in the riparian zone cannot sustain the groundwater flow that was observed in the basin over the study period. Much of the wetted perimeter of the stream is composed of an organic-rich loam and measured hydraulic conductivities range from  $1.7 \times 10^{-6}$  to  $6.7 \times 10^{-6} \text{ m s}^{-1}$ . These materials form the top metre of riparian soils, while underlying materials in the upper portion of the basin consist of compact Maryhill till (Harris, 1999). Measured hydraulic conductivities in these deeper soil horizons (e.g. 1.5 m – 2 m) range from  $1.2 \times 10^{-7}$  to  $6.7 \times 10^{-7} \text{ m s}^{-1}$ . The lower hydraulic conductivities in deeper soil horizons restrict vertical groundwater movement and cause shallow groundwater to flow laterally across the riparian zone (Harris, 1999; Mengis *et al.*, 1999).

Table 4.1 illustrates the upper and lower range in hydraulic gradients measured in basin riparian areas over the one-year period. Darcy's equation is used to estimate groundwater fluxes into the stream based on these hydraulic gradients and measured

**Table 4.1: Estimates of groundwater discharge to the stream based on Darcy's Law and the measured range of hydraulic gradients (dh/dx) and measured hydraulic conductivities ( $K_{HS}$ ). Groundwater gained per metre of stream length (GW/m) and total groundwater gained along the entire stream reach ( $\Sigma GW_{Reach}$ ) are also shown.**

	dh/dx	$K_{HS}$ ( $m\ s^{-1}$ )	Wetted Perimeter ( $m^2$ )	GW/m ( $m^3\ s^{-1}$ )	$\Sigma GW_{Reach}$ ( $m\ s^{-1}$ )
<b>High</b>	0.25	$3 \times 10^{-6}$	2.3	$2 \times 10^{-5}$	$4 \times 10^{-2}$
<b>Low</b>	0.03	$3 \times 10^{-6}$	1.0	$9 \times 10^{-8}$	$2 \times 10^{-4}$

hydraulic conductivities to determine 'predicted groundwater flow' ( $Q_D$ ). The quantity of observed groundwater flow is always higher than groundwater flow predicted using Darcy's Law. In order to support the diffuse flow contributing to the stream (based on the measured hydraulic gradients), true hydraulic conductivities must be 100x higher (on the order of  $10^{-4}\ m\ s^{-1}$ ). No overland flow occurred during these periods. Thus, this large discrepancy between measured hydraulic conductivities and 'calculated' hydraulic conductivities is likely explained by the presence of preferential flowpaths and macropores in upland and riparian soils. Preferential groundwater transport is likely a substantial contributor to discharge from this basin.

The contribution of groundwater and various tiles in the basin is determined as a residual based on measured export from the basin and what is observed at the basin outflow (Figure 4.6). Clearly, tiles dominate a substantial amount of overall basin discharge and this is evenly distributed among tiles. However, a substantial amount of flow comes from groundwater.

**Figure 4.6 Contribution of tiles and diffuse groundwater sources to basin discharge over a one year period. The stream hydrograph (line) and sampling periods (red dots) are shown in (a). The contribution of tiles (stacked bars) and streamflow at the outflow (black dots) are shown in (b). If black dots are above the bars, the difference between the dots and bars is water coming from diffuse sources.**

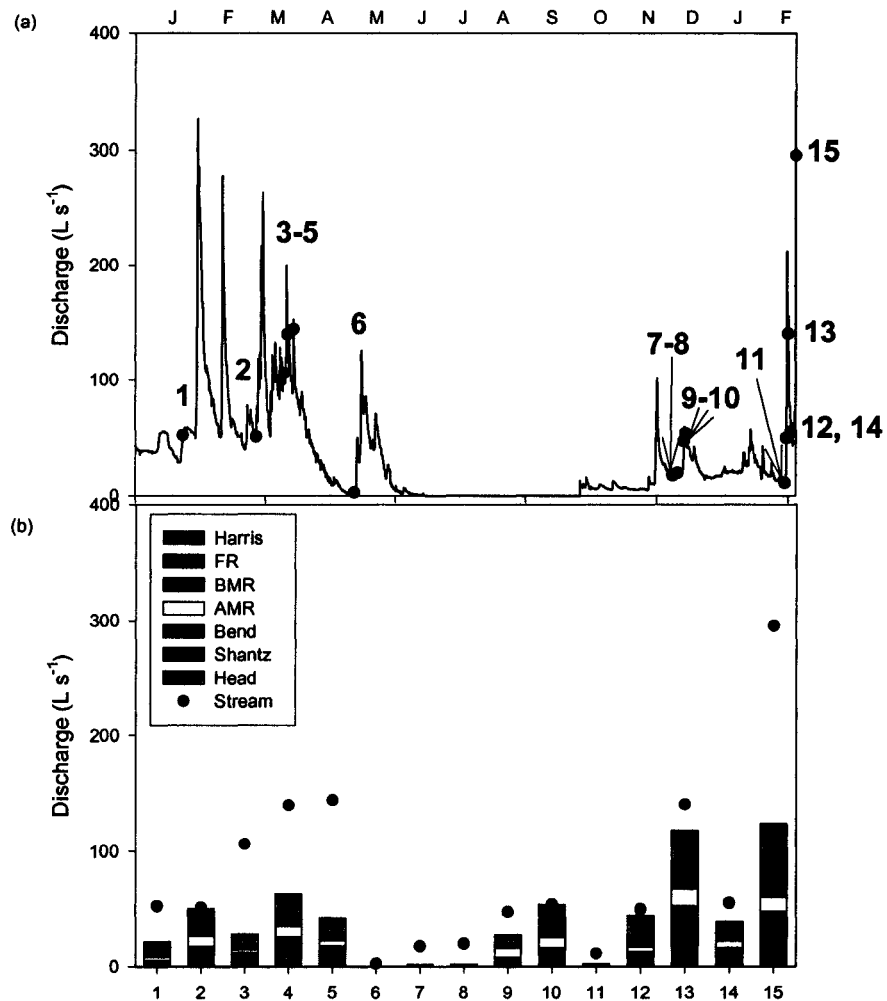
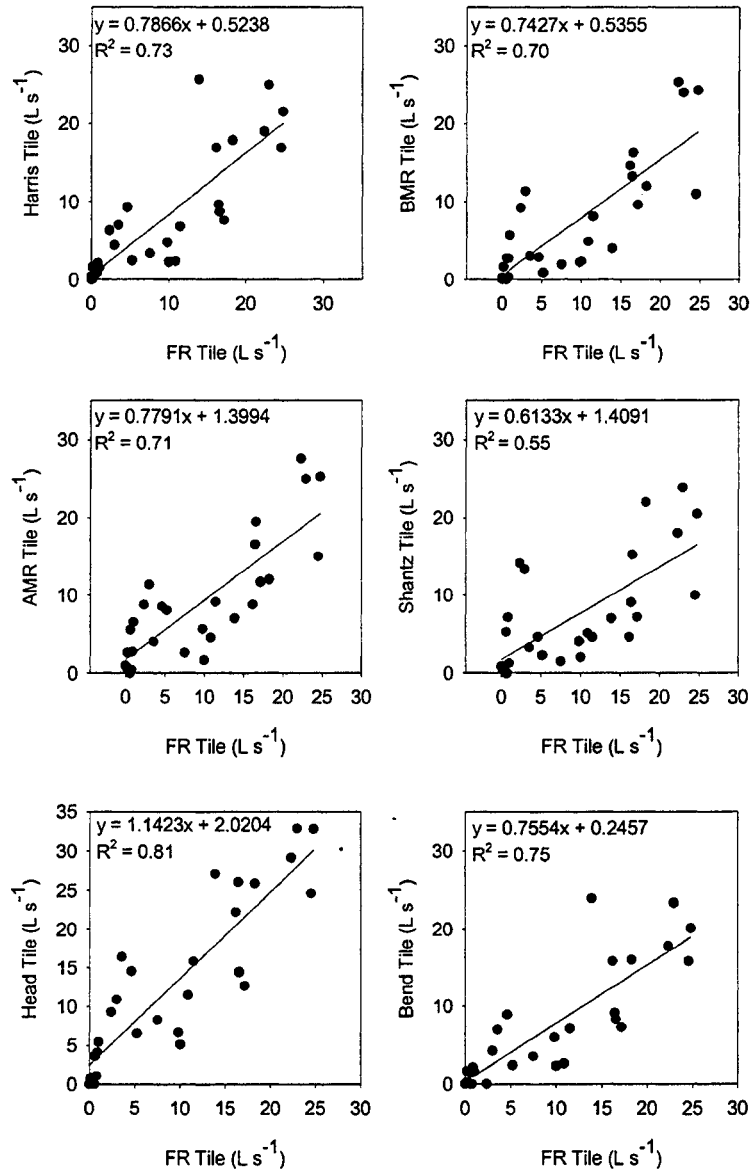


**Figure 4.7: Correlations (95% Confidence Interval) between the continuously monitored FR tile and instantaneous measurements of hydrologic discharge from 6 other tiles in the basin. Measured contribution of tiles is shown by black circles.**



#### 4.3.1.3 Empirical Relationships in Tile Discharge: Predicting the Annual Role of Tiles in Basin Discharge

Discharge from the continuously monitored (FR) tile is compared to instantaneous discharge (32 sampling dates) from six other tiles in the study basin (Fig. 4.7). While there is some scatter in the data, all of the relationships are statistically significant. This suggests that discharge patterns from other tiles in a basin can be predicted from one continuously monitored tile, although there will be some quantifiable error. Although correlations can be found between the continuously monitored tile and other tiles in the basin, stronger correlations are present among specific tiles within the basin, especially those draining the same fields (Table 4.2).

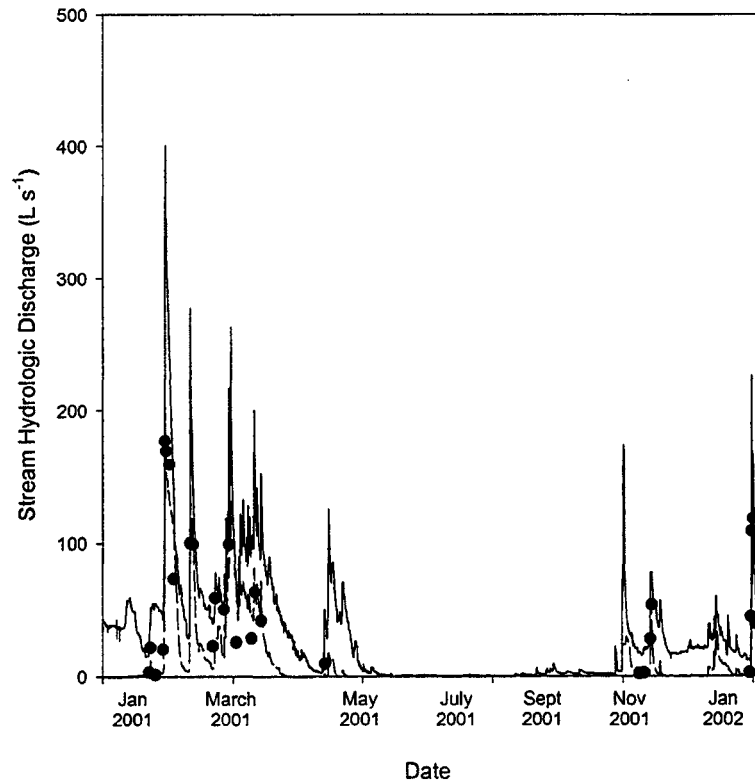
**Table 4.2: Pearson Correlation (r) of various tiles in the study basin. The FR tile was continuously monitored, whereas other tiles were monitored with spot samplings during all seasons, and during wet, dry, storm and snowmelt periods.**

	<b>FR</b>	<b>Harris</b>	<b>BMR</b>	<b>AMR</b>	<b>Shantz</b>	<b>Head</b>	<b>Bend</b>
<b>FR</b>	1.00						
<b>Harris</b>	0.85	1.00					
<b>BMR</b>	0.83	0.78	1.00				
<b>AMR</b>	0.83	0.76	0.95	1.00			
<b>Shantz</b>	0.71	0.74	0.87	0.86	1.00		
<b>Head</b>	0.89	0.94	0.83	0.84	0.77	1.00	
<b>Bend</b>	0.85	0.99	0.74	0.75	0.70	0.94	1.00

Some variability in the response of drainage tiles to various events is demonstrated as a result of spatial heterogeneity among fields in the basin. If more than one drainage tile was monitored continuously, error in the predicted results would likely be minimized. However, from a logistical standpoint, this is not an efficient solution.

The relationships in Figure 4.7 are used to predict the hydrologic contribution of all drainage tiles within the basin over a one year period. The contribution of tiles and diffuse sources to annual basin discharge are shown in Figure 4.8. Our confidence in

**Figure 4.8: Contribution of Point sources to annual streamflow, predicted from the continuously monitored FR tile data. Total streamflow is shown by the solid line. The modelled contribution of all tiles in the basin is shown by the dashed line. The observed contribution of tiles to discharge is shown with black dots.**



predicting patterns of other tiles in the basin from the FR tile varies with flow. Predicted results are most similar to observed results during higher and low flow periods, but not intermediate periods. During dry periods, not all of the tiles in the basin flow. When tiles in the basin are collectively contributing  $50 \text{ L s}^{-1}$  or higher, the error between predicted and observed tile discharge ranges from 20 to 30%. However, when the total contribution of tiles is less than  $50 \text{ L s}^{-1}$ , it is more difficult to predict tile export from the continuously monitored tile as error then ranges between 10 and 150%. Based on the empirical relationships between the continuously monitored tile and other tiles in the basin, the estimated total annual contribution of drainage tiles within the basin is 42% of basin discharge but may range from 21-45% (based on the error associated with our ability to predict tile export when total tile export is less than  $50 \text{ L s}^{-1}$ ). In a plot scale study in southern Ontario, Culley *et al.* (1983) observed that 60% of annual runoff was from a drainage tile.

### ***4.3.2 The Role of Drainage Tiles in Basin Phosphate Export***

#### **4.3.2.1 Spatiotemporal Variability in Phosphate Concentrations in Tile Effluent**

Figures 4.9 and 4.10 show the geometric means and ranges in SRP and TP concentrations in tile effluent over time. Substantial spatiotemporal variability exists in the data. Tile concentrations of SRP and TP are often higher during (a) storm periods; and (b) following the application of both organic and inorganic fertilizers in spring, and the spreading of manure in autumn.

**Figure 4.9: Tile Concentrations of SRP are shown against the basin hydrograph (solid line) illustrating seasonal and storm-related patterns in concentrations in tile effluent. The geometric mean concentration in seven tiles (solid circles) is shown in (a), and the observed range in concentrations (max and min) is shown by the error bars in (b).**

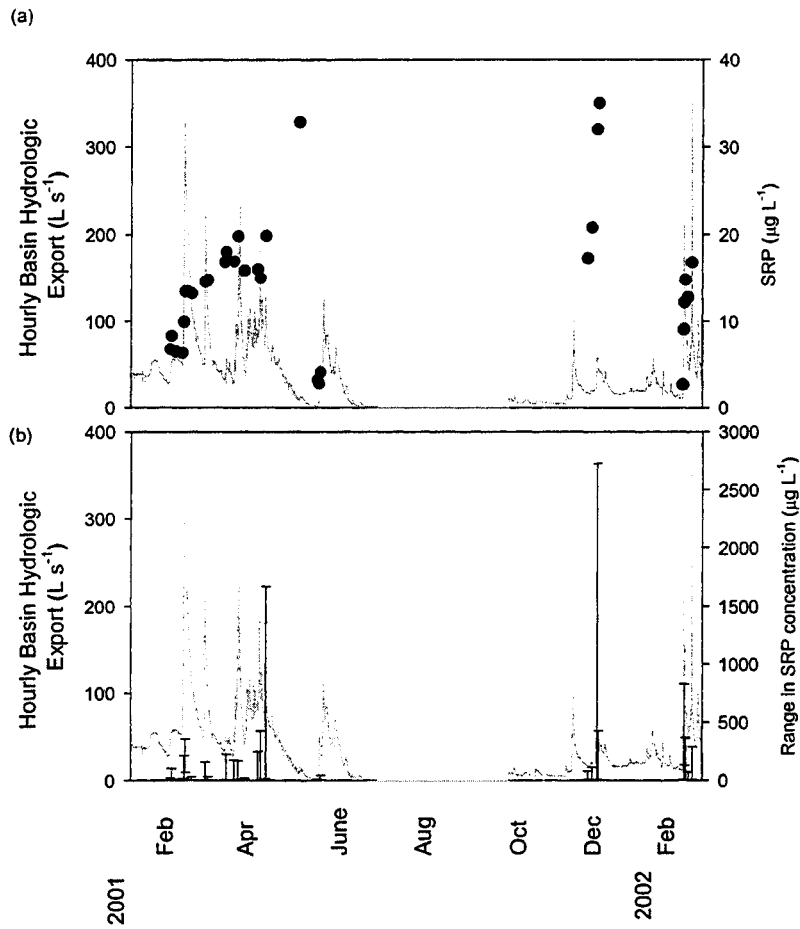
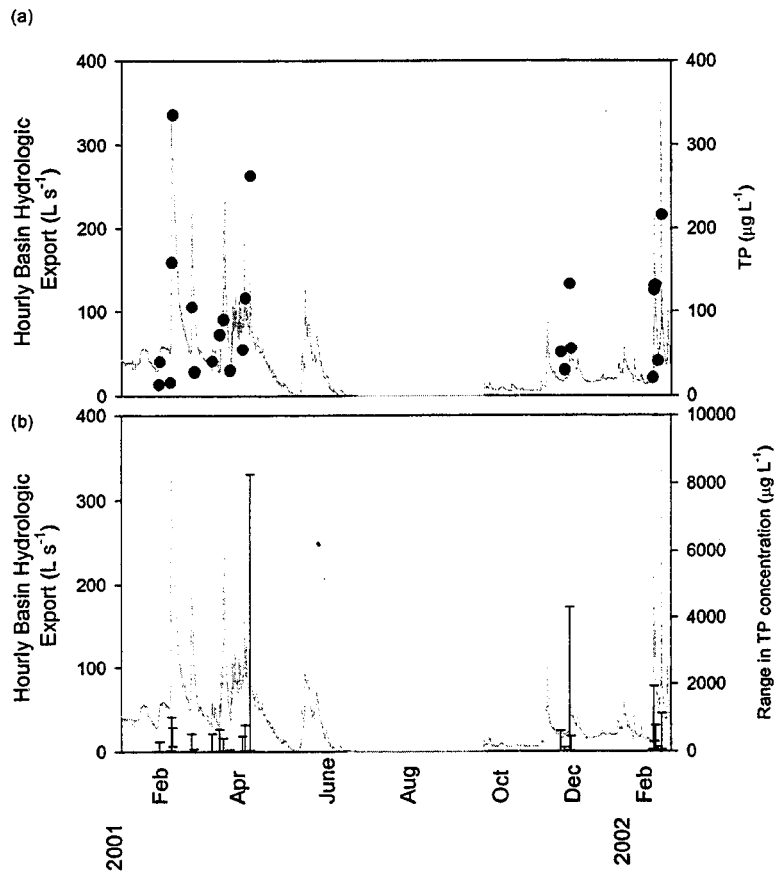




**Figure 4.10: Tile Concentrations of TP are shown against the basin hydrograph (solid line) illustrating seasonal and storm-related patterns in concentrations in tile effluent. The geometric mean concentration in seven tiles (solid circles) is shown in (a), and the observed range in concentrations (max and min) is shown by the error bars in (b)**



In general, SRP and TP concentrations in tile effluent were low (10-35  $\mu\text{g L}^{-1}$  and 10-350  $\mu\text{g L}^{-1}$ , respectively), although SRP and TP concentrations in tile effluent varied temporally. While tiles were generally low in P, they were occasionally very high in both SRP and TP concentrations. The same pattern in P concentrations has also been shown by Dils and Heathwaite (1999), Laubel et al. (1999) and Ulen (1995). The highest concentrations of SRP were observed in tile effluent in the autumn of 2001 following an extended period of drought. No increase in TP concentrations was observed during this period. SRP and TP concentrations were also high in the effluent of one tile (Bend Tile, cornfields fertilized with manure) in April following several successive thunderstorms (1700  $\mu\text{g L}^{-1}$  and 8200  $\mu\text{g L}^{-1}$ , respectively). These high concentrations are comparable to those observed by Laubel *et al.* (1999).

Tiles draining areas receiving organic fertilizers are much more significant sources of P than tiles draining fields receiving inorganic fertilizers (Table 4.3). Tiles in the basin that received inorganic fertilizers (e.g. Harris, FR) always exported minimal quantities of phosphorus, irrespective of antecedent conditions.

P concentrations in tile effluent vary between and within storms. The hydrologic and chemical responses of the continuously monitored FR tile following rainstorms can be used to assist in identifying important processes occurring within the fields. Figures 4.11 and 4.12 demonstrate variability in P concentrations in effluent of the FR tile for five successive rainstorms in April 2001. Antecedent hydrologic conditions in the basin prior to these events were wet as a result of a major snowmelt period that had taken place over a period of three weeks prior to the April events.

**Table 4.3: Average, standard deviation and range in nutrient concentrations for tiles in the study basin over the study period. Land use and fertilizer type are also shown in the table.**

<b>TILE</b>	<b>Harris</b>	<b>FR</b>	<b>BMR</b>	<b>AMR</b>	<b>Bend</b>	<b>Shantz</b>	<b>Head</b>
<b>Land Use</b>	strawberries	soybeans	soybeans	corn	corn	Corn	Corn
<b>Fertilizer Type</b>	inorganic	inorganic	organic	organic	organic	organic	Organic
<b>SRP (<math>\mu\text{g P L}^{-1}</math>)</b>							
Average	9	11	60	55	549	23	86
Std. Dev.	16	11	76	81	828	36	171
Max	96	48	355	361	2854	165	1030
Min	1	1	2	3	3	2	2
<b>NO<sub>3</sub><sup>-</sup> (mg NO<sub>3</sub><sup>-</sup>-N L<sup>-1</sup>)</b>							
Average	26	7	26	22	25	14	14
Std. Dev.	13	5	12	9	11	8	4
Max	96	33	53	39	45	41	23
Min	2	2	0	4	2	1	5
<b>TP (<math>\mu\text{g P L}^{-1}</math>)</b>							
Average	44	47	253	102	1553	117	591
Std. Dev.	66	40	613	112	2317	196	1471
Max	351	196	3538	532	8275	909	8056
Min	5	10	12	8	42	11	11

The available hydrologic storage in the FR field prior to each event and the gains and losses of water by the field throughout each of the events are summarized in Table 4.4. Prior to rainstorm #1, the water table was 94 cm beneath the ground surface and runoff from snowmelt was draining through the FR tile at a rate of approximately  $7 \text{ L s}^{-1}$ .

There was nearly 30 mm of storage potential in the upper 50 cm of the field but little storage capacity in lower horizons. A 4.6 mm rainstorm (storm #1) had no effect on tile discharge, although elevated levels of SRP and TP were observed in the tile effluent throughout the rainstorm. This suggests that a small pulse of P from surface soils was passing through macropores into the tile drain. Shortly after the start of the second rainstorm after 1.3 mm of rain had fallen (therefore, a cumulative total of 5.9 mm) a response in the FR tile discharge was observed. Although there was nearly 30 mm of

**Figure 4.11 SRP export from FR tile during five successive rainstorms in April 2001. Precipitation is shown in (a), the FR tile hydrograph (solid line) and SRP concentrations (black dots) are shown in (b), and mass SRP export from the FR tile is shown in (c).**

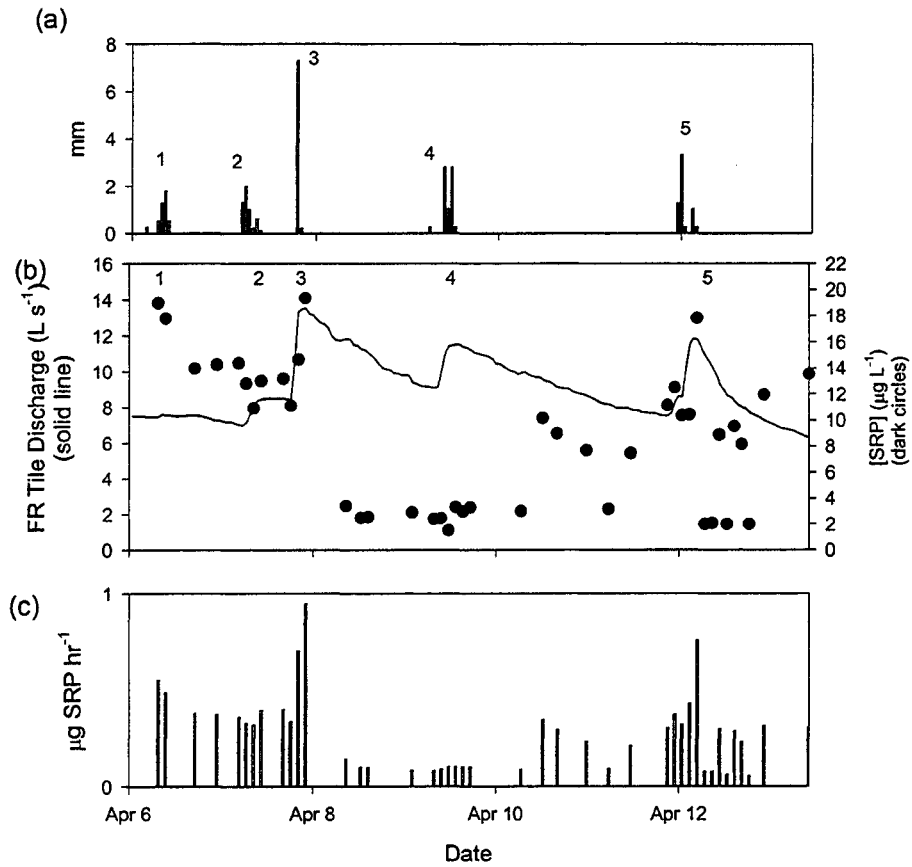
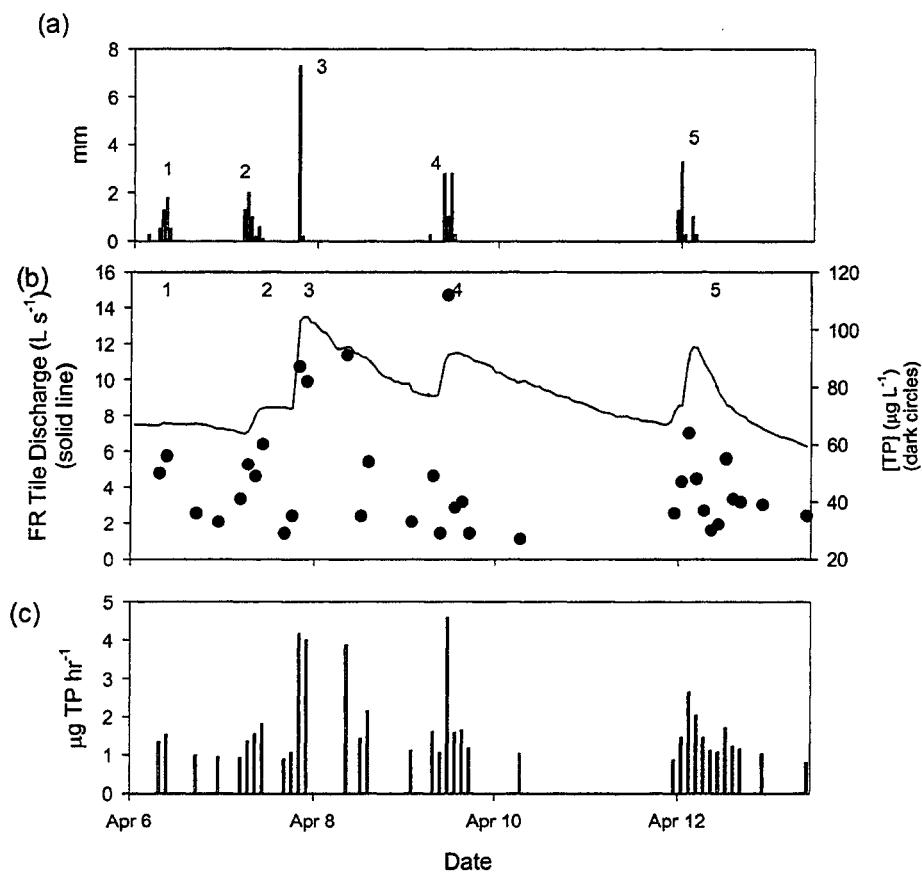


**Figure 4.12 TP export from FR tile during five successive rainstorms in April 2001. Precipitation is shown in (a), the FR tile hydrograph (solid line) and TP concentrations (black dots) are shown in (b), and mass TP export from the FR tile is shown in (c).**



storage in the field, there was only 8.8 mm of available storage in surface soil horizons and a gain of 5.9 mm of rainfall would have made surface horizons exceptionally wet.

SRP and TP export in tile effluent increased throughout rainstorm #2 as more rain fell. This pattern is likely due to the presence of preferential flowpaths where P from surface horizons was rapidly routed into drainage tiles through macropores. Kung (2000b) suggested that increasingly larger macropores are activated as conditions become wetter in a basin and that chemicals may be rapidly routed through these macropores into tile drains. The observed increase in P export through the FR tile throughout the rainstorm is in agreement with these findings. A decrease in P export is observed after the rainstorm ends. This may have been due to a finite source of P feeding the macropores or because runoff into the tile may have been diluted by groundwater.

A total of 9.8 mm of rain fell during rainstorms 1 and 2 (Table 4.4), of which 0.7 mm was discharged through the FR tile. Thus, 9.1 mm of the rain added to storage in the fields. Surface soils were very wet following these events.

A subsequent thunderstorm (#3) contributed 7.5 mm of rainfall over a one hour period to the field that was likely already very wet due to rainstorms 1 and 2. Thus, the hydrologic response of the tile was immediate (Figs 4.11, 4.12). Nearly all of the hydrologic inputs from rain were balanced by discharge through the FR tile (6.6 mm, Table 4.4). A substantial increase in both SRP and TP was observed during the early portion of this event (Figs 4.11, 4.12) suggesting substantial connectivity between the surface soils and the FR tile and increased access to other sources of P as the vadose zone wet up. As a result, P rapidly passed into the tile drain where it was exported.

**Table 4.4 Changes in Hydrologic Storage in the FR Field During Successive Rainstorms. Available storage ( $S_A$ ) is calculated from Measured soil moisture ( $\theta_V$ ) and a measured porosity of 0.5. Rainfall prior to the tile response ( $PPT_{resp}$ ), the total rainfall throughout the event ( $\Sigma PPT$ ), the total tile discharge throughout the event ( $\Sigma Q_{tile}$ ), and storage in the fields throughout the event ( $S_F$ ) are also shown.**

Date	Soil Horizon	$\theta_V$ (%)	$S_A$ (mm)	$PPT_{resp}$ (mm)	$\Sigma PPT$ (mm)	$\Sigma Q_{tile}$ (mm)	$S_F$ (mm)
Storms 1 and 2	0-25 cm	93	8.8				
	25-50 cm	85	18.8				
	50-75 cm	98	2.5				
	75-100 cm	100	0				
	Total		30.1	5.9	9.8	0.7	9.1
Storm 3				7.5	7.5	6.6	0.9
Storm 4	0-25 cm	99	1.3				
	25-50 cm	100	0				
	50-75 cm	100	0				
	75-100 cm	100	0				
	Total		1.3	2.8	7.1	6.3	0.8
Storm 5	0-25 cm	91	11.3				
	25-50 cm	86	17.5				
	50-75 cm	100	0				
	75-100 cm	100	0				
	Total		28.8	1.6	6.4	2.4	4.0

Soils in the basin were close to saturation when a subsequent rainstorm (#4) occurred. The water table at the boundary of the field and riparian zone was 0.33 m beneath the surface (Table 4.4). Thus, the available storage in the basin prior to this event was small and consequently, most of the 7.1 mm of rainfall were exported by the FR tile

(Table 4.4). A pulse of TP through the tile was observed early in the event although the same pattern was not observed for SRP. Aside from the TP pulse, TP export increased throughout the rainstorm, and P was likely being routed into the FR tile through preferential flowpaths.

A fifth rainstorm occurred several days after rainstorm #4. During this rainstorm, 6.4 mm of rain fell, of which 2.4 mm were exported through the FR tile. Conditions in the field prior to rainstorm #5 were similar to conditions prior to rainstorms #1 and #2, although the water table was higher during storm #5 (0.50 m beneath the surface) (Table 4.4). As in the preceding rainstorms, SRP and TP export throughout the event increased throughout the rainstorm and then decreased after it ended. It is likely that the observed increase in SRP and TP in tile effluent throughout the rainstorms was due to the movement of SRP and TP through preferential pathways into the FR tile. As conditions became progressively wetter throughout a given event (as rainfall occurred), larger macropores were likely activated and greater quantities of P were routed into the tiles. Once the rainstorms ended, large pores progressively ceased to flow and P export decreased.

P export varied both within events but also throughout events. During storms #1 #2 and #3 the field was becoming progressively wetter. The field reached saturation during storm #3, and consequently, during storms #4 and #5, the field could not become any wetter and no new pores could be accessed. Thus the overall P export through the FR tile increased progressively from event #1 to event #3, at which point it decreased successively during events #4 and #5. Furthermore, it is possible that the available pool of P in surface soils was reduced following storm #3.



Temporal variability in P export through tiles has been observed in other studies (e.g. Ulen, 1995; Beauchemin *et al.*, 1998; Stamm *et al.*, 1998; Dils and Heathwaite, 1999; Ulen and Persson, 1999; Gentry *et al.*, 2000; Hodgkinson *et al.*, 2002; Stone and Krishnappan, 2003). Temporal variability in P export through tiles has been linked to macropores during both dry periods (e.g. Stamm *et al.*, 1998) and wet periods (Biron *et al.*, 1999; Welsch *et al.*, 2001).

Figures 4.13 and 4.14 show SRP and TP Q-C relationships for various drainage tiles in the basin. In all cases, the correlations are weak. The poor Q-C relationships for P in tile effluent are due to the episodic nature of P delivery into tile drains that was demonstrated in Figures 4.11 and 4.12. However, to generate a crude estimate of the annual contribution of drainage tiles to nutrient export, the relationships in Figures 4.13 and 4.14 and the predicted tile discharge rates (Figs. 4.7, 4.8) are employed. Export from drainage tiles in the basin is estimated to represent 156% of annual basin SRP and 87% of annual basin TP export. However, given the error associated with these calculations, these values should be treated with extreme caution.

#### 4.3.2.2 The Role of Tiles and Diffuse Groundwater Flow in Basin Phosphate Export

Figures 4.15 and 4.16 present SRP and TP export observed at the basin outflow and from individual tiles in the basin during selected events over the study period. Figure 4.6 showed that a substantial proportion of basin discharge comes from diffuse groundwater sources. However, Figures 4.15 and 4.16 demonstrate that drainage tiles account for the majority of P export from the basin and that P export from the basin is often dominated by only a few tiles. These tiles drain fields receiving manure and during

**Figure 4.13: Q-C relationship for SRP concentrations in effluent of 7 tiles in the basin are shown in (a) through (g).**

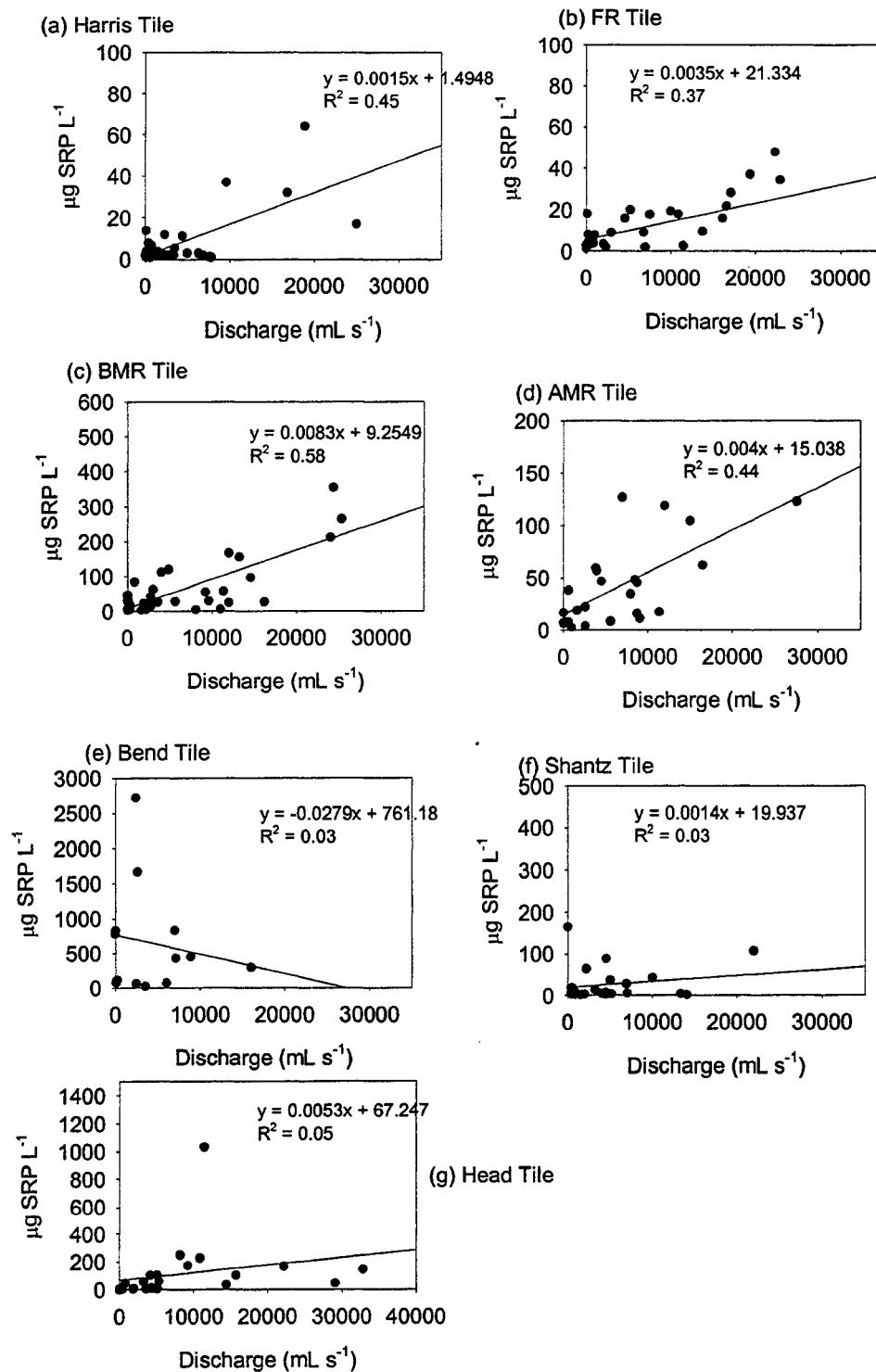


**Figure 4.14: Q-C relationship for TP concentrations in effluent of 7 tiles in the basin are shown in (a) through (g).**

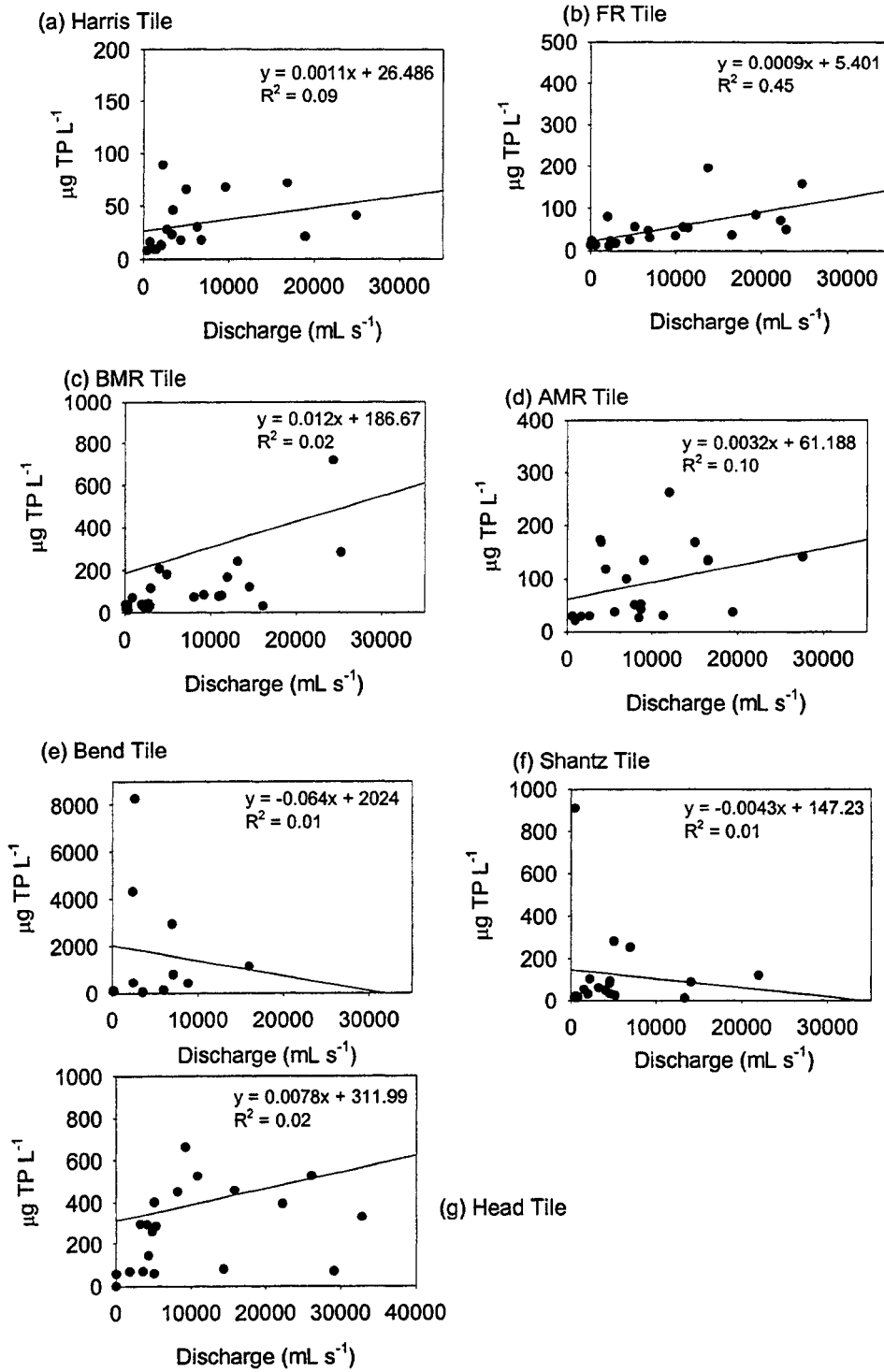


**Figure 4.15 Contribution of tiles and diffuse groundwater sources to basin SRP export over a one year period. The stream hydrograph (line) and sampling periods (red dots) are shown in (a). SRP export from tiles (stacked bars) and in streamflow at the basin outflow (black dots) are shown in (b). If black dots are above the bars, the difference between the dots and bars is water coming from diffuse sources. If the dots are below the bars some retention is occurring in the stream.**

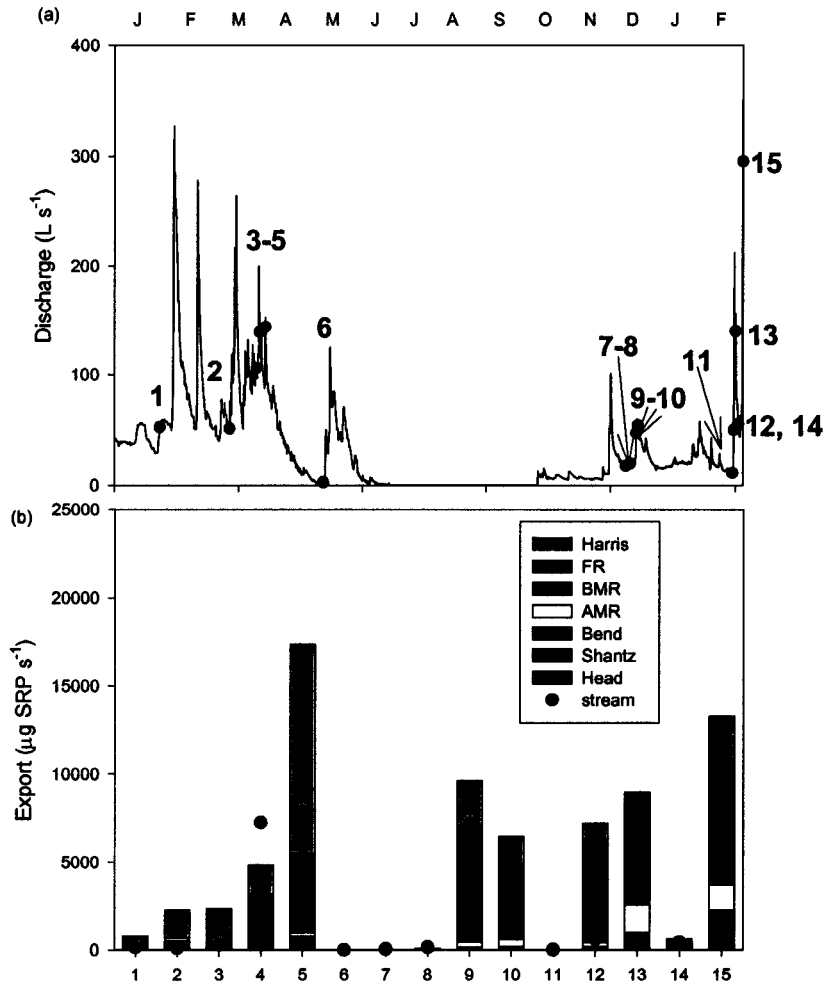
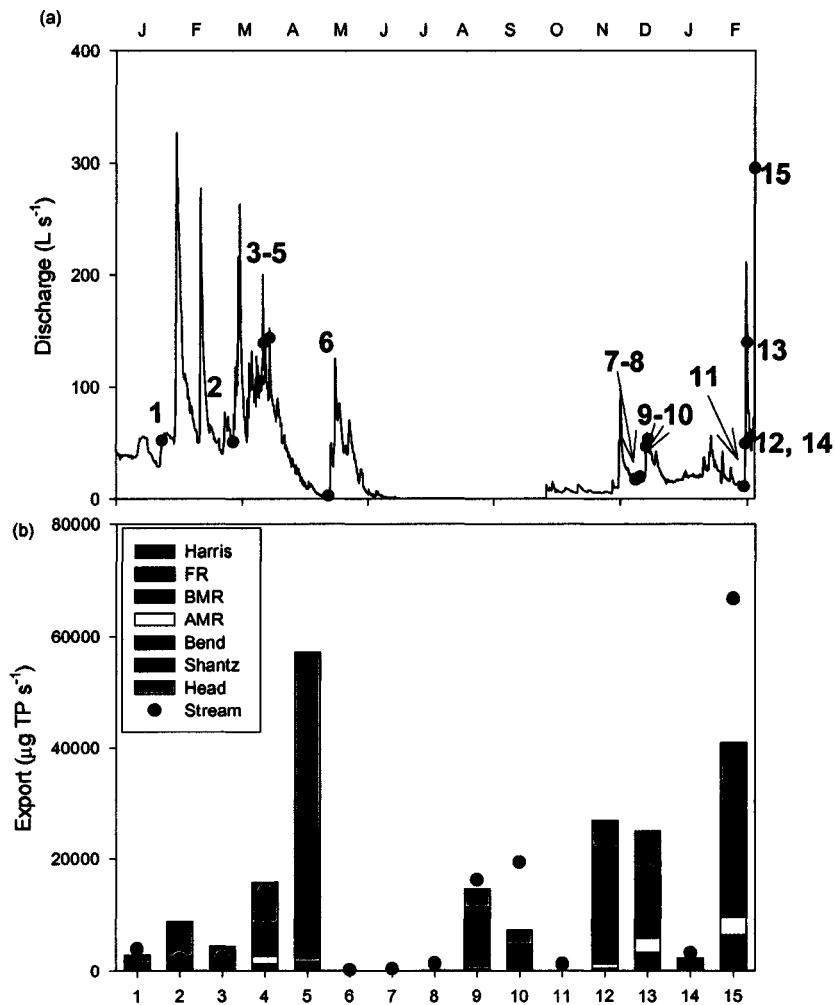


**Figure 4.16 Contribution of tiles and diffuse groundwater sources to basin TP export over a one year period. The stream hydrograph (line) and sampling periods (red dots) are shown in (a). TP export from tiles (stacked bars) and in streamflow at the basin outflow (black dots) are shown in (b). If black dots are above the bars, the difference between the dots and bars is water coming from diffuse sources. If the dots are below the bars some retention is occurring in the stream.**



some periods, P export from tiles exceeds P export from the basin. It is likely that some of the P exported by tiles is retained in the stream during these periods.

The contribution of diffuse groundwater sources is examined along a small segment of the stream reach adjacent to the FR field (Fig. 4.1) in Table 4.5. The observed inputs from groundwater flow (Obs $\Delta$ P) are always less than the inputs of groundwater that are predicted from piezometers in the riparian zone (Pred $\Delta$ P). Although these estimates are crude, a comparison of the estimated retention (R), which is the difference between the observed and predicted inputs from groundwater, and the retention (R<sub>RZ</sub>) that is observed in the riparian zone between piezometers at GW2 and GW1 (Figure 4.1) are comparable.

Thus, it is possible that substantial SRP retention is occurring in the portion of the riparian zone that rests between the monitored piezometers (GW1, Figure 4.1) and the stream. This may be a critical place in the riparian zone that is missed when the existing piezometers are sampled. Alternatively, the SRP may be retained in the stream bed. Given the fact that SRP has been shown to be strongly sorbed to stream bed sediments (e.g. Meyer, 1979; Hill, 1981), this is a plausible explanation.

**Table 4.5: Comparison of P Mass Export from Diffuse Groundwater Sources and Drainage Tiles in the FR Cultivated Fields. Discharge, (Q) (L s<sup>-1</sup>), P concentrations, [P] ( $\mu$ g L<sup>-1</sup>), and the calculated mass of P,  $\Sigma$ P ( $\mu$ g s<sup>-1</sup>) are shown at upstream (1) and downstream (2) locations along the reach and in the FR tile to calculate the observed change in P mass along the reach, Obs $\Delta$ P ( $\mu$ g s<sup>-1</sup>). This is compared to the estimated flux of groundwater, Pred $\Delta$ P ( $\mu$ g s<sup>-1</sup>) to calculate P retention, R.**

Date	Q1	[P] 1	$\Sigma$ P 1	Q2	[P] 2	$\Sigma$ P 2	Q <sub>Tile</sub>	[P] <sub>Tile</sub>	Obs $\Delta$ P	Pred $\Delta$ P	R	R <sub>RZ</sub>
Mar 19	22.0	2	44	34.3	2	69	2.4	2	+20	+47	-27	-24
Apr 8	94.1	12	1129	132.1	4	528	11.5	3	-635	+73	-708	-954
May 23	19.1	33	630	23.2	19	441	0.2	3	-190	+66	-256	-

### ***4.3.3 The Role of Drainage Tiles in Basin Nitrate Export***

#### **4.3.3.1 Spatiotemporal Variability in Nitrate Concentrations in Tile Effluent**

Concentrations of  $\text{NO}_3^-$  in tile effluent typically ranged from 5 to 25  $\text{mg N L}^{-1}$ , but were as low as  $< 1 \text{ mg N L}^{-1}$  during low summer flows and higher than 30  $\text{mg N L}^{-1}$  during storms. The highest  $\text{NO}_3^-$  concentration recorded was 95  $\text{mg N L}^{-1}$  from one tile (Harris Tile, Strawberries fertilized with inorganic N/P/K mixture) during an extremely wet period (June, 2000) in which riparian areas were inundated and saturation overland flow occurred for several days (Figure 4.17). These concentrations are comparable to those reported by Haag and Kaupenjohann (2001) and Bronswijk *et al.* (1995).

As in the case of P,  $\text{NO}_3^-$  export also varies throughout events and between different events. Figure 4.18 demonstrates variability in  $\text{NO}_3^-$  in effluent of the FR tile for five successive rainstorms in April 2001. Since the individual storms have been discussed in detail previously, they will not be discussed again here. In general,  $\text{NO}_3^-$  export increases throughout events as conditions become wetter, and  $\text{NO}_3^-$  export patterns are therefore similar to P export patterns. However, a pulse of  $\text{NO}_3^-$  export is not observed through drainage tiles as in the case of P (Figs 4.11 and 4.12). It is likely that as conditions become wetter and larger macropores are activated, greater quantities of  $\text{NO}_3^-$  from upper soil layers are flushed through macropores into tiles. A slight increase in overall  $\text{NO}_3^-$  export is observed in storms #1 - #3, and a decrease is observed during storms #4 and #5. As in the case of P, it is assumed that since the fields were the wettest during storm #3, no new sources could be accessed during subsequent events. A large increase in  $\text{NO}_3^-$  export was observed following rainstorm #5. A previously untapped source of  $\text{NO}_3^-$  may have been accessed.

**Figure 4.17: Tile Concentrations of  $\text{NO}_3^-$  shown against the basin hydrograph (solid line) illustrating seasonal and storm-related patterns in concentrations in tile effluent. The geometric mean concentration in 7 tiles (black dots) is shown in (a), and the observed range in concentrations (max and min) is shown by the error bars in (b).**

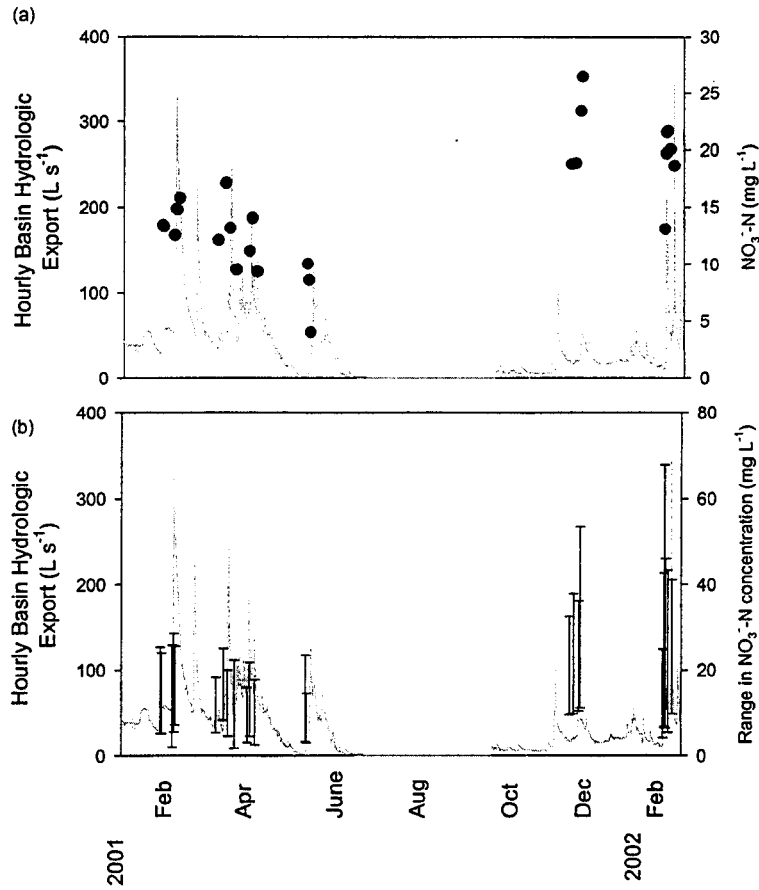
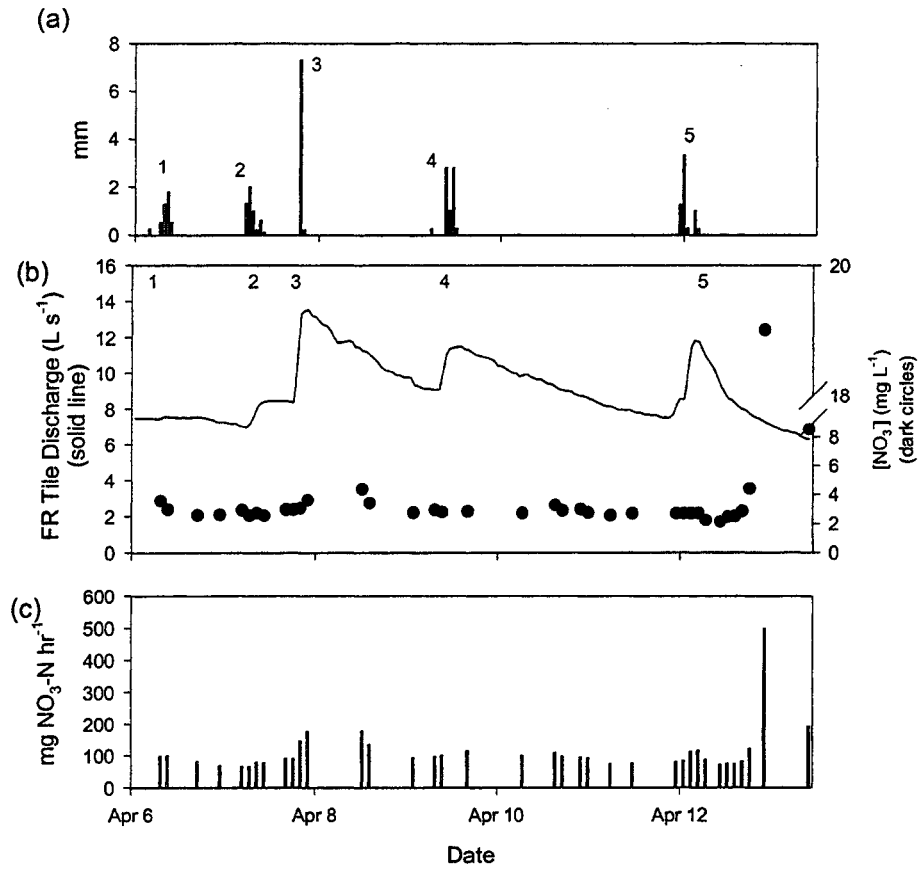




**Figure 4.18**  $\text{NO}_3^-$  export from FR tile during three successive thunderstorms in April 2001. Precipitation is shown in (a), the FR tile hydrograph (solid line) and  $\text{NO}_3^-$  concentrations (black dots) are shown in (b), and mass  $\text{NO}_3^-$  export from the FR tile is shown in (c).



As in the case of P,  $\text{NO}_3^-$  Q-C relationships in the FR tile are weak (Fig. 4.19). Based on the relationships in Figure 4.19 and Figures 4.7 and 4.8, it is estimated that 62% of annual  $\text{NO}_3^-$  export from the basin originates from drainage tiles. Thus, diffuse groundwater sources account for a greater proportion of  $\text{NO}_3^-$  export than for P export.

#### 4.3.3.2 The Role of Tiles and Diffuse Groundwater Flow in Basin Nitrate Export

Harris (1999) monitored  $\text{NO}_3^-$  attenuation along small transects in riparian areas in the Strawberry Creek Watershed and observed that large amounts of  $\text{NO}_3^-$  were exported into the stream along with groundwater during storms. Basin  $\text{NO}_3^-$  export and  $\text{NO}_3^-$  from tiles are quantified in Figure 4.20.  $\text{NO}_3^-$  from diffuse sources is determined as a residual between basin and tile export.

Unlike P,  $\text{NO}_3^-$  export is not dominated by only a few tiles, and  $\text{NO}_3^-$  is exported from all tiles in the basin. However, a substantial amount of  $\text{NO}_3^-$  originates from diffuse sources within the basin. Some  $\text{NO}_3^-$  also appears to be attenuated in the stream. Both Cabrera (1998) and House (2000) observed minimal quantities of  $\text{NO}_3^-$  in hyporheic areas of Strawberry Creek in summer, although Harris (1999) observed that  $\text{NO}_3^-$  attenuation in these zones is reduced in winter. Significant quantities of  $\text{NO}_3^-$  exported by tiles may be attenuated in the stream and hyporheic zone during some periods. This is an area where future research is necessary.

The contribution of diffuse groundwater sources to stream  $\text{NO}_3^-$  along a small segment of the stream reach adjacent to the FR field is shown in Table 4.6. As in the case of SRP, observed inputs from groundwater flow are less than the inputs of groundwater that are predicted from piezometers in the riparian zone on two of the three dates (April 8

**Figure 4.19: Q-C relationship for  $\text{NO}_3^-$  concentrations in effluent of 7 tiles in the basin are shown in (a) through (g).**

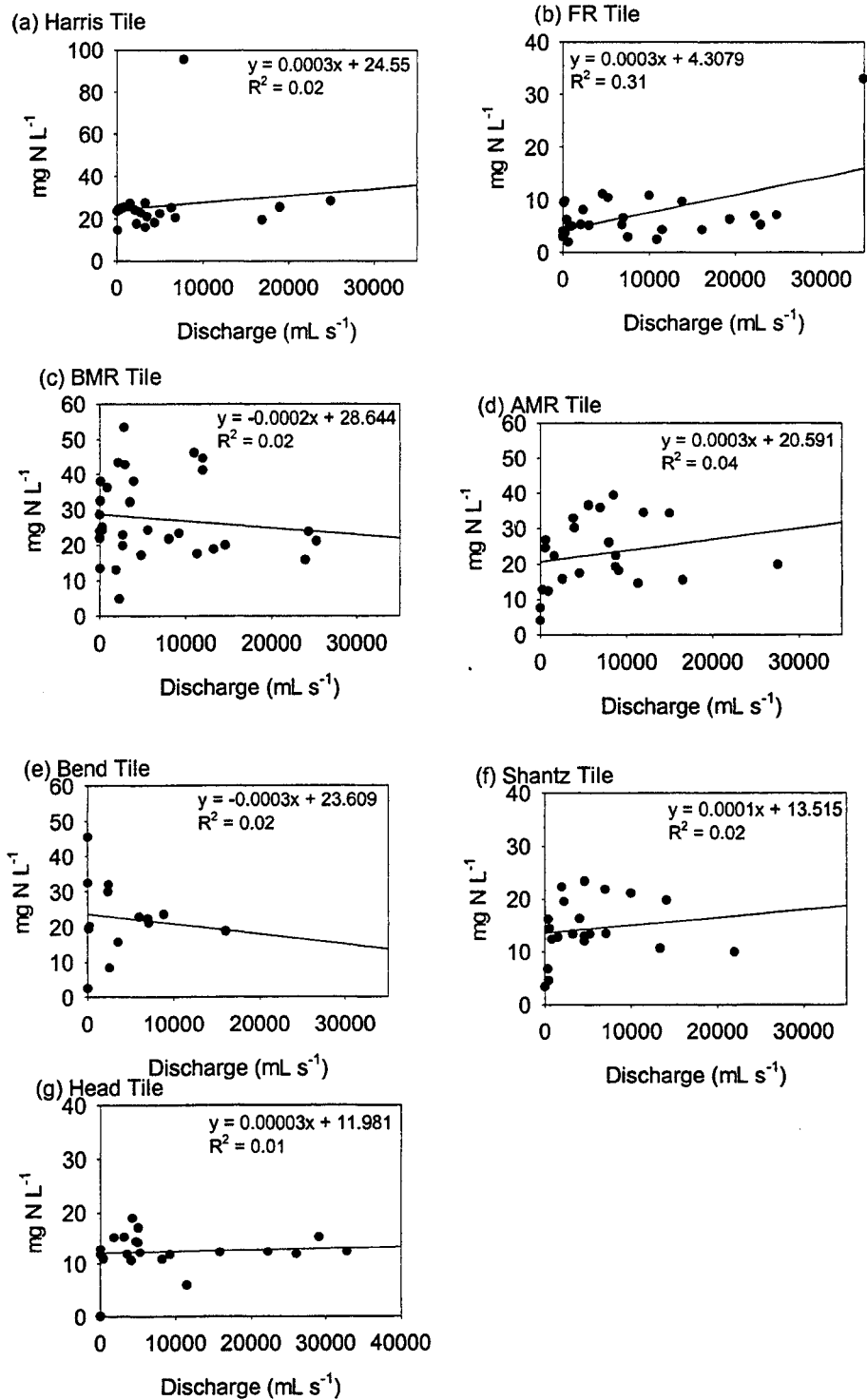
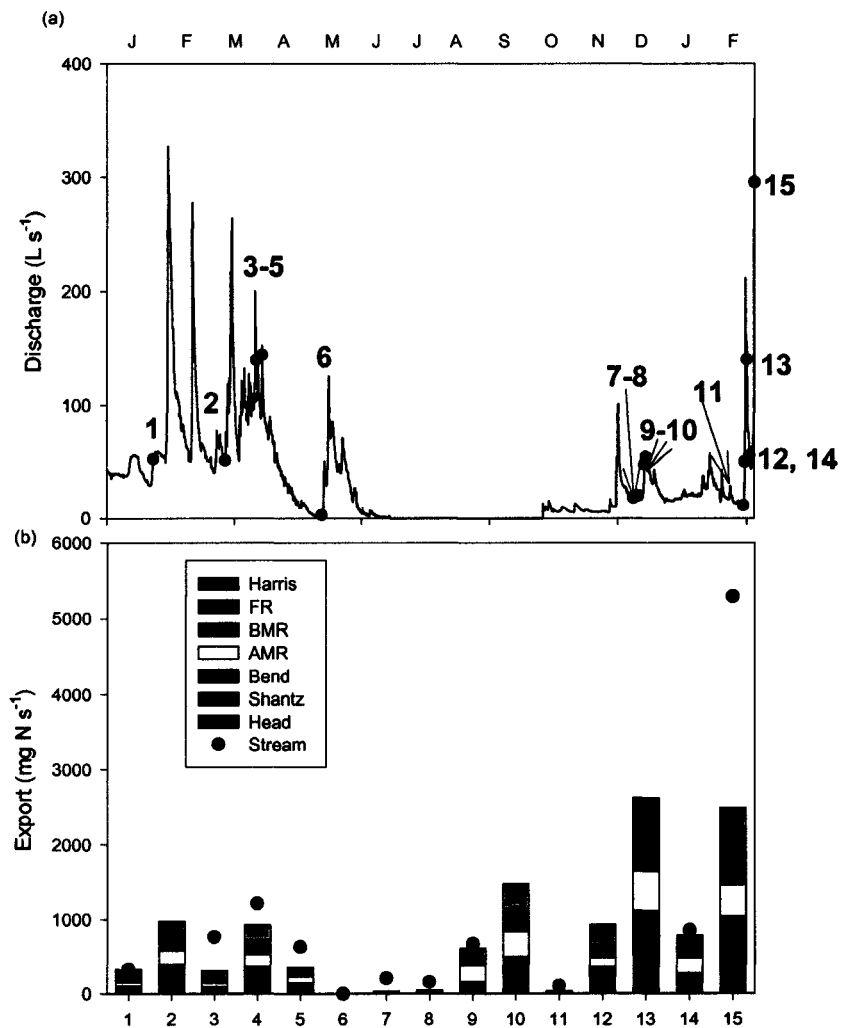


**Figure 4.20 Contribution of tiles and diffuse groundwater sources to basin  $\text{NO}_3^-$  export over a one year period. The stream hydrograph (line) and sampling periods (red dots) are shown in (a).  $\text{NO}_3^-$  export from tiles (stacked bars) and in streamflow at the basin outflow (black dots) are shown in (b). If black dots are above the bars, the difference between the dots and bars is water coming from diffuse sources. If the dots are below the bars some retention is occurring in the stream.**



and May 23), but less on March 19. Table 4.6 indicates that groundwater  $\text{NO}_3^-$  inputs (based on measured piezometers) may be attenuated either within the riparian zone or the stream bed.

**Table 4.6: Comparison of  $\text{NO}_3^-$  Mass Export from Diffuse Groundwater Sources and Drainage Tiles in the FR Cultivated Fields. Discharge (Q), ( $\text{L s}^{-1}$ ),  $\text{NO}_3^-$  concentrations, [N] ( $\text{mg N L}^{-1}$ ), and the calculated mass of N,  $\Sigma\text{N}$  ( $\text{mg N s}^{-1}$ ) are shown at upstream (1) and downstream (2) locations along the reach and in the FR tile to calculate the observed change in  $\text{NO}_3^-$  mass along the reach,  $\text{Obs}\Delta\text{N}$  ( $\text{mg N s}^{-1}$ ). This is compared to the estimated flux of groundwater,  $\text{Pred}\Delta\text{N}$  ( $\text{mg N s}^{-1}$ ) to calculate  $\text{NO}_3^-$  attenuation, R.**

	Q1	[N]1	$\Sigma\text{N}$ 1	Q2	[N]2	$\Sigma\text{N}$ 2	$Q_{\text{Tile}}$	[N] <sub>Tile</sub>	Obs $\Delta\text{N}$	Pred $\Delta\text{N}$	R	$R_{\text{RZ}}$
Mar 19	22	8.4	185	34.3	6.8	233	2.37	3.88	+ 39	30	+ 9	-50
Apr 8	94.1	7.2	678	132.1	6.7	885	11.49	3.35	+170	186	- 16	-93
May 23	19.1	8.8	168	23.2	6.9	160	0.2	4.08	- 9	20	- 29	-39

Alternatively, the piezometers sampled are not representative of true  $\text{NO}_3^-$  concentrations along the reach. It should be noted that the small differences between the  $\text{Obs}\Delta\text{N}$  and  $\text{Pred}\Delta\text{N}$  are well within the range of error associated with this crude technique and these values should therefore be treated with caution.

A comparison of the estimated retention (R), which is the difference between the observed and predicted inputs from groundwater and the retention that is observed in the riparian zone ( $R_{\text{RZ}}$ ) are comparable for the March 19 and May 23 events. Thus, it is possible that substantial  $\text{NO}_3^-$  is attenuated in the portion of the riparian zone that rests between the monitored piezometers (GW1, Figure 4.1) and the stream. Harris (1999) also observed that critical zones of denitrification could easily be missed by sampling piezometers in riparian areas. Alternatively, the  $\text{NO}_3^-$  may also have been attenuated along the stream reach.

#### 4.4 The Contribution of Overland Flow to Basin Hydrochemical Export

Overland flow is a flowpath that is of interest to many managers because of its potential for exporting sediments and nutrients from agricultural catchments. However, overland flow is difficult to quantify because it is very difficult to measure. This is largely why it was not quantified in this thesis. However, to provide some discussion of overland flow in the context of its contribution to basin discharge, overland flow can be crudely estimated from a statistical analysis of flow during periods when overland flow is not occurring.  $\Sigma GW_{\text{basin}}$  can be estimated from  $\Sigma Q_{\text{tiles}}$  and  $\Sigma Q_{\text{basin}}$  during periods when overland flow is not occurring (equation 4.1) and yields the following relationship:  $\Sigma GW_{\text{basin}} = 0.4136 * \Sigma Q_{\text{basin}} + 3.193$ ;  $r^2 = 0.80$ . This relationship can be applied to periods when overland flow was observed, and the contribution of overland flow can be estimated from

$$OF = \Sigma Q_{\text{basin}} - \Sigma GW_{\text{basin}} \quad (4.4)$$

where  $OF$  is the contribution of overland flow ( $L s^{-1}$ ). It is important to note that this calculation is crude, as error exists within each set of calculations, thus making errors cumulative. During periods when overland flow was observed, it was contributing between between 15 – 44  $L s^{-1}$  and accounting for 10-30% of total basin discharge.

$NO_3^-$  and P export via overland flow is impossible to quantify for several reasons. First, as discussed above, the proportion of discharge from overland flow is nearly impossible to quantify. Second, concentrations of  $NO_3^-$  and P in standing water on the various fields vary substantially within the basin on any given occasion. For example, during a storm on April 12 2001, SRP concentrations in overland flow were 2200  $\mu g L^{-1}$  in one field (manure), 131  $\mu g L^{-1}$  in another field (inorganic fertilizers) and 60  $\mu g L^{-1}$  in

another field (fallow). Since an estimated  $27 \text{ L s}^{-1}$  entered the stream via overland flow, the quantity of SRP exported from the basin via overland flow may have been anywhere from  $0.5$  to  $18.4 \text{ g ha}^{-1} \text{ day}^{-1}$  (18-1000% of basin SRP export). Drainage tiles on the same day contributed  $5.3 \text{ g SRP ha}^{-1} \text{ day}^{-1}$  (250% of basin SRP export). During the same storm, TP concentrations in overland flow within the basin ranged from  $150 \mu\text{g L}^{-1}$  to  $8800 \mu\text{g L}^{-1}$ . Thus, TP exported via overland flow on April 12 may have been anywhere from  $1.3$  to  $73.6 \text{ g ha}^{-1} \text{ day}^{-1}$  (20-750% of basin TP export). Drainage tiles on the same day contributed  $17.7 \text{ g TP ha}^{-1} \text{ day}^{-1}$  (220% of basin TP export).  $\text{NO}_3^-$  concentrations in overland flow were lower than in tiles. For example, overland flow in various fields within the basin contained between  $3$  and  $5 \text{ mg NO}_3\text{-N L}^{-1}$ . Thus, between  $25.0$  and  $41.8 \text{ g NO}_3\text{-N ha}^{-1} \text{ day}^{-1}$  (12-20% of basin  $\text{NO}_3^-$  export) may have been exported via overland flow on April 12 2001, compared to  $109.0 \text{ g NO}_3\text{-N ha}^{-1} \text{ day}^{-1}$  (55% of basin  $\text{NO}_3^-$  export) from tiles. This suggests that overland flow was not a significant contributor to basin  $\text{NO}_3^-$  export on April 12 2001, but may have been a significant source of basin P export. These estimates are crude and must be treated with extreme caution. Given the error associated with estimating the contribution of overland flow to hydrochemical export, its importance on an annual basis cannot be quantified at this time.

#### **4.5 Summary and Conclusions**

This chapter has demonstrated the importance of tile drainage in hydrochemical export from the Strawberry Creek Watershed. Although a substantial portion of the discharge from the basin comes from diffuse groundwater sources, tiles are generally the dominant source of nutrients to the stream. As such, tiles are acting as the most important source of nutrients from this basin.

There is spatiotemporal variability in hydrochemical export from drainage tiles within this basin. Higher concentrations of SRP and TP are linked to fields receiving manure. No spatial patterns are evident with  $\text{NO}_3^-$  export through tiles. While there is within-event variability in the contribution of tiles to basin discharge, this can be predicted empirically from one continuously monitored tile. The error in predicted tile discharge is greatest during low flow periods. Strong correlations between other tiles in the basin suggest that simultaneously monitoring another one or two tiles in the basin will reduce the error in the predicted tile discharge.

This chapter has shown the dominance of drainage tiles in nutrient export from this basin. However, it has also shown that tiles are highly variable in both their hydrologic and chemical export. Such complexities complicate modelling endeavours. The temporal patterns in nutrient export throughout events suggest that macropores are an important pathway by which nutrients are transported into tiles and that this role changes under variable antecedent hydrologic conditions. Improving our understanding of the temporally dynamic role of tiles, and being able to quantify and predict this variability are areas where future research is necessary.



## **5.0 Influence of Antecedent Hydrologic Conditions on Patterns of Hydrochemical Export from a First-Order Agricultural Basin in Southern Ontario**

### **5.1 Introduction**

There is considerable interest among the scientific community in quantifying and predicting hydrochemical export patterns from agricultural catchments for both scientific and practical reasons. Spatial variables such as land use, soil type, topography, and drainage characteristics have all been empirically linked to hydrochemical export from various basins (McDowell *et al.*, 2001; Arheimer and Liden, 2000; Sims *et al.*, 1998; Stamm *et al.*, 1998; Jordan *et al.*, 1997; Beaulac and Reckhow, 1982; Welsch *et al.*, 2001). However, the specific reasons why similar precipitation events produce entirely different nutrient export patterns are poorly understood. Hydrochemical export cannot be easily predicted because export patterns are complicated by antecedent hydrologic conditions (AHC) in upland areas (Jenkins *et al.*, 1994; Biron *et al.*, 1999) as well as precipitation intensity (Muscutt *et al.*, 1993; Biron *et al.*, 1999). AHC have the potential to affect hydrochemical export by influencing both the quantity and quality of runoff following precipitation events. AHC can affect the storage of hydrologic inputs (rainfall, snowmelt) by influencing the storage capacity and the hydraulic conductivity of soils in the basin. During dry periods, the storage capacity of the basin is high and a substantial proportion of precipitation falling on the basin is expected to be retained. Under wetter conditions, the storage capacity of the basin is reduced and the hydraulic conductivity of soils increases causing increased runoff through upper soil horizons. Under very wet conditions, the storage capacity of the basin is low and the majority of precipitation that falls on the basin is expected to be exported as runoff.

AHC also govern the chemical constituents in runoff by influencing (a) the hydrologic flowpaths through which runoff moves; and (b) the 'available' pool of nutrients in basin soils. Factors such as soil temperature (Welsch *et al.* 2001), antecedent precipitation (Welsch *et al.* 2001) and antecedent wetness (Biron *et al.* 1999) have been identified as important in governing patterns of chemical export, but the effects of AHC on chemical export patterns are unclear (Muscutt *et al.*, 1993; Biron *et al.*, 1999; Welsch *et al.*, 2001). The chemical constituents in runoff have been found to vary depending on whether a given event is preceded by drought or wet conditions. Some authors report a pulse of nutrients following periods of drought, while others report an increase in nutrient export as moisture levels rise. For example, Biron *et al.* (1999) and Walling and Foster (1975) showed that initial chemical concentrations were higher following a period of drought rather than following a period of wet antecedent conditions. In laboratory tests Pote *et al.* (1998) showed that soluble reactive phosphorus (SRP) was more easily desorbed following the drying of soil samples and implied that this may lead to variable losses in runoff in different seasons and/or under variable AHC. Welsch *et al.* (2001) linked  $\text{NO}_3^-$  export to topographic indices and found that such relationships were strengthened as moisture levels increased due to increased hydrologic connectivity in the basin. Hydrologic connectivity with upper soil horizons appears to be critical in flushing chemicals into streams (Creed and Band, 1998; Biron *et al.*, 1999; Welsch *et al.*, 2001) and, such connectivity has been linked to AHC in several studies (Biron *et al.*, 1999; Welsch *et al.*, 2001).

Elevated nutrient losses have long been associated with surface runoff (e.g. Gburek and Sharpley, 1998). Since fertilizers are surface applied, surface soil horizons

contain the highest levels of nutrients. Therefore, runoff passing over and through upper soil horizons should contain higher quantities of nutrients due to the fact that there is a greater potential stock of nutrients in surface horizons due to the application of fertilizers and manure. Consequently, under exceptionally wet conditions when stormflow is passing over or through upper horizons of the soil, runoff is expected to contain higher quantities of SRP and  $\text{NO}_3^-$ . Under saturated conditions when overland flow is occurring, TP in runoff is expected to be highest due to surface erosion.

Losses of nutrients via runoff from soils may also occur under dry or moist conditions due to drainage through macropores and preferential flow pathways. These large pores have been identified as a major source of nutrients to surface waters (e.g. Stamm *et al.*, 1998; Beauchemin *et al.*, 1998; Kung *et al.*, 2000b). Under very dry conditions, runoff is forced to move via preferential 'finger like' flow (e.g. Ritsema *et al.*, 1998), thereby allowing surface waters to bypass natural soil processes and be exported to drainage tiles and/or surface waters (Beauchemin *et al.*, 1998; Gachter *et al.*, 1998; Ritsema *et al.*, 1998; Stamm *et al.*, 1998). 'Pulses' of nutrient losses are often observed under such dry conditions following rainfall (e.g. Beauchemin *et al.*, 1998; Stamm *et al.*, 1998) or irrigation (Stone and Krishnappan, 2002; 2003).

However, as soils become wet, the role of macropores and preferential flow pathways appears to increase. Kung *et al.* (2000) showed that water movement and contaminant transport shifts toward increasingly larger pores of preferential flow pathways as soils wet up. As soils become wetter during an event or with successive events, new and larger pores may be 'activated' and rapidly transport runoff from surface horizons into drainage tiles or waterways. Increasing soil wetness causes greater pore

sizes to be 'activated'. Thus, under more wet antecedent conditions, greater volumes of surface runoff are transported through larger pore spaces and greater losses of nutrients should be observed.

However, the available pool of nutrients in soils may also be affected by AHC. Throughout the course of any given year, the availability of nutrients is largely a function of the application of fertilizer and/or manure, where nutrient availability should obviously be highest following the application of these materials. As successive events occur and nutrients are exported from soils, the available pool of nutrients in soils is expected to decrease. As time passes between events, the pool of nutrients in soils may be replenished through biological activity. Thus, in addition to the application of fertilizers and manure, the distribution of storm events (and therefore AHC) may also affect nutrient export following precipitation events.

This chapter examines the relationship between hydrochemical export patterns and AHC in a first-order agricultural basin in Southern Ontario. The specific objectives of this chapter are:

- (1) to show linkages between AHC in the basin and the proportion of hydrologic inputs (rainfall, snowmelt) that are lost via discharge; and
- (2) to show linkages between AHC in the basin and the export of SRP, TP and  $\text{NO}_3^-$  in streamflow
- (3) to describe prevalent types of hysteresis loops that are found in storms in the study basin and link these to AHC.

## 5.2 Site Description and Methods

The research site description and methods are provided in detail in Chapter Two. Briefly, the data presented in this chapter are grouped on the basis of individual events (as outlined in detail in Chapter Two), and, are the same events explored in Chapters Three and Four. A total of 64 events, occurring over 25 months (all seasons) are described in this chapter.

In this chapter, AHC in the basin are related to basin retention of precipitation. The total discharge for a given event ( $Q$ ) is compared to the total hydrologic inputs (rain or snowmelt) throughout that event (PPT) and, this is presented as  $Q/PPT$  in the text and figures.

Variables such as water table position immediately prior to the event ( $WT_0$ ), stream flow rate immediately prior to the event ( $Q_0$ ) as well as over a two-week period prior to the event ( $Q_{2wks}$ ), season, and soil moisture are used to define AHC in this chapter.  $WT_0$  was selected as an indication of AHC because it provides a measurement of the upper limit of the saturated zone, and therefore influences both basin storage potential and also affects connectivity between deeper groundwater and surface soil horizons. The use of  $WT_0$  may be problematic, however, as this value is for one location in the basin only, and therefore may not reflect conditions elsewhere in the basin. Soil moisture was selected for a number of reasons. First, the hydraulic conductivity of soils, and therefore the routing of subsurface runoff, is strongly influenced by soil moisture. Also, soil moisture gives an indication of how close to saturation soils are. As soils become wetter, larger pores are 'activated', enhancing the rapid transport of runoff from surface horizons to tiles or surface waters. Furthermore, soil moisture may also have an effect on the

available nutrient pool in soils. For example, the amount of easily desorbed phosphorus increases in dry soils (Pote *et al.*, 1998), whereas  $\text{NO}_3^-$  may be reduced in saturated conditions if anoxia persists.  $Q_0$  was selected as a proxy for overall basin wetness (water table position and vadose zone moisture) immediately prior to the event. However, since  $Q_0$  is only indicative of conditions at the event onset, it does not give an indication of whether the basin is on a wetting or drying trend. Consequently, basin discharge over a two-week period prior to the event ( $Q_{2\text{wks}}$ ) was also employed as an indication of AHC. The small time interval of two weeks was arbitrarily selected to demonstrate basin wetness prior to each event because the basin is a small first-order stream. A larger time interval of one or more months may be too long a time interval. Season was also selected as an indication of AHC because of the influence of climatic variables on basin storage (e.g. frozen soils are less permeable), and also on the processes that govern nutrient cycling (e.g. biological activity is reduced in winter).

### **5.3 Results and Discussion**

Precipitation and/or thaw events are the driving force behind nutrient export at Strawberry Creek (Fig. 5.1) where the magnitude of nutrients exported generally increases with the magnitude of precipitation/snowmelt water added to the basin. However, these relationships are highly variable (Fig 5.1).

#### **5.3.1 Hydrology**

The relationship between discharge and a wide range of singular precipitation events, including snowmelt and resulting runoff volume is weak (60%) (Fig 5.2) and  $Q/PPT$  can range from 0 to 1.

Figure 5.1 Total nutrient losses ( $\text{kg ha}^{-1}$ ) for each event for SRP (a), TP (b) and  $\text{NO}_3^-$  (c).are plotted against the total hydrologic inputs (precipitation = rainfall + snowmelt) to the basin for a given event

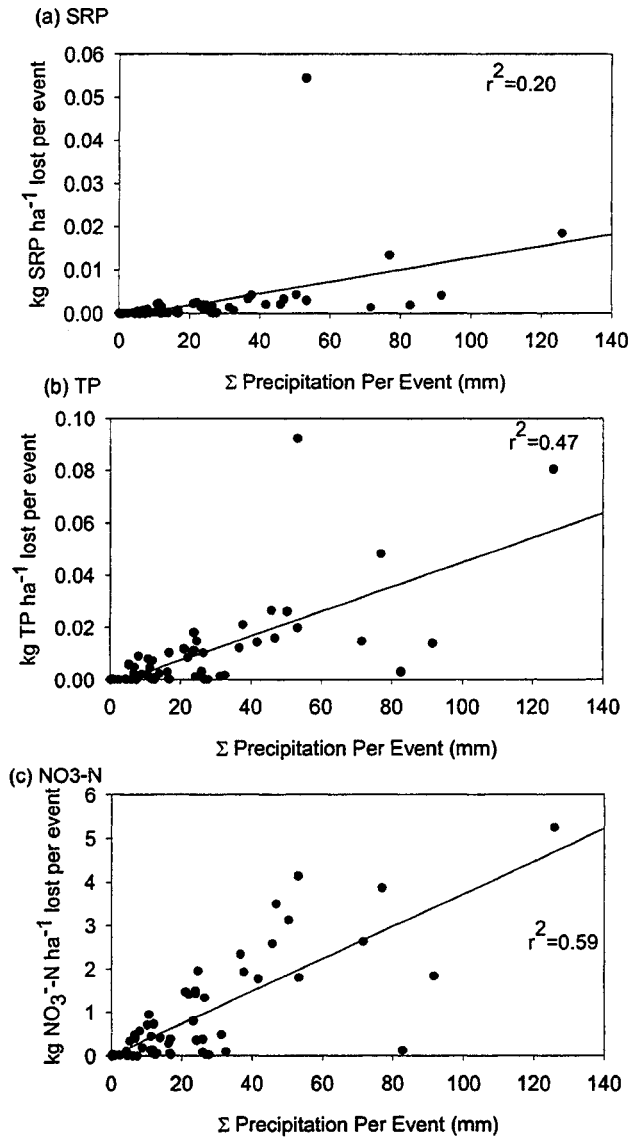
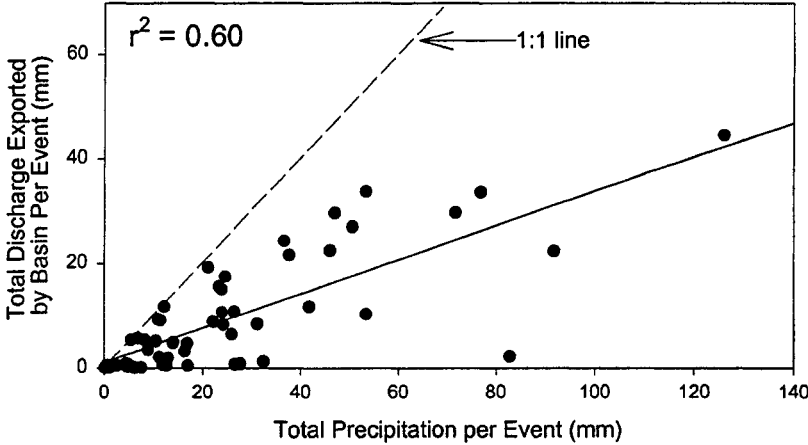


**Figure 5.2** The total discharge for a given event is plotted against the total hydrologic inputs to the basin (precipitation, = rainfall + snowmelt) for that event





The proportion of hydrologic inputs exported from the basin should be linked to the storage potential of the basin in some capacity. However, relationships between Q/PPT and the 'indices' of AHC are weak (Fig. 5.3). Figure 5.3a shows the relationship between  $Q_o$  and Q/PPT. Although the relationship is weak, the relationship appears to differ above and below the streamflow rate of  $40 \text{ L s}^{-1}$ . This is indicative of the drainage characteristics of the basin. At streamflow rates above  $40 \text{ L s}^{-1}$ , Q/PPT is always higher than 0. This is a result of the presence of drainage tiles in this basin. Chapter 4 of this thesis showed that at streamflow rates between 25 and  $40 \text{ L s}^{-1}$ , tiles began to flow and at streamflow rates above  $40 \text{ L s}^{-1}$  all tiles flowed. Consequently, if tiles are flowing, some fraction of hydrologic inputs will be exported from the basin. However, at streamflow rates below  $40 \text{ L s}^{-1}$ , the basin demonstrates a large amount of temporal variability in the proportion of hydrologic inputs that it can store, and may export between 0 and 100% of hydrologic inputs.

$Q_o$  may not be a good indication of the true AHC in the basin as it is an instantaneous value and is not a good indication of AHC in the basin over longer timescales. Figure 5.3b plots  $Q_{2\text{wks}}$  against Q/PPT for 64 events. Although there seems to be an increase in Q/PPT with increasing  $Q_{2\text{wks}}$ , the relationship is very poor.

Pre-event water table position ( $WT_o$ ) at the basin outflow shows absolutely no relationship with Q/PPT (Fig 5.3c). This is surprising, given that the position of the saturated zone should be a strong indication of the storage potential of the basin. However, a comparison of pre-event water table position at other locations in the basin, in both riparian and upland (field) areas, yields stronger relationships (Fig. 5.4),

**Figure 5.3** Indicators of antecedent hydrologic conditions (AHC) in the basin are plotted against the ratio of total hydrologic outputs to total hydrologic inputs (Q/PPT) for 64 events. The various indicators of AHC are (a) pre-event streamflow ( $Q_o$ ), Discharge lost over 2 weeks prior to the event onset ( $Q_{2wks}$ ), and pre-event water table position ( $WT_o$ ). The control of event ‘magnitude’ (total hydrologic inputs) on Q/PPT is shown in (d).

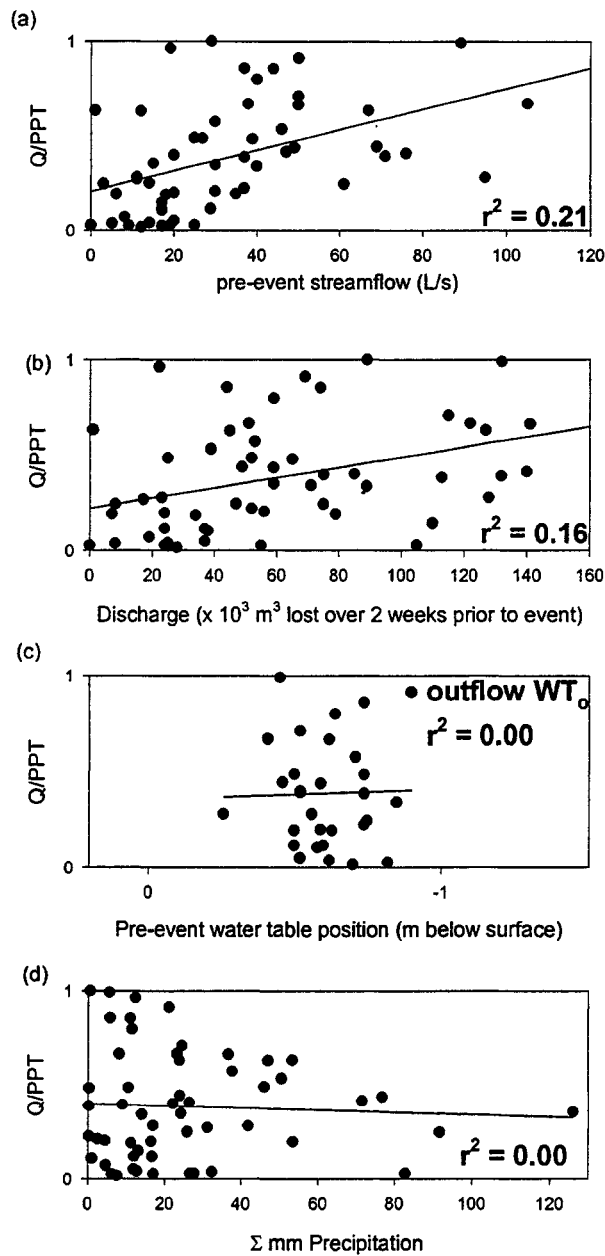
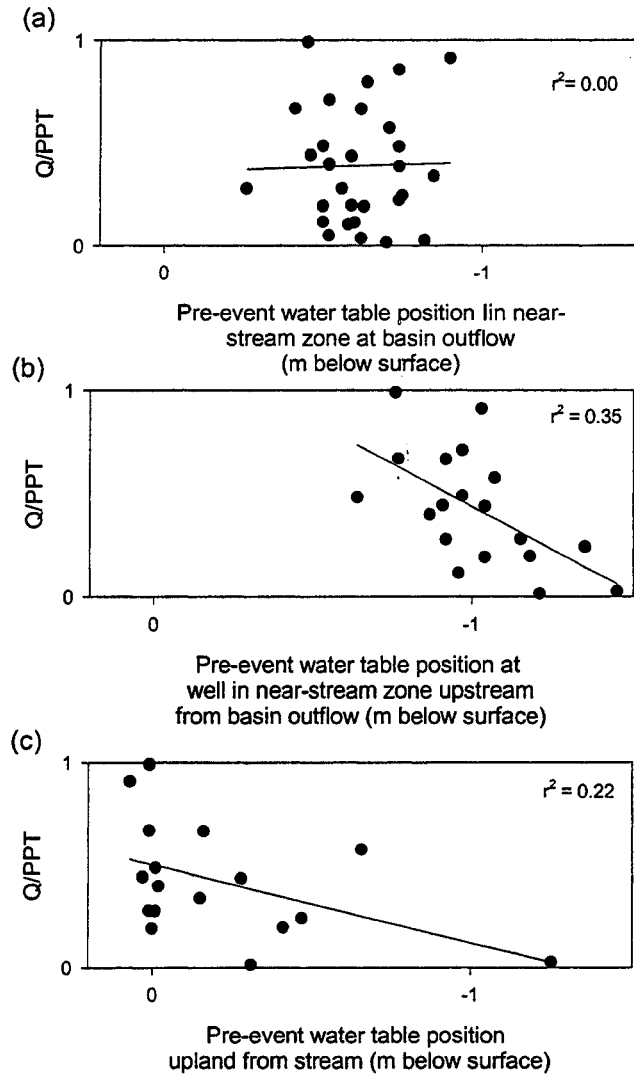


**Figure 5.4 Influence of pre-event water table position at various locations in the basin on the ratio of total hydrologic outputs to total hydrologic inputs (Q/PPT) for 64 events. Pre-event water table position in the riparian zone at the basin outflow, in the riparian zone upstream from the basin outflow, and in a field upland from the stream are shown in (a), (b) and (c), respectively.**



suggesting the pre-event water table position may in fact influence basin hydrologic response to precipitation events.

The magnitude of precipitation also does not appear to strongly affect Q/PPT (Fig 5.3d). However, rainfall amounts exceeding 40 mm do appear to represent a 'threshold' in this basin (Fig. 5.3d). Over the study period, 20% of precipitation events exceeded 40 mm. Rainfall amounts that are less than 40 mm may have a variable response, and Q/PPT may range from 0 to 1. However, at precipitation magnitudes greater than 40 mm, some fraction of the hydrologic input is generally exported. It is likely that events exceeding 40 mm are sufficient to induce tile flow in this basin even when conditions are dry in the basin. One exception to this is present in the data set. Several successive rainstorms (exceeding 80 mm of rainfall in total) in the summer of 2001 (August) were retained by the basin. These rainstorms followed several months of drought conditions during which there was no streamflow and the water table position was nearly 1 m beneath the streambed. These were anomalously dry conditions.

Rainfall intensity has also been found to influence Q/PPT in some studies (Muscutt *et al.*, 1993). During most of the storms that occurred over the study period, rainfall intensities ranged between 0 and 8 mm hr<sup>-1</sup>. Occasionally, intensities exceeded this and rain fell at rates of 20 mm hr<sup>-1</sup> and higher. In general, rainfall intensity did not affect Q/PPT in the study basin.

Season also does not appear to play a large role in governing Q/PPT. In general, very low Q/PPT values are not observed during winter events, unless the magnitude of the precipitation/thaw event is very small. Winter events are expected to have a reduced

ability to retain hydrologic inputs compared to summer events due to the presence of ground frost; however, clear seasonal trends are not apparent in the data set.

Stepwise linear regressions combining  $Q_o$ , ( $WT_o$  in the near-stream zone upstream from the basin outflow), soil moisture, and  $Q_{2wks}$  increase our confidence in predicting Q/PPT, although the relationships between these parameters are weak (Fig.5.5). The stepwise regressions demonstrate that a complex suite of AHC are likely working together to influence basin hydrologic response.

Table 5.1 shows several series of successive storms/thaw events. Variables such as  $WT_o$  and  $Q_o$  are also included in the table. The table demonstrates that Q/PPT increases for successive events, but some variables ( $WT_o$  and  $Q_o$ ) are less sensitive, which partly explains the poor relationships shown in Figure 5.3. While quantifiable variables such as  $WT_o$ ,  $Q_o$  and soil moisture may not change between successive events, AHC in the basin are still wetter with each event, as inputs of precipitation have occurred that have not been exported by the basin. Biron *et al.* (1999) also observed increased Q/PPT with successive events.

Figures 5.2 and 5.3, and Table 5.1 show that Q/PPT is highly variable temporally. Many variables work together to influence how much of the precipitation is able to pass through basin soils into the stream. This makes empirical modelling endeavours in this basin difficult.

### ***5.3.2 Nutrient Export***

The relationships between runoff volume and nutrient export on an event basis are strong (Fig. 5.6), indicating that if storm runoff can be quantified and predicted, nutrient

**Figure 5.5** Stepwise linear regressions showing the combined influences of the various indicators of AHC on the ratio of total hydrologic outputs to total hydrologic inputs (Q/PPT) for 64 events.  $Q_o$  ( $L s^{-1}$ ),  $WT_o$  in riparian zone upstream from basin outflow (m beneath soil surface), soil moisture at 25 cm (% saturation), and  $Q_{2ks}$  (mm) are shown in the various plots.

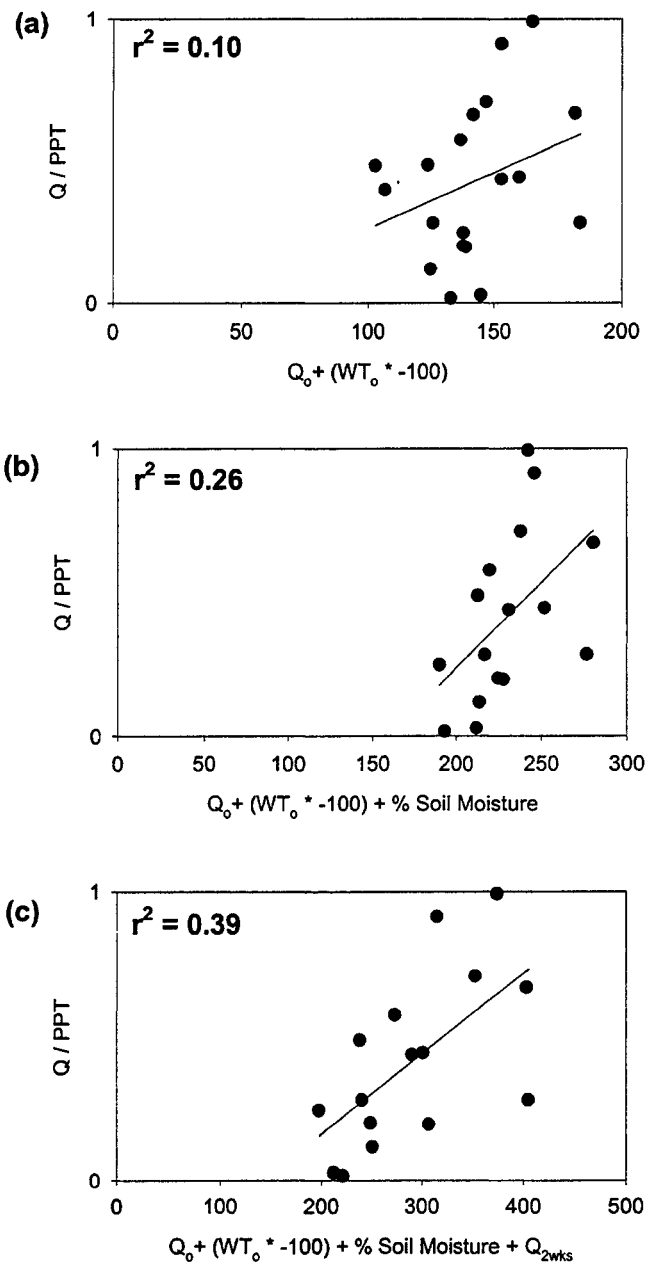
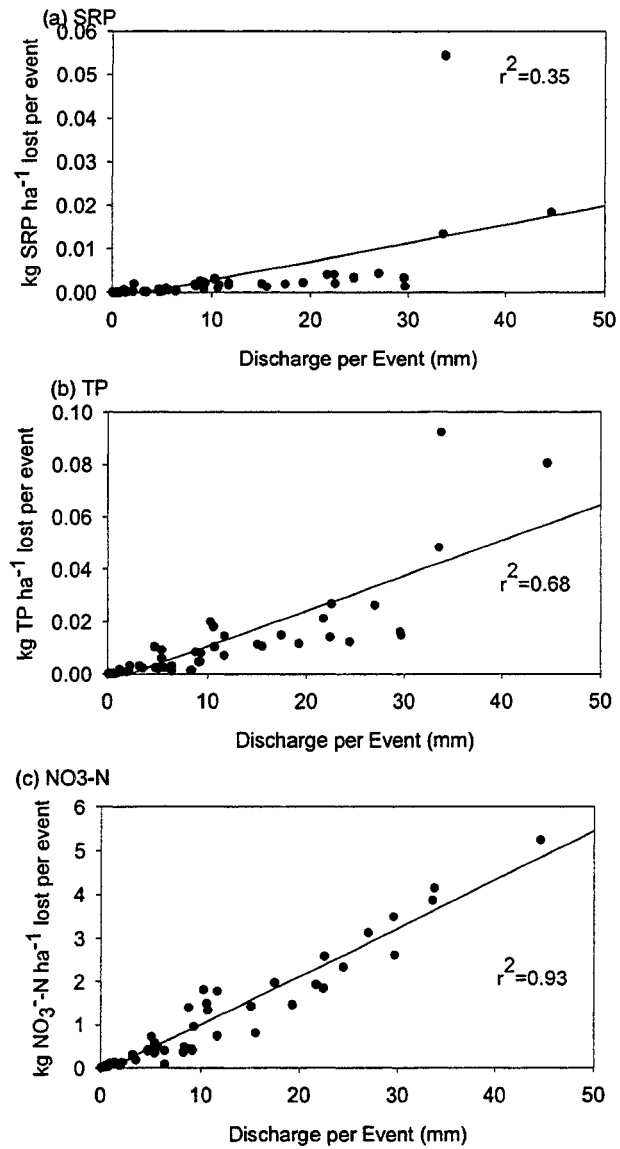


Figure 5.6 Total hydrologic losses (discharge) from the basin for a given event are plotted against the total nutrient losses ( $\text{kg ha}^{-1}$ ) for each event for SRP (a), TP (b) and  $\text{NO}_3^-$  (c).



**Table 5.1: Proportion of Precipitation Discharged from Basin During Successive Storms**

Date	PPT Duration (hrs)	Response Duration (hrs)	PPT (mm)	Q (mm)	Q <sub>o</sub> (L s <sup>-1</sup> )	WT <sub>o</sub> at basin outflow	WT <sub>o</sub> in near stream zone up from basin outflow	Soil Moisture at 25 cm depth (%)	Q/ PPT
Jan 30/01	10	621	37.7	21.7	30	-0.74	-1.07	83%	0.57
Feb 8/01	20	390	76.8	33.6	49	-0.59	-1.04	78%	0.44
Feb 25/01	8	476	36.7	25.1	50	-0.62	-0.92	-	0.68
May 8/01	2	59	7.5	0.1	12	-0.70	-1.21	60%	0.02
May 24/01	40	404	91.7	22.4	3	-0.75	-1.35	52%	0.24
June 3/01	2	365	11.4	9.1	40	-0.64	-	-	0.80
Oct 12/01	66	482	82.8	2.2	0	-0.82	-1.45	67%	0.03
Nov 2/01	12	540	32.5	1.2	5	-0.62	-	-	0.04
Nov 25/01	8	446	53.4	10.3	6	-0.63	-	-	0.19
Jan 6/02	6	298	16.7	0.6	17	-0.60	-	-	0.03
Jan 23/02	24	63	4.4	0.9	20	-0.59	-1.18	87%	0.20
Jan 26/02	10	270	10.4	5.1	27	-0.50	-0.97	89%	0.49
Feb 6/02	3	269	11.9	1.4	29	-0.50	-0.96	89%	0.12
Feb 19/02	40	154	41.8	11.8	11	-0.56	-1.15	91%	0.28
Feb 25/02	9	124	23.9	10.6	69	-0.46	-0.91	92%	0.44

mass export can also be predicted and/or quantified reasonably well. Although the relationships are strong, there is some variability in these relationships and events exporting similar amounts of discharge can export different masses of nutrients (Table 5.2).

### 5.3.2.1 Individual Events

In order to understand physical processes contributing to patterns of nutrient export, a series of events is explored in more detail in Figures 5.7 - 5.18. Given the close correlation among tile discharge rates in the basin (see Chapter Four) discharge patterns



from a continuously monitored tile are assumed to represent the behaviour of all tiles in the drainage basin.

**Table 5.2: Comparison of Variability in the Magnitude of Nutrient Export During Events with Similar Discharge**

<b>Discharge Lost</b>	<b>Date</b>	<b>SRP export (kg P ha<sup>-1</sup>)</b>
<b>5 mm</b>	Jan 26/02	2.9 x 10 <sup>-4</sup>
	Apr 6/01	7.9 x 10 <sup>-4</sup>
<b>9 mm</b>	Dec 17/01	2.5 x 10 <sup>-3</sup>
	Apr 12/01	5.0 x 10 <sup>-4</sup>
<b>22 mm</b>	Feb 25/01	3.4 x 10 <sup>-3</sup>
	Mar 18/01	2.4 x 10 <sup>-3</sup>
		<b>TP export (kg P)</b>
<b>5 mm</b>	Jan 14/01	2.5 x 10 <sup>-3</sup>
	Apr 6/01	1.0 x 10 <sup>-2</sup>
<b>9 mm</b>	Dec 17/01	8.2 x 10 <sup>-3</sup>
	Apr 12/01	5.8 x 10 <sup>-3</sup>
<b>22 mm</b>	Apr 19/00	2.7 x 10 <sup>-2</sup>
	Mar 18/01	1.2 x 10 <sup>-2</sup>
		<b>NO<sub>3</sub><sup>-</sup> export (kg N)</b>
<b>5 mm</b>	Jan 26/02	7.2 x 10 <sup>-1</sup>
	Apr 6/01	3.9 x 10 <sup>-1</sup>
<b>9 mm</b>	Dec 17/01	1.4
	Apr 12/01	3.4 x 10 <sup>-1</sup>
<b>22 mm</b>	Apr 19/00	2.6
	Mar 18/01	1.5

**Figure 5.7 Hydrologic and SRP export for a sequence of radiation melt days in March, 2001. Precipitation is shown in (a), stream discharge (solid line), discharge from one continuously monitored drainage tile (dashed line), and water table position (dotted line) are shown in (b), stream SRP concentration (dots) and mass output (bars) are shown in (c) and Q-SRP relationships are shown in (d). Melt 'days' are labelled (1-5) in (b) and (d).**

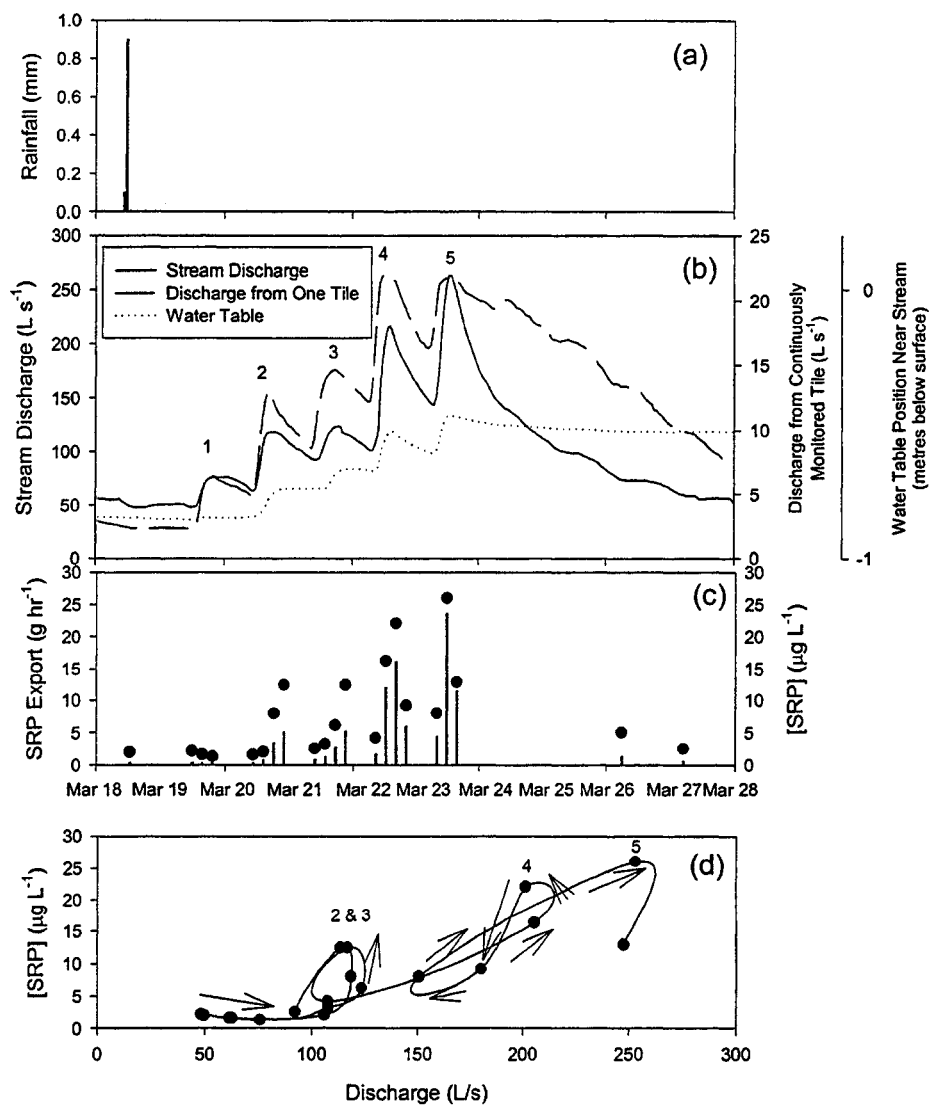


**Figure 5.8 Hydrologic and TP export for a sequence of radiation melt days in March, 2001. Precipitation is shown in (a), stream discharge (solid line), discharge from one continuously monitored drainage tile (dashed line), and water table position (dotted line) are shown in (b), stream TP concentration (dots) and mass output (bars) are shown in (c) and Q-TP relationships are shown in (d). Melt ‘days’ are labelled (1-5) in (b) and (d).**

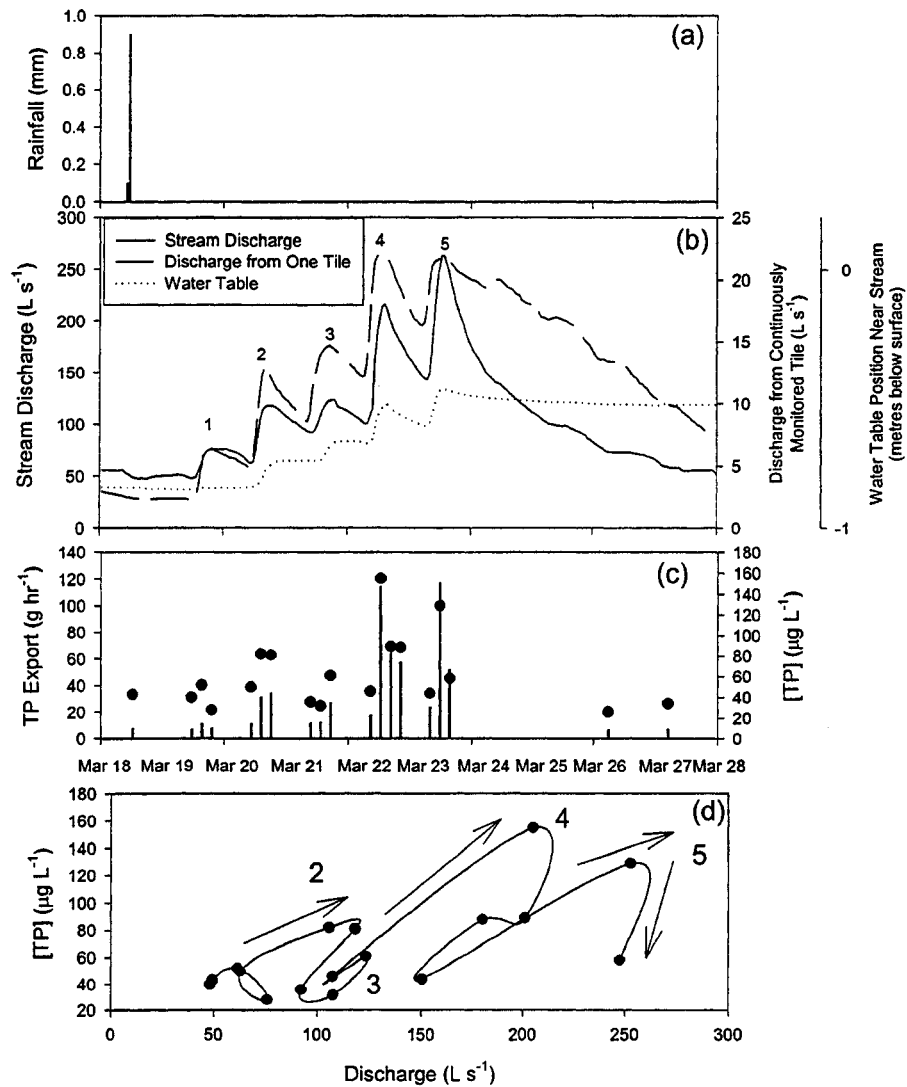


**Figure 5.9 Hydrologic and  $\text{NO}_3^-$  export for a sequence of radiation melt days in March, 2001. Precipitation is shown in (a), stream discharge (solid line), discharge from one continuously monitored drainage tile (dashed line), and water table position (dotted line) are shown in (b), stream  $\text{NO}_3\text{-N}$  concentration (dots) and mass output (bars) are shown in (c) and Q-  $\text{NO}_3\text{-N}$  relationships are shown in (d). Melt 'days' are labelled (1-5) in (b) and (d).**

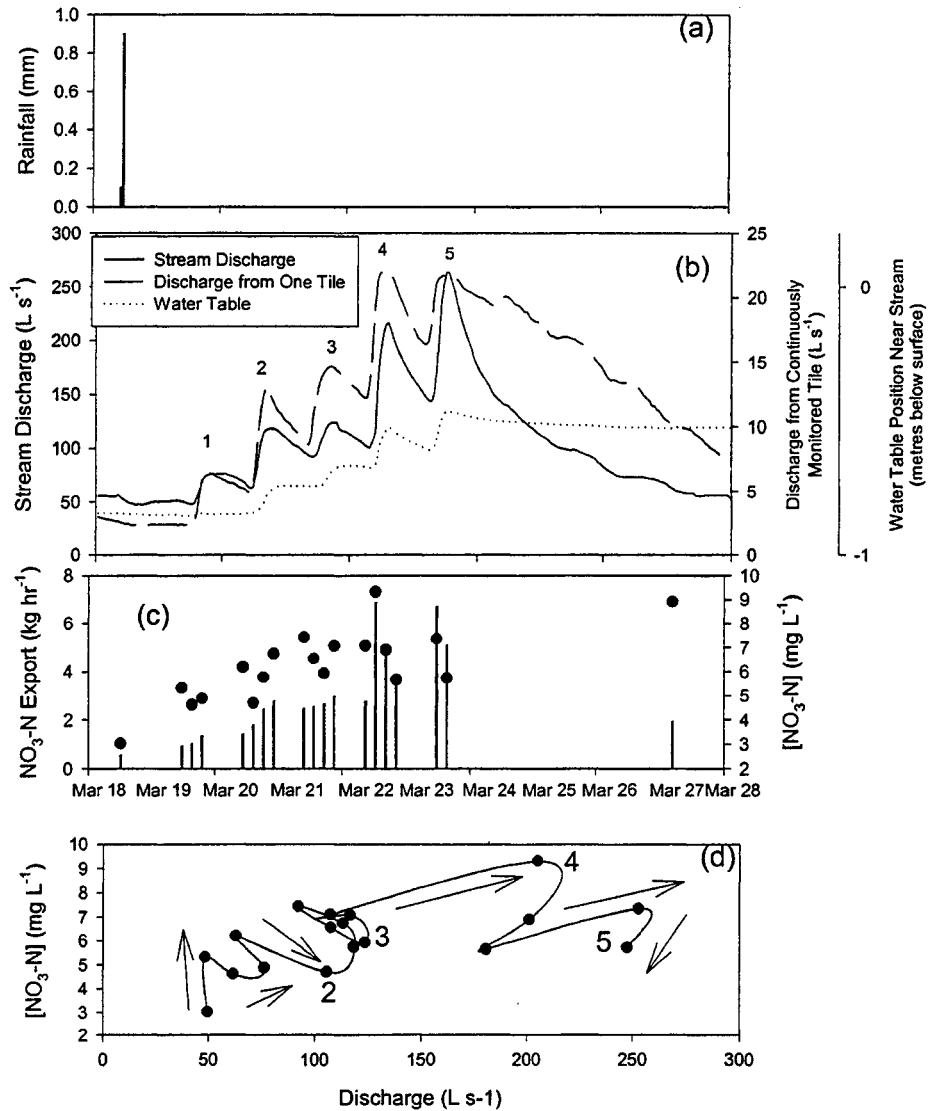


**Figure 5.10 Hydrologic and SRP export for a sequence of rainstorms in April, 2001, following a prolonged wet period. Precipitation is shown in (a), stream discharge (solid line), discharge from one continuously monitored drainage tile (dashed line), and water table position (dotted line) are shown in (b), stream SRP concentration (dots) and mass output (bars) are shown in (c) and Q-SRP relationships are shown in (d). Individual storms are labelled (1-3) in (b) and (d).**

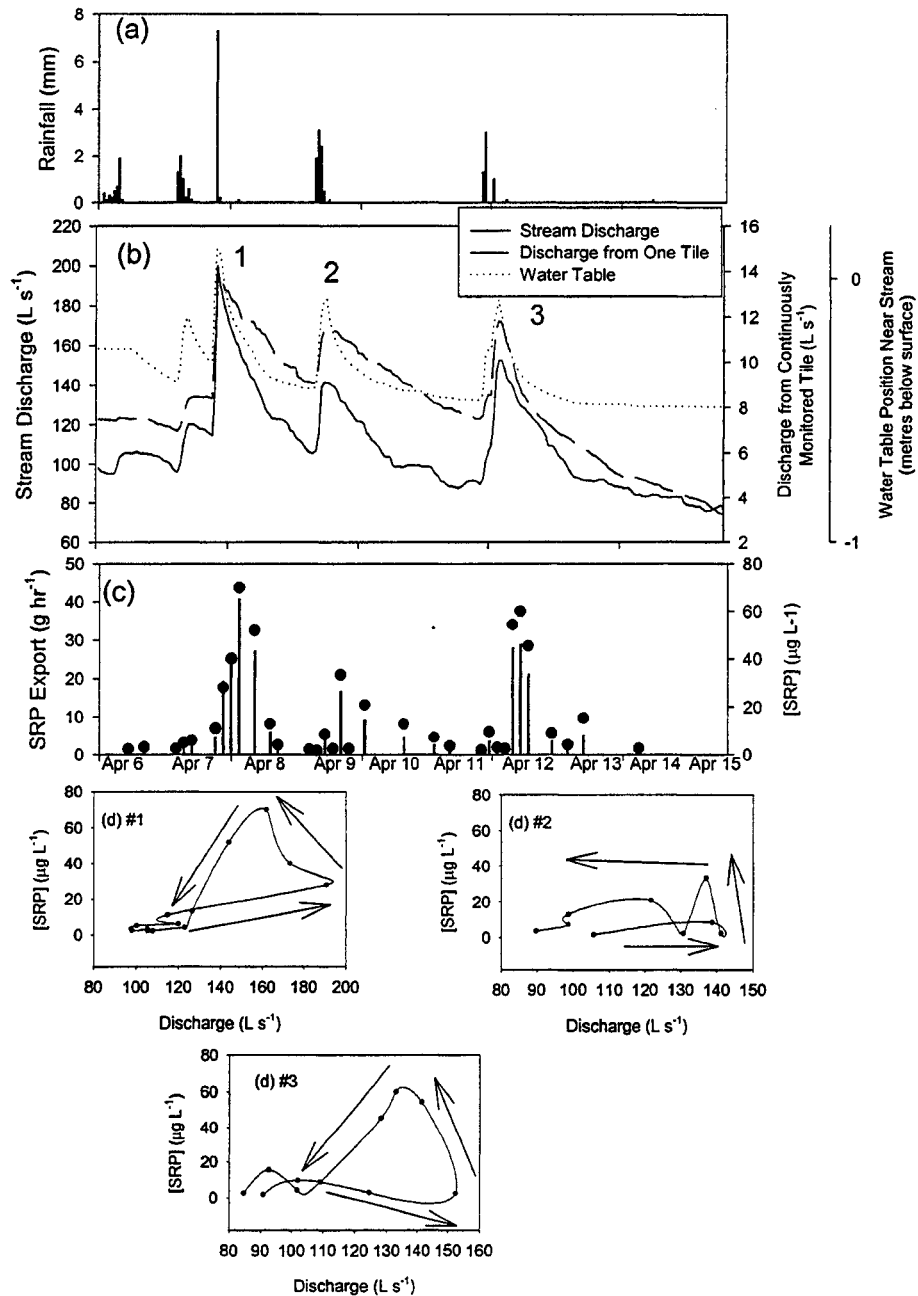


**Figure 5.11 Hydrologic and TP export for a sequence of rainstorms in April, 2001, following a prolonged wet period. Precipitation is shown in (a), stream discharge (solid line), discharge from one continuously monitored drainage tile (dashed line), and water table position (dotted line) are shown in (b), stream TP concentration (dots) and mass output (bars) are shown in (c) and Q-TP relationships are shown in (d). Individual storms are labelled (1-3) in (b) and (d).**

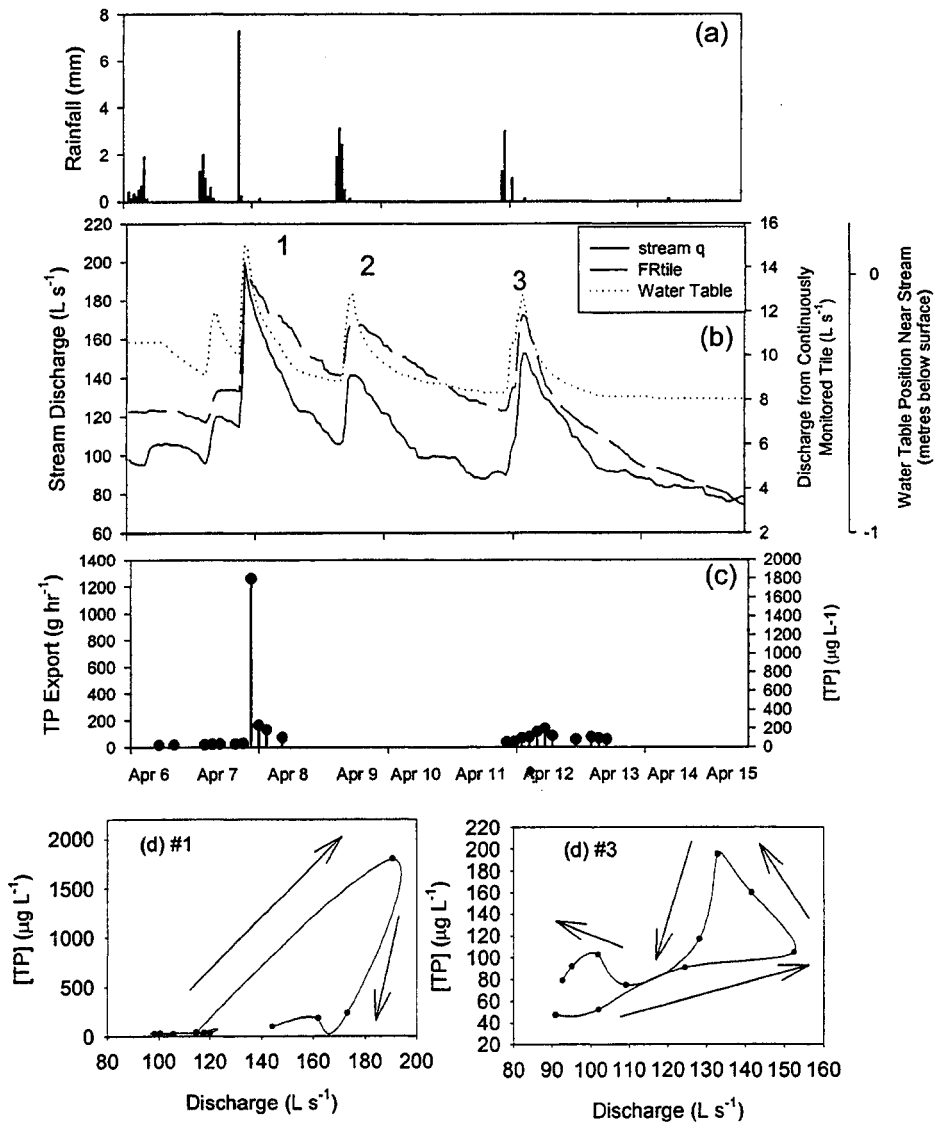


**Figure 5.12 Hydrologic and  $\text{NO}_3^-$  export for a sequence of rainstorms in April, 2001, following a prolonged wet period. Precipitation is shown in (a), stream discharge (solid line), discharge from one continuously monitored drainage tile (dashed line), and water table position (dotted line) are shown in (b), stream  $\text{NO}_3\text{-N}$  concentration (dots) and mass output (bars) are shown in (c) and Q-  $\text{NO}_3\text{-N}$  relationships are shown in (d). Individual storms are labelled (1-3) in (b) and (d).**

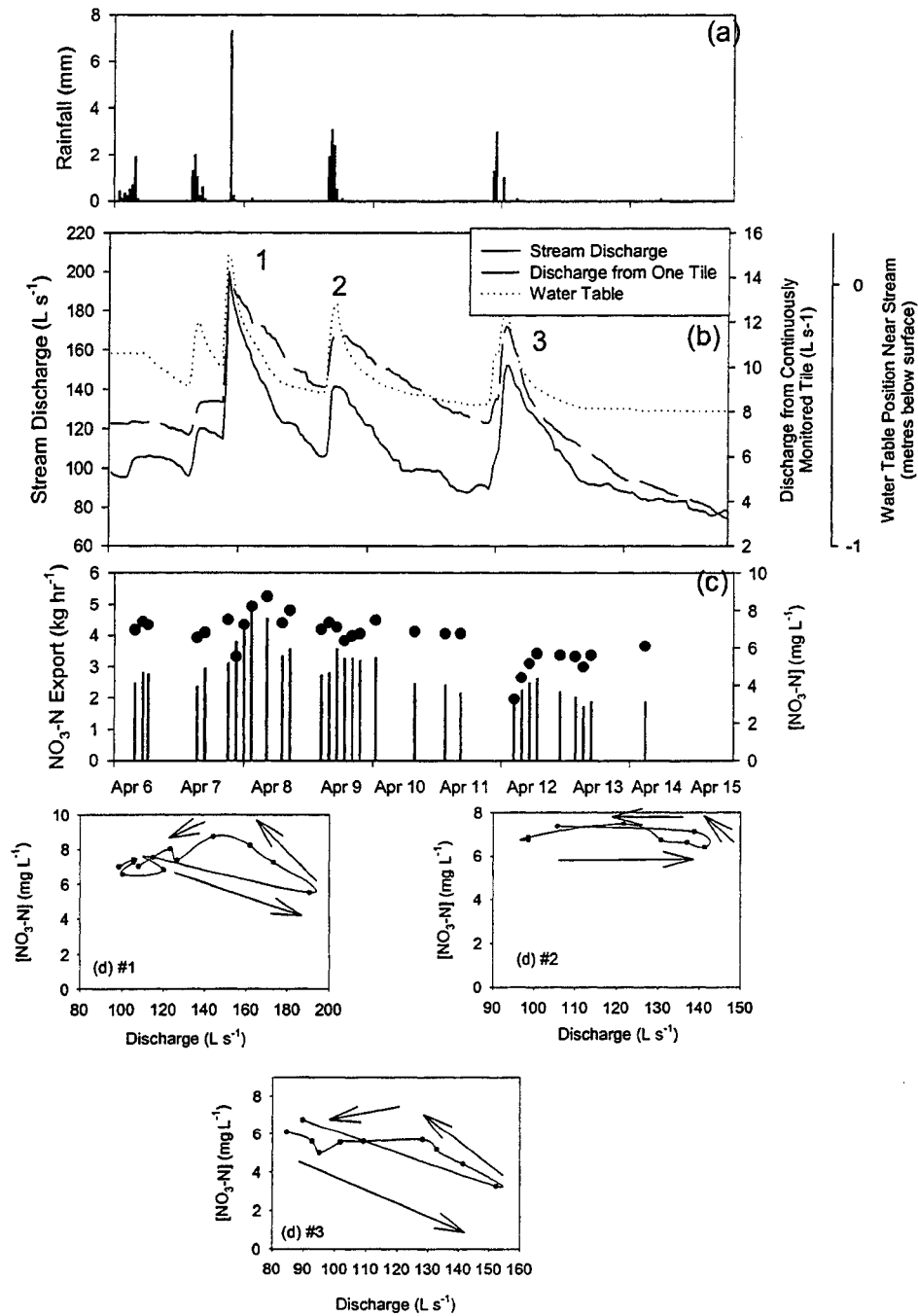


**Figure 5.13 Hydrologic and SRP export for a sequence of rainstorms in October, 2001, following a prolonged dry period. Precipitation is shown in (a), stream discharge (solid line), discharge from one continuously monitored drainage tile (dashed line), and water table position (dotted line) are shown in (b), stream SRP concentration (dots) and mass output (bars) are shown in (c) and Q-SRP relationships are shown in (d). Individual storms are labelled (1-3) in (b) and (d). Individual storms are labelled (1-3) in (b) and (d).**

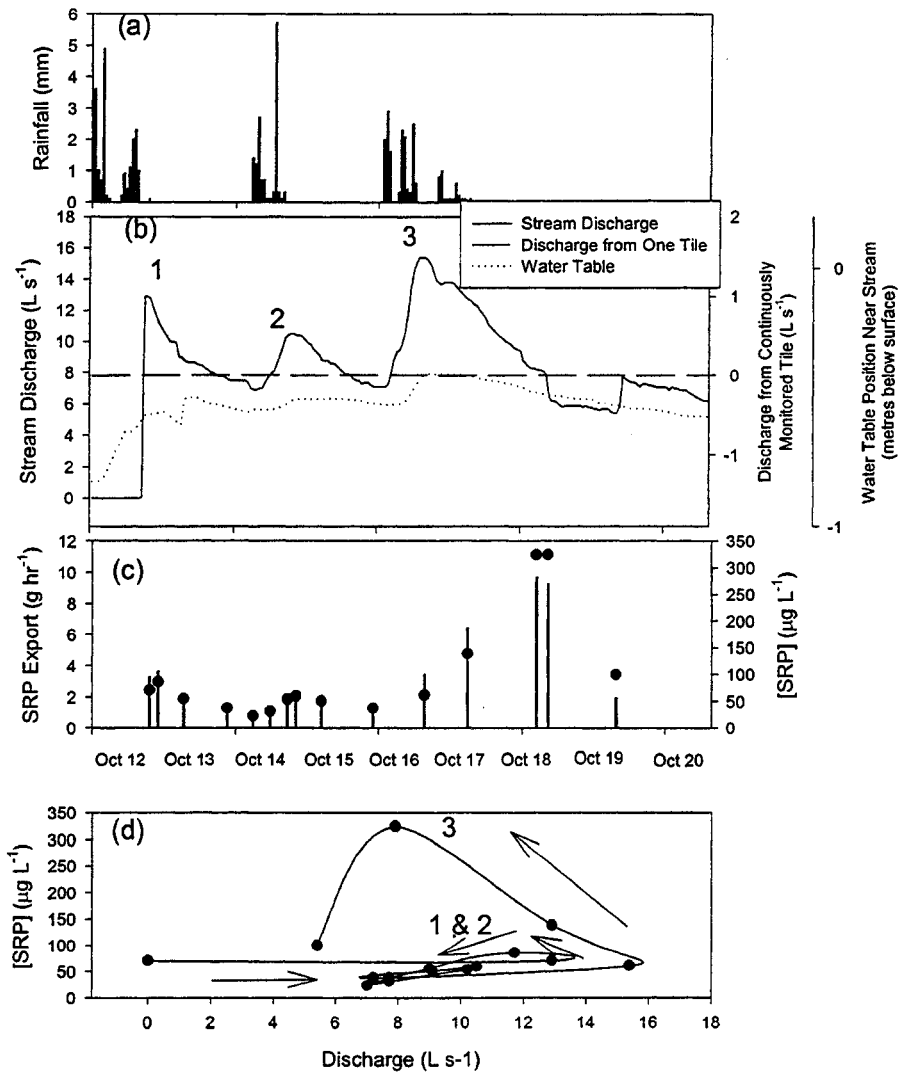
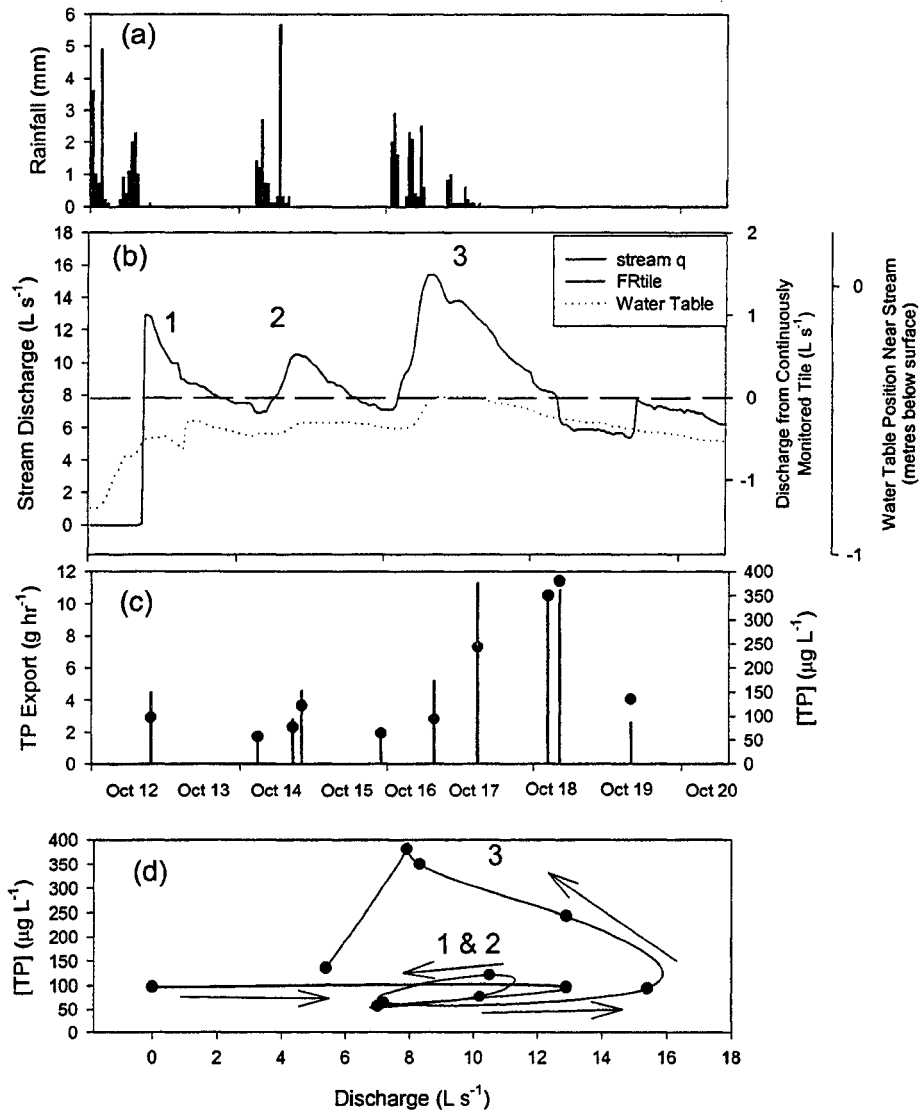
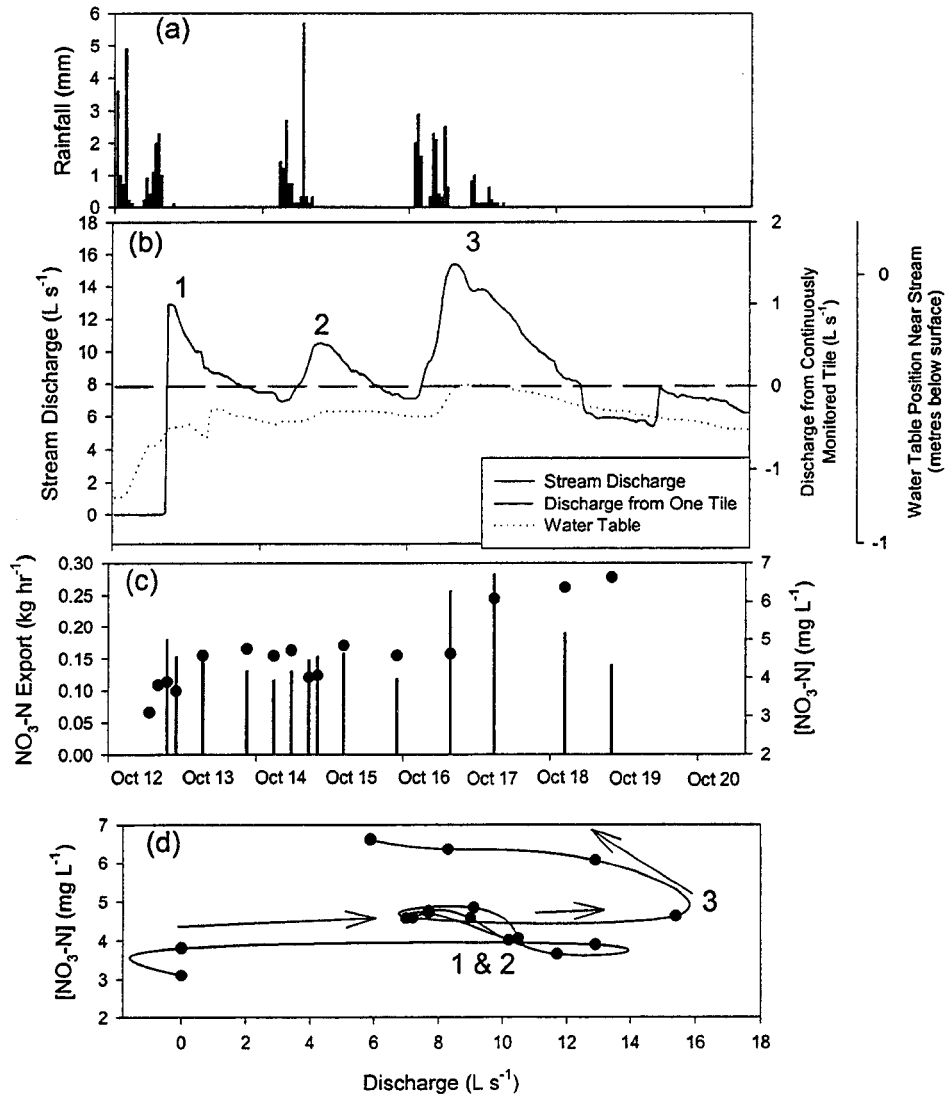




Figure 5.14 Hydrologic and TP export for a sequence of rainstorms in October, 2001, following a prolonged dry period. Precipitation is shown in (a), stream discharge (solid line), discharge from one continuously monitored drainage tile (dashed line), and water table position (dotted line) are shown in (b), stream TP concentration (dots) and mass output (bars) are shown in (c) and Q-TP relationships are shown in (d). Individual storms are labelled (1-3) in (b) and (d). Individual storms are labelled (1-3) in (b) and (d).



**Figure 5.15 Hydrologic and  $\text{NO}_3^-$  export for a sequence of rainstorms in October, 2001, following a prolonged dry period. Precipitation is shown in (a), stream discharge (solid line), discharge from one continuously monitored drainage tile (dashed line), and water table position (dotted line) are shown in (b), stream  $\text{NO}_3\text{-N}$  concentration (dots) and mass output (bars) are shown in (c) and  $Q\text{-NO}_3\text{-N}$  relationships are shown in (d). Individual storms are labelled (1-3) in (b) and (d).**



**Figure 5.16 Hydrologic and SRP export for a rain-on-snow winter thaw event in December, 2001. Precipitation is shown in (a), stream discharge (solid line), discharge from one continuously monitored drainage tile (dashed line), and water table position (dotted line) are shown in (b), stream SRP concentration (dots) and mass output (bars) are shown in (c) and Q-SRP relationships are shown in (d).**

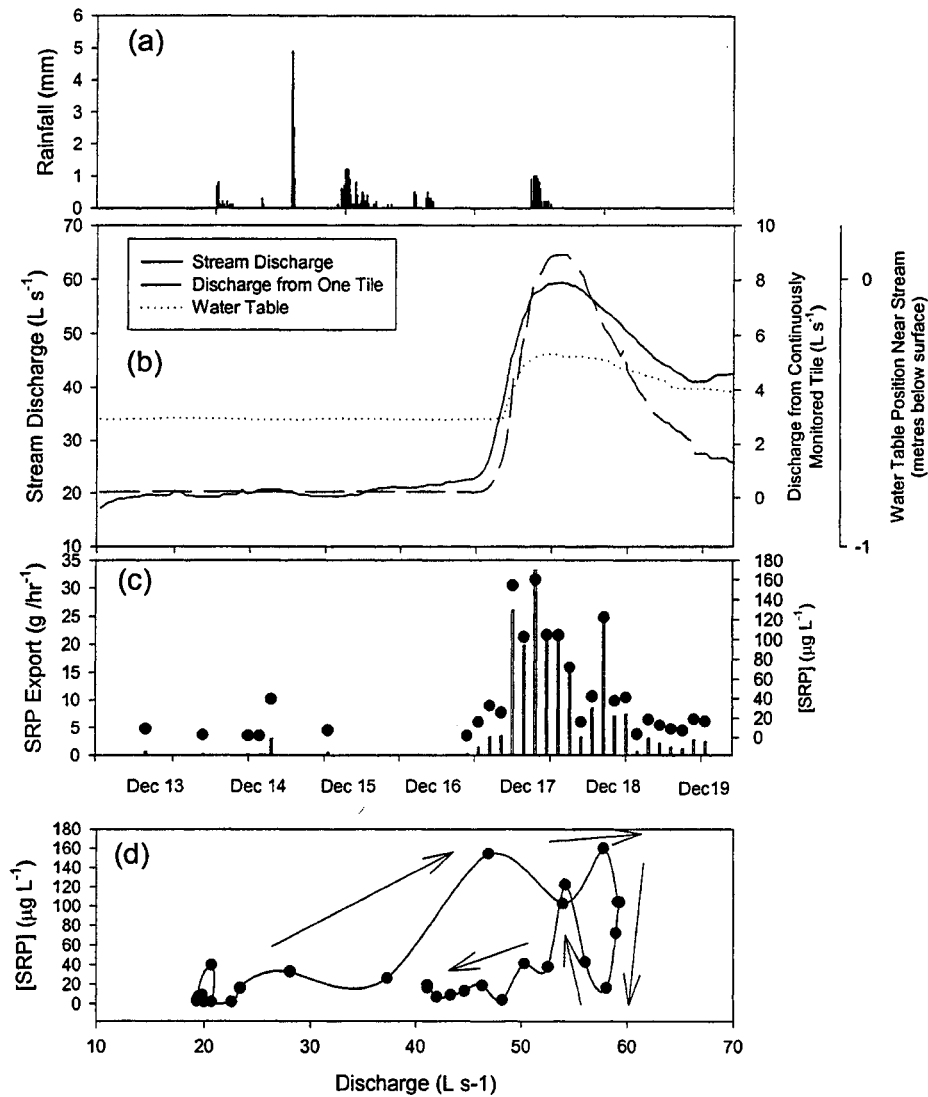


**Figure 5.17 Hydrologic and TP export for a rain-on-snow winter thaw event in December, 2001. Precipitation is shown in (a), stream discharge (solid line), discharge from one continuously monitored drainage tile (dashed line), and water table position (dotted line) are shown in (b), stream TP concentration (dots) and mass output (bars) are shown in (c) and Q-TP relationships are shown in (d).**

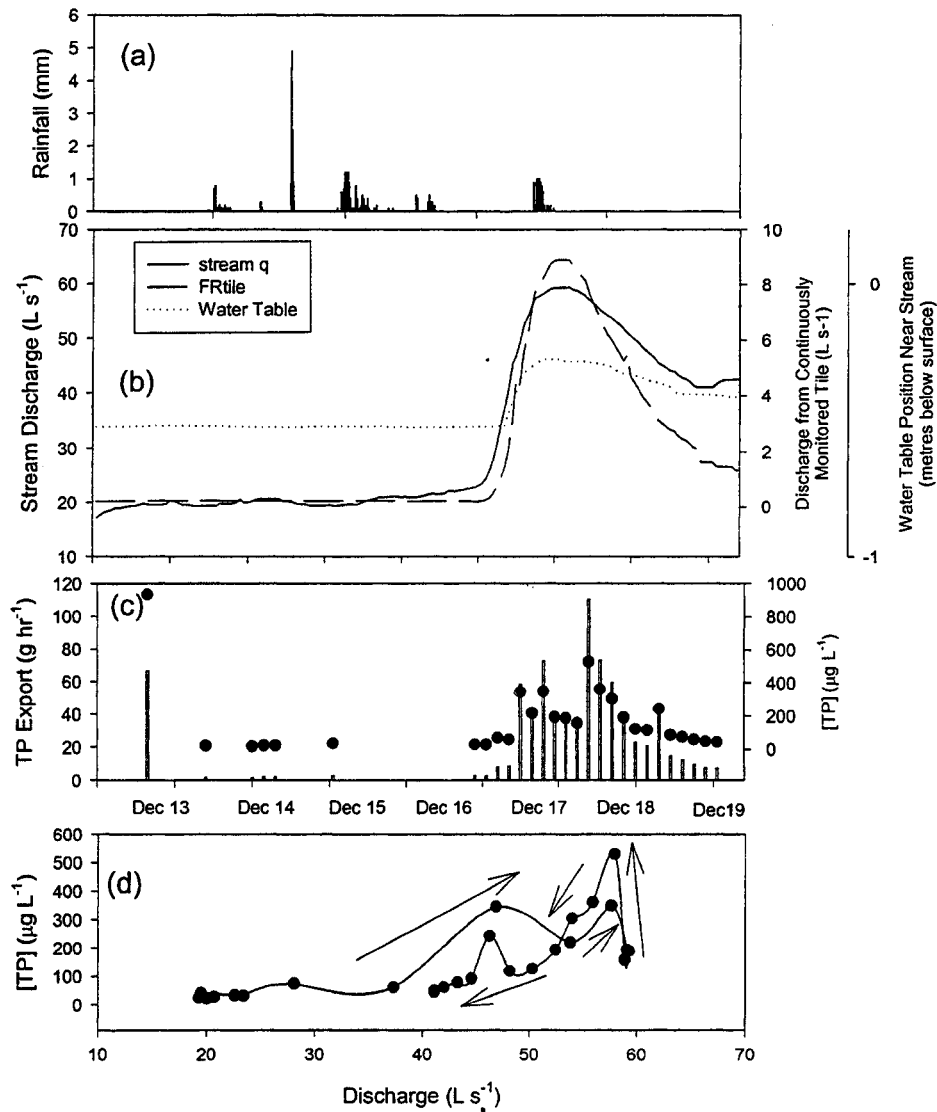
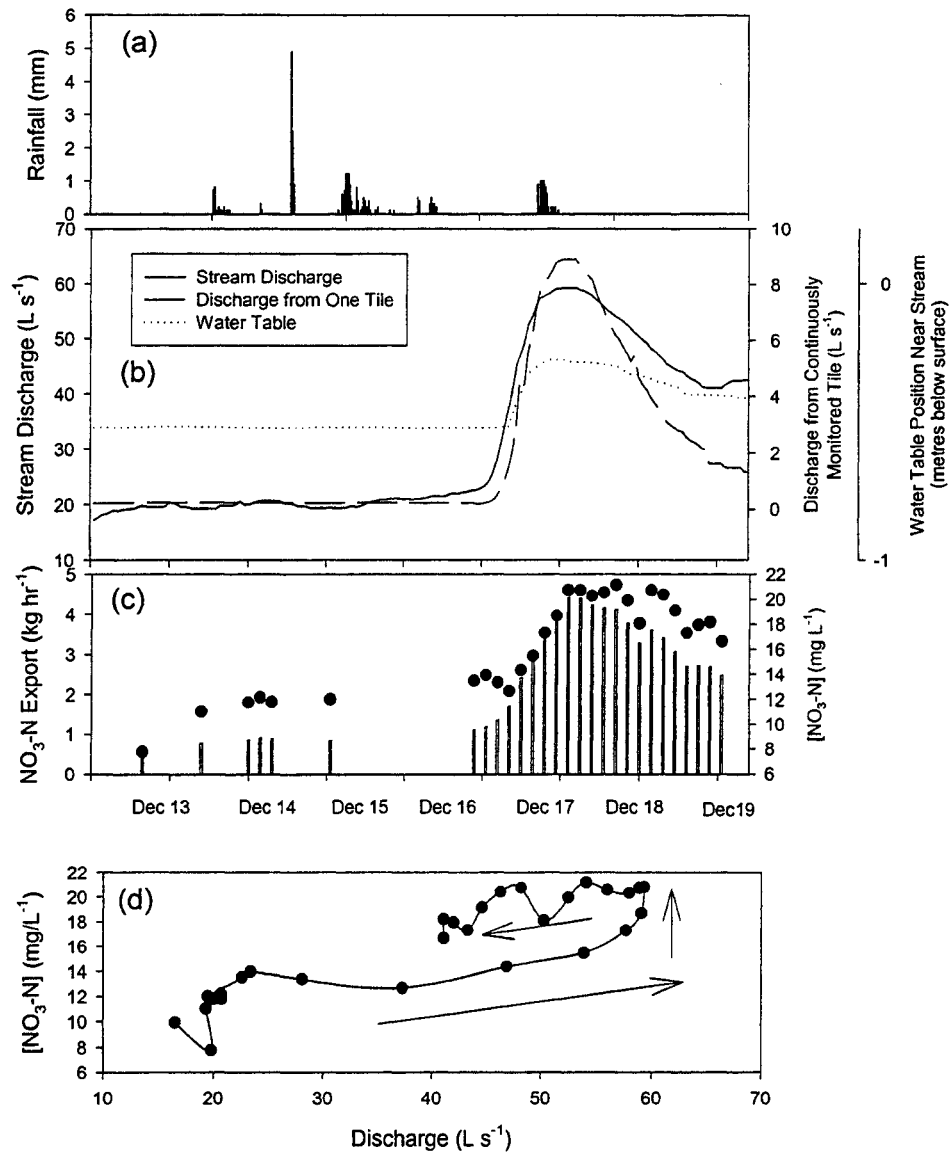


**Figure 5.18 Hydrologic and  $\text{NO}_3^-$  export for a rain-on-snow winter thaw event in December, 2001. Precipitation is shown in (a), stream discharge (solid line), discharge from one continuously monitored drainage tile (dashed line), and water table position (dotted line) are shown in (b), stream  $\text{NO}_3\text{-N}$  concentration (dots) and mass output (bars) are shown in (c) and Q-  $\text{NO}_3\text{-N}$  relationships are shown in (d).**



### March 18 – 23, 2001

Hydrologic and nutrient export data for SRP, TP and  $\text{NO}_3^-$  are illustrated in Figures 5.7, 5.8 and 5.9, respectively. Cold weather occurred for a period of two weeks prior to onset of this March event (mean air temperature over the two weeks prior to this event was  $-3.3^\circ\text{C}$ ), and no precipitation fell during this period. The water table was relatively low prior to this event (0.80 m beneath the surface in the near-stream zone), although soil moisture was close to saturation (91% saturated in top 25 cm of soil). Two major thaw events (rain-on-snow) preceded this event in February, and a substantial amount of the winter snow pack was lost during the February melt events. This period of elevated discharge in March was a series of small events (radiation melt) in which 20 mm of snow water equivalent were lost over a period of 7 days. The water table increased in a stepwise manner during the first few days of the melt event (Figs. 5.7b-5.9b #2 and #3), but began to rise and fall during the latter days of the event (#4 and #5). Correspondingly, a strong diurnal trend is seen in stream and tile discharge as well as water table position (Figs. 5.7b, 5.8b and 5.9b).

#### *P Export*

SRP mass export and concentrations in streamwater are shown in Figure 5.7c and Q-[SRP] relationships are shown in Figure 5.7d. During the first day of the melt event, no change is observed in water table position or stream water SRP concentrations although a small change in stream discharge and tile discharge occurred. During the second and third days of the event, an increase in both SRP concentrations and mass export occurred with successive days which corresponds with the diurnal rise in water table and tile discharge.

These counter-clockwise hysteresis loops for the successive events (Fig. 5.7d) and the corresponding rise in the water table indicate that SRP concentrations were greater on the falling limb of the hydrograph, after the water table peaked. It is assumed that either a 'new' nutrient pool is available as the water table moves into higher soil horizons, or, new pores in the vadose zone are 'activated' as wetness increases, thereby allowing more runoff from surface horizons to pass through soils unhindered. During the latter portion of the 4<sup>th</sup> day and during the 5<sup>th</sup> day, there is still an increase in discharge but only a slight increase in the water table position and no increase in soil moisture. The Q-[SRP] plot shows a shift from a counter-clockwise hysteresis pattern to a clockwise hysteresis pattern at this point in the event. Ulen and Persson (1999) suggested that a clockwise hysteresis loop suggests either (a) a finite amount of SRP available or a decrease of available SRP due to prolonged runoff and dilution effects. It is possible that the 'stabilization' of the water table during the latter stages of the event partly caused this pattern. It is possible that the SRP pool in the contributing areas of the soil was depleted and new 'pools' of SRP were not accessed because either (a) the water table failed to move into higher soil horizons or (b) no new pores were 'activated' within the vadose zone.

Q-[TP] relationships (Fig. 5.8d) are less clear and appear to exhibit clockwise hysteresis loops rather than counter-clockwise loops evident in the Q-[SRP] relationships. In the latter stages of the event (days #4 and 5), there is a decrease in TP output. The 'activation' of new pores with wetter AHC may explain the successive clockwise hysteresis loops. Fine grained particles are selectively lost early in events, often through

preferential flow paths. Thus, as ‘new’ pores are ‘activated’ under successive events, a ‘new’ pulse of TP may occur with each event.

#### *NO<sub>3</sub><sup>-</sup> Export*

Q-[NO<sub>3</sub>-N] relationships show hysteresis loops (Fig 5.9d) that appear to be counter-clockwise in nature in the early portion of the event (days 2 and 3) but these successive loops also exhibit an increase in NO<sub>3</sub><sup>-</sup> concentrations between successive events (Fig 5.9c-d) in the latter stages of the event (days 4 and 5). However, the hysteresis loops shift to clockwise loops as with SRP and the response of SRP and NO<sub>3</sub><sup>-</sup> were similar during this period. The successive counter-clockwise loops suggest that new sources or pathways within the soil were accessed as conditions became successively wetter. The clockwise loops during the latter stages of the event suggest that the NO<sub>3</sub><sup>-</sup> pool may have been depleted in the soils. Alternatively, other flowpaths (*e.g.* overland flow) may have been contributing to the stream and diluting NO<sub>3</sub><sup>-</sup> concentrations in the streamwater.

#### April 6 – 20, 2001

A series of successive rainstorms occurred following the March events (Figures 5.7-5.9). Mean air temperatures for 10 days prior to this event were warmer than prior to the March event noted above (2.7°C), and no precipitation fell prior to this event. Approximately 4.6 mm of snow melted in the basin in the three weeks prior to this event and basin soils were very wet (93% saturated in top 25 cm of soil). The water table was



0.89 m beneath the surface in the near-stream zone upstream from the basin outflow but was only 0.26 m beneath the surface in the near-stream zone at the basin outflow.

Hydrologic and nutrient export data for SRP, TP and  $\text{NO}_3^-$  are shown in figures 5.10, 5.11 and 5.12, respectively. As during the March events (Figs. 5.7-5.9), stream discharge and drainage from the continuously monitored tile are related. However, what differs from the March events is that there is an overall ‘drying trend’ rather than a ‘wetting trend’ in basin AHC (Figs. 5.10b-5.12b).

### *P Export*

The drying trend throughout this series of events has important implications for SRP export from the basin (Figure 5.10). The water table peaks on April 6 (storm #1) and overland flow occurs for a short period. With each successive event (storms #2 and #3), an increase in SRP mass is observed on the falling limb of each of the individual hydrograph peaks but the magnitude appears to decrease with each successive event. This seems to indicate that although successive events are occurring, AHC are not ‘wetting up’ with each successive event (as they were in March) and instead AHC are drier. This decline in SRP losses may be due to a depletion of the available SRP pool in the soil, as the “peak” water table position during each successive storm does not access a ‘new’ soil horizon but re-enters a soil horizon that was accessed during the preceding event. Alternatively, large pores in the vadose zone may be ‘inactivated’ as conditions dry out and drainage may be restricted to smaller pores.

The effect of wetting conditions and pore size is also evident for TP although the pattern is muted in the TP plots due to the substantial pulse of TP that occurred during the

short period of overland flow (storm #1). This pulse was likely due to erosion of surficial soils. Ulen and Persson (1999) observed reduced TP fluxes in tile drains during successive events and attributed this to a reduced pool of TP in subsoils.

### *NO<sub>3</sub><sup>-</sup> Export*

NO<sub>3</sub><sup>-</sup> shows the same decreasing trend as SRP and TP with each successive storm. During storms #1 and #3, NO<sub>3</sub><sup>-</sup> concentrations were diluted on the rising limb of the hydrograph. It is possible that streamflow during these periods may have been partially from overland flow which is low in NO<sub>3</sub><sup>-</sup> concentration and would therefore have diluted NO<sub>3</sub><sup>-</sup> in the streamwater. However, during all three storms, Q-[NO<sub>3</sub><sup>-</sup>] plots showed counter-clockwise hysteresis loops indicating that a new source of NO<sub>3</sub><sup>-</sup> was accessed as conditions became wetter.

### October 12 – 21, 2001

This event resembles the March events (Figs 5.7-5.9) in that AHC are ‘wetting up’, however, it differs from the March event in that it follows several months of summer drought rather than moist winter AHC. Mean daily air temperatures during July and August were 18.7°C, but temperatures had cooled in late September and early October, and averaged 9.6°C over the two week period prior to October 12. 82.8 mm of rainfall fell over the first two weeks of October, prompting the response on October 12. Prior to October 12, there had been no surface water discharge from the basin for three months.

Hydrologic and nutrient export data for SRP TP and NO<sub>3</sub><sup>-</sup> are presented in Figures 5.13, 5.14, and 5.15, respectively.

### *P Export*

As in the March event (Figs. 5.7-5.9), SRP concentrations increase in discharge as AHC become wetter. However, SRP concentrations were very high in October compared to March and April storms. This may be the result of several factors. First, solid manure had been applied to 10% of the basin less than two weeks prior to this event which was preceded by several months of drought. Most of the TP loss during this event was as SRP rather than PP. The direct leaching of SRP following the recent application of manure has been observed in other systems (e.g. Stone and Krishnappan, 2003). SRP export was also high during a subsequent event (Nov. 2), but was less than the October 12 event, indicating that the pool of SRP may have been depleted with successive rain events. It is likely that a pulse of SRP passed through macropores into the stream during the October event. Pulses of SRP via macropore flow into drainage tiles following dry conditions have been observed elsewhere (e.g. Stamm *et al.*, 1998; Beauchemin *et al.*, 1998).

The patterns of SRP export observed throughout October and November were most likely a result of manure application rather than hydrology and AHC. SRP was likely leached from the newly applied manure and lost during the October 12 event. Smaller quantities were lost during the November 2 event. Subsequent events decreased in their export of SRP because the available pool of nutrients was depleted over time. However, throughout each of the events, successive counter-clockwise hysteresis loops were observed in Q-C plots for both SRP and TP (Figs 5.13d, 5.14d), indicating that a new 'pool' was accessed as AHC increased between October 12-20. This is due to either the water table rising into higher soil horizons or new pores in the vadose zone being 'activated'.

### *NO<sub>3</sub><sup>-</sup> Export*

As in the case of P, NO<sub>3</sub><sup>-</sup> export also showed successive counter clockwise hysteresis loops with each storm (Fig 5.15d) but the first event (storm #1) exhibited a very small clockwise loop. The extreme drought that preceded this event may have affected the available 'pool' of NO<sub>3</sub><sup>-</sup> as NO<sub>3</sub><sup>-</sup> concentrations were high during this event. It is likely that the prolonged drought and warm temperatures allowed substantial quantities of NO<sub>3</sub><sup>-</sup> to accumulate in soils. As the fields wet up, NO<sub>3</sub><sup>-</sup> was flushed into the stream. NO<sub>3</sub><sup>-</sup> losses subsequently increased with successive events as the water table rose and new pores in the vadose zone were likely 'activated'.

### December 17 – 20, 2001

Cool, dry conditions preceded this event for approximately ten days and mean daily air temperatures were 0.2°C. Aside from the 9 mm of rainfall on December 6<sup>th</sup>, conditions were relatively dry in the basin. The water table position in the near stream zone at the basin outflow was 0.52 m beneath the ground surface.

Hydrologic and nutrient export data for SRP, TP and NO<sub>3</sub><sup>-</sup> are presented in Figures 5.16, 5.17 and 5.18, respectively.

### *P Export*

This winter thaw event, in which several short rainstorms occurred, showed an increase in SRP and TP export in response to wetter AHC. During this time period, an interesting pattern was observed for SRP export. During this event, as well as during four of the five rain-on-snow events over the study period, the Q-C plot showed a hysteresis

pattern where a clockwise loop was observed on the rising limb and then a counter clockwise loop was observed on the falling limb. During these events, an elevated SRP concentration is observed early in the event, prior to the peak of the hydrograph and water table. Elevated nutrient losses are subsequently observed on the falling limb of the hydrograph. It is hypothesized that the pulse of P observed early in the event and the increased losses of P on the falling limb of the hydrograph may be due to preferential flow through macropores.

#### *NO<sub>3</sub><sup>-</sup> Export*

NO<sub>3</sub><sup>-</sup> concentrations in discharge increased throughout this series of events as AHC became wetter. A counter-clockwise loop was observed for NO<sub>3</sub><sup>-</sup> as in other events. However, the export of NO<sub>3</sub><sup>-</sup> was quite high during this event compared to the March winter event. The effects of the extreme summer drought in 2001 may have still been affecting the basin during the December event. Harris (1999) observed reduced NO<sub>3</sub><sup>-</sup> attenuation in groundwater in riparian areas during the winter months and suggested that winter storms were more vulnerable to NO<sub>3</sub><sup>-</sup> export. This could explain seasonal differences between the winter (March, December 2001) and non-winter storms (April, October 2001). However, NO<sub>3</sub><sup>-</sup> export is much greater during the December 2001 event (Fig.5.18) than the March 2001 event (Fig. 5.9). AHC prior to the March 2001 event were much wetter than prior to the December 2001 event. It is possible that a substantial portion of the available NO<sub>3</sub><sup>-</sup> was lost prior to the March 2001 event and there was therefore more available NO<sub>3</sub><sup>-</sup> prior to the December event. These results suggest that

$\text{NO}_3^-$  export patterns are a result of the combined influences of season, hydrology (AHC) and the availability of  $\text{NO}_3^-$ .

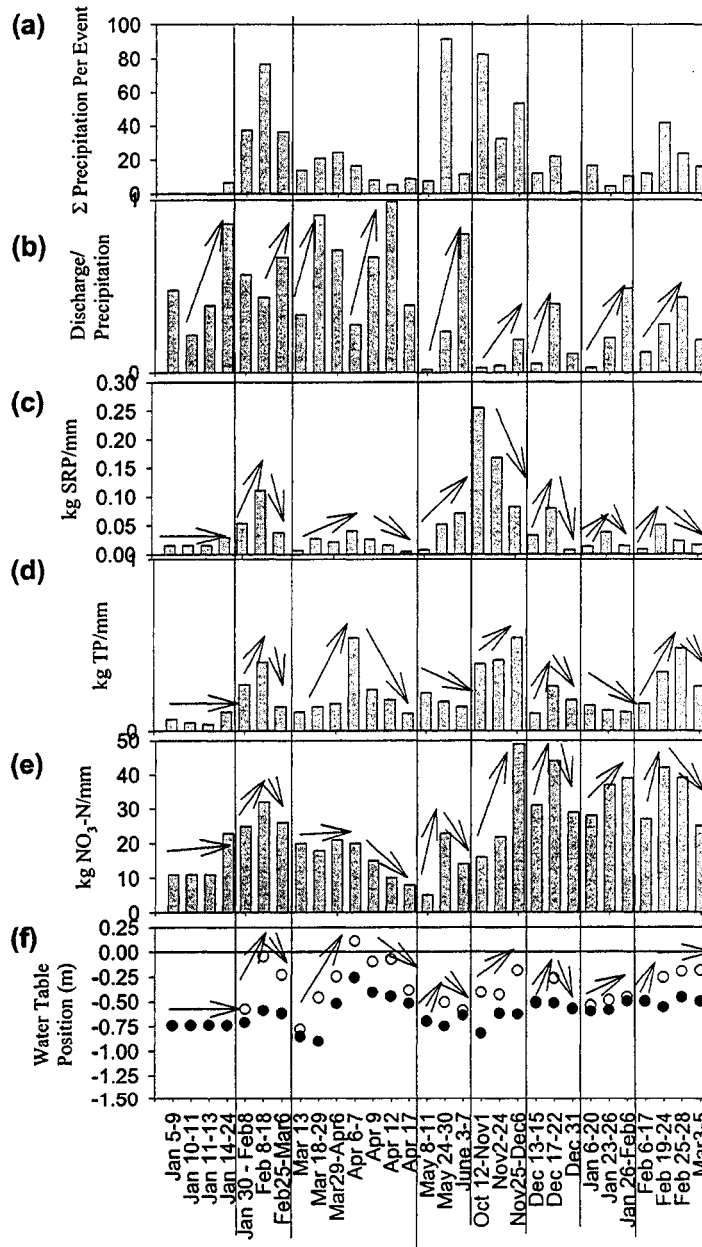
### 5.3.2.2 Summary of Individual Successive Events

Several sets of successive events (including those in Figures 5.7 – 5.18) are summarized in Figure 5.19. The magnitude of event (e.g. hydrologic inputs) and Q/PPT are shown in Figure 19 a and b. P and  $\text{NO}_3^-$  export per event is ‘normalized’ to account for differences in discharge [nutrient mass per event (kg) /  $\Sigma$  discharge per event (mm)] and is shown as the mass of nutrients per mm of discharge (Fig. 5.19 c-e) (hereafter referred to as  $N_{\text{EFF}}$ ). Water table position prior to the event ( $\text{WT}_0$ ) (dark circles) and peak water table position during the event ( $\text{WT}_{\text{peak}}$ ) (white circles) are shown in (f).

Figure 5.19c-e shows that  $N_{\text{EFF}}$  changes with successive events as well as among different series of events. Within a given sequence of successive events, successive events may increase in  $N_{\text{EFF}}$ , or decrease in  $N_{\text{EFF}}$ . This seems to be linked to AHC, which are indicated by the behaviour of the water table ( $\text{WT}_0$  and  $\text{WT}_{\text{peak}}$ ), although empirical relationships are not evident. Figures 5.7 – 5.18 demonstrated how successive events could result in increased or decreased nutrient mass export, depending on whether AHC were wet or dry. Several additional storms are examined in Figure 5.19. The same effect that was observed at a fine timescale in Figures 5.7 – 5.18 can also be seen at a less intensive timescale in Figure 5.19.

Arrows are used in Figure 5.19c-e to show how  $N_{\text{EFF}}$  changes with successive events. When successive events occur, either an increase in the  $N_{\text{EFF}}$  is observed (or remains the same) as the water table rises with each event (indicating a successive

**Figure 5.19 Summary of 30 selected events. Sequences of successive events are divided by the solid vertical lines. Total precipitation (hydrologic inputs, sum of rainfall and snowmelt) for each event is shown in (a). Q/PPT is shown in (b). Nutrient export 'efficiency' ( $N_{EFF}$ ) for SRP, TP and  $NO_3^-$  are shown in (c-e).  $N_{EFF}$  is the mass of nutrients exported per mm of discharge. Initial water table position ( $W_0$ ) (black dots) and peak water table position ( $W_{peak}$ ) (white dots) are shown in (f). Arrows indicate a rising or declining trend in the various variables.**



wetting up of AHC). Thus,  $WT_{\text{peak}}$  may be more important than  $WT_0$  in describing AHC during a given event. It is hypothesized that either (a) the water table accesses a new pool within the new soil horizon in order to increase  $N_{\text{EFF}}$ ; or (b) new and larger preferential flow paths are ‘activated’ as the basin becomes successively wetter (e.g. March, Figures 5.7-5.9 and 5.19).

If successive storms follow a ‘drying’ trend and have the water table peaking at the same soil horizon or lower than a previous event,  $N_{\text{EFF}}$  will decrease over time (e.g. April, May-June, December, Figs 5.10-5.12, 5.16-5.18, 5.19). It is possible that ‘nutrient availability’ is decreasing in the soil horizon with each successive event or preferential flow paths are ‘inactivated’ as the basin dries out.

Finally, storms may decrease in their  $N_{\text{EFF}}$  even though the basin is ‘wetting up’. This was only observed for SRP in October and November and followed a prolonged period of drought as well as the recent application of manure to 10% of the basin. The high export of SRP during the October-November sequence of events is likely due to the combined influence of preferential flow paths (which are linked to AHC) and the application of manure in the basin (*i.e.* P availability).

### 5.3.2.3 Hysteresis Patterns

Fig. 5.20 summarizes the six types of hysteresis loop patterns observed Q-C plots in the current study (when comparing stream discharge to stream water nutrient concentration). Three types of hysteresis loops are most prevalent in this basin: clockwise, counterclockwise, and clockwise followed by counter clockwise loops.



## *Phosphate*

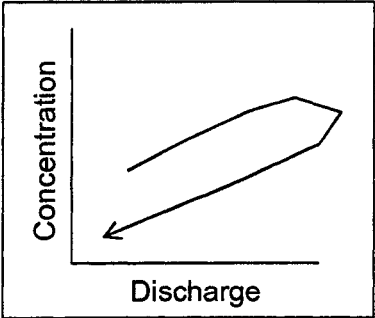
Clockwise patterns were observed for both SRP and TP but were more common for TP than SRP. The observed pattern for TP is likely a result of sediment availability. A clockwise pattern (Fig 5.20a) is particularly common when the water table intersects the soil surface and overland flow occurs for a short period of time. This 'clockwise' pattern is not observed in tile effluent, implying that the observed nutrient pulses are a result of overland flow rather than a pulse through drainage tiles. It is likely that fine grained sediments are entrained early in an event and lost via a short burst of overland flow. This explains why such patterns are common for TP and not SRP or  $\text{NO}_3^-$ . Successive clockwise loops (Fig 5.20e) were only observed for TP during the March event (Figs 5.7-5.9).

Counter-clockwise loops (Fig 5.20b) were observed for both TP and SRP. In fact, this pattern was the most commonly observed type of hysteresis loop for P. The increased concentration on the falling limb of the hydrograph is likely due to either (a) the water table accessing a 'pool' of nutrients in upper soil horizons; or (b) new preferential flow paths being 'activated' under wetter soil moisture conditions. Successive loops (Fig. 5.20f) are observed with successive events.

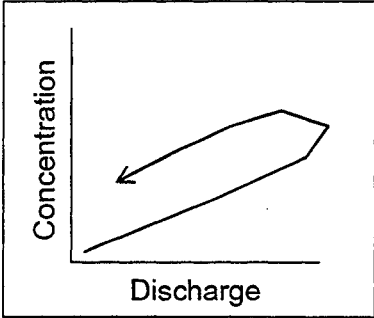
Clockwise followed by counter clockwise loops (Fig 5.20c) are also observed with SRP and TP but are only seen during rain-on-snow events (e.g. Fig 5.16-5.18). Drainage tile effluent also typically shows this pattern during the same events, suggesting that a pulse of SRP is rapidly routed through the tiles early in the event. This is most likely due to preferential transport through macropores into the tiles (Stamm *et al.*, 1998). During such events, a 'pulse' through the tiles occurs prior to the peak of the hydrograph.

**Figure 5.20 Summary of prevalent forms of hysteresis loops observed in Q-C plots for various events throughout the study period.**

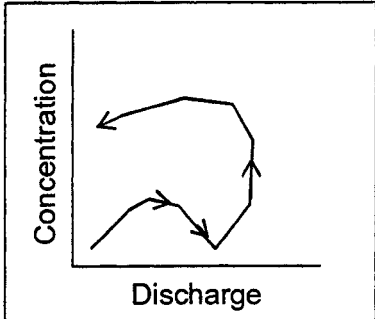
**(a) Clockwise**



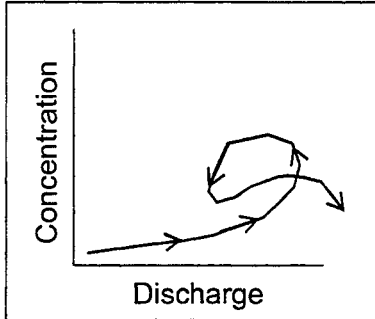
**(b) Counter clockwise**



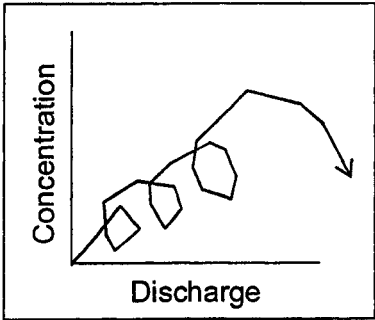
**(c) Clockwise-Counter-clockwise**



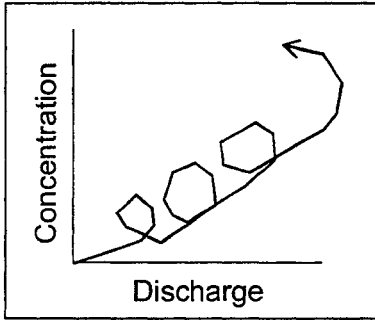
**(d) Counterclockwise – Clockwise**



**(e) Successive clockwise**



**(f) Successive counter-clockwise**



As the water table, tile and stream discharge start to decline following the peak, increased concentrations of SRP and TP are observed which are assumed to be a result of water draining from the vadose zone.

Finally, Q-[P] plots occasionally exhibited hysteresis patterns that were counter-clockwise loops followed by clockwise loops (Fig 5.20d). This was observed during the March 2001 series of events (Figs. 5.7-5.9) where a prolonged period of wet conditions had occurred in which the water table remained at the same depth instead of rising into upper soil horizons. It is assumed that the available pool of nutrients in the contributing areas (e.g. unsaturated and saturated soils) was depleted due to prolonged runoff.

#### *Nitrate*

Counter-clockwise loops (Fig 5.20b) were most commonly observed for Q-[NO<sub>3</sub><sup>-</sup>] plots. The increased concentrations of NO<sub>3</sub><sup>-</sup> in streamflow on the falling limb of the hydrograph are likely a result of new pools of NO<sub>3</sub><sup>-</sup> being accessed within the vadose zone as soils increase in wetness. As in the case of P, successive loops are observed with successive events (Fig. 5.20f).

Although Q-[NO<sub>3</sub><sup>-</sup>] plots most commonly exhibited counter-clockwise hysteresis loops, some storms exhibited counter-clockwise loops followed by clockwise loops (Fig 5.20d). These patterns were observed following prolonged periods of wet conditions (e.g. March Figs 5.7-5.9). As in the case of P, it is assumed that the available pool of nutrients in the contributing areas (e.g. unsaturated and saturated soils) was depleted due to prolonged runoff.

## 5.4 Summary and Conclusions

This chapter has shown that AHC in the basin may affect hydrochemical export from a basin. However, such conditions are complex and quantitative relationships between 'indicators' of AHC (e.g.  $WT_o$ ,  $Q_o$ ,  $Q_{2wks}$ , season) and storm response (Q/PPT) are unclear. Q/PPT increases with successive storms even when indicators of AHC do not change between events. AHC must be increasing in the basin as there are successive inputs of water to the basin; however, the empirical indices considered in this paper do not provide relationships with Q/PPT. Clearly, the effects of AHC on hydrochemical export are difficult to quantify.

In general, nutrient export is strongly linked to stream export (positive linear relationship). Some of the scatter is explained by successive events, where the  $N_{EFF}$  of a given event depends on basin AHC.  $N_{EFF}$  will increase or stay the same with successive events as AHC increase. However,  $N_{EFF}$  will decrease with successive events if AHC are on a 'drying' trend.

## **6.0 Phosphate Retention in an Agricultural Stream Using Experimental Additions of Phosphate**

### **6.1 Introduction**

Nutrient loading from point and non-point sources has contributed to the eutrophication of aquatic systems in many agricultural catchments (Carpenter *et al.*, 1998). Streams and wetlands have been identified as a critical interface between uplands and receiving water bodies due to their ability to retain nutrients (Meyer, 1979; Klotz, 1985; Richardson, 1985; Reddy *et al.*, 1999).

Phosphorus (P) is an important factor in the eutrophication of freshwater systems (Carpenter *et al.*, 1998). P may be exported in both dissolved and particulate forms. Dissolved phosphorus (DP) and soluble reactive phosphorus (SRP) are of particular interest as these forms are available for use in biotic cycles.

The degree of SRP retention is a function of a number of biotic and abiotic processes (Reddy *et al.*, 1999). Biotic mechanisms of P retention include assimilation by vegetation, plankton, periphyton and microorganisms, whereas abiotic mechanisms include sedimentation, adsorption by sediments and precipitation (Reddy *et al.*, 1999). While biotic mechanisms play an important role (Meyer, 1979; Hill, 1982; Mulholland *et al.*, 1985), the abiotic exchange of P between the water column and suspended and/or bottom sediments is a major component of the P cycle in many fluvial systems (McCallister and Logan, 1978; Meyer, 1979; Hill, 1982; Klotz, 1985). Exchange processes are governed by factors such as pH, redox potential, and organic matter content, but appear to be most affected by sediment composition (mineralogy and texture) (Syers *et al.*, 1973; Patrick and Khalid, 1974; Meyer, 1979; Hill, 1982; Klotz,

1985; Stone and Mudroch, 1989; Stone and English, 1993). P retention can vary within stream reaches depending on stream morphometry and vegetation cover (Meyer, 1979; Munn and Meyer, 1990). For instance, finer sediments found in pools have been found to have a higher SRP retention capacity than coarser sediments in riffles (Hill, 1982; Munn and Meyer, 1990).

During baseflow, in-stream processes can regulate nutrient export from agricultural catchments (e.g. Svendsen *et al.*, 1995), but the majority of P export from agricultural catchments typically occurs during storm periods (e.g., Svendsen *et al.*, 1995; Gburek and Sharpley, 1998). During storms associated with high rates of discharge, P originally retained in stream vegetation and sediments can be subsequently transported as particulate P (PP) due to the resuspension of streambed sediments (Hill, 1982; Svendsen *et al.*, 1995). However, storm events can increase SRP concentrations above ambient levels even if high rates of discharge do not occur. Such conditions exist in streams receiving drainage tile effluent following the application of liquid manure on irrigated systems (Stone and Krishnappan, 2003) or when P is accidentally applied into stream channels or ditches. Several studies have examined the retention of SRP by sediments in streams receiving effluent from point sources (e.g., McCallister and Logan, 1978; Hill, 1982; Fogal *et al.*, 1995; Haggard *et al.*, 2001a; Haggard *et al.*, 2001b). However, few studies have evaluated the SRP retention rates of streams when concentrations are highly elevated, and hydrologic discharge rates are low.

Experiments were conducted to examine the SRP retention potential of an agricultural stream under highly elevated SRP concentrations at low flows. Various concentrations of SRP were added to the stream to simulate elevated SRP concentrations

found in streams receiving effluent from upland areas. The objectives of the study are: (1) to determine SRP retention rates when SRP concentrations in the stream are highly elevated during low flow periods; (2) to examine whether retention rates vary spatially among areas having different physical characteristics such as horizontal gradient, groundwater flux direction, bathymetry, and vegetative cover; and (3) to examine the effects of dredging the stream bottom on the ability of the stream to retain SRP.

## **6.2 Study Site and Methods**

The study site description and methods are provided in detail in Chapter Two. Methods specific to this chapter are discussed below.

### ***6.2.1 Characterization of Study Reaches***

To evaluate SRP retention in the stream, three 70 m stream segments were chosen with differing bathymetry, streambed vegetation coverage, and groundwater flow direction (Figs. 6.1-6.3). The experimental additions of SRP were not conducted in sections of the stream receiving direct effluent from drainage tiles to avoid possible confounding contributions of tile drainage.

Over each of the study segments, streambed area was quantified at 1-5 m intervals and streambed coverage (% coverage by vegetation, cobbles, sediments) was determined at 5 m intervals. The gradient of the streambed was determined using both a Total Station (Leica Model T1600) (error  $\pm 5$  ppm) and GPS system (Leica Model SR530) (error  $\pm 7$  ppm).

Site 1 is a well-defined channel, and is deeper (7.1 - 25.2 cm) and has a lower elevation gradient (0.007) than the two other study reaches. Streambed coverage at Site 1 is dominated by a combination of fine and coarse textured sediments and some areas of the stream bottom are covered by periphyton. In-stream vegetation species and coverage did not differ between the June and October experiments. Riffle and pool sequences are present throughout this segment (Fig. 6.1a). During both experiments, surface flow velocities ranged from 0.01-0.06 m s<sup>-1</sup>, and vertical hydraulic gradients in groundwater 1 m beneath the streambed (sampled at 10-20 m intervals along the reaches) ranged from -0.028 to +0.043 in this section of the stream. The hydraulic gradients observed during both experiments are typical of what has been observed in this section of the reach under dry conditions. Under wet conditions, hydraulic gradients are often positive within this segment of the stream.

Site 2 (Fig. 6.2) is straighter and shallower (1 - 10 cm) than Site 1. The streambed is covered by a mixture of exposed fine sediments and aquatic grasses (Fig.6.2c). This did not change between the June and October experiments. The elevation gradient along this stretch is 0.009. Surface flow velocities ranged from 0.02 to 0.13 m s<sup>-1</sup> during both experiments. This section of the stream neither gained nor lost groundwater during either experiment as vertical hydraulic gradients were zero. These groundwater vertical gradients are typical of what is generally observed within this section of the stream under both wet and dry conditions.



**Figure 6.1: Morphological characteristics of experimental Site 1. Water and streambed surfaces (m.a.s.l.) are shown in (a), and streambed coverage is shown in (b). Locations of the point source addition of SRP, and sampling points *a* through *e* are shown in (a).**

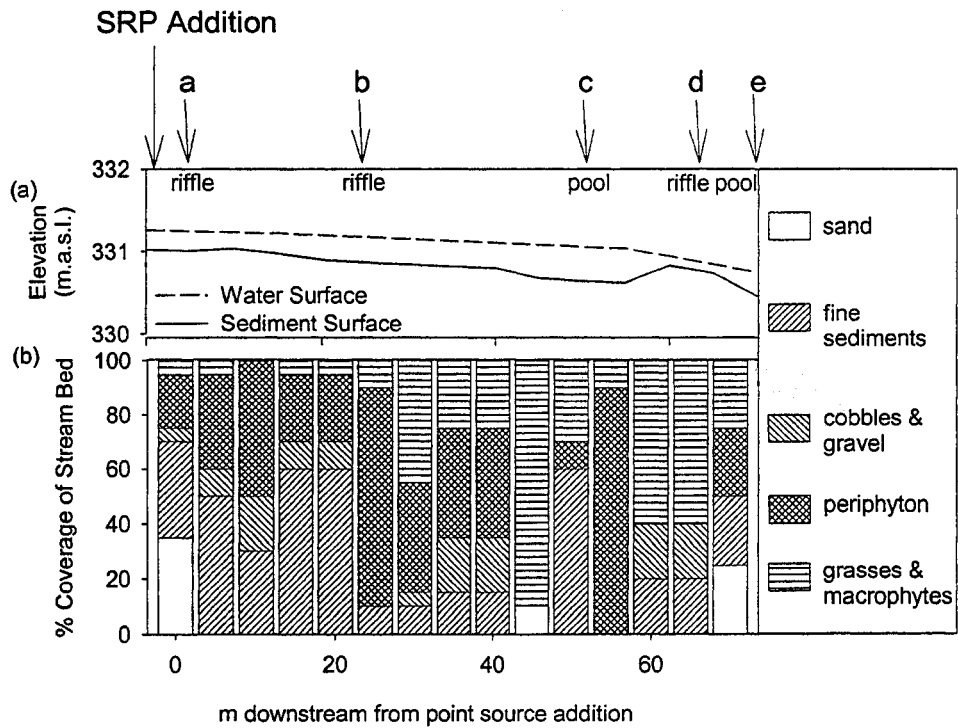


**Figure 6.2: Morphological characteristics of experimental Site 2. Water and streambed surfaces (m.a.s.l.) are shown in (a), and streambed coverage is shown in (b). Locations of the point source addition of SRP, and sampling points *a* through *e* are shown in (a).**

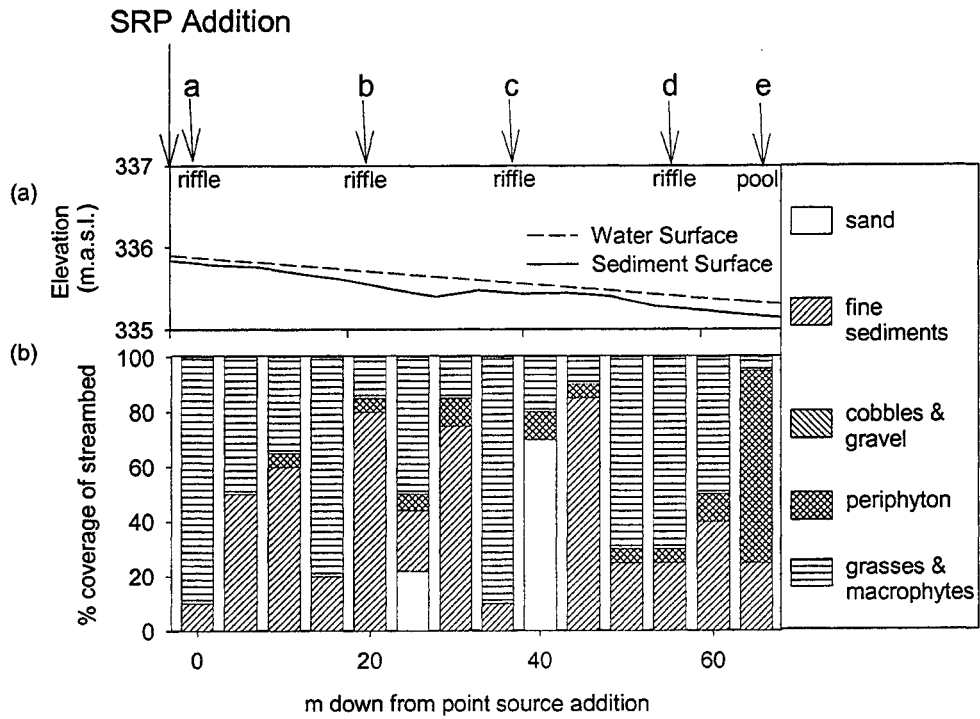
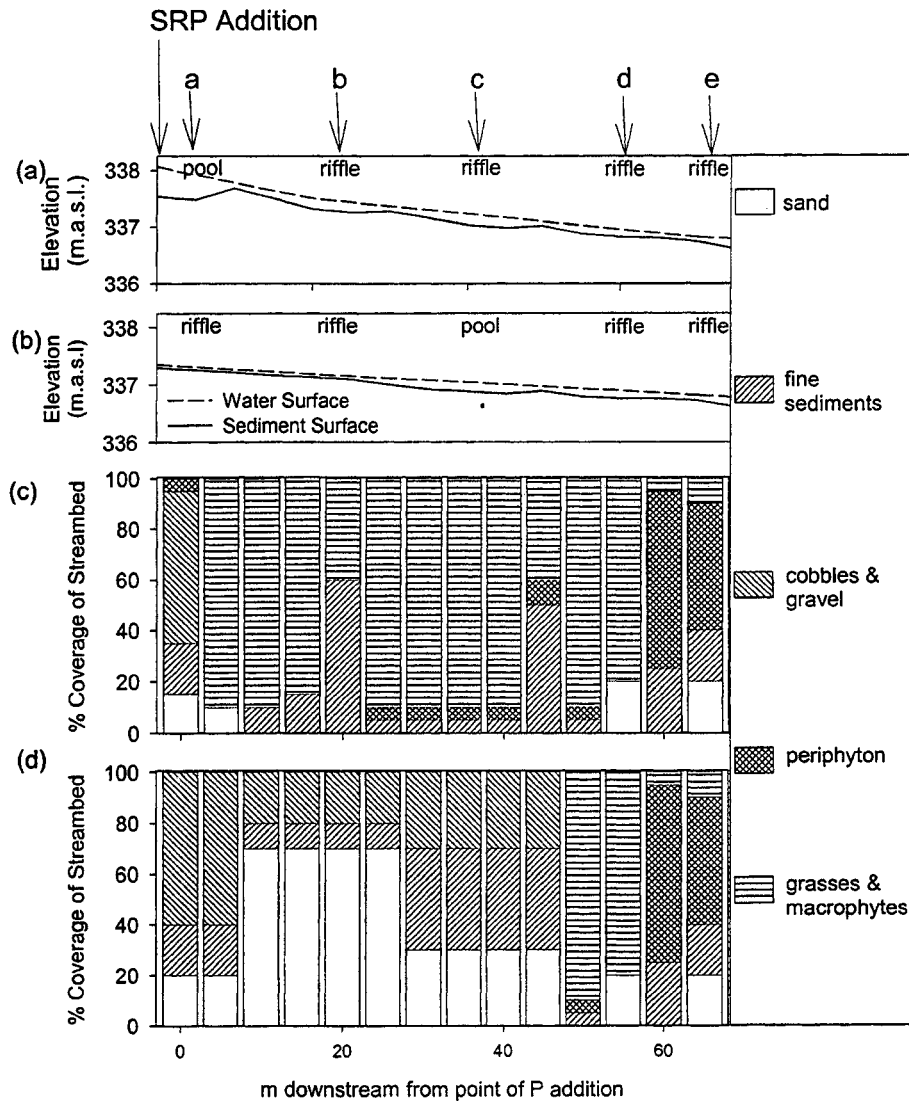


**Figure 6.3: Morphological characteristics of experimental Site 3. Water and streambed surfaces (m.a.s.l.) for June and October are shown in (a) and (b), and streambed coverage for June and October are shown in (c) and (d). Locations of the point source addition of SRP, and sampling points *a* through *e* are shown in (a).**



Textural composition and vegetation characteristics of the streambed in June for Site 3 are shown in Figure 6.3c. During the June experiment, the streambed was covered by a mixture of fine sediments and aquatic grasses, and riffle and pool sequences were present. In the upper section of Site 3 during the June experiment, surface flow velocities were  $0.01 - 0.04 \text{ m s}^{-1}$ , whereas in the lower section of Site 3, surface flow velocities were  $0.01 - 0.12 \text{ m s}^{-1}$ . Prior to the October experiment, the upper 50 m of the 75 m of the experimental reach was dredged and the top 25 cm of sediments and all in-stream vegetation was removed (Fig. 6.3d). Following the dredge, the streambed in the upstream 50 m of Site 3 consisted of exposed compact sediments (coarse sands and clays). Approximately 25 m downstream from the point of SRP addition, the stream widened into a small pool. Otherwise, the stream channel was narrow and straight. During the October experiment (following the dredge) flow velocities in the lower portion of the experimental reach were similar to those observed during the June experiment, whereas flow velocities in the upper portion of the study reach were much higher after the removal of the vegetation ( $0.07-0.20 \text{ m s}^{-1}$ ). Dredging of the stream bottom changed the horizontal gradient along this stretch from 0.012 in June (Fig. 6.3a) to 0.008 in October (Fig. 6.3b). Groundwater vertical hydraulic gradients beneath the streambed ranged from +0.109 to +0.325 during both experiments, which is typical for this section of the stream under both wet and dry conditions.

### **6.2.2 Experimental Approach**

Concentrated  $\text{K}_2\text{HPO}_4$  solution was added to each of the three stream segments on two dates (June 12 and October 18, 2001). The SRP additions occurred on the same day

during both experiments and were conducted sequentially, starting at the lower end of the stream, so that successive experiments would not interfere with one another. A conservative tracer (NaCl) was simultaneously injected into the stream at the top of the experimental segment at the upstream location to raise the stream conductivity by a factor of 3, and monitored as it passed through all three study reaches using a field conductivity probe. Both the NaCl and K<sub>2</sub>HPO<sub>4</sub> solutions were injected via continuous drips (5 mL s<sup>-1</sup> each) that were regulated by maintaining constant head in the container from which each of the tracers were being injected. Constant head was maintained by a peristaltic pump which transferred the tracer solution from another container into the container from which the tracer was being injected. Samples were collected throughout the stream prior to and following the addition of the NaCl over a period of 15 hours. Samples were analysed for conductivity in the laboratory following the experiments. Stream dilution was determined from conductivity values using

$$Q_n = \frac{(C_t - C_n)}{(C_n - C_o)} Q_t \quad (6.1)$$

where  $Q_n$  is the stream discharge at location  $n$  (L s<sup>-1</sup>),  $C_t$  is the conductivity of the added solution (µmhos cm<sup>-1</sup>),  $C_n$  is the final conductivity at location  $n$  (µmhos cm<sup>-1</sup>),  $C_o$  is the background conductivity at location  $n$  (µmhos cm<sup>-1</sup>), and  $Q_t$  is the tracer injection rate (L s<sup>-1</sup>). Discharge within the three study reaches was also calculated using K<sup>+</sup> concentrations during the K<sub>2</sub>HPO<sub>4</sub> treatments. Discharge rates calculated using conductivity and K<sup>+</sup> were in agreement, suggesting that K<sup>+</sup> was acting conservatively during the experiments. Stream discharge measured manually at the upstream and downstream transects of the three study reaches using a velocity metre (Marsh-McBirney) was also in agreement with discharge rates calculated using tracers.

During the June experiment, SRP was increased in the three stream reaches from 32, 40, and 29  $\mu\text{g L}^{-1}$  to approximately 697, 2121 and 1134  $\mu\text{g L}^{-1}$ , respectively. During the October experiment, SRP concentrations were increased from 246, 319, and 397  $\mu\text{g L}^{-1}$  to approximately 2897, 4225, and 3308  $\mu\text{g L}^{-1}$ , respectively. These high concentrations have been observed in this stream in the past, as well as in tile effluent draining into the stream.

Prior to the SRP additions, the stream was sampled for background concentrations of SRP, total phosphorus (TP), potassium ( $\text{K}^+$ ), and total suspended sediments (TSS) at 20 m intervals (five sub-sections) within each study reach. SRP was added 1-2 m above the most upstream sampling point within each reach, and stream water was gently stirred to ensure that mixing had been achieved in the water column, but the sediments were not disturbed. Any SRP retention occurring as a result of stirring the water column was not factored into calculations of retention rates as all estimates of retention were relative to initial samples taken below the upper 1-2 m of each study reach. Samples were collected at the same five points within each study segment for SRP, TP, and  $\text{K}^+$  analysis 35, 45, and 55 minutes after the beginning of the SRP treatments, and two hours and 24 hours after the SRP treatments had ended. It was assumed that TSS concentrations would not change significantly over the one hour period, and TSS was therefore only measured once. In a catchment and stream similar to the one in the current study, Fogal *et al.*, (1995) found that TSS did not vary over the course of a day under low flow conditions. Stream water samples were also collected at the catchment outflow by an automated ISCO sampler at 20-minute intervals throughout the duration of the experiments in

October, and at two hour intervals for 12 hours following the cessation of the October experiments.

Samples were filtered (0.45  $\mu\text{m}$ ) on the day of sampling, stored at 2°C and analyzed for SRP and TP (within one week) using colorimetric analysis (Stannous-Chloride/Ammonium Molybdate Method) with a Technicon Auto-analyser linked to NAP software. TP samples were digested with persulfate prior to colorimetric analysis. All samples were run in duplicate for SRP and TP. Duplicates were on average within  $\pm 30 \mu\text{g P L}^{-1}$  and  $\pm 94 \mu\text{g P L}^{-1}$  for SRP, and within  $\pm 37 \mu\text{g P L}^{-1}$  and  $\pm 77 \mu\text{g P L}^{-1}$  for TP in June and October, respectively. Water samples were analysed for  $\text{K}^+$  using a Perkin-Elmer 3100 Atomic Absorption Spectrophotometer. TSS concentrations were determined by filtering 1 L samples (in replicate) through pre-weighed 0.45  $\mu\text{m}$  filters. The 0.45  $\mu\text{m}$  pore diameter was selected so that TSS could be compared to PP. PP was determined by subtracting SRP from TP. All forms of P other than SRP are included in PP. TP and SRP concentrations at 35, 45 and 55 minutes were averaged at each sampling location to give an average TP and SRP concentration over the time period for the June and October SRP treatments.

Measured SRP concentrations were compared to *expected* (dilution corrected) SRP concentrations to infer SRP retention efficiency of the stream, but no distinction was made between sediment and vegetative retention. Expected SRP calculations were calculated by

$$[\text{SRP}]_{(F)} = \frac{(Q_I * [\text{SRP}]_I) + ((Q_F - Q_I) * [\text{SRP}]_o)}{Q_F} \quad (6.2)$$

where  $[SRP]_{(F)}$  ( $\mu\text{g L}^{-1}$ ) is the *expected* SRP concentration at the downstream location based on dilution alone,  $Q_I$  and  $Q_F$  are discharge at the upstream and downstream locations, respectively ( $\text{L s}^{-1}$ ),  $[SRP]_I$  is the elevated concentration at the upstream location ( $\mu\text{g L}^{-1}$ ), and  $[SRP]_o$  is the background concentration at the downstream location ( $\mu\text{g L}^{-1}$ ). SRP retention rates per unit area of stream bed were determined using the approach of Munn and Meyer (1990). Briefly, the change in SRP mass is divided by streambed surface area to yield a retention rate in  $\mu\text{g m}^{-2} \text{s}^{-1}$ .

$$\text{Retention Rate } (\mu\text{g m}^{-2} \text{s}^{-1}) = \frac{([SRP]_U * Q_U) - ([SRP]_L * Q_L)}{A_o} \quad (6.3)$$

where  $[SRP]_U$  and  $[SRP]_L$  are the SRP concentrations at the upper and lower end of a given stream segment, respectively ( $\mu\text{g L}^{-1}$ ),  $Q_U$  and  $Q_L$  are the discharge rates at the upper and lower end of a given stream reach, respectively ( $\text{L s}^{-1}$ ), and  $A_o$  is the surface area of the stream bed between the two points of interest. Retention rates were determined among each of the five sampling points in the three stream segments. A mean ‘whole-reach’ retention rate, calculated from concentration changes between the top of the study reach and the lowest point along the study reach where data are available, was also determined for each reach.

## 6.3 Results and Discussion

### 6.3.1 Environmental Conditions Prior to the SRP Addition Experiment Occasions

Several differences in stream conditions were observed between the June and October experiments. The June experiment followed a wet spring. The October experiment followed a prolonged period of drought (two months) where groundwater



discharge to the stream and stream discharge ceased. Rain events occurred two days prior to both experiments (8 mm in June, 17 mm in October) and several rain events of the same magnitude had occurred over a ten-day period prior to the October experiment. Discharge was low during both experiments, more so in October ( $1.5 - 3.3 \text{ L s}^{-1}$ ) than in June ( $4.5-7.3 \text{ L s}^{-1}$ ). Drainage tiles were not flowing during either experiment. During the June and October experiments, increases in discharge were observed between the upper and lower ends of the study reaches:  $0.2$  to  $1.8 \text{ L s}^{-1}$  and  $0.2$  to  $0.9 \text{ L s}^{-1}$ , respectively. Ambient SRP concentrations in the stream in October ( $\sim 300 \text{ ug L}^{-1}$ ) were higher than in June ( $\sim 30 \text{ ug L}^{-1}$ ). This may have resulted from different antecedent conditions within the catchment, or the application of organic fertilizers two weeks prior to the October experiment.

### **6.3.2 SRP Retention**

Changes in SRP concentrations as a result of retention (Figs. 6.4 and 6.5) over the entire length of the three experimental reaches ranged from  $2$  to  $321 \text{ ug L}^{-1}$  in June and from  $-76$  to  $660 \text{ ug L}^{-1}$  in October (Figs. 6.4 and 6.5). Although SRP retention along the study reaches was a maximum of 23%, retention was most often between 5% and 10% of the experimentally elevated SRP concentrations ( $0.7 - 4.2 \text{ mg L}^{-1}$ ) (Figs. 6.4 and 6.5). Temporal variability in SRP retention was apparent between the 35 minute and 45 and 55 minute samplings for both the June and October experiments, with SRP retention decreasing slightly over time during the experiment. This may have been due to the fact that available sediment sorption sites were filled as the experiment progressed.

The elevated SRP concentrations employed in the experiments were substantially higher than typical SRP concentrations in streams in Southern Ontario, which range from 20 to 60  $\mu\text{g L}^{-1}$  at low flows (Stone and Mudroch, 1989; Stone and English, 1993). There are a few possible explanations for the small amounts of SRP retained by the stream: (1) there is a limit to the SRP retention potential of the sediments, and the experimental concentrations of SRP were approaching this limit; or (2) low flow conditions in the stream caused it to be poorly mixed, thus limiting the contact between the sediments and the bulk of the overlying water column. The low retention observed is in contrast to the results of McCallister and Logan (1978) where SRP was rapidly retained by stream sediments. The study by McCallister and Logan (1978) was conducted on sediments from fluvial systems (Maumee River Catchment, Ohio) larger than Strawberry Creek.

Quantities of SRP retained in October were higher than in June (Figs. 6.4 and 6.5); however this may be due to the fact that more SRP was added to the stream in October than in June. The proportion and amount of SRP retained during experimental additions is directly related to the level of SRP added (Mulholland *et al.*, 1990). Mean whole-reach rates of SRP retention (Table 6.1) were similar for all three reaches during the June experiment (3.4 – 5.3  $\mu\text{g m}^{-2} \text{s}^{-1}$ ). During the October experiment, mean whole-reach retention rates were slightly higher at Site 2 (6.3  $\mu\text{g m}^{-2} \text{s}^{-1}$ ) than during the June experiment and much higher at Sites 1 and 3 (11.4 and 9.4  $\mu\text{g m}^{-2} \text{s}^{-1}$ ).

Retention rates were calculated for specific points within the various reaches (Table 6.1) to potentially isolate factors affecting SRP retention. Retention rates in sections of the stream that were not dredged ranged from 0.2  $\mu\text{g m}^{-2} \text{s}^{-1}$  to 20.8  $\mu\text{g m}^{-2} \text{s}^{-1}$ .

Figure 6.4: Difference between expected SRP concentration and observed SRP concentrations downstream from point source addition of  $K_2HPO_4$  in June. Observations 35 minutes (circles), 45 minutes (squares), and 55 minutes (triangles) after the beginning of the additions are shown. Data for 35 minutes is missing from Site 1 as the SRP plume had not passed the lower sections of the reach by 35 minutes into the experiment. SRP concentrations at Sites 1, 2 and 3 were elevated to 697, 2121, and 1134  $\mu g L^{-1}$ , respectively (shown in brackets in each graph). Analytical error calculated from replicate analysis of samples is shown by error bars.

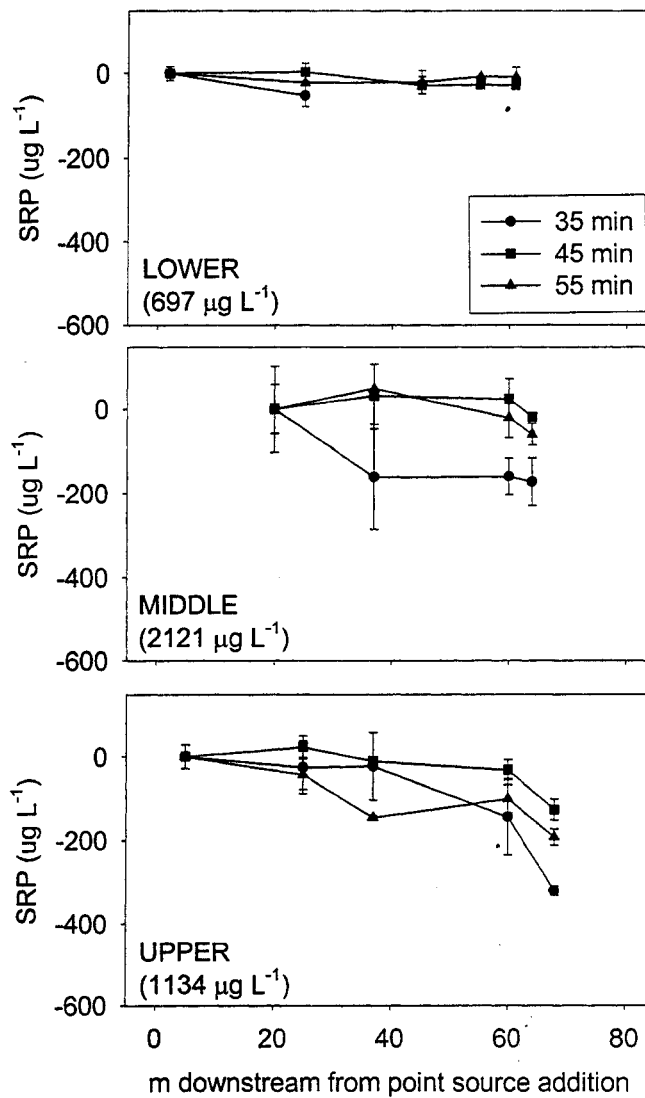


**Figure 6.5: Difference between expected SRP concentration and observed SRP concentrations downstream from point source addition of  $K_2HPO_4$  in October. Observations 35 minutes (dark circles), 45 minutes (dark squares), and 55 minutes (dark triangles) after the beginning of the additions are shown. Data is missing from Site 1 as the SRP plume did not pass into the lower sections of Site 1 at all during the 55-minute experiment in October. However, the plume was caught at the outflow (30 m downstream of Site 1) by the automated sampler 30 minutes later. SRP concentrations observed at the catchment outflow are shown for Site 1 (white symbols). SRP concentrations at Sites 1, 2 and 3 were elevated to 2897, 4225, and 3308  $\mu g L^{-1}$ , respectively. Analytical error calculated from replicate analysis of samples is shown by error bars.**

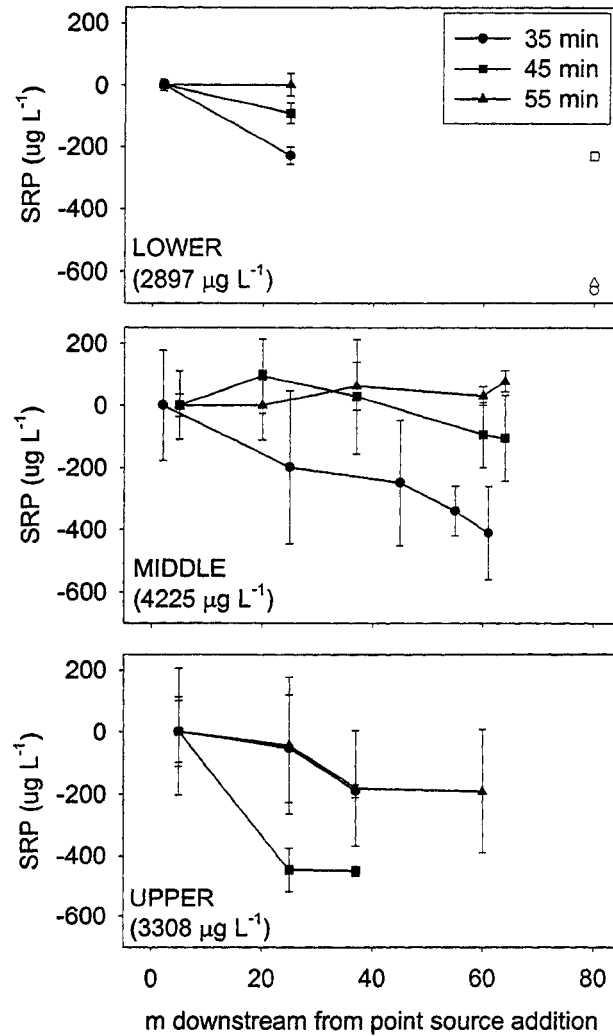


**Table 6.1: SRP Retention Rates Along Three Experimental Reaches for Two Experiments. All units are in  $\mu\text{g m}^{-2} \text{s}^{-1}$ . Retention rates between each of the sampling points (*a* through *e*) were calculated from the mean retention for the 35, 45 and 55 minutes sampling intervals.**

June Experiment	Upstream (a-b)	(b-c)	(c-d)	Downstream (d-e)	Mean Reach
<b>Site 1</b>	5.9	0.2	n.d.	n.d.	3.4
<b>Site 2</b>	n.d.	7.5	12.2	0.8	5.2
<b>Site 3</b>	1.8	7.7	6.0	n.d.	5.3
October Experiment	Upstream (a-b)	(b-c)	(c-d)	Downstream (d-e)	Mean Reach
<b>Site 1</b>	16.6	n.d.	n.d.		11.4
<b>Site 2</b>	10.2	1.3	20.8	1.7	6.7
<b>Site 3</b>	24.1	2.3	3.0	n.d.	9.4

These rates are higher than those reported for natural baseflow conditions by Hill (1982) in agricultural streams ( $0.07 - 0.89 \mu\text{g m}^{-2} \text{s}^{-1}$ ) and Munn and Meyer (1990) in forested streams ( $0.05 - 0.37 \mu\text{g m}^{-2} \text{s}^{-1}$ ). However, direct comparisons cannot be made between SRP retention rates of Hill (1982) and Munn and Meyer (1990) and our study because of the much higher concentrations of SRP we employed. Variability in SRP retention within a given study reach appears to be linked to riffle-pool sequences (Figs. 6.1-6.3, Table 6.1). Variability between riffles does not appear to correspond with channel shape or morphology, groundwater flow direction, or the presence or absence of vegetation in the stream channel. Retention rates are lowest in pools in all three study reaches. This is in contrast to the results of laboratory sediment-P equilibrium experiments by Hill (1982) and Munn and Meyer (1990) who observed that pools had a higher retention capacity than riffles. Both Hill (1982) and Munn and Meyer (1990) linked this variability in sediment retention of SRP to particle size, where coarser sands found in riffles had a lower sorption capacity than finer sediments found in pools. However, SRP retention by stream sediments can also be affected by exchange in the hyporheic zone and/or turbulent mixing in the water column (Tate *et al.*, 1995; Jones and Mulholland, 2000;

Haggard *et al.*, 2001b). The lowest degree of mixing is expected to occur in pools, thereby leading to reduced interaction between the water column and sediments, and consequently leading to reduced retention rates. The discrepancy between the laboratory-based conclusions and this in situ field study indicate that several sediment and flow characteristics interactively affect phosphorus retention in agricultural streams. The relative importance of these characteristics (factors) may change as a function of discharge or antecedent conditions.

A dredging did not substantially increase SRP retention. Increased retention was observed in the uppermost section of Site 3 following the dredging of this section ( $24.1 \mu\text{g m}^{-2} \text{s}^{-1}$  in October compared to  $1.8 \mu\text{g m}^{-2} \text{s}^{-1}$  in June). The midsection of Site 3 was also dredged between the June and October experiments. However, SRP retention in this section of the stream was lower in October than in June even though SRP additions were higher in October. This pattern may be explained by changes to the stream morphometry as dredging changed the upper portion of the reach from a pool in June to a riffle in October, and changed the middle portion of the reach from a riffle in June to a pool in October. It is possible therefore, that the variability in SRP retention rates was a result of the movement of the pool in the stream rather than the dredging of the stream bottom.

The SRP retention rates observed for the entire reach of Site 3 following the dredge were similar to retention rates observed in sections of the stream that were not dredged. Exposed bed sediments following the dredging consisted largely of clays, which should have enhanced P retention. Sediments at this site had not been exposed to high concentrations of SRP prior to the experimental additions. Groundwater SRP concentrations in this section of the stream (measured over a two year period) were

always lower than  $10 \mu\text{g L}^{-1}$ . This suggests that any effect of dredging the stream bottom on SRP retention did not last long. Furthermore, the lack of vegetation in the channel did not appear to have an effect on SRP retention. The change in stream channel shape (pool-riffle) appears to have had a much more notable effect on SRP retention than the exposure of fresh sediments and the removal of vegetation caused by the dredge.

### **6.3.3 Mechanisms of SRP Retention**

SRP retention at high SRP concentrations in this stream is limited. Although the relative importance of the specific removal mechanisms cannot be determined directly, SRP retention patterns in the stream suggest that abiotic sorption of SRP to bottom sediments was likely the dominant mechanism of SRP retention during both experiments. This is consistent with observations in other agricultural systems (*e.g.* Hill, 1982). It is unlikely that biotic mechanisms of SRP retention were important on either sampling date. Mulholland *et al.* (1990) suggested that biotic communities became saturated at low SRP concentrations, and, biotic uptake would not vary over short-term SRP additions.

During the experiments, SRP concentrations greatly exceeded PP concentrations. PP concentrations in the water column throughout all three reaches before the experiment were variable and notably higher in October ( $37$  to  $266 \mu\text{g L}^{-1}$ ) than in June ( $3$  to  $64 \mu\text{g L}^{-1}$ ) (Figs. 6.6 and 6.7). TSS concentrations ranged from  $0.76$  to  $11.78 \text{ mg L}^{-1}$  in June, and from  $4.44$  to  $77.29 \text{ mg L}^{-1}$  in October (Figs. 6.6 and 6.7). During the June and October treatments, PP concentrations in the water column ranged within the variability observed for background PP concentrations. The lack of increase in PP during the experiments suggests that the elevated load of SRP was not converted to PP.

**Figure 6.6: TSS (squares) (left y-axis) and PP (right y-axis) at sampling points along the three stream reaches during the June experiment. [PP] prior to and during the  $K_2HPO_4$  additions are shown with diamonds and triangles, respectively. Error bars on the elevated PP symbols (triangles) show one standard deviation of the range of PP values observed at 35, 45 and 55 minutes at each location throughout the experiments.**

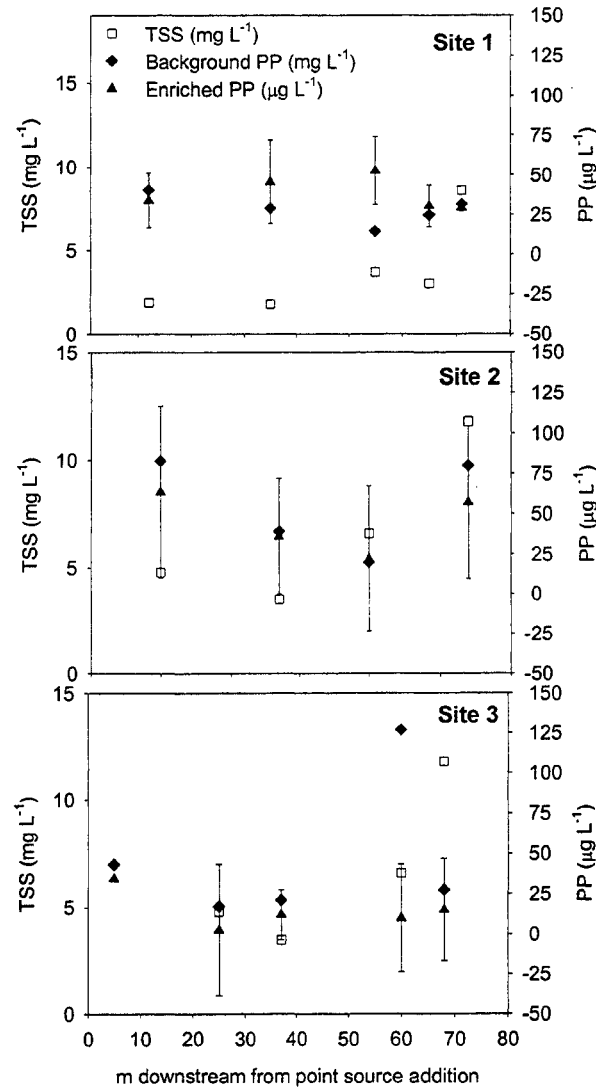
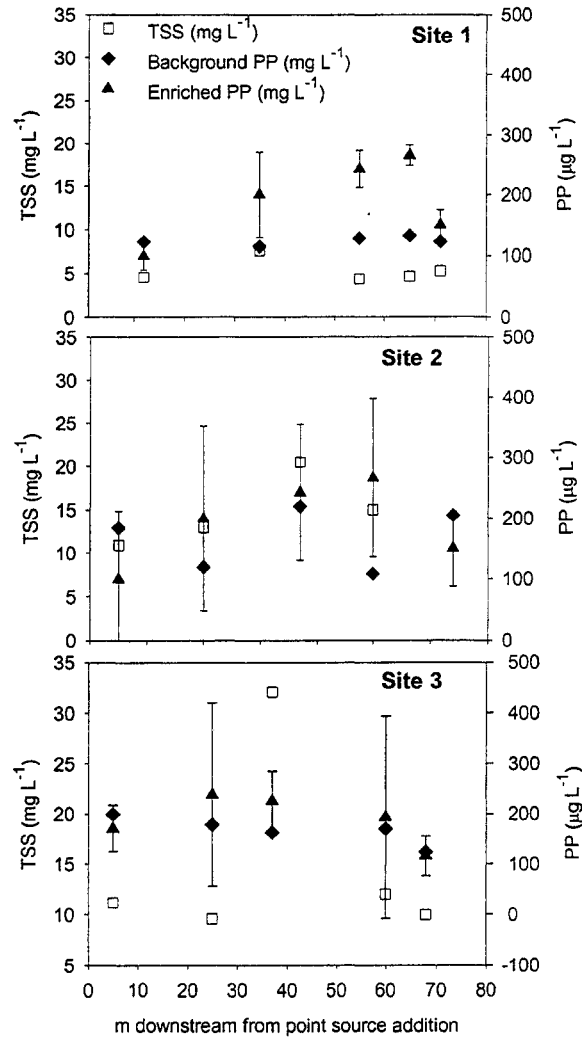




**Figure 6.7: TSS (squares) (left y-axis) and PP (right y-axis) at sampling points along the three stream reaches during the October experiment. [PP] prior to and during the  $K_2HPO_4$  additions are shown with diamonds and triangles, respectively. Error bars on the elevated PP symbols (triangles) show one standard deviation of the range of PP values observed at 35, 45 and 55 minutes at each location throughout the experiments.**

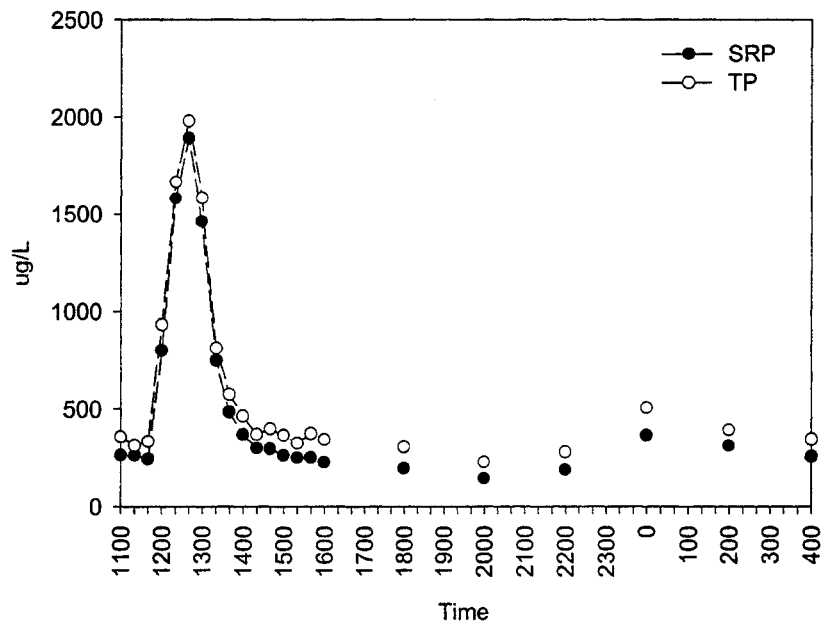


Stream SRP concentrations quickly returned to background levels after the experiments. Most of the P in stream water leaving the catchment was in the dissolved form prior to, during, and following the experiments (Fig. 6.8). The elevated SRP concentrations observed at the outflow following the SRP additions at Site 1 returned to background levels within two hours of the experiments during the October experiment (Fig. 6.8). The plumes from the SRP treatments at Sites 2 and 3 were missed by the automated sampler as a result of the sampling interval. The brief disturbance caused by the experimental additions is consistent with samples taken at each of the experimental reaches two hours and 24 hours following the cessation of the SRP additions at all three sites during both the June and October experiments.

#### **6.4 Conclusions**

This first-order agricultural stream did not retain substantial quantities of SRP under low flow conditions at concentrations of SRP elevated to  $0.7 - 4.2 \text{ mg L}^{-1}$ . The potential for streambed retention was expected to be high due to the low flow conditions. However, SRP retention by stream sediments appeared to be limited by mixing in the water column. Changes in SRP retention along the stream length corrected for dilution were generally less than 10% of the high SRP concentrations employed in the experiments. Given that most SRP is lost when SRP concentrations are elevated (at either high or low flows) this stream is a poor buffer of SRP export from an agricultural system.

Figure 6.8: TP (white circles) and SRP (black circles) observed at the catchment outflow prior to, during and following the October additions of  $K_2HPO_4$ .



## **7.0 Summary and Major Conclusions of Thesis**

The goal of this thesis is to improve our understanding of nutrient transport in agricultural systems. Four areas have been identified where knowledge is lacking and each of these areas has been explored in one of the four major chapters of the thesis.

A substantial amount of literature exists on nutrient export in agricultural watersheds. However, while it is possible to conceptually model dominant processes and variability in nutrient export patterns, factors affecting these processes (e.g. basin land use, soil characteristics, management practices, topography, and flow paths) cannot yet be adequately predicted and quantified in numerical models. This is because there are still gaps in our understanding of processes that govern variability of nutrient export in time and space. Four specific areas where knowledge is lacking include (1) temporal variability at a range of scales (annual, between and within storm); (2) the role of drainage tiles in basin discharge and nutrient export throughout all seasons of the year; (3) the role of basin antecedent hydrologic conditions (AHC) in temporal variability in nutrient export; and (4) temporal variability in the effectiveness of riparian wetlands and/or instream processes.

### **7.1 Long- and Short-term Temporal Variability in Nutrient Export Patterns**

Before quantitative and predictive models of nutrient export patterns can be generated, it is necessary to characterize the range of event magnitudes. In determining the range of events that occur, we can subsequently select specific storms and identify processes that lead to variability among events. This also enables us to focus our sampling regimes around critical periods. Chapter Three has shown that hydrochemical

export varies significantly in the study basin at a range of temporal scales. Much of the annual hydrochemical export occurs during storm and thaw events rather than baseflow conditions, and the bulk of nutrients are exported within a few high magnitude events. In general, high magnitude hydrologic events also export high magnitudes of nutrients.

This is the first comprehensive study to examine the role of high magnitude events in annual  $\text{NO}_3^-$ , SRP and TP export from small first-order agricultural catchments in Southern Ontario and describe the dominant processes leading to the observed patterns of nutrient export. Chapter Three has shown the significance of winter thaws and in particular major snowmelt events in annual nutrient export from agricultural catchments in Southern Ontario, and has identified the need to include the winter period in sampling regimes. In both study years, the major snowmelt event exported high magnitudes of discharge and nutrients.

Chapter Three also illustrates the importance of sampling frequency in generating estimates of hydrochemical export. Not only is storm selection important, but also the sampling frequency that is employed throughout the duration of the event. Error decreases substantially with increased sampling frequency. This is true for all storms, rather than just storms that are large in magnitude. Intensive sampling frequencies are critical in obtaining precise estimates of nutrient export rates. Estimates of nutrient export generated from infrequent sampling frequencies can generate errors of more than 100% per event, and such errors can cumulatively result in major inaccuracies over time. An improved monitoring strategy may be to intensively sample a study basin during a range of hydrologic events to generate a discharge-mass relationship and predict nutrient export from subsequent events using this relationship. However, since discharge-mass

relationships for P change during high magnitude events, and, substantial quantities of nutrients are exported during these periods, it is critical that such events are monitored intensively each time they occur.

## **7.2 The Role of Drainage Tiles Within Various Watersheds**

In order to understand temporal variability in hydrochemical export patterns, we must first identify the dominant sources of nutrients within catchments. The role of tiles in export from agricultural areas has been the focus of several studies, yet factors governing temporal variability in nutrient export from tiles are still poorly understood. Much of the current understanding of hydrochemical export patterns from tiles has been developed in warmer geographic regions, and little is known about nutrient export from tiles during winter months.

This study is one of the first studies to examine nutrient export patterns from drainage tiles in the winter months. Chapter Four has shown that hydrochemical export originates from a combination of drainage tiles and diffuse groundwater sources but in general, drainage tiles export the majority of nutrients from the study basin.

Chapter Four has shown that hydrologic export from tiles in this basin is predictable during very dry and wet conditions, but, unpredictable at low to moderate flow periods. It is estimated that 42% of annual basin discharge originates from drainage tiles. However, during storm and thaw events, tiles may contribute between 0 and 90% of basin discharge.

Nutrient export from tiles within the basin varies both spatially and temporally. All tiles demonstrated temporal variability in hydrochemical export throughout the study

period. Pulses of P export were often observed from tiles, although pulses of  $\text{NO}_3^-$  were not observed. Instead  $\text{NO}_3^-$  concentrations in tile effluent were often elevated for several days throughout storm events.

Although tiles appear to export the majority of nutrients during storm periods, not all tiles behave in a similar manner. Some tiles routinely export higher quantities of nutrients than other tiles. For example, fields receiving manure applications tended to export higher quantities of P than tiles in fields receiving inorganic fertilizers during some storm periods. However, during some storm periods and also during lower flow periods, all tiles in the basin exported minimal quantities of P. All tiles in the basin exported substantial quantities of  $\text{NO}_3^-$  during both high and moderate flow periods.

Overland flow has been identified as a major nutrient source in many studies. When overland flow occurred in the study basin, P concentrations in overland flow were high and overland flow was likely a major P source during those periods. This was not the case for  $\text{NO}_3^-$ . Overland flow seldom occurs in the study basin, and generally only occurred during high magnitude even within the study period. However, tiles also contributed substantial quantities of nutrients during both high magnitude and smaller events.

The consistently low P concentrations in groundwater suggest that soils are effectively retaining P in matrix flow. The work of Cabrera (1998), Harris (1999) and Mengis et al., (1999) has shown that some  $\text{NO}_3^-$  is attenuated in riparian areas in this basin, but this varies both spatially and temporally. Harris (1999) observed reduced rates of denitrification in winter months. Substantial amounts of  $\text{NO}_3^-$  were exported to the

stream through diffuse groundwater flow suggesting that not all  $\text{NO}_3^-$  in groundwater is attenuated in riparian areas within this basin.

During periods of moderate flow, tiles are low in their export of both P and  $\text{NO}_3^-$ , but during large storm events tiles export substantial quantities of both nutrients. This appears to be a result of connectivity with surface layers, where nutrients from surface layers are routed into drainage tiles via preferential flowpaths. Given the fact that tiles bypass natural processes in soils that attenuate nutrients, the only way to reduce nutrient losses in tile effluent is to reduce rates of nutrient application. In the case of P, McDowell et al. (2001) advocate a 'maintenance' philosophy to soil P levels rather than a 'build-up' philosophy and suggest that once adequate soil P concentrations are reached, optimum crop yields can be maintained by replenishing that taken off with fertilizer or manure. Thus, limiting the application rates of fertilizers and manure is a good way to reduce P export from agricultural catchments.

A substantial quantity of  $\text{NO}_3^-$  is also lost through tiles, reducing the effectiveness of riparian buffer strips. Thus, as in the case of P, we must manage N application rates rather than rely on riparian buffer strips to attenuate  $\text{NO}_3^-$  in groundwater.

### **7.3 The Effects of Antecedent Hydrologic Conditions on Nutrient Export Patterns**

Chapters Three and Four of this thesis have shown that the study basin is temporally variable in nutrient export, and that the majority of the nutrients exported by the basin originate from drainage tiles, particularly in the case of P. Chapter Five links temporal variability in hydrochemical export to AHC in the basin, and demonstrates that basin discharge and nutrient export change during successive events and under variable



AHC. Successive storms appear to increase the proportion of precipitation that is lost as discharge from the basin. This complicates the relationship between precipitation and discharge. Weak relationships between basin discharge and AHC such as pre-event streamflow, season, water table behaviour and precipitation type and magnitude demonstrate the complex hydrology of heterogeneous agricultural catchments such as the study catchment.

The quantity of nutrients exported is a function of a suite of factors, including antecedent conditions in the basin, precipitation received, and the availability of nutrients which is partly a function of the timing of fertilizer application. Antecedent conditions are particularly important for several reasons. First, they affect how much water may actually pass through the basin following a storm event. Second, antecedent conditions affect the 'efficiency' of the runoff that does pass through the basin in exporting nutrients to surface water bodies. As stated above, AHC affect the quantity of water that passes through the basin, which affects the mass of nutrients that can be exported. Furthermore, the behaviour of the water table strongly impacts the export of nutrients. An incrementally rising water table will lead to a constant or increasing mass of nutrients lost per mm of discharge, as long as the water table is moving into new soil horizons and the system is becoming wetter. During such periods, larger macropores and flowpaths may be accessed, increasing connectivity with surface soils and possibly accessing new sources of nutrients in the vadose zone. However, if the basin is on a drying trend, and the basin is not becoming 'wetter' with successive events (evidenced by the water table simply passing into a soil horizon that it recently 'accessed' during a preceding storm) the nutrient loading potential of the event is diminished.

In summary, the role of AHC in hydrochemical export from agricultural catchments is poorly understood. AHC are frequently referred to in the literature, yet the scientific community has been unable to quantify these relationships. Consequently, it is difficult to incorporate AHC into predictive models. Chapter Five is a first step towards solving this problem and has shown there is strong temporal variability in hydrochemical export in this basin and this variability can be linked to a complex suite of factors, the most important of which include antecedent conditions, precipitation type and quantity received, and the availability of nutrients/timing of fertilizer application. Chapter Five shows the complexities in predicting nutrient and hydrologic export from agricultural basins. The goal of future research is to quantitatively incorporate the effects of antecedent conditions into physically-based models.

#### **7.4 Temporal Variability in the Effectiveness of Riparian Buffer Strips and/or Instream Processes**

The fourth 'gap' in our understanding of nutrient dynamics in agricultural catchments is temporal variability in the effectiveness of riparian buffer strips and in-stream processes. This is a large gap, and could easily comprise an entire thesis. Thus, one specific area (SRP attenuation by in-stream processes at low flows) was the focus of Chapter Six.

Nutrient retention by biogeochemical processes in riparian areas was not focused on in this thesis.  $\text{NO}_3^-$  attenuation in riparian areas has been studied previously in this basin by Cabrera (1998), Harris (1999) and Mengis et al. (1999) and has been shown to vary spatially and temporally. The in-stream retention of  $\text{NO}_3^-$  has not been examined in

this basin, although both Cabrera (1998) and House (2000) observed very low concentrations of  $\text{NO}_3^-$  in the hyporeic zone of the stream. The removal of  $\text{NO}_3^-$  from streamwater by in-stream processes is an area where future work is necessary.

P removal in riparian areas was also not focused on in this thesis. Throughout the entire study period, SRP concentrations in groundwater piezometers were very low, suggesting that diffuse groundwater flow is not an important source of P in the study basin. Chapter Four demonstrated that the bulk of P observed at the outflow was due to drainage tiles. Thus, the contribution of drainage tiles was focused on rather than P in diffuse groundwater.

Chapter Six focuses on in-stream retention of SRP, and shows that stream sediments are unable to retain large pulses of P during very low flow periods, due to poor mixing in the water column. Occasionally, tiles export a pulse of SRP under low flow conditions, such as occasions following the irrigation of fields receiving liquid manure applications, or, when fertilizers are directly applied into ditches. Chapter Six demonstrates that the stream is unable to retain such pulses.

The stream is also likely unable to retain P during high flow periods. It is generally agreed that streams export previously retained sediments during high flow periods (e.g. Haggard et al., 2001a; Hill, 1981). Observation of the streambed prior to and following high flow events and the elevated PP in stream discharge during such periods suggests that the same is true in the study basin.

Calculations of tile and groundwater discharge into the stream suggest that some retention is occurring during moderate flows, although in-stream retention under these conditions was not focused on in this thesis. However, since the stream sediments are

exported during high flow events, P retention by sediments is transient and cannot be viewed as a true attenuation mechanism.

### **7.5 Summary of Major Processes Controlling Nutrient Export in the Strawberry Creek Watershed and Major Conclusions of Thesis**

Attempting to understand the mechanisms driving the export of nutrients by monitoring the basin outflow alone is difficult. The basin, typical of Southern Ontario, is composed of a mosaic of source areas that differ in land use, drainage characteristics and structure. As such, they respond differently to hydrologic events and range in their ability to export nutrients. In order to understand patterns observed at the basin scale, it is important to first understand processes occurring at smaller spatial and temporal scales within the basin. Thus, temporal patterns of hydrochemical export were examined at the outflow and AHC, the contribution of drainage tiles and some groundwater flow were monitored simultaneously to tie processes occurring at different scales within the catchment to what was being observed at the outflow.

Based on the scientific literature and the findings of this thesis, conceptual diagrams of the major processes controlling P and NO<sub>3</sub><sup>-</sup> export have been constructed (Figures 7.1 and 7.2). Since most nutrients are lost during hydrologic events (rainstorm, winter thaw), it is important to focus on what is happening during these events rather than during baseflow periods. This thesis and the work of others have shown that in order to have high losses of nutrients, there must be a nutrient *source* and a *pathway*. However, antecedent hydrologic conditions in the basin cause variability in nutrient availability and the flowpaths through which nutrients are transported.

**Figure 7.1 Conceptual Diagram of Major Sources, Pathways and Fate of Phosphate in the Study Basin**

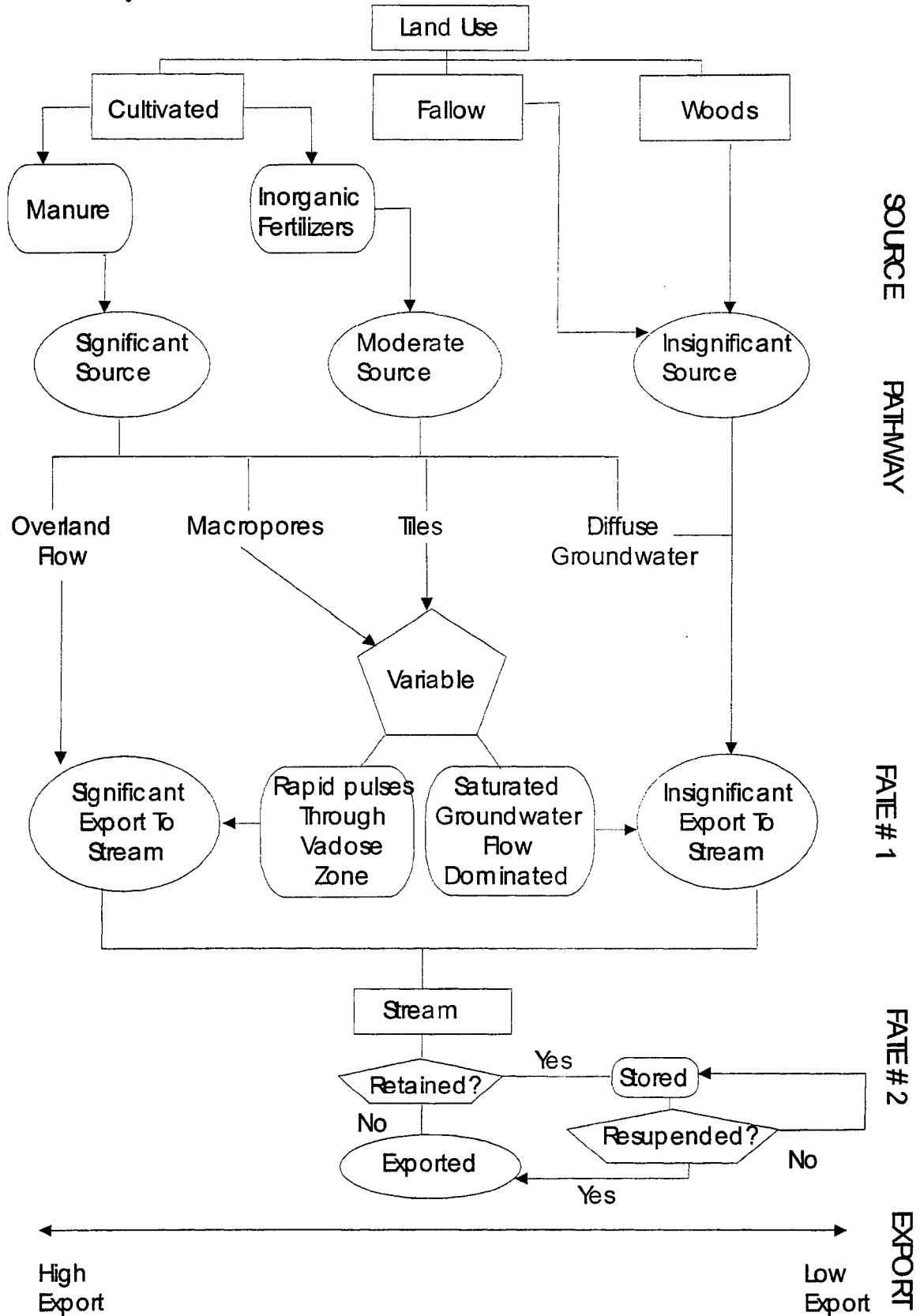
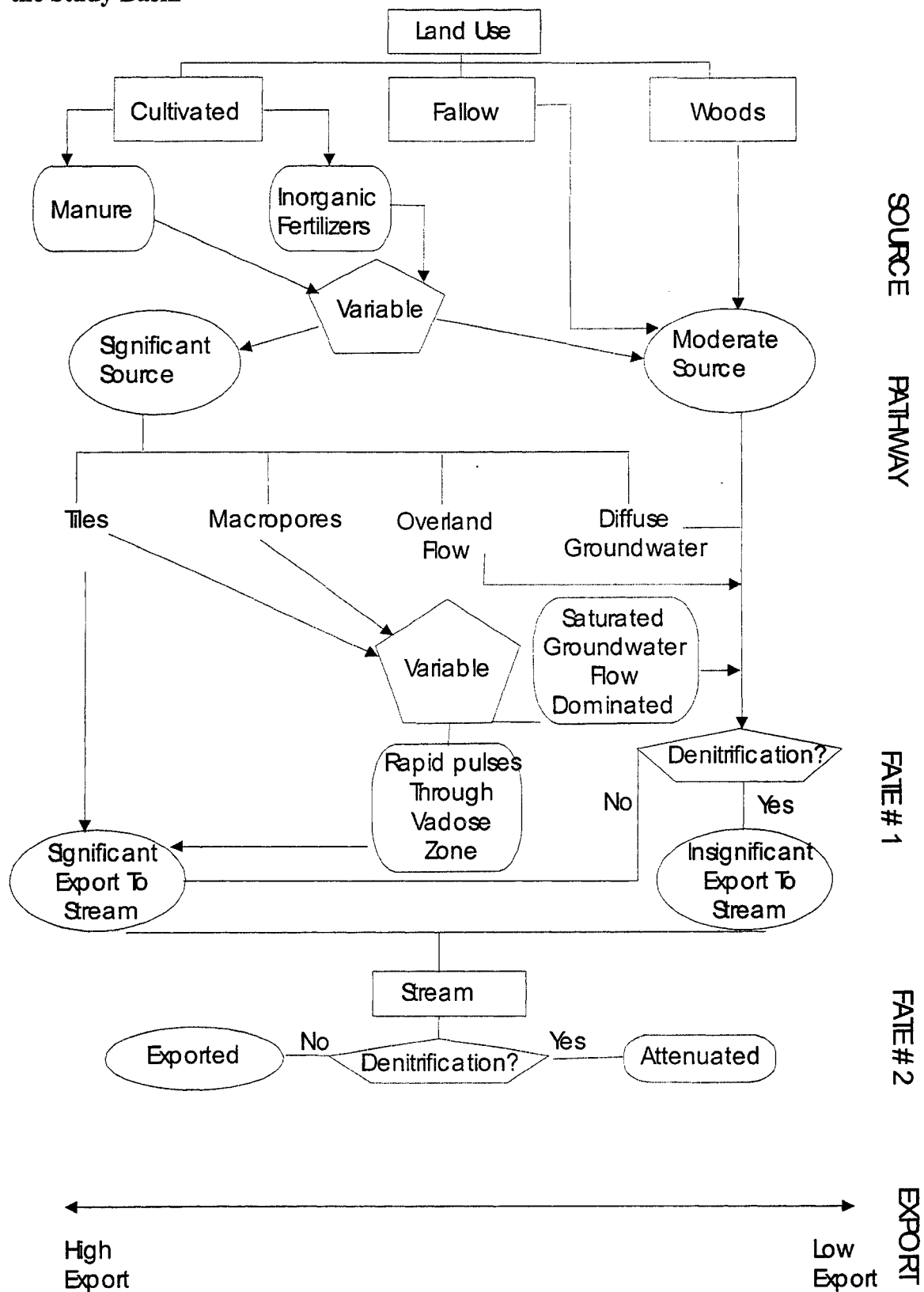


**Figure 7.2 Conceptual Diagram of Major Sources, Pathways and Fate of Nitrate in the Study Basin**



The highest TP export is observed due to erosion when surface runoff interacts with P pools in surface soils. Such conditions may be very wet antecedent conditions (i.e. saturated conditions), or, frozen and impermeable soils (i.e. thaw events). If these conditions are coupled with the recent application of manure, exceptionally high export of SRP is observed (e.g. February 2000). SRP and TP export may also be very high through tiles. Pulses of P may occur during somewhat dry conditions, or, very wet conditions. Such pulses often occur following the application of manure to contributing areas, and likely can be attributed to drainage through macropores into the tiles.

Moderate to low  $\text{NO}_3^-$  export is observed during dry conditions and high  $\text{NO}_3^-$  export occurs as conditions become increasingly wetter. The highest  $\text{NO}_3^-$  export is observed during wet periods that follow drought periods (e.g. Autumn, 2001). A high water table, and connectivity between surface layers and tile drains via macropores appears to be very important in  $\text{NO}_3^-$  export in this basin. It is hypothesized that as conditions become wetter, larger preferential flow pathways are 'activated' and transport larger quantities of  $\text{NO}_3^-$  through drainage tiles. Although a substantial quantity of  $\text{NO}_3^-$  is transported through tiles, moderate amounts of  $\text{NO}_3^-$  are also exported through diffuse groundwater flow.

In summary, the major findings of the thesis are:

- (1) There is strong temporal variability in discharge and SRP, TP and  $\text{NO}_3^-$  export from the basin and a few high magnitude events account for the bulk of this export;
- (2) Snowmelt is very important in this region, and often results in the export of high magnitudes of discharge and SRP, TP and  $\text{NO}_3^-$  export;

- (3) The majority of SRP, TP and  $\text{NO}_3^-$  originates from drainage tiles rather than diffuse groundwater flow. This is particularly true in the case of P.
- (4) SRP, TP and  $\text{NO}_3^-$  export varies spatially and temporally among tiles within the same basin. The greatest P losses are observed from areas where manure is applied; however, such occurrences are episodic. This demonstrates the importance of sampling frequency in characterizing nutrient levels in tile effluent.
- (5) Hydrologically, tiles within the basin behave in a similar manner during dry or wet conditions, but behave differently during periods of moderate flow.
- (6) Antecedent hydrologic conditions in the basin have a substantial effect on basin hydrochemical export, and the ability of the basin to store water and retain nutrients changes during successive events.
- (7) Although antecedent hydrologic conditions have a dramatic effect on hydrochemical export, their effects are complex and cannot be quantified at this time.
- (8) Although some P retention occurs in this stream during periods of moderate flow, Strawberry Creek is not able to retain pulses of P during low flow periods.



## 8.0 References

- Arheimer, B and R Liden, 2000. Nitrogen and phosphorus concentrations from agricultural catchments – influence of spatial and temporal variables. *J. Hydrology* 227: 140-159.
- Baker DB, 1993. The Lake Erie Agroecosystem Program: Water quality assessments. *Agricult. Ecosyst. Environ.* 46: 197-215.
- Baker RS and D Hillel, 1990. Laboratory tests of a theory of fingering during infiltration into layered soils. *Soil Science Society of America Journal* 54: 20-30.
- Barrow NJ, 1978. The description of phosphate adsorption curves. *J. Soil. Sci.* 29: 447-462.
- Beauchemin S, RR Simard, and D Cluis, 1998. Forms and concentration of phosphorus in drainage water of twenty-seven tile-drained soils. *J. Environ. Qual.* 27:721-728.
- Beaulac, MN and KH Reckhow, 1982. An examination of land use-nutrient export relationships. *Water Resources Bull.* 18: 1013 – 1024.
- Berner, EK and RA Berner, 1996. *Global Environment: Water, Air, and Geochemical Cycles*. U.S.A.: Prentice-Hall, Inc.
- Bevan K and P Germann, 1982. Macropores and water flow in soils. *Water Resources Research* 18: 1311-1325.
- Biron PM, AG Roy, F Courchesne, WH Hendershot, B Côté, and J Fyles, 1999. The effects of antecedent moisture conditions on the relationship of hydrology to hydrochemistry in a small forested watershed. *Hydrological Processes* 13:1541-1555.
- Bronswijk JJB, W Hamminga, and K Oostindie, 1995. Rapid nutrient leaching to groundwater and surface water in clay soil areas. *Eur. J. Agron.* 4: 431-439.
- Brunet R.-C, and KB Astin, 1998. Variation in phosphorus flux during a hydrological season: the River Adour. *Water Research* 32(3): 547-558.
- Burns D, 1998. Retention of NO<sub>3</sub><sup>-</sup> in an upland stream environment: A mass balance approach. *Biogeochemistry* 40: 73-96.
- Burwell RE, DR Timmons, and RF Holt, 1975. Nutrient transport in surface as influenced by soil cover and seasonal periods. *Soil Soc. Sci. Am. Proc.* 39: 523-528.

- Cabrera F, 1998. Investigating the impact of variable riparian zone geometry on the attenuation of nitrate in the Strawberry Creek Watershed. M.S.C. Project, Waterloo Centre for Groundwater Research, Univ. of Waterloo.
- Carlyle GC and AR Hill, 2001. Groundwater phosphate dynamics in a river riparian zone: effects of hydrologic flowpaths, lithology and redox chemistry. *J. Hydrology* 247: 151-168.
- Carpenter SR, NF Caraco, DL Correll, RW Howarth, AN Sharpley, and VH Smith, 1998. Nonpoint pollution of surface waters with phosphorus and nitrogen. *Ecol. Applic.* 8: 559-568.
- Chapman LJ and DF Putnam, 1984 *The Physiography of Southern Ontario, 3rd edition*. Toronto.
- Christensen PB, LP Nielson, J Sorenson and NP Revsbech, 1990. Denitrification in nitrate-rich streams – diurnal and seasonal variation related to benthic metabolism. *Limnol. Oceanogr.* 35: 640-651.
- Cirno CP and JJ McDonnell, 1997. Linking the hydrologic and biogeochemical controls of nitrogen transport in near-stream zones of temperate-forested catchments: a review. *J. Hydrology* 199: 88-120.
- Cleresci NL, SJ Curran, and RI Sedlak, 1986. Nutrient loads to Wisconsin lakes: Part I. Nitrogen and phosphorus export coefficients. *Water Resources Bull.* 22: 983-990.
- Cook MJ and JL Baker, 1998. Bacteria and nutrient transport to tile lines shortly after application of large volumes of liquid swine manure. *Paper 98-2035. ASAE*, St. Joseph, MI.
- Cooke SE and EE Prepas, 1998. Stream phosphorus and nitrogen export from agricultural and forested watersheds on the Boreal Plain. *Can. J. Fish. Aquat. Sci.* 55: 2292-2299.
- Cooper JR and JW Gilliam, 1987. Phosphorus redistribution from cultivated fields into riparian areas. *Soil Sci.Soc.Am.J.* 51: 1600-1604.
- Correll DL, TE Jordan, and DE Weller, 1999. Effects of precipitation and air temperature on phosphorus fluxes from Rhode River watersheds. *J. Environ. Qual.* 28: 144-154.
- Cosser PZ, 1989, Nutrient concentration-flow relationships and loads in the South Pine River, Southeastern Queensland. I. Phosphorus loads. *Aust. J. Mar Freshwater Res.* 40: 613-630.
- Creed IF and LE Band, 1998. Export of nitrogen from catchments within a temperate forest: Evidence for a unifying mechanism regulated by variable source area dynamics. *Water Resources Res.* 24: 3105-3120.

- Culley JL, EF Bolton, and V Bernyk, 1983. Suspended solids and phosphorus loads from a clay soil: I plot studies. *J. Environ. Qual.* 12(4): 493-503.
- Daniel TC, AN Sharpley, and JL Lemunyon, 1998. Agricultural phosphorus and eutrophication: A symposium overview. *J. Environ. Qual.* 27: 251-257.
- Daniels RB and JW Gilliam, 1996. Sediment and chemical load reduction by grass and riparian filters. *Soil Sci. Soc. Am. J.*, 60: 246-251.
- David M, LE Gentry, DE Kovacic and KM Smith, 1997. Nitrogen balance in and export from an agricultural watershed. *J. Environ. Qual.* 26: 1038-1048.
- Dean DM and ME Foran, 1992. The effect of farm liquid waste application on tile drainage. *J. Soil Water Conserv.* 47:368-369.
- Devito KJ, PJ Dillon, and BD Lazerte, 1990. Phosphorus and nitrogen retention in five Precambrian Shield wetlands. *Biogeochemistry* 8: 185-204.
- Dillon PJ and WB Kirchner, 1975. The effects of geology and land use on the export of phosphorus from watersheds. *Water Research* 9: 135-148.
- Dillaha TA, JH Sherrard, and D Lee, 1989. Long-term effectiveness of vegetative filter strips. *Water Environ. Technol.* (November), 419-421.
- Dils RM and AL Heathwaite, 1999. The controversial role of tile drainage in phosphorus export from agricultural land. *Wat. Sci. Tech* 39(12): 55-61.
- Dingman, SL, 2002. *Physical Hydrology (2nd Edition)*. Prentice-Hall Inc. USA.
- Dolezal F, Z Kulhavy, M Soukup and R Kodesova, 2001. Hydrology of Tile Drainage Runoff. *Phys. Chem. Earth (B)*, 26(7-8): 623-627.
- Douglas CL Jr., KA King, JF and Zuzel, 1998. Nitrogen and phosphorus in surface runoff and sediment from a wheat-pea rotation in Northeastern Oregon. *J. Environ. Qual.* 27: 1170-1177.
- Douglas CL Jr., RW Rickman, JF Zuzel, and BL Klepper, 1988. Criteria for delineation of agronomic zones for the dryland Pacific Northwest. *J. Soil Water Conserv.* 43: 415-418.
- Duff JH and FJ Triska, 1990. Denitrification in sediments from the hyporheic zone adjacent to a small forested stream. *Can. J. Fish. Aquat. Sci.* 47: 1140-1147.
- Edwards WM and LB Owens, 1991. Large storm effects on total soil erosion. *J. Soil Water Conserv.* 46: 75-78.

Environment Canada, 2003. Canadian Climate Normals, Meteorological Service of Canada.

Environment Canada, 1979. *Analytical Methods Manual*. Ottawa, Canada.

Fennessy MS and JK Cronk, 1997. The effectiveness and restoration potential of riparian ecotones for the management of non-point source pollution, particularly nitrate. *Crit. Rev. Environ. Sci. Technol.* 27: 285-317.

Findlay S. 1995. Importance of surface-subsurface exchange in stream ecosystems: the hyporheic zone. *Limnol. Oceanogr.* 40:159-164.

Fleming R and M Ford, 2001. Humans Vs. Animals – Comparison of Waste Properties. Available Online: [www.ridgetownc.on.ca/Research/Rfleming/Reports/huvsanim0107.pdf](http://www.ridgetownc.on.ca/Research/Rfleming/Reports/huvsanim0107.pdf)  
Date accessed: September 15, 2003.

Fogal R, G Mulamootil, M Stone and L Logan, 1995. Longitudinal and Seasonal Patterns of Phosphorus in Riverbed Sediments. *Journal of Environmental Planning and Management* 38(2): 167-179.

Foth HD and BG Ellis, 1997. *Soil Fertility*. CRC Press, UK.

Gachter R. and JS Meyer, 1993. The role of microorganisms in mobilization and fixation of phosphorus in sediments. *Hydrobiologia* 253:103-121.

Gachter R, JM Ngatiah, and C Stamm. 1998. Transport of phosphate from soil to surface waters by preferential flow. *Environ. Sci. & Tech.* 32(13):1865-1869.

Gburek WJ and AN Sharpley, 1998. Hydrologic controls on phosphorus loss from upland agricultural watersheds. *J. Environ. Qual.* 27: 267-277.

Gentry LE, MB David, KM Smith-Starks, and DA Kovacic, 2000. Nitrogen fertilizer and herbicide transport from tile drained fields. *Journal of Environmental Quality* 29(1): 232-240.

Ghodrati M and WA Jury, 1990. A field study using dyes to characterize preferential flow of water. *Soil Science Society of America Journal* 54: 1558-1563.

Gilbert J, M Dole-Olivier, P Marmonier, and P Vervier, 1990. Surface-groundwater ecotones. In: Naiman, RJ, Decamps, H (eds). *Ecology and Management of Aquatic-terrestrial Ecotones*. UNESCO, Paris: pp.7-21.

Glass RJ, S Cann, J King, N Baily, J-Y Parlange, and TS Steenhuis, 1990. Wetting front instability in unsaturated porous media: a three-dimensional study in initially dry sand. *Transp. Porous Media*, 5: 247-268.

- Geohring LD, PE Wright and TS Steenhuis, 1998. Preferential flow of liquid manure to subsurface drains. In *Drainage in the 21<sup>st</sup> Century: Food Production and the Environment*, L. Brown (ed.). Pub. No. 02-98. ASAE, St. Joseph, MI. pp. 1-8.
- Goss MJ, DAJ Barry, and DL Rudolph, 1998. Contamination in Ontario farmstead domestic wells and its association with agriculture: 1. Results from drinking water wells. *Journal of Contaminant Hydrology* 32 (3): 267-293.
- Grant DM, 1981. *Open Channel Flow Measurement Handbook* (2<sup>nd</sup> Ed.). ISCO, Inc. Lincoln, Nebraska.
- Grand River Conservation Authority, 1998. *State of the Watershed Report: Background Report on the Health of the Grand River Watershed 1996-97*. Cambridge, Ontario: Grand River Conservation Authority.
- Haag D and M Kaupenjohann, 2001. Landscape fate of nitrate fluxes and emissions in Central Europe: A critical review of concepts, data, and models for transport and retention. *Agriculture, Ecosystems and Environment* 86: 1-21.
- Haggard BE, DE Storm, and EH Stanley, 2001a. Effect of a point source input on stream nutrient retention. *Journal of the American Water Resources Association* 37(5): 1291-1299.
- Haggard BE, DE Storm, RD Tejral, YA Popova, VG Keyworth, and EH Stanley, 2001b. Stream nutrient retention in three Northeastern Oklahoma agricultural catchments. *Transactions of the ASAE* 44(3): 597-605.
- Harris M, 1999. Nitrate attenuation in a narrow non-forested riparian buffer zone in an agricultural watershed in Southern Ontario, M.Sc. Thesis, Wilfrid Laurier University.
- Haygarth PM, L Hepworth, and SC Jarvis, 1998. Forms of phosphorus transfer in hydrological pathways from soil under grazed grassland. *Eur J Soil Sci* 49: 65-72.
- Haygarth PM, 1997. Agriculture as a Source of Phosphorus Pollution in Water: Sources and Pathways. *Scientific Committee in Phosphates in Europe*, Paris.
- Henderson-Sellers B. and HR Markland, 1987. *Decaying Lakes: The Origins and Control of Cultural Eutrophication*. Great Britain: John Wiley and Sons.
- Hewlitt JD and AR Hibbert, 1967. Factors affecting the response of small watersheds to precipitation in humid areas, In WE Sopper and HW Lull (eds) *International Symposium on Forest Hydrology*, The Pennsylvania State University, 29 August – 10 September 1965. Pergamon Press, Oxford, pp. 275-290.
- Hill AR, 1997. The potential role of in-stream and hyporheic environments as buffer zones. In: Naycock, RE, Burt, TP, Goulding, KW, and Pinay, G (eds.) *Buffer Zones:*

*Their Processes and Potential in Water Protection*. Quest Environment, Hertfordshire, pp. 115-127.

Hill AR, 1996. Nitrate removal in stream riparian zones. *J. Environ. Qual.* 25: 743-755.

Hill AR, 1990. Groundwater flowpaths in relation to nitrogen chemistry in the near-stream zone. *Hydrobiologia* 206: 29-52.

Hill AR, 1982. Phosphorus and major cation mass balances for two rivers during low summer flows. *Freshwater Biology* 12:293-304.

Hill AR, 1981. Stream phosphorus exports from watersheds with contrasting land uses in Southern Ontario. *Wat. Res. Bull.*, 17(4): 627-635.

Hillel D, 1998. *Environmental Soil Physics*. Academic Press: USA.

Hillel D and RS Baker, 1988, A descriptive theory of fingering during infiltration into layered soils. *Soil Science* 146: 51-56.

Hodgkinson, RA, BJ Chambers, PJA Withers and R Cross, 2002. Phosphorus losses to surface waters following organic manure applications to a tile drained clay soil. *Agricultural Water Management* 57(2): 155-173.

Holtan H, L Kamp-Nielson and AO Stuanes, 1988. Phosphorus in soil, water and sediment: an overview. *Hydrobiologia* 170:19-34.

House A, 2000. Examination of the role of macropores and subsurface drainage in the delivery of NO<sub>3</sub>-N to a small first-order agricultural stream in Southern Ontario. MES Thesis, Wilfrid Laurier University.

Hvorslev MJ, 1951. Time lag and soil permeability in ground water observations. *US Army Corps of Engineers Waterways Experimental Station Bulletin* 36. Vicksburg, Mississippi.

International Joint Commission (IJC), 2000. *10th Biennial Report on Great Lakes Water Quality*. Windsor: International Joint Commission.

Jaffe DA, 1992. The Nitrogen Cycle, In, *Global Biogeochemical Cycles*, SS Butcher, RJ Charlson, GH Orians, and GW Wolfe (eds). Academic Press Ltd: USA.

Jahnke RJ, 1992. The Phosphorous Cycle, In, *Global Biogeochemical Cycles*, SS Butcher, RJ Charlson, GH Orians, and GW Wolfe (eds). Academic Press Ltd: USA.

Jenkins A, RC Ferrier, R Harriman, and YO Ogunkoya, 1994. A case study in catchment hydrochemistry: Conflicting interpretations from hydrological and chemical observations. *Hydrological Processes* 8: 335-349.

- Johnson AH, DR Bouldin, EA Goyette, and AM Hedges, 1999. Phosphorus loss by stream transport from a rural watershed: Quantities, processes and sources. *J. Environ. Qual.* 5(2): 148-157.
- Jones JB and PJ Mulholland, 2000. *Streams and Ground Waters*. London: Academic Press, 425 pp.
- Jordan TE, DL Correll, and DE Weller, 1997. Relating nutrient discharges from watersheds to land use and streamflow variability. *Water Resources Res.* 33: 2579-2590.
- Ju S-H, K-JS Kung, and C Helling, 1997. Simulating impact of funnel flow on contaminant sampling in sandy soils. *Soil Society of America Journal* 61: 409-415.
- Jury WA and K Roth, 1990. *Transfer Functions and Solute Transport Through Soil: Theory and Applications*. Birkhaeuser Publ. Basel.
- Karr JR and IJ Schlosser, 1978. Water resources and the land-water interface. *Science*, 201: 229-234.
- Karrow PF, 1974. Till stratigraphy in parts of Southwestern Ontario. *Geological Society of America Bulletin*, 761-768.
- Klotz RL, 1985. Factors controlling phosphorus limitation in stream sediments. *Limnology and Oceanography* 30:543-553.
- Khaleel R, 1980. Hydrologic Processes Affecting Non-point Pollution from Agricultural Lands, In *Environmental Impact of Non-point Source Pollution* (M.R. Overcash and J.M. Davidson, Eds.). U.S.A.: Ann Arbor Science Publishers.
- Kohl DH, GB Shearer, and B Commoner, 1971. Fertilizer nitrogen: contribution to nitrate in surface water in a cornbelt watershed. *Science* 174: 1331-1334.
- Kucey RMN, 1983. Phosphate solubilizing bacteria and fungi in various cultivated and virgin Alberta soils. *Can.J.Soil Sci.* 63: 671-678.
- Kung KJ-S, EJ Kladvko, TJ Gish, TS Steenhuis, G Bubenzer, and CS Helling, 2000a. Quantifying Preferential Flow by Breakthrough of Sequentially Applied Tracers. *Soil Science Society of America Journal* 64: 1296-1304.
- Kung KJ-S, TS Steenhuis, EJ Kladvko, G Bubenzer, TJ Gish, and CS Helling, 2000b. Impact of preferential flow on the transport of adsorbing and non-adsorbing tracers. *Soil Science Society of America Journal* 64: 1290-1296.
- Lindstrom MJ, WW Nelson, and TE Schumacher, 1992. Quantifying tillage erosion rates due to mouldboard ploughing. *Soil and Tillage Research* 24: 243-255.

- Laubel A, OH Jacobsen, B Kronvang, R Grant, and HE Andersen, 1999. Subsurface drainage loss of particles and phosphorus from field plot experiments and a tile-drained catchment. *Journal of Environmental Quality*, 28: 576-584.
- Lauzon J. 2003. Department of Land-Resource Science, University of Guelph. Personal Communication.
- Lee D, TA Dillaha, and JH Sherrard, 1989. Modelling phosphorus transport in grass buffer strips. *Journal of Environmental Engineering*, 115: 409-427.
- Lindsay WL, 1979. *Chemical Equilibria in Soils*. John Wiley & Sons Ltd., Chichester.
- Logan TJ, 1990. Sustainable agriculture and water quality. In *Sustainable Agricultural Systems*, Edwards, C.A., Lal, R., Madden, P., Miller, R.H., and House, G., (Eds). Soil and Water Conservation Society, Ankeny, Iowa, USA.
- McCallister DL and TJ Logan, 1978. Phosphate adsorption-desorption characteristics of soils and bottom sediments in the Maumee River Basin. *Journal of Environmental Quality* 7: 87-92.
- McCool DK, WH Wischmeier, and LC Johnson, 1982. Adapting the universal soil loss equation to the Pacific Northwest. *Trans. AWAE* 25: 928-934.
- McCuen RH, 1998. *Hydrologic Analysis and Design*, 2<sup>nd</sup> Ed. USA: Prentice-Hall.
- McDowell RW, AN Sharpley, LM Condrón, PM Haygarth, and PC Brookes, 2001. Processes controlling soil phosphorus release to runoff and implications for agricultural management. *Nutrient Cycling in Agroecosystems* 59: 269-284.
- Mengis M, SL Schiff, M Harris, MC English, R Aravena, RJ Elgood, and AM MacLean, 1999. Multiple geochemical and isotopic approaches for assessing ground water attenuation in a riparian zone. *Ground Water* 37: 448-457.
- Meyer JL, 1979. The role of sediments and bryophytes in phosphorus dynamics in a headwater stream ecosystem. *Limnology and Oceanography* 24:365-375.
- Miller MH, 1979. Contribution of nitrogen and phosphorus to subsurface drainage water from intensively cropped mineral and organic soils in Ontario. *J. Environ. Qual.* 8: 42-48.
- Miller RW and RL Donahue, 1990. *Soils: An Introduction to Soils and Plant Growth*. New Jersey: Prentice Hall.
- Mosley MP, 1982. Subsurface flow velocities through selected forest soil. South Island, New Zealand. *J. Hydrology* 55: 225-248.



- Mueller DK, PA Hamilton, DR Helsel, KJ Hitt, and BC Ruddy, 1995. Nutrients in groundwater and surface water of the United States – An analysis of data through 1992. *United States Geological Survey Water-Resources Investigations Report* 95-4031.
- Mulholland PJ, AD Steinman AD, and J Elwood, 1990. Measurement of Phosphorus uptake length in streams: comparison of radiotracer and stable PO<sub>4</sub> releases. *Canadian Journal of Fisheries and Aquatic Sciences* 47: 2351-2357.
- Mulholland PJ, JD Newbold and J Elwood, 1985. Phosphorus spiralling in a woodland stream: seasonal variations. *Ecology* 66(3): 1012-1023.
- Mulholland PJ, 1992. Regulation of nutrient concentrations in a temperate forest stream: roles of upland, riparian and instream processes. *Limnol. Oceanogr.* 37: 1512-1526.
- Munn NL and JL Meyer, 1990. Habitat-specific solute retention in two small streams: an intersite comparison. *Ecology* 71(6): 2069-2082.
- Muscutt AD, GL Harris, SW Bailey and DB Davies, 1993. Buffer zones to improve water quality: a review of their potential use in UK agriculture. *Agriculture, Ecosystem and Environment*, 45: 59-77.
- Norris V, 1993. The use of buffer zones to protect water quality: a review. *Water Resources Management* 7: 257-272.
- Osborne LL and DA Kovacic, 1993. Riparian vegetated buffer strips in water quality restoration and stream management. *Freshwater Biology* 29: 243-258.
- Parfitt RL, 1978. Anion adsorption by soils and soil materials. *Adv. Agron.* 30: 1-50.
- Patrick WH Jr and RA Khalid, 1974. Phosphate release and sorption by soils and sediments: effect of aerobic and anaerobic conditions. *Science* 186: 53-55.
- Pionke HB, WJ Gburek, AN Sharpley, and RR Schnabel, 1996. Flow and nutrient export patterns for an agricultural hill-land watershed. *Water Resources Res.* 32:1795-1804.
- Pollution from Land Use Activities Reference Group (PLUARG), 1978. *Environmental Management Strategy for the Great Lakes System*. Windsor: International Joint Commission.
- Pote DH, TC Daniel, DJ Nichols, PA Jr. Moore, DM. Miller, and DR Edwards, 1998. Seasonal and Soil-Drying Effects on Runoff Phosphorus Relationship to Soil Phosphorus. *Soil Sci. Soc. Am. J.* 63:1006-1012.
- Present RC, and RE Wicklund, 1971. The Soils of Waterloo Country *Ontario Soil Survey Report* 44.

- Puckett LJ, 1995. Identifying the major sources of nutrient water pollution. *Environ. Sci. Tech.* 29: 408-414.
- Reddy KR, RH Kadlec, E Flaig and PM Gale, 1999. Phosphorus retention in streams and wetlands: a review. *Critical Reviews in Environmental Science and Technology* 29: 83-146.
- Renkema, P. 2003. Land Owner and Farmer, Maryhill Ontario.
- Richards TL and TS Steenhuis, 1988. Tile drain sampling of preferential flow on a field scale. *Journal of Contaminant Hydrology* 3: 307-325.
- Richardson CJ, 1985. Mechanisms controlling phosphorus retention capacity in freshwater wetlands. *Science* 228: 1424-1427.
- Ritsema CJ, JL Nieber, LW Dekker, and TS Steenhuis, 1998. Stable or unstable wetting fronts in water repellent soils – effect of antecedent soil moisture content. *Soil and Tillage Research* 47: 111-123.
- Ritsema CJ and LW Dekker, 1994, Soil moisture and dry bulk density patterns in bare dune sands. *Journal of Hydrology* 154: 107-131.
- Ryden JC, JK Syers, and RF Harris, 1973. Phosphorus in runoff and streams. *Adv. Agron.* 25: 1-45.
- Sample EC, RI Soper, and GJ Racz, 1980, Reactions of phosphate fertilizers in soils. In *The Role of Phosphorus in Agriculture*. FE Khasawneh, EC Sample and EJ Kamprath (Eds.). Madison, WI: ASA-CSSA-SSSA
- Scheider WA, JJ Moss, and PJ Dillon, 1979. Measurement and uses of hydraulic and nutrient budgets. In *Lake Restoration*. Proceedings of a National Conference, NTIS, EPA 440/5-79-001, Washington, D.C.
- Schindler DW, 1977. Evolution of phosphorus limitation in lakes. *Science* 195: 260-262.
- Schlosser IJ and JR Karr, 1981. Water quality in agricultural watersheds: impact of riparian vegetation during baseflow. *Water Resources Bulletin*, 17(2): 233-240.
- Schnabel RR, 1986. Nitrate concentrations in a small stream as affected by chemical and hydrologic interactions in the riparian zone. In *Watershed Research Perspectives*. DL Correll (Ed.) Smithsonian Press, Washington, D.C.
- Schuman GE, RG Spomer, and RF Piest, 1973. Phosphorus losses from four agricultural watersheds on Missouri Valley loess. *Soil Sci. Amer. Proc.* 37: 424-427.

- Sharpley AN, 1995a. Identifying sites vulnerable to phosphorus loss in agricultural runoff. *J. Environ. Qual.* 24: 947-951.
- Sharpley AN, 1995b. Soil phosphorus dynamics: agronomic and environmental impacts. *Ecological Engineering* 5:261-279.
- Sharpley AN, SC Chapra, R Wedepohl, JT Sims, TC Daniel, and KR Reddy, 1994, Managing agricultural phosphorus for the protection of surface waters: Issues and options. *J. Environ. Quality* 23: 437-451.
- Sharpley AN, JK Syers, and RW Tillman, 1983. Transport of ammonium- and nitrate-nitrogen in surface runoff from pasture as influenced by urea application. *Water, Air and Soil Pollution* 20: 425-430.
- Sharpley AN and JK Syers, 1981. Amounts and relative significance of runoff types in the transport of nitrogen into a stream draining an agricultural watershed. *Water, Air and Soil Pollution* 15: 299-308.
- Sharpley AN, LR Ahuja, and RG Menzel, 1981. The release of phosphorus to runoff in relation to the kinetics of desorption. *J. Environ. Qual.* 10(3), 387-391.
- Sims JT, RR Simard, and BC Joern, 1998. Phosphorus loss in agricultural drainage: Historical perspective and current research. *J. Environ. Qual.* 27: 277-293.
- Smeck NE, 1985. Phosphorus dynamics in soils and landscapes. *Geoderma* 36: 185-199.
- Sommers LE, DW Nelson, and B Kaminsky, 1975. *Non-point Source Pollution Seminar* (EPA-905/9-75-007, Environmental Protection Agency, Chicago).
- Stamm C, H Fluhler, R Gachter, J Leuenberger, and H Wunderli, 1998. Preferential transport of phosphorus in drained grassland soils. *J. Environ. Qual.* 27: 515-522.
- Steinheimer TR, KD Scoggin, and LA Kramer, 1998. Agricultural chemical movement through a field-size watershed in Iowa: Surface hydrology and nitrate losses in discharge. *Environ. Sci. Technol.* 32: 1048-1052.
- Stoddard JL, 1994. Long-term changes in watershed retention of N. In: Baker LA (Ed) *Chemistry of Lakes and Reservoirs*. ACS Advances in Chemistry Series No. 237, American Chemical Society, pp. 223-284.
- Stone M, 1993. Sediment and nutrient transport dynamics in two Lake Erie tributaries: implications for external phosphorus loading estimates. Ph.D. Thesis, University of Waterloo. Waterloo, Ontario, Canada.
- Stone M and BG Krishnappan, 2002. The effect of irrigation on tile sediment transport in a headwater agricultural stream. *Water Research.* 36:3439-3448.

Stone M and BG Krishnappan, 2003 Floc morphology and size distributions of cohesive sediment in steady-state flow. *Water Research* 37(11): 2739-274.

Stone M and MC English, 1993. Geochemical composition, phosphorus speciation and mass transport characteristics of fine-grained sediment in two Lake Erie tributaries. *Hydrobiologia* 253:17-29.

Stone M and A Mudroch, 1989. The effect of particle size, chemistry and mineralogy of river sediments on phosphate adsorption. *Environmental Technology Letters* 10: 501-510.

Svendsen LM, B Kronvang, P Kristensen, and P Graesbol, 1995. Dynamics of phosphorus compounds in a lowland river system: importance of retention and non-point sources. *Hydrological Processes* 9: 119-142.

Syers JK, RF Harris, and DE Armstrong, 1973. Phosphate chemistry in lake sediments. *Journal of Environmental Quality* 2(1): 1-14.

Tate CM, RE Broshears, and DM McKnight, 1995. Phosphate dynamics in an acidic mountain stream: Interactions involving algal uptake, sorption by iron oxide and photoreduction. *Limnology and Oceanography*, 40(5): 938-946.

Topp GC, JL Davis and AP Annan, 1980. Electromagnetic determination of soil water content: Measurements in coaxial transmission lines. *Water Resour. Res.* 16(1), 574-588.

Triska FJ, JH Duff and RJ Avanzino, 1990. Influence of exchange flow between the channel and hyporheic zone on nitrate production in a small mountain stream. *Can. J. Fish. Aquat. Sci.* 47: 2099-2111.

Triska FJ, JH Duff and RJ Avanzino, 1993. The role of water exchange between a stream channel and its hyporheic zone in nitrogen cycling at the terrestrial-aquatic interface. *Hydrobiologia* 251: 167-184.

Triska FJ, VC Kennedy, RJ Avanzino GW Zellweger and KE Bencala, 1989. Retention and transport of nutrient in a third-order stream in northwestern California: hyporheic processes. *Ecology* 70: 1893-1905.

Troeh FR, and LM Thompson, 1993. *Soils and Soil Fertility*, 5<sup>th</sup> Ed. College of Agriculture, Iowa State University. Oxford University Press: New York.

Ulen B and K Persson, 1999. Field-scale phosphorus losses from a drained clay soil in Sweden. *Hydrological Proc.* 13: 2801-2812.

Ulen B, 1995. Episodic precipitation and discharge events and their influence on losses of phosphorus and nitrogen from tile drained arable fields. *Swedish J. Agric. Res.* 25: 25-31.

Updegraff K, J Pastor, SD Bridgham and CA Johnston, 1995. Environmental and substrate controls over carbon and nitrogen mineralization in northern wetlands. *Ecol. Applic.* 5: 151-163.

Vanni MJ, WH Renwick, JL Headworth, JD Auch, and MH Schaus, 2001. Dissolved and particulate nutrient flux from three adjacent agricultural watersheds: A five-year study. *Biogeochemistry* 54: 85-114.

Van Schilfgaarde J, 1974. *Drainage for Agriculture*. Agronomy Series No. 17, Am. Soc. Agron., Madison, pp. 245-270.

Villee CA, EP Solomon, CE Martin, DW Martin, LR Berg, and PW Davis, 1989. *Biology*, 2<sup>nd</sup> Ed. U.S.A.: Saunders College Publishing.

Vymazal J, 1995. *Algae and Element Cycling in Wetlands*. U.S.A.: CRC Press, Inc.

Wetzel RG, 1983. The Phosphorus Cycle, In RG Wetzel (ed.), *Limnology*, 2nd ed. CBS College Publishing, U.S.A.

Walling DE and IDL Foster, 1975. Variations in the natural chemical concentration of river water during flood flows, and the lag effect: Some further comments. *J. Hydrol.* 26: 237-244.

Welsch DL, CN Kroll, JJ McDonnell, and DA Burns, 2001, Topographic controls on the chemistry of subsurface stormflow: *Hydrological Processes* 15: 1925-1938.

Zuzel JF, RR Allmaras, and R Greenwalt, 1993. Temporal distribution of runoff and soil erosion from small agricultural plots in northeastern Oregon. *Soil Sci.* 156: 111-117.